

Copyright Warning & Restrictions

The copyright law of the United States (Title 17, United States Code) governs the making of photocopies or other reproductions of copyrighted material.

Under certain conditions specified in the law, libraries and archives are authorized to furnish a photocopy or other reproduction. One of these specified conditions is that the photocopy or reproduction is not to be “used for any purpose other than private study, scholarship, or research.” If a user makes a request for, or later uses, a photocopy or reproduction for purposes in excess of “fair use” that user may be liable for copyright infringement,

This institution reserves the right to refuse to accept a copying order if, in its judgment, fulfillment of the order would involve violation of copyright law.

Please Note: The author retains the copyright while the New Jersey Institute of Technology reserves the right to distribute this thesis or dissertation

Printing note: If you do not wish to print this page, then select “Pages from: first page # to: last page #” on the print dialog screen

The Van Houten library has removed some of the personal information and all signatures from the approval page and biographical sketches of theses and dissertations in order to protect the identity of NJIT graduates and faculty.

ABSTRACT

THERMOCHEMICAL PROPERTIES OF FLUORINATED HYDROCARBONS, HYDROPEROXIDES, AND FLUORINATED HYDROPEROXIDES; THERMOCHEMISTRY AND KINETICS ON DISSOCIATION AND ASSOCIATION REACTIONS OF OXIRANYL RADICAL

by
Heng Wang

Thermochemical properties on fluorinated hydrocarbons, alcohol, hydroperoxides, and alkyl hydroperoxides are determined. Reaction kinetics and modeling on the three member ring cyclic ether radical, oxiranyl radical, are studied under atmospheric and combustion environments.

Molecular geometries, vibration frequencies, internal rotor potentials, and thermochemical properties ($\Delta_f H^\circ_{298}$, $S^\circ(T)$ and $C^\circ_p(T)$) for fluorinated-hydrocarbons, thermochemical properties and bond energies, for alkyl and fluoro hydroperoxides and fluoro alcohols are determined with comparison of data from a number of different ab initio, density functional theory (DFT) and composite calculation methods, and basis sets.

Kinetic parameters for unimolecular decomposition and isomerization reactions of the oxiranyl radical are determined versus pressure and temperature. Kinetic parameters for chemically activated bimolecular oxidation reaction of the oxiranyl radical with 3O_2 are determined for the formation and unimolecular dissociation of the formed peroxy radical. Kinetic calculations use multi-frequency quantum RRK analysis for the energy dependent rate constant with Master Equation analysis for fall-off. Computer modeling for simulation and identification of the primary products, important reaction paths and thermal characteristics under atmospheric and combustion conditions are evaluated.

Thermochemical and kinetic properties developed during this work illustrate the effects of fluorine substitution on structures and bonding in C1 to C4 normal hydrocarbons, fluoro-alcohols, fluoro-hydroperoxides based on standard enthalpies of formation and bond dissociation energies.

Thermochemical kinetic calculations for the unimolecular dissociation (ring opening) and molecular oxygen oxidation association reactions of oxiranyl radical show important reaction paths and their changes as function of temperature and pressure.

**THERMOCHEMICAL PROPERTIES OF FLUORINATED HYDROCARBONS,
HYDROPEROXIDES, AND FLUORINATED HYDROPEROXIDES;
THERMOCHEMISTRY AND KINETICS ON DISSOCIATION AND
ASSOCIATION REACTIONS OF OXIRANYL RADICAL**

**by
Heng Wang**

**A Dissertation
Submitted to the Faculty of
New Jersey Institute of Technology
in Partial Fulfillment of the Requirements for the Degree of
Doctor of Philosophy in Chemistry**

Department of Chemistry and Environmental Science

May 2016

Copyright © 2016 by Heng Wang

ALL RIGHTS RESERVED

APPROVAL PAGE

**THERMOCHEMICAL PROPERTIES OF FLUORINATED HYDROCARBONS,
HYDROPEROXIDES, AND FLUORINATED HYDROPEROXIDES;
THERMOCHEMISTRY AND KINETICS ON DISSOCIATION AND
ASSOCIATION REACTIONS OF OXIRANYL RADICAL**

Heng Wang

Dr. Joseph W. Bozzelli, Dissertation Advisor Date
Distinguished Professor of Chemistry and Environmental Science, NJIT

Dr. Lev N. Krasnoperov, Committee Member Date
Professor of Chemistry and Environmental Science, NJIT

Dr. Tamara Gund, Committee Member Date
Professor of Chemistry and Environmental Science, NJIT

Dr. Alexie Khalizov, Committee Member Date
Assistant Professor of Chemistry and Environmental Science, NJIT

Dr. Chiung-chu Chen, Committee Member Date
Physical Scientist, U.S. Army, Maryland

BIOGRAPHICAL SKETCH

Author: Heng Wang
Degree: Doctor of Philosophy
Date: May 2016

Undergraduate and Graduate Education:

- Doctor of Philosophy in Chemistry,
New Jersey Institute of Technology, Newark, NJ, 2016
- Master of Science in Chemistry,
New Jersey Institute of Technology, Newark, NJ, 2011
- Bachelor of Science in Applied Chemistry,
Beijing University of Chemical Technology, Beijing, P. R. China, 2010

Major: Chemistry

Publications:

Heng Wang, Alvaro Castillo, and Joseph W. Bozzelli, "Thermochemical Properties Enthalpy, Entropy, and Heat Capacity of C1-C4 Fluorinated Hydrocarbons: Fluorocarbon Group Additivity", *J. Phys. Chem. A*. DOI. 10.1021/acs.jpca.5b03912, 2015.

Heng Wang and Joseph W. Bozzelli, "Thermochemical Properties and Bond Dissociation Energies for C1-C4 Normal Hydroperoxides and Peroxy Radicals", Accepted by *J. Chem. Eng. Data*. 2016.

Heng Wang and Joseph W. Bozzelli, "Thermochemistry and Kinetic Analysis on Unimolecular Dissociation Reaction of Oxiranyl Radical: A Theoretical Study", *ChemPhysChem*. DOI. 10.1002/cphc.201600152, 2016.

Extended Abstract Publications:

Heng Wang and Joseph W. Bozzelli. "Quantum Chemical Study on α -Acrolein Radicals Associate With $^3\text{O}_2$ ", ESSCI Spring Meeting, Princeton University, New Jersey. March 2016.

Heng Wang and Joseph W. Bozzelli, "Cyclic Ether Mechanism for 2-Oxiranyl and 2-Oxetanyl Radicals: A Theoretical Study", 10th Asian-Pacific Combustion Conference, Beijing, China. June 2015.

Heng Wang and Joseph W. Bozzelli, "Cyclic Ether Mechanism for 2-Oxiranyl and 2-Oxetanyl Radicals: A Theoretical Study", 9th U.S. National Combustion Meeting, Cincinnati, Ohio. May 2015.

Presentations:

Heng Wang and Joseph W. Bozzelli, "Quantum Chemical Study on α - Acrolein Radicals Association With Molecular Oxygen", the Dana Knox Research Showcase, NJIT, New Jersey. Oral Presentation. April 2016.

Heng Wang and Joseph W. Bozzelli, "Quantum Chemical Study on α - and β - Acrolein Radicals Association With Molecular Oxygen", ESSCI Spring Meeting, Princeton University, New Jersey. Oral Presentation. March 2016.

Heng Wang and Joseph W. Bozzelli, "Dissociation and Association Kinetics of Oxiranyl Radical: A Theoretical Study", KAUST Future Fuels Workshop, Thuwal, Saudi Arabia. March 2016. Poster Presentation. Won travel fellowships which sponsored by the KAUST office of sponsored research.

Heng Wang and Joseph W. Bozzelli, "Thermochemistry and Kinetic Analysis on Unimolecular Dissociation Reaction of Oxiranyl Radical: A Theoretical Study", 34th Regional Meeting on Kinetics and Dynamics, Brown University, Rhode Island. Oral Presentation. January 2016.

Heng Wang and Joseph W. Bozzelli, " β -Scission Ring Opening Unimolecular Dissociation Kinetics of 2-Oxetanyl and 3-Oxetanyl Radical and Thermochemistry Properties", 11th Annual Graduate Student Research Day, NJIT, New Jersey. Oral Presentation. Won first prize in Chemistry and Environmental Science Department and won second prize in University. October 2015.

Heng Wang and Joseph W. Bozzelli, "Dissociation and Association Kinetics of Oxiranyl Radical: A Theoretical Study", 9th International Conference on Chemical Kinetics, Ghent, Belgium. Poster Presentation. June 2015.

Heng Wang and Joseph W. Bozzelli, "Dissociation and Oxidation Mechanism for Oxiranyl Radical: A Theoretical Study", the Dana Knox Research Showcase, NJIT, New Jersey. Oral Presentation. Won second prize in graduate student's category. April 2015.

- Heng Wang and Joseph W. Bozzelli, "Dissociation Kinetics of 3 to 5 Member Ring Cyclic Ether Radicals and Thermochemistry Properties", 15th International Congress of Quantum Chemistry, Beijing, China. Oral Presentation. June 2015.
- Heng Wang and Joseph W. Bozzelli, "Cyclic Ether Dissociation and Oxidation Mechanism for 2-Oxiranyl and 2-Oxetanyl Radicals: A Theoretical Study", 10th Asian-Pacific Combustion Conference, Beijing, China. Oral Presentation. June 2015.
- Heng Wang and Joseph W. Bozzelli, "Cyclic Ether Oxidation Mechanism for 2-Oxiranyl and 2-Oxetanyl Radicals: A Theoretical Study", 9th U.S. National Combustion Meeting, Cincinnati, Ohio. Oral Presentation. May 2015.
- Heng Wang and Joseph W. Bozzelli, "A Detailed Cyclic Ether Oxidation Mechanism for 2-Oxiranyl and 2-Oxetanyl Radicals: A Theoretical Study", 33rd regional meeting on kinetics and dynamics, University of Massachusetts -Amherst, Amherst, MA. Oral Presentation. January 2015.
- Heng Wang, Itsaso Ayzmendi-Murua, and Joseph W. Bozzelli, "Dissociation Kinetics of 3-5 Member Ring Cyclic Ether Radicals and Thermochemistry for Hydroperoxides, Alcohols, and Peroxy Radicals", 23rd International Symposium on Gas Kinetics and Related Phenomena, Szeged, Hungary. Oral Presentation. June 2014.
- Heng Wang and Joseph W. Bozzelli, "Dissociation Kinetics of Oxetanyl Radicals and Thermochemical Properties", 10th Annual Graduate Student Research Day, NJIT, New Jersey. Poster and Oral Presentation. September 2014.
- Heng Wang, Alvaro Castillo, and Joseph W. Bozzelli, "Thermochemical Properties Enthalpy, Entropy, and Heat Capacity of C1-C4 Fluorinated Hydrocarbons: Fluorocarbon Group Additivity", 32nd regional meeting on kinetics and dynamics, Trinity College, Hartford, CT. Oral Presentation. January 2014.
- Douglas Purnell, Heng Wang, and Joseph W. Bozzelli, "Thermochemistry and Kinetic Parameters for Diethyl Ether and Diethyl Ether-lyl Radicals Reactions with Oxygen: Atmospheric and Lower Temperature Initiation", 32nd regional meeting on kinetics and dynamics, Trinity College, Hartford, CT. Oral Presentation. January 2014.
- Heng Wang and Joseph W. Bozzelli, "Thermochemical Properties Enthalpy, Entropy, and Heat Capacity of C1-C4 Fluorinated Hydrocarbons: Fluorocarbon Group Additivity", 9th Annual Graduate Student Research Day, NJIT, New Jersey. Poster Presentation. September 2014.

< 谨以此献给无怨无悔无条件爱我理解我支持我的爸爸，王宝利，妈妈，王金霞。
感谢你们对我从始至终的溺爱与纵容。 >
< To Mom and Dad, I love you forever. Many thanks for your unlimited love and support
in my entire life. >

ACKNOWLEDGMENT

First and foremost, I wish to express my appreciation to my advisor, Dr. Joseph W. Bozzelli, not only for his professional advice but also for his encouragement, patience, and support throughout this research. I also wish to thank Mrs. Bozzelli for her kindness. Without them, life would not be that easy.

I would also like to thank to my dissertation committee members, Dr. Lev. N. Krasnoperov, Dr. Tamara Gund, Dr. Alexie Khalizov, and Dr. Chiung-chu Chen for their helpful corrections and suggestions.

I am exceptionally appreciative to the members of Bozzelli Research Group - Dr. Alvaro Castillo, Dr. Itsaso Auzmendi-Murua, Dr. Suarwee Snitsirawat, Dr. Suriyakit Yommee, Mr. Francisco Guzman. They have provided friendship, assistance, and encouraging conversations to me during my studies.

I also dedicate my special thanks to Dr. Carol A. Venanzi, Dr. William Skawinski, Dr. Pin Gu, Dr. Zhiqian Wang, Dr. Han Jia, Ms. Sylvana L. Brito, Ms. Genti M. Price, Ms. Xinglei Liu, Mrs. Lingjie (Selina) He, Mr. Pengfei Yin, Mr. Yiwen Wu, Ms. Megha Thakkar, Ms. Clarisa González-Lenahan, and Mr. Yogesh Gandhi. I also wish to thank Lei Li for his unlimited love and support.

TABLE OF CONTENTS

Chapter	Page
1 OVERVIEW.....	1
2 THERMOCHEMICAL PROPERTIES ENTHALPY, ENTROPY, AND HEAT CAPACITY OF C1-C4 FLUORINATED HYDROCARBONS: GROUP ADDITIVITY.....	8
2.1 Overview	8
2.2 Computational Methods	10
2.2.1 Ab Initio Calculation for Fluoromethane via Atomization Reaction	10
2.2.2 Density Functional Theory and Composite Calculations for Fluorinated Hydrocarbons C1-C4 via Series of Isodesmic Reactions	12
2.2.3 Enthalpy of Formation Calculations	13
2.2.4 Entropy, Heat capacity, and Internal Rotor Analysis for 14 Fluorinated Hydrocarbons	17
2.2.5 Group Additivity	19
2.3 Results and Discussion	20
2.3.1 Enthalpy of Fluoromethane	20
2.3.2 Geometries and Frequencies	21
2.3.3 Enthalpies of Formation of C2-C4 Target Molecules	22
2.3.4 Internal Rotor Potential Energy Diagrams	28
2.3.5 Entropy and Heat Capacity	29
2.3.6 Group Additivity.....	31
2.3.7 Monofluoro to Pentafluoro Ethanes Comparisons and Revaluation of Groups for Fluorocarbons with Fluorine Atoms on Adjacent Carbons.....	32

TABLE OF CONTENTS
(Continued)

Chapter	Page
2.4 Summary	35
3 THERMOCHEMICAL PROPERTIES ($\Delta_{\text{F}}H^{\circ}(298 \text{ K})$, $S^{\circ}(298 \text{ K})$, $C_{\text{p}}(T)$) AND BOND DISSOCIATION ENERGIES FOR C1-C4 NORMAL HYDROPEROXIDES AND PEROXY RADICALS.....	36
3.1 Overview	36
3.2 Computational Methods	40
3.2.1 Enthalpies of Formation	41
3.2.2 Entropy and Heat Capacity	46
3.3 Results and Discussion	47
3.3.1 Geometries	47
3.3.2 Enthalpies of Formation for C1-C4 Stable Molecules.....	48
3.3.3 Enthalpies of Formation for C1-C4 Peroxy Radicals	52
3.3.4 Internal Rotor Potential Energy Diagrams	59
3.3.5 Entropy and Heat Capacity	60
3.3.6 Bond Dissociation Energies at 298 K	64
3.4 Summary	66
4 THERMOCHEMICAL PROPERTIES ($\Delta_{\text{F}}H^{\circ}(298 \text{ K})$, $S^{\circ}(298 \text{ K})$, $C_{\text{p}}(T)$) AND BOND DISSOCIATION ENERGIES FOR FLUORINATED METHANOL AND FLUORINATED METHYL HYDROPEROXIDES: $\text{CH}_{3-\text{x}}\text{F}_{\text{x}}\text{OH}$, AND $\text{CH}_{3-\text{x}}\text{F}_{\text{x}}\text{OOH}$.....	67
4.1 Overview	67
4.2 Computational Methods	68

TABLE OF CONTENTS
(Continued)

Chapter	Page
4.2.1 Enthalpies of Formation	68
4.2.2 Entropy and Heat Capacity	70
4.2.3 Bond Dissociation Energies	71
4.3 Results and Discussion	71
4.3.1 Geometries	71
4.3.2 Enthalpies of Formation	77
4.3.3 Internal Rotor Potential Energy Diagrams	82
4.3.4 Entropy and Heat Capacity	85
4.3.5 Bond Dissociation Energies at 298 K	86
4.4 Summary	88
5 THERMOCHEMISTRY AND KINETIC ANALYSIS OF UNIMOLECULAR OXIRANYL RADICAL DISSOCIATION REACTION: A THEORETICAL STUDY.....	89
5.1 Overview	89
5.2 Computational Methods	92
5.2.1 Enthalpy of Formation	92
5.2.2 Entropy and Heat Capacity	94
5.2.3 Rate Constants	95
5.3 Results and Discussion	96
5.3.1 Potential Energy Diagrams.....	97
5.3.2 Enthalpy of Formation for the Transition States	98

TABLE OF CONTENTS
(Continued)

Chapter	Page
5.3.3 Entropy and Heat Capacity	105
5.3.4 Beta-Scission Ring-Opening Reaction Kinetics	106
5.4 Summary	112
6 THERMOCHEMISTRY AND KINETIC ANALYSIS ON MOLECULAR OXYGEN ASSOCIATION REACTION OF OXIRANYL RADICAL: A THEORETICAL STUDY.....	113
6.1 Overview	113
6.2 Computational Methods	115
6.2.1 Enthalpy of Formation	115
6.2.2 Entropy and Heat Capacity	116
6.2.3 Rate Constants	117
6.3 Results and Discussion	118
6.3.1 Potential Energy Diagrams.....	119
6.3.2 Enthalpy of Formation for the Transition States	120
6.3.3 Entropy and Heat Capacity	135
6.3.4 Kinetic Parameters.....	137
6.3.5 Comparison of Dissociation and Association Reaction of Oxiranyl	144
6.4 Summary	149
7 CONCLUSION	150
APPENDIX A ENTHALPY OF FORMATION OF REFERENCE SPECIES	151
APPENDIX B GEOMETRIES OF STUDIED MOLECULES	153

TABLE OF CONTENTS
(Continued)

Chapter	Page
APPENDIX C VIBRATIONAL FREQUENCIES OF STUDIED MOLECULES	166
APPENDIX D MOMENTS OF INERTIA OF STUDIED MOLECULES	176
APPENDIX E WORK REACTIONS OF STUDIED MOLECULES	178
APPENDIX F OPTIMIZED STRUCTURES OF STUDIED MOLECULES	190
APPENDIX G POTENTIAL ENERGY PROFILES.....	198
APPENDIX H ORBITAL ANALYSIS.....	207
REFERENCES	209

LIST OF TABLES

Table	Page
2.1 Isodesmic Reactions and Enthalpy of Formation for Fluoromethane from the Selected Calculation Method.....	14
2.2 Enthalpies of Formation for Fluoromethane.....	20
2.3 Carbon-Fluorine Bond Length for C2-C4 Fluorinated Hydrocarbons at the B3LYP/6-311+G(d,p) and QCISD/6-311G(d,p) Levels of Theory	22
2.4 The Method Average Under Each Calculation Level and the Overall Average of Enthalpy of Formation of 14 Fluorinated Hydrocarbons and the Differences Between Our Calculation with Experimental Reference Values or Literature Reference Values.....	24
2.5 Change in the Enthalpy of Formation by Inserting One CH ₂ Group in the Carbon Chain, and in Replacing An H Atom with A Fluorine Atom	26
2.6 Enthalpy of Formation for C5 Fluorinated Hydrocarbons Estimated Using the CH ₂ Insertion and F/H Substitution Trends, and Comparison to Group Additivity (kcal mol ⁻¹).....	27
2.7 Ideal Gas Phase Entropy and Heat Capacity Obtained by B3LYP/6-31+G(d,p) Calculation, Comparison with Literature.....	29
2.8 Composition of Groups for Ten C2-C4 Fluorocarbons.....	31
2.9 Thermodynamic Properties of Related Groups.....	32
2.10 Re-evaluation of the Enthalpy of Formation from Previous Study.....	33
2.11 Enthalpies of Formation: Difluoro- to Pentafluoro- Ethanes.....	34
3.1 Calculated $\Delta_{\text{rxn}}H_{298}$ from Work Reactions: Hydroperoxides and Peroxy Radicals.....	42
3.2 Comparison of Major Bond Lengths and Dihedral Angles Between Each Target.....	47
3.3 Work Reactions and Heat of Formation for C1-C4 Alkyl Hydroperoxides.....	49

LIST OF TABLES
(Continued)

Table	Page
3.4 Work Reactions and Heat of Formation Using Enthalpy Values of CH ₃ OOH, CH ₃ CH ₂ OOH from Above as Reference Species.....	50
3.5 Comparison of Calculated $\Delta_f H^\circ_{298}$ Values for C1-C4 Alkyl Hydroperoxides to Available Literature Data.....	52
3.6 Work Reactions for Peroxy Radical	54
3.7 Isodesmic Reactions for Peroxy Radicals: CH ₃ OOj, CH ₃ CH ₂ CH ₂ OOj, and CH ₃ CH ₂ CH ₂ CH ₂ OOj. CH ₃ CH ₂ OOj is Used as A Reference Species.....	55
3.8 Isodesmic Reactions and Enthalpy of Formation for C1-C4 Peroxy Radicals.....	56
3.9 Work Reactions and Enthalpy of Formation Including Target CH ₃ OOj, CH ₃ CH ₂ OOj, and CH ₃ CH ₂ CH ₂ OOj as Reference Species for C2-C4 Peroxy Radicals.....	57
3.10 Comparison of Calculated $\Delta_f H^\circ_{298}$ Values for C1-C4 Peroxy Radicals to Available Literature Data.....	59
3.11 Idea Gas Entropy and Heat Capacity Obtained by B3LYP/6-31+G(d,p) Calculation, Comparison with Available Literature.....	63
3.12 Bond Dissociation Energies of ROO-H, RO-OH, R-OOH, RO-Oj, and R-OOj. Comparison with Available Literature.....	65
4.1 Important Geometry Parameters of Methyl Hydroperoxide and Mono- to Tri-Fluoro Methyl Hydroerpxides. Bond Lengths in Å, Dihedral Angles in Degree...	73
4.2 Important Geometry Parameters of Methyl Hydroperoxy and Mono- to Tri-Fluoro Methyl Hydroperoxy. Bond Lengths in Å, Dihedral Angles in Degrees....	73
4.3 Important Geometry Parameters ofMethanol and Mono- to Tri-Fluoro Methanol. Bond Lengths in Å, Dihedral Angles in Degrees.....	75
4.4 Important Geometry Parameters of Methoxy and Mono- to Tri-Fluoro Methoxy. Bond Lengths in Å, Dihedral Angles in Degrees.....	76
4.5 Isodesmic Reactions and Heat of Formation for Fluoro Methyl Hydroperoxides. (All in kcal mol ⁻¹).....	77

LIST OF TABLES
(Continued)

Table	Page
4.6 Enthalpy of Formation of Each Target Molecules in this Study Compare to Available Literatures. (All in kcal mol ⁻¹).....	81
4.7 Energy Barrier for Each Internal Rotor in Methyl Hydroperoxide and Mono- to Tri-Fluoro Methyl Hydroperoxides. (Units in kcal mol ⁻¹).....	82
4.8 Energy Barrier for Each Internal Rotor in Methyl Hydroperoxy and Mono- to Tri-Fluoro Methyl Hydroperoxy Radicals. (Units in kcal mol ⁻¹).....	84
4.9 Energy Barrier for Each Internal Rotor in Methanol and Mono- to Tri-Fluoro Methanol. (Units in kcal mol ⁻¹).....	84
4.10 Ideal Gas Phase Entropy and Heat Capacity Obtained by B3LYP/6-31+G(d,p) Calculation, Comparison with Available Literature.....	85
4.11 Summary and Comparison of Bond Dissociation Energies with Available Literature (All in kcal mol ⁻¹).....	87
5.1 Standard Enthalpy of Formation at 298.15 K of Reference Species and Comparison with Available Literature.....	96
5.2 Calculated Standard Enthalpy of the Transition State Structures at 298 K for the Oxiranyl Radical β -Scission Ring Opening Reaction System (Data Recommended in This Study are Indicated by *).....	99
5.3 Ideal Gas Phase Entropy and Heat Capacity Obtained by B3LYP/6-31+G(d,p) Calculation, Comparison with Available Literature.....	105
5.4 High Pressure Limit Elementary Rate Parameters for the Unimolecular Dissociation Reaction of Oxiranyl Radical.....	106
5.5 Reversible Elementary Rate Parameters for the Unimolecular Dissociation Reaction of Oxiranyl Radical.....	110
6.1 Nomenclature and Figures of the Oxiranyl Radical and Its Derivative Compounds.....	119
6.2 Calculated Standard Enthalpy of Formation of the Transition State Structures at 298 K for the Oxiranyl Radical Oxidation Reaction System. See Figure 6.2. (Data Recommended in This Study are Indicated by *)	121

LIST OF TABLES
(Continued)

Table	Page
6.3 Calculated Standard Enthalpy of Formation of the Transition State Structures at 298 K for the Unimolecular Dissociation Reaction of $\gamma(\text{cjoo})$ and $\gamma(\text{coc})\text{-oj}$. See Figure 6.2 and Figure 6.3. (Data Recommended in This Study are Indicated by *)	130
6.4 Ideal Gas Phase Entropy and Heat Capacity Obtained by B3LYP/6-31+G(d,p) Calculation, Comparison with Available Literature.....	135
6.5 High Pressure Limit Elementary Rate Parameters for the Unimolecular Dissociation Reaction of Oxiranyl Radical.....	139

LIST OF FIGURES

Figure	Page
2.1 Standard deviation range of each calculation method	15
2.2 Potential energy profiles of the C-CCCF, CC-CCF, and CCC-CF internal rotors for 1-fluorobutane (symbol). The solid line is the fit of the Fourier series expansions.....	28
3.1 Potential energy profiles of the CCCO-OH, CCC-OOH, CC-COOH, and C-CCOOH internal rotors for propyl peroxy (symbols). The solid line is the fit of the Fourier series expansions.....	60
4.1 Geometry of methyl hydroperoxide and mono- to tri- fluoro methyl hydroperoxide molecules calculated by CBS-APNO method. Bond lengths in Å, bond angles in degrees, dihedral angles in degree.....	72
4.2 Geometry of methyl hydroperoxy and mono- to tri- fluoro methyl hydroperoxy molecules calculated by CBS-APNO method. Bond lengths in Å, bond angles in degree, dihedral angles in degree.....	73
4.3 Geometry of methanol and mono- to tri- fluoro methanol molecules calculated by CBS-APNO method. Bond lengths in Å, bond angles in degree, dihedral angles in degree.....	75
4.4 Geometry of methoxy and mono- to tri- fluoro methoxy molecules calculated by CBS-APNO method. Bond lengths in Å, bond angles in degree, dihedral angles in degree.....	76
4.5 Potential energy profiles of the internal rotors of the methyl hydroperoxide and mono- to tri- fluoro hydroperoxides (a-d). The solid lines are the fit of the Fourier series expansions.....	83
4.6 Potential energy profiles of internal rotors of the methyl hydroperoxy and mono- to tri- fluoro hydroperoxy radicals (e-h). The solid lines are the fit of the Fourier series expansions.....	83
4.7 Potential energy profiles of the internal rotors of the Methanol and mono- to tri- fluoro methanol (i-l). The solid lines are the fit of the Fourier series expansions.....	84

LIST OF FIGURES
(Continued)

Figure	Page
5.1 Nomenclature and figures of the oxirane (Left) and oxiranyl radical (right) with detailed geometry parameters. Bond length in Å, bond angle in degree.....	91
5.2 Potential energy diagram for unimolecular dissociation reaction of oxiranyl radical (energy barriers in parenthesis). Enthalpy of formation for TS1 are taken average of CBS-APNO and CCSD(T)/aug-cc-pVTZ.....	97
5.3 Enthalpy differences (kcal mol ⁻¹) between each method from the recommended enthalpy for each transition state. Transition state 1(I) to transition state 5(V), (a), (b), and (c) indicates 6-31G(d,p), 6-31+G(d,p), 6-311+G(2d,d,p), respectively, for each DFT method	105
5.4 Rate constant plot as a function of 1000/T(K) ranging from 298 K to 2000 K at 2 atm for comparison of this study with Joshi et al.....	107
5.5 Rate constant plot as a function of temperature ranging from 298 K to 2000 K under 0.01 atm and 100 atm.....	108
5.6 Rate constant plot as a function of pressure ranging from 0.01 atm to 100 atm under 600 K and 1500 K.....	109
5.7 Chemkin modeling of β-scission ring opening reaction of oxiranyl radical at 1 atm, 600 K, 1% of oxiranyl radical with 99% of N ₂	110
5.8 Chemkin modeling of β-scission ring opening reaction of oxiranyl radical at 1 atm, 800 K, 1% of oxiranyl radical with 99% of N ₂	111
6.1 Potential energy diagram for oxidation reaction of oxiranyl radical. Enthalpy of formation for each TS (energy barrier in parenthesis). Data are taken from Table 6.2. Units in kcal mol ⁻¹	120
6.2 Potential energy diagram for ring opening reaction of dioxirane radical (energy barrier in parenthesis). Enthalpy of formation for each TS is taken from Table 6.3 Units in kcal mol ⁻¹	129
6.3 Potential energy diagram for ring opening reaction of alkoxy radical (energy barrier in parenthesis). Enthalpy of formation for each TS is taken from Table 6.3 Units in kcal mol ⁻¹	130

LIST OF FIGURES
(Continued)

Figure	Page
6.4 Potential energy surface for dissociation of the oxiranyl hydroperoxide, $y(\text{coc})\text{-oo}\bullet$, $\text{R-O}_2 \rightarrow \text{R}\bullet + \text{O}_2$ with $\omega\text{B97XD/6-31+G(d,p)}$ calculation method.....	137
6.5 Potential energy surface for dissociation of the oxiranyl hydroperoxide, $y(\text{coc})\text{-oo}\bullet$, $\text{R-O}_2 \rightarrow \text{RO}\bullet + \text{O}$ with $\omega\text{B97XD/6-31+G(d,p)}$ calculation method.....	138
6.6 Rate constants as a function of temperature at 0.01 atm (left) and at 1 atm (right).....	140
6.7 Rate constants as a function of pressure at 298 K, 600 K, 800 K, and 1500 K.....	141
6.8 Chemkin modeling of oxidation reaction of oxiranyl radical at 1 atm, 600 K. 1% of oxiranyl radical, 6% of O_2 , 93% of N_2	143
6.9 Chemkin modeling of oxidation reaction of oxiranyl radical at 1 atm, 800 K. 1% of oxiranyl radical, 6% of O_2 , 93% of N_2	143
6.10 Chemkin modeling of competition between the dissociation reaction and oxidation reaction of oxiranyl radical at 1 atm, 298 K, 1% of oxiranyl radical, 6% of O_2 , 93% of N_2	144
6.11 Chemkin modeling of competition between the dissociation reaction and oxidation reaction of oxiranyl radical at 1 atm, 400 K, 1% of oxiranyl radical, 6% of O_2 , 93% of N_2	145
6.12 Chemkin modeling of competition between the dissociation reaction and oxidation reaction of oxiranyl radical at 1 atm, 430 K, 1% of oxiranyl radical, 6% of O_2 , 93% of N_2	145
6.13 Chemkin modeling of competition between the dissociation reaction and oxidation reaction of oxiranyl radical at 1 atm, 500 K, 1% of oxiranyl radical, 6% of O_2 , 93% of N_2	147
6.14 Chemkin modeling of competition between the dissociation reaction and oxidation reaction of oxiranyl radical at 1 atm, 600 K, 1% of oxiranyl radical, 6% of O_2 , 93% of N_2	148
6.15 Chemkin modeling of competition between the dissociation reaction and oxidation reaction of oxiranyl radical at 1 atm, 600 K, 1% of oxiranyl radical, 6% of O_2 , 93% of N_2	148

CHAPTER 1

OVERVIEW

One of the most important components of this study is to use the computational and quantum chemistry theories, principles, and postulations to determine the thermochemistry properties and chemical kinetics for fluorinated hydrocarbons, hydroperoxides, fluorinated hydroperoxides, and cyclic ether systems. In the quantum mechanics, several theories, principles, and approximations have been introduced to solve the atomic scale microcosms problems which have different situation with the macrocosm.

In 1913, quantum chemistry is early developed and described by Bohr who describes the atom as a small and positively charged nucleus surrounded by electrons that travel in circular orbits around the nucleus but with attraction provided by electrostatic forces rather than gravity. Bohr introduced: electrons in atoms orbit the nucleus; the electrons can only orbit stably, without radiating, in certain orbits at a certain discrete set of distances from the nucleus; electrons can only gain and lose energy by jumping from one allowed orbit to another.

The Heisenberg's principle, also known as the uncertainty principle, describes that the complementary variables cannot be determined simultaneously, such as the position and the momentum is also an important contribution to Quantum Mechanics.

In 1926, the Austrian physicist Erwin Schrödinger, enlightened by De Broglie's matter wave hypothesis, established the revolutionary basic equation of Quantum theory, an exploit that signified the formation of theory revealing the basic dynamic law in the microscopic matter world, namely Quantum Mechanics Theory with applications to

structure, bonding and energies of chemical specie. With the invention of computer and its continued improvements, the application to Quantum Theoretical Chemistry has developed. It has become a progressively accurate, effective, advanced and powerful field of study for thermochemical properties and understanding on reaction paths and kinetics. The Schrödinger equation is a partial differential equation that describes how the quantum state of a quantum system changes with time. It is not a simple algebraic equation, but in general a linear partial differential equation, describing the time-evolution of the system's wave function. However, except for the H like atom, people cannot solve the Schrödinger equation completely. Thus, scientists developed modified corrections or approximations to solve the multiple atoms system with the Schrödinger equation.

Several calculation methods have been involved and applied to this study. The fundamental assumption of HF theory, that each electron sees all of the others as an average field, allows for tremendous progress to be made in carrying out practical MO calculations. However, neglect of electron correlation can have profound chemical consequences when it comes to determine accurate wave functions and properties derived from the calculations. Hartree-Fock theory makes the fundamental approximations that each electron moves in the static electric field created by all of the other electrons, and then proceeds to optimize orbits for all of the electrons in a self-consistent fashion subject to a variational constraint. The resulting wave function, when operated upon by the Hamiltonian, delivers as its expectation value the lowest possible energy for a single-determinant wave function formed from the chosen basis set.

Density Functional Theory (DFT), function of another function, which is the spatially dependent electron density for a many-electron system. Thus, the name density

functional theory comes from the use of functional of the electron density. DFT is among the most popular and versatile methods available in current use of computational chemistry. In DFT, the functional is the electron density which is a function of space and time. The electron density is used in DFT as the fundamental property unlike Hartree-Fock theory which deals directly with the many-body wave function. Using the electron density significantly speeds up the calculation.

This study is focused on the development of accurate thermochemical properties ($\Delta_f H^\circ_{298}$, ΔS°_{298} , $C_p(T)$), reaction paths and reaction kinetics on chemical systems related to atmospheric chemistry, and to thermal and combustion related elementary reaction systems. Organic molecules, fluorinated hydrocarbons, fluorinated alcohols, fluorinated hydroperoxides, hydroperoxides, and cyclic ether radicals, have been studied. Quantum chemistry, coupled with statistical mechanics, has been applied to a number of chemical systems to study Chemical Thermodynamics, Chemical Reaction Paths, Kinetics, and Chemical Statistical Mechanics have been applied to practical issues. A combination of mathematical treatment with computational platform helps solving thermodynamic and kinetic problems regarding the target systems.

Enthalpy of formation for 14 C₂-C₄ fluorinated hydrocarbons are calculated with nine popular ab initio and density functional theory methods: B3LYP, CBS-QB3, CBS-APNO, M06, M06-2X, ω B97X, G4, G4(MP2)-6X, and W1U via several series of isodesmic reactions. The recommended ideal gas phase ΔH°_{f298} (kcal mol⁻¹) values calculated in this study are the following: -65.4 for CH₃CH₂F; -70.2 for CH₃CH₂CH₂F; -75.3 for CH₃CHFCH₃; -75.2 for CH₃CH₂CH₂CH₂F; -80.3 for CH₃CHFCH₂CH₃; -108.1 for CH₂F₂; -120.9 for CH₃CHF₂; -125.8 for CH₃CH₂CHF₂; -133.3 for CH₃CF₂CH₃; -166.7

for CHF₃; -180.5 for CH₃CF₃; -185.5 for CH₃CH₂CF₃; -223.2 for CF₄; and -85.8 for (CH₃)₃CF. Standard entropies are estimated using B3LYP/6-31+G(d,p) computed frequencies and geometries. Rotational barrier are determined and hindered internal rotational contributions for S[°]₂₉₈ and C_p(T) are calculated using the rigid rotor harmonic oscillator approximation, with direct integration over energy levels of the intramolecular rotation potential energy curve. Thermochemical properties for the fluorinated carbon groups C/C/F/H₂, C/C₂/F/H, C/C/F₂/H, C/C₂/F₂, and C/C/F₃ are derived from the above target fluorocarbons. Previously published enthalpies and groups for 1,2-difluoroethane, 1,1,2-trifluoroethane, 1,1,2,2-tetrafluoroethane, 1,1,1,2-tetrafluoroethane, 1,1,1,2,2-pentafluoroethane, 2-fluor-2-methylpropane that are previously determined via work reaction schemes are revised using updated reference species values. Standard deviations are compared for the calculation methods.

Structure and thermochemical properties of the normal hydroperoxides, C_nH_{2n+1}OOH (1 ≤ n ≤ 4), and corresponding peroxy radicals, C_nH_{2n+1}OO• (1 ≤ n ≤ 4), are determined by density functional M06-2X, multilevel G4, composite CBS-QB3 and CBS-APNO level calculations. Unique to this study is that the Δ_fH[°]₂₉₈ values are determined using several isodesmic reactions which utilize experimental standard enthalpy data for CH₃OOCH₃ and CH₃CH₂OOCH₂CH₃ as reference species, where previous studies used atomization or work reactions with alcohols or other non-peroxide species. The S[°]₂₉₈ and C_p(T)'s (300 ≤ T/K ≤ 1500) from vibration, translation, and external rotation contributions are calculated based on the vibration frequencies and structures obtained from the density functional study. Potential barriers for the internal rotations are calculated at B3LYP/6-31+G(d,p) level with scale factor 0.964, and hindered rotational contributions

to S°_{298} and $C_p(T)$'s are calculated using direct integration over energy levels of the internal rotational potentials. The results show the following $\Delta_f H^{\circ}_{298}$ values (units in kcal mol⁻¹):

CH₃OOH (-30.96), CH₃CH₂OOH (-38.94), CH₃CH₂CH₂OOH (-44.03),
 CH₃CH₂CH₂CH₂OOH (-48.86), CH₃OO• (2.37), CH₃CH₂OO• (-6.19), CH₃CH₂CH₂OO•
 (-11.35), and CH₃CH₂CH₂CH₂OO• (-16.58). Bond dissociation energies for the R-OOH,
 RO-OH, ROO-H, R-OOj and RO-Oj bonds are reported. The enthalpy values from use of
 experimental data as reference show very good agreement and support the data obtained
 from calculation methods. They should be used for reference values. Entropy and heat
 capacity values show good agreement with the calculation literature. The standard entropy
 for butyl hydroperoxide, propyl peroxy, and butyl peroxy are corrected.

Oxygenated fluorocarbons are routinely found in sampling of environmental soils and waters as a result of the wide spread use of fluoro and chlorofluoro carbons as heat transfer fluids, inert materials and solvents; their influence on the environment is a growing concern. The thermochemical properties of these species are needed for understanding their stability and reactions in the environment and in thermal process. Structures and thermochemical properties on the mono- to tri- fluoro methanol, CH_{3-x}F_xOH, and fluoro methyl hydroperoxide, CH_{3-x}F_xOOH (1 ≤ x ≤ 3), are determined by CBS-QB3, CBS-APNO, and G4 calculations. Entropy and heat capacities from vibration, translation, and external rotation contributions are calculated based on the vibration frequencies and structures obtained from the B3LYP/6-31+G(d,p) density functional method. Potential barriers for the internal rotations are also calculated from this method and used to calculate hindered rotor contributions to S°_{298} and $C_p(T)$'s using direct integration over energy levels of the internal rotational potentials. Standard enthalpy of formation, $\Delta_f H^{\circ}_{298}$, (units in kcal mol⁻¹)

are: CH₂FOOH (-83.7), CHF₂OOH (-138.1), CF₃OOH (-193.6), CH₂FOO• (-44.9), CHF₂OO• (-99.3), CF₃OO• (-153.8), CH₂FOH (-101.9), CHF₂OH (-161.6), CF₃OH (-218.1), CH₂FO• (-49.1), CHF₂O• (-97.8), CF₃O• (-150.5), CH₂F• (-7.6), CHF₂• (-58.8), CF₃• (-112.6). Bond dissociation energies for the R-OOH, RO-OH, ROO-H, R-OO•, RO-O•, R-OH, RO-H, R-O•, and R-H bonds are determined and compared with methyl hydroperoxide to observe the trends from added fluoro- substitutions.

Oxirane structures are important in organic synthesis, being important initial products in the oxidation reactions of alkyl radicals. The thermochemical properties for the reaction steps of the unimolecular oxiranyl radical dissociation reaction are determined and compared with the available literature. The overall ring opening and subsequent steps involve four types of reactions: β -scission ring opening, intramolecular hydrogen transfer, β -scission hydrogen elimination, and β -scission methyl radical elimination. The enthalpies of formation of the transition states are determined and evaluated using six popular DFT calculation methods (B3LYP, B2PLYP, M06, M06-2X, ω B97X, ω B97XD), each combined with three different basis sets. The DFT enthalpy values are compared with five composite calculation methods (G3, G4, CBS-QB3, CBS-APNO, W1U), and by CCSD(T)/aug-cc-pVTZ. Kinetic parameters are determined versus pressure and temperature for the unimolecular dissociation pathways of an oxiranyl radical, which include the chemical activation of the ring-opened oxiranyl radical relative to the ring-opening barrier. Multifrequency quantum Rice Ramsperger Kassel (QRRK) analysis is used to determine $k(E)$ with Master Equation analysis for fall-off. The major overall reaction pathway at lower combustion temperatures is oxiranyl radical dissociation to a

methyl radical and carbon monoxide. Oxiranyl radical dissociation to a ketene and hydrogen atom is the key reaction path above 700 K.

Cyclic ether radicals are formed in combustion and in atmospheric oxidation reactions, where they undergo abstraction reactions to form cyclic ether radicals. The cyclic ether radicals then undergo unimolecular dissociation or a chemical activation reaction with $^3\text{O}_2$ to form peroxy radicals, that further react to form new reactive oxygenated intermediates, in combustion and thermal oxidation processes. Density functional theory (B3LYP, B2PLYP, M06, M06-2X, ωB97X , and ωB97XD) and higher level composite ab initio calculations (CBS-QB3, CBS-APNO, and G4) are used to calculate the thermochemical properties (enthalpy of formation, entropy, and heat capacity) of the oxidation reaction of oxiranyl radical with molecular oxygen. Kinetic parameters are determined versus pressure and temperature for the chemical activated formation and unimolecular dissociation of the peroxide adducts. Multi-frequency quantum RRRK (QRRK) analysis is used for $k(E)$ with master equation analysis for falloff. At room temperature and 1 atm, the major reaction path is the stabilization to peroxy radical pathway over the entire pressure range. The stabilization starts to fall off around 600 K. Formation of glyoxal (CHOCHO) and a bicyclic (dual-dioxirane) are dominant forward reactions paths. At 1000 K and above chain branching to a dioxirane alkoxy radical plus ^3O atom is the dominant forward reaction product. The competition between the β -scission ring-opening dissociation reaction and the molecular oxygen association reaction of oxiranyl radical has been simulated with Chemkin code. The $^3\text{O}_2$ association reaction dominates below 430 K whereas the unimolecular dissociation reaction is dominant above 430 K.

CHAPTER 2

THERMOCHEMICAL PROPERTIES ENTHALPY, ENTROPY, AND HEAT CAPACITY OF C1-C4 FLUORINATED HYDROCARBONS: FLUOROCARBON GROUP ADDITIVITY

2.1 Overview

Fluorinated hydrocarbons are present in the atmosphere, hydrosphere and lithosphere as a result of past use as solvents and propellants as well as past and current use as refrigerants and heat exchange fluids and in polymers. They were regarded as the replacement of greenhouse gas like chlorofluorocarbons because of their none or less adverse effects on the stratospheric ozone layer.¹ They exist in the environment from pure compounds to partially oxidized intermediates resulting from environmental driven oxidation of the molecular structures. The fundamental thermodynamic and chemical properties of the fluorocarbons and their oxygenated breakdown intermediates are critical to understand in order to study their lifetimes and reactivity in biological processes and in the environment. Thermochemical properties are also needed in kinetic modeling and in equilibrium codes.

There are several studies on the thermochemistry of fluorinated alkanes with one and two carbon atoms in the literature²⁻⁹. In 1994, Chen et al³. studied thermodynamic properties of CH₂FCHF₂ and CHF₂CHF₂ using RHF, MP2, and MP4 calculation methods. Zachariah et al⁹. employed the BAC-MP4 method and expanded the database for thermochemistry of C/H/F/O species significantly as the data was needed for construction of a mechanism to model oxidation of partially fluorinated hydrocarbons of C₁ and C₂. Berry et al². studied fluorinated C₁ species with bromine using G2(MP2), CBS, and BAC-MP4 methods. Berry et al². reported that the negative errors in the calculated enthalpies by atomization methods were observed to be linearly dependent upon the

number of C-F bonds in the molecule. Yamada et al^{6,8}. leveraged the isodesmic reaction method with literature data for highly fluorinated $C_2H_XF_{6-X}$ ethanes using MP2 and G2. Yamada et al^{6,8}. also updated the thermochemical enthalpy data of C/F/H groups needed for use of the Group Additivity¹⁰ method, where they reported that interaction groups had to be used to correct for fluorine atoms when they occurred on adjacent carbons. Yamada and Berry⁷ together continued using G2MP2 to expanded the data to C_3 hydro-fluorocarbons.

In 2000, Haworth et al⁴. published a study on more than one hundred , fluorinated C_1 and C_2 hydrocarbons, including stable molecules and radicals. They evaluated differences in enthalpy data between the values from isodesmic reaction versus atomization energies and recommended use of the G3 method data.

Recently, Nagy et al⁵. has used Weizmann-n methods (for total energies) and CCSD(T) (for conformer energies and rotational barriers) to study enthalpies on a series of multi-fluoro $C_2H_XF_{6-X}$ molecules. They did not report entropy and heat capacity data on monofluoro hydrocarbons or larger C_3 and C_4 fluorocarbons.

This study verifies the standard enthalpy of formation for fluoromethane with that of the literature^{4, 11-14}, and uses these molecules as reference species in isodesmic work reactions for fluorocarbons with a higher carbon content. This study shows and compares the performance of nine different ab initio, composite and density functional calculation methods for accuracy, and this study determines the ideal gas thermodynamic properties and compare the data in this study with that from experiments. The calculation from this study on the C_1 and C_2 fluorocarbons are used to calculate C_3 and C_4 related fluoro-hydrocarbons. This study uses between four and twenty-nine work reactions for

error cancellation in the calculation enthalpy for each species. This study re-evaluates group contribution values (for group additivity) for C/C/F/H₂, C/C₂/F/H, C/C/F₂/H, C/C₂/F₂, C/C/F₃ based on their calculated values. This study uses the previous calculated thermal enthalpies and enthalpies of work reactions of Yamada et al⁶⁻⁸. with more accurate data for the reference molecules and show good agreement with current literature values. The data of this study and of Yamada et al^{6,8}. has been used to build group additivity terms for calculation of thermochemical properties of fluorocarbons, including interactions between fluorine atoms on adjacent carbons. Group Additivity¹⁰ is a popular method for estimation of thermochemical properties on hydrocarbons and oxygenated hydrocarbons, but it is not widely used for fluorohydrocarbons.

2.2 Computational Methods

2.2.1 Ab Initio Calculation for Fluoromethane Via Atomization Reaction

This study considers fluoromethane as core reference species in the isodesmic reactions; hence it is important that the standard enthalpy of formation of fluoromethane that use is accurate. In addition to evaluating data in the literature this study has calculated the enthalpy of formation of fluoromethane using extrapolated CCSD(T)¹⁵⁻¹⁸ energies with atomization reactions.

The accurate calculation of electronic energies requires the extrapolation of the calculated values to the basis set limit, and that the Hartree-Fock (self-consistent field) energies and the correlation energies converge to this limit differently¹⁹. HF-SCF energies

are calculated with the augmented correlation consistent basis set (X= T, Q, 5),²⁰⁻²² and extrapolated as suggested by Feller²³, $E_{\text{HF}}^X = E_{\text{HF}}^{\infty} + ae^{-bX}$, with E_{HF}^X being the three calculated HF-SCF energies using the aug-cc-pVXZ basis sets. The E_{HF}^{∞} extrapolated energy and parameters a and b can then be calculated with X as the cardinal number of the basis set (T:3, Q:4, and 5). CCSD(T) correlation energies were calculated with the aug-cc-pVXZ (X= Q, 5), and extrapolated following the atomic partial wave expansion of Helgaker et al.²⁴, $E_{\text{corrCCSD(T)}}^X = E_{\text{corrCCSD(T)}}^{\infty} + AX^{-3}$, where $E_{\text{corrCCSD(T)}}^X$ are the CCSD(T) correlation energies using the aug-cc-pVXZ basis sets. The $E_{\text{corrCCSD(T)}}^{\infty}$ and parameter A can then be calculated with simple algebra as for the HF-SCF energies. Enthalpies of formation were then calculated using atomization reactions, with Ruscic's Active Thermochemical Tables for the experimental atomic enthalpies: H=51.63±0.00 kcal/mol ; C=170.12±0.05 kcal/mol ; F=18.45±0.06 kcal/mol,²⁵⁻²⁶ and they include thermal corrections for enthalpy. Molecular geometries were calculated using CCSD(T)/cc-pVTZ because it has been shown that this method presents a mean absolute error of 0.0023 Å and a maximum absolute error of 0.0045 Å for a set of 19 molecules that include atoms of the first row (including HF, F₂, and HOF)²⁷. Geometry optimization is carried out with the Gaussian09²⁸ set of programs, frequency and single point energy calculations are carried out with GAMESS.²⁹⁻³²

2.2.2 Density Functional Theory and Composite Calculations for Fluorinated Hydrocarbons C₁-C₄ via Series of Isodesmic Reactions

All calculations for the C₁-C₄ fluorocarbons, (excluding CH₃F as above) are performed using the Gaussian 09²⁸ program. Structures, vibration frequencies, zero-point vibrational and thermo energies, and internal rotor potentials are initially analyzed with the hybrid density functional theory (DFT) method B3LYP. This method combines the three-parameter Becke exchange functional B3³³, with Lee-Yang-Parr correlation functional, LYP³⁴, and is used here with the 6-31G+(d,p) basis set. B3LYP/6-31G+(d,p) is chosen because it is computational economical and, thus, possibly applicable to larger molecules.

Energies are further refined using the procedures of the complete basis method developed by Petersson and coworkers, CBS-QB3.³⁵ It utilizes B3LYP/6-311G(2d,d,p) level of theory to calculate geometries and frequencies followed by single-point calculations using the CCSD(T) MP4(SDQ), and MP2 level.

The CBS-APNO³⁶ method performs an initial geometry optimization and frequency calculation at the HF/6-311G(d,p) level, followed by a higher-level QCISD/6-311G(d,p) geometry optimization. A single point energy calculation is then performed at the QCISD(T)/6-311++G(2df,p) level, followed by extrapolation to the complete basis set limit.

In 2007, two new hybrid meta exchange-correlation functional, M06 and M06-2X were reported³⁷. A third new hybrid density functional method, that includes 100% long-range exact exchange and 16% of exact short-exchange, called ω B97X,³⁸ was developed in 2008. These three modified DFT calculation levels are further used and evaluated in this fluorocarbons study.

This study also utilizes the W1U³⁹ theory, a modification of W1⁴⁰ (Weizmann 1), as fluorine is in the first row of the periodic table. W1U theory is an unrestricted coupled cluster spin contamination corrected [UCCSD(T)] method. Due to the large computational requirements of the CCSD(T)-FC\AugH-CC-pVTZ+2df and CCSD-FC\AugH-CC-pVQZ+2df energy calculations in the W1U method, this method is not applicable to the larger molecules used in this study.

Gaussian-4 theory (G4)⁴¹ is the fourth in the Gaussian-n series of quantum chemical methods based on a sequence of single point energy calculations. This method performs an initial geometry optimization and frequency calculation at the B3LYP/6-31G(2df, p) level, followed by a series of single point correlation energy calculations started from CCSD(T), MP4SDTQ, until MP2-Full.

Regarding the computational time cost of the G4 composite calculation methods, a cost-effective improvement to G4 had been presented in 2011, called G4(MP2)-6X⁴². This calculation method is reported to have a cost comparable to that of G4(MP2) but performance approaching that of G4.

2.2.3 Enthalpy of Formation Calculations

The basic requirement of an isodesmic reaction is that the number of each bond type is conserved in products and reactants, which leads to the cancellation of systematic errors in the molecular orbital calculations.⁴³ The careful choice of the isodesmic reactions allowed evaluation of enthalpies of formation to accuracies approaching the sum of the uncertainties of the other – often experimental – values involved in the isodesmic

reactions. Taking fluoroethane as an example, the following four isodesmic reactions (Table 2.1) are selected to determine the $\Delta H_{f,298}^{\circ}$ of the target molecule, fluoroethane.

Table 2.1 Isodesmic Reactions and Enthalpy of Formation for Fluoroethane from the Selected Calculation Method

Work Reactions	$\Delta H_{f,298}^{\circ}$ ^a	
$\text{CH}_3\text{CH}_2\text{F} + \text{CH}_4 \rightarrow \text{CH}_3\text{F} + \text{CH}_3\text{CH}_3$	-65.28 ^b	a1
$\text{CH}_3\text{CH}_2\text{F} + \text{CH}_3\text{CH}_3 \rightarrow \text{CH}_3\text{F} + \text{CH}_3\text{CH}_2\text{CH}_3$	-65.51 ^b	a2
$\text{CH}_3\text{CH}_2\text{F} + \text{CH}_3\text{CH}_2\text{CH}_3 \rightarrow \text{CH}_3\text{F} + \text{CH}_3\text{CH}_2\text{CH}_2\text{CH}_3$	-65.41 ^c	a3
$\text{CH}_3\text{CH}_2\text{F} + \text{CH}_3\text{OH} \rightarrow \text{CH}_3\text{F} + \text{CH}_3\text{CH}_2\text{OH}$	-65.50 ^b	a4

^a Unit in kcal mol⁻¹. ^b average of enthalpy of formation of fluoroethane over seven selected calculation methods (CBS-QB3, CBS-APNO, M06, M06-2X, ω B97X, G4, and W1U). ^c average of enthalpy of formation of fluoroethane over six selected calculation methods (CBS-QB3, CBS-APNO, M06, M06-2X, ω B97X, and G4).

Since the $\Delta H_{f,298}^{\circ}$ values of all species but fluoroethane in a1-a4 (Table 2.1) are known, the $\Delta H_{f,298}^{\circ}$ of the target species fluoroethane, is obtained from this data and the calculated $\Delta H_{rxn,298}^{\circ}$. This study has calculated thirty-five $\Delta H_{f,298}^{\circ}$ values (from nine different calculation levels on each of the four isodesmic reactions, a1-a4) are determined for the unknown target molecule, fluoroethane. Several of the evaluated fluorinated hydrocarbons in this study are further used in some of the isodesmic reactions, as reference species so that this study can achieve error cancellation.

The nine computation methods combined with up to twenty-nine work reactions provides several methods to formulate averages for evaluation of the standard enthalpy of formation on the target molecules. (i) Method average: uses the average of the calculation method values for each target molecule over the series of isodesmic reactions. (ii) Selected average: reports the average $\Delta H_{f,298}^{\circ}$ values from the selected set of seven calculation methods (CBS-QB3, CBS-APNO, M06, M06-2X, ω B97X, G4, and W1U) from the

respective isodesmic reaction sets. B3LYP and G4(MP2)-6X are excluded based on the large standard deviation range as shown in Figure 3.1. The selected average enthalpy values are the recommended values and those which have been reported below. (iii) Overall average: the average of all calculated ΔH_{f298}° values from all of the nine calculation levels on the isodesmic reactions.

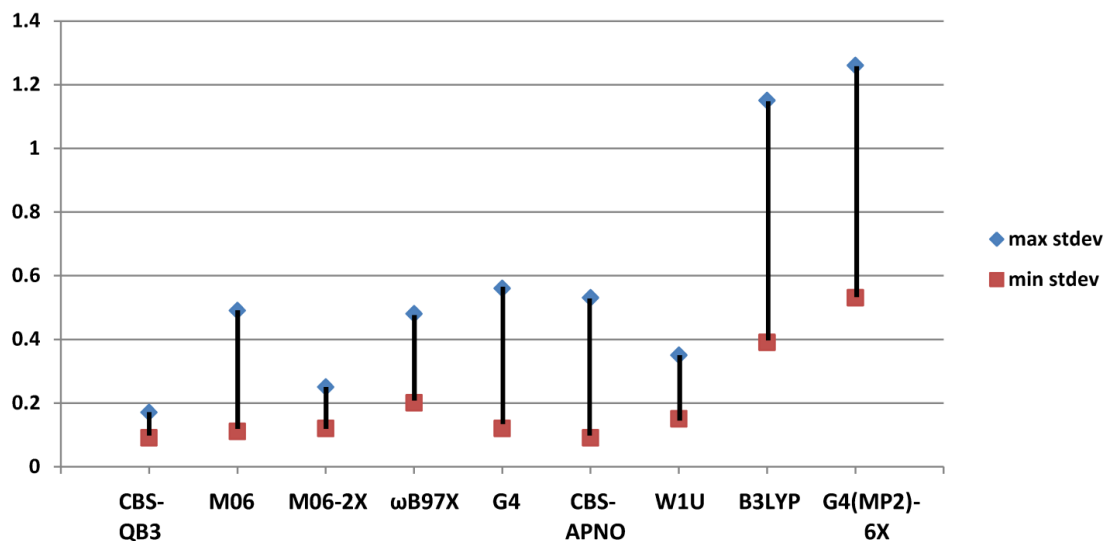


Figure 2.1 Standard deviation range of each calculation method.

This study uses fluoroethane as an example: the method average under B3LYP is the average of four values determined by the four isodesmic reactions using B3LYP, $-65.92 \text{ kcal mol}^{-1}$. The selected method averages for fluoroethane are: CBS-QB3 (-65.28), CBS-APNO (-65.28), M06 (-65.68), M06-2X (-65.42), ω B97X (-65.76), W1U (-65.32), G4(-65.21), G4(MP2)-6X (-65.25) kcal mol^{-1} . The overall average for fluoroethane is the average of all calculated ΔH_{f298}° values from the nine methods over the set of isodesmic reactions, $-65.46 \text{ kcal mol}^{-1}$. The selected average for fluoroethane, which this study recommends for the enthalpy of formation values (from CBS-QB3, CBS-APNO, M06,

M06-2X, ω B97X, G4, and W1U methods over the set of isodesmic reactions) is $-65.42 \text{ kcal mol}^{-1}$.

These averaging methods are used for the fourteen target molecules of this study. The method average enthalpy of formation is initially determined for each method. This study then calculates the selected method average enthalpy of formation from the seven method calculation set. This study notes that in order to have good cancelation of error in the work reactions, this study uses one of the smaller fluorocarbons, as reference species for larger target molecules. Here, the method, selected and overall average enthalpy of formation of the target is then determined using the respective ‘method, selected and overall’ average enthalpy of formation of the reference fluorocarbon.

The isodesmic reactions used for each of the $\text{C}_2 - \text{C}_4$ fluorinated hydrocarbons and their enthalpies of formation are illustrated in the Appendix E Table E.1-E.14. The reference species in the isodesmic reactions are listed in the Appendix Table A along with the uncertainties. This study uses the standard enthalpy of formation for methanol determined by Pedley⁴⁴ as $-48.16 \pm 0.07 \text{ kcal mol}^{-1}$ and not the value recommended in NIST Webbook⁴⁵ ($-49.0 \pm 3.0 \text{ kcal mol}^{-1}$). The calculation for the enthalpy of methanol in this study, $-48.15 \text{ kcal mol}^{-1}$ is in the Appendix E Table E.15.

The uncertainty for the target molecules incorporates: (i) uncertainty of the work reaction calculation method, (ii) the number of work reactions and (iii) uncertainty of the reference species. Uncertainty of the work reaction computational method was derived from analysis of the calculated ΔH_{rxn} for a series of twelve work reactions versus the ΔH_{rxn} of evaluated literature data. Appendix E Table E.16 shows the standard deviation (std) for the twelve work reactions was $0.69 \text{ kcal mol}^{-1}$. This std value was then used in a

Student's t-test for the number of work reactions used for each fluorocarbon at the 95% confidence limit. Separately the sum of three reference species uncertainties for each work reaction of the target molecule was calculated. The std of the two values: (a) calculation method - Student's t-test value and (b) sum reference species uncertainty. The average value of this std over the set of work reactions was calculated and reported as the uncertainty for that species.

As an example four work reactions are used for fluoroethane. The Student's t-test using the std of the twelve reference reactions 0.69, applied for four reactions, resulted in a Student's t-test uncertainty of 1.09 for the work reaction method. The sum or the uncertainties over the three reference species for each of the four work reactions was: 0.1, 0.1, 0.2, 0.1 kcal mol⁻¹. Calculation of the std of these two values, the (a) reaction and t test method and (b) the sum species uncertainty was 1.1, 1.1, 1.2, 1.1 (four work reactions) resulting in an average uncertainty of 1.1 kcal mol⁻¹.

The calculated computational method uncertainty for each molecule is (in kcal mol⁻¹): ±1.09 for CH₃CH₂F, ±0.72 for CH₃CH₂CH₂F, ±0.72 for CH₃CHFCH₃, ±0.53 for CH₃CH₂CH₂CH₂F, ±0.46 for CH₃CHFCH₂CH₃, ±0.64 for CH₂F₂, ±0.49 for CH₂CHF₂, ±0.42 for CH₃CH₂CHF₂, ±0.42 for CH₃CF₂CH₃, ±0.40 for CHF₃, ±0.34 for CH₃CF₃, ±0.30 for CH₃CH₂CF₃, ±0.26 for CF₄, and ±1.09 for (CH₃)₃CF.

2.2.4 Entropy, Heat Capacity, and Internal Rotor Analysis for 14 Fluorinated Hydrocarbons

Entropy and heat capacity contributions as a function of temperature are determined from the calculated structure, moments of inertia, vibration frequencies, symmetry, electron

degeneracy, number of optical isomers, and the known mass of each molecule. The entropies and heat capacities are calculated using the geometry, symmetry, frequencies, and moments of inertia of the B3LYP/6-31+G(d,p) optimized structures. The calculations use standard formulas from statistical mechanics for the contributions of translation, external rotation, and vibrations using the “SMCPS”⁴⁶ program. This program utilizes the rigid-rotor-harmonic oscillator approximation from the frequencies along with moments of inertia from the optimized structures. Contributions from internal rotors using the program “Rotator”⁴⁷ are substituted for contributions from the corresponding internal rotor torsion frequencies. The “Rotator” program calculates the thermodynamic functions from hindered rotations with arbitrary potentials based on the method developed by Krasnoperov, Lay, and Shokhirev⁴⁷. This technique employs expansion of the hindrance potential in the Fourier series, calculation of the Hamiltonian matrix in the basis of the wave functions of free internal rotation, and subsequent calculation of energy levels by direct diagonalization of the Hamiltonian matrix. All potential curves of rotational barrier versus dihedral angle are fit by a cosine curve. In this work, the torsional potential calculated at discrete torsional angles is represented by a truncated ten-parameter Fourier series of the following form:

$$V(\varnothing) = a_0 + \sum_{i=1}^{10} a_i \cos(i\varnothing) + \sum_{j=1}^{10} b_j \cos(j\varnothing) \quad (\text{Eq. 2.1})$$

The values of the coefficients a_i and b_j are calculated to provide the minima and maxima of the torsional potentials with allowance for a shift of the theoretical extreme angular positions.

Vibrational frequencies are scaled by a factor of 0.964 for the B3LYP/6-31+G(d,p) calculation method for the use in calculation of standard entropy and heat capacity based on the computational chemistry comparison and benchmark database⁴⁸.

2.2.5 Group Additivity

Group additivity¹⁰ is a straightforward and reasonably accurate calculation method to estimate thermodynamic properties of hydrocarbons and oxygenated hydrocarbons; ⁴⁹ it is particularly useful for application to larger molecules and in codes or databases for the estimation of thermochemical properties in reaction mechanism generation. Selection of values for the initial groups in a series is critical to development of a group additivity scheme for accurate property estimation. This study updates several fluorocarbon alkane groups from the previous research^{6, 8} in the same research group and develops several new fluorocarbon alkane groups derived from use of thermodynamic property data. Data for the C/C/F/H₂ group is derived from fluoroethane, 1-fluoropropane, and 1-fluorobutane. There are no other halogens or bulky groups/fragments on the carbon atoms adjacent to the carbon atoms containing the fluorine in the defining group. The enthalpy of formation and heat capacities of C/C/F/H₂ is calculated by the average from the following:

$$(\text{CH}_3\text{CH}_2\text{F}) = (\text{C/C/H}_3) + (\text{C/C/F/H}_2) \quad (\text{Eq. 2.2})$$

$$(\text{CH}_3\text{CH}_2\text{CH}_2\text{F}) = (\text{C/C/H}_3) + (\text{C/C}_2\text{/H}_2) + (\text{C/C/F/H}_2) \quad (\text{Eq. 2.3})$$

$$(\text{CH}_3\text{CH}_2\text{CH}_2\text{CH}_2\text{F}) = (\text{C/C/H}_3) + 2(\text{C/C}_2\text{/H}_2) + (\text{C/C/F/H}_2) \quad (\text{Eq. 2.4})$$

The standard entropy of C/C/F/H₂ is calculated from

$$(\text{CH}_3\text{CH}_2\text{F}) = (\text{C/C/H}_3) + (\text{C/C/F/H}_2) - R \ln (\sigma) \quad (\text{Eq. 2.5})$$

$$(\text{CH}_3\text{CH}_2\text{CH}_2\text{F}) = (\text{C}/\text{C}/\text{H}_3) + (\text{C}/\text{C}_2/\text{H}_2) + (\text{C}/\text{C}/\text{F}/\text{H}_2) - R \ln(\sigma) \quad (\text{Eq. 2.6})$$

$$(\text{CH}_3\text{CH}_2\text{CH}_2\text{CH}_2\text{F}) = (\text{C}/\text{C}/\text{H}_3) + 2(\text{C}/\text{C}_2/\text{H}_2) + (\text{C}/\text{C}/\text{F}/\text{H}_2) - R \ln(\sigma) \quad (\text{Eq. 2.7})$$

$R = 1.987 \text{ cal mol}^{-1} \text{ K}^{-1}$ and σ is symmetry number, which is 3 for fluoroethane, 1-fluoropropane, and 1-fluorobutane.

The groups C/C/F/H₂, C/C₂/F/H, C/C/F₂/H, C/C₂/F₂, and C/C/F₃ are also updated in the basis of the well-known accuracy and validity of group additivity for hydrocarbons. For halocarbons with halogen atoms on adjacent atoms interaction terms⁶ are needed to account for intermolecular interactions.

2.3 Results and Discussion

2.3.1 Enthalpy of Fluoromethane

Table 2.2 shows the calculation for enthalpy of fluoromethane via atomization reaction.

Table 2.2 Enthalpies of Formation for Fluoromethane

Compound	This work ^{a,b}	Literature ^b	Δ^b (this study, lit.)
CH ₃ F	-56.3	-56.0 ^c	-0.3
		-56.3 (G3[MP2(full)]) ^d	0.0
		-56.9 (G3) ^d	0.6
		-56.54 ± 0.07 ^e	0.2
		-56.62 ± 0.48 ^f	0.3
		-57.1 ± 0.2 ^g	0.8

^a See Methods for details. ^b Units in kcal mol⁻¹. ^c Chase¹¹. ^d Haworth⁴. ^e Goos¹³. ^f Csontos¹². ^g Kormos¹⁴.

Goos et al.¹³ report an evaluated enthalpy for fluoromethane of $-56.54 \text{ kcal mol}^{-1}$, with uncertainty of ± 0.07 ; this value is $0.24 \text{ kcal mol}^{-1}$ lower energy than the extrapolated CCSD(T) value calculated in this study. This study has used the value of Goos et al.¹³ as a reference species value in the work reactions that provided in this study.

2.3.2 Geometries and Frequencies

The optimized geometries at the B3LYP/6-31+G(d,p) density functional calculation level for $\text{CH}_3\text{CH}_2\text{F}$, $\text{CH}_3\text{CH}_2\text{CH}_2\text{F}$, $\text{CH}_3\text{CHFCH}_3$, $\text{CH}_3\text{CH}_2\text{CH}_2\text{CH}_2\text{F}$, $\text{CH}_3\text{CHFCH}_2\text{CH}_3$, CH_2F_2 , CH_3CHF_2 , $\text{CH}_3\text{CH}_2\text{CHF}_2$, $\text{CH}_3\text{CF}_2\text{CH}_3$, CHF_3 , CH_3CF_3 , $\text{CH}_3\text{CH}_2\text{CF}_3$, CF_4 , and $(\text{CH}_3)_3\text{CF}$ are presented in the Appendix. The Cartesian coordinates (Appendix Table B), vibrational frequencies (Appendix Table C), and moments of inertia (Appendix Table D) are also listed. The structures are shown in Figures F.1-F.14 of the Appendix F.

Trends in C-F single bond lengths are illustrated in Table 2.3, which includes bond lengths from QCISD/6-311G(d,p) optimized geometries in the CBS-APNO calculations. Using the data in Table 2.3, this study compares the B3LYP calculation to the higher-level QCISD calculations. The B3LYP geometries and frequencies follow the same trends as the QCOSD, and the C-F bond lengths optimized by QCISD are approximately 1.5% shorter than optimized by B3LYP. The data also show that primary C-F bonds are shorter than secondary C-F bonds.

Table 2.3 Carbon-Fluorine Bond Length for C2-C4 Fluorinated Hydrocarbons at the B3LYP/6-31+G(d,p) and QCISD/6-311G(d,p) Levels of Theory

	Bond length (C-F) (Å)	
	B3LYP ^b	QCISD ^c
CH ₃ CH ₂ F	1.4104	1.3892
CH ₃ CH ₂ CH ₂ F	1.4116	1.3911
CH ₃ CHFCH ₃	1.4219	1.3978
CH ₃ CH ₂ CH ₂ CH ₂ F	1.4122	1.3912
CH ₃ CHFCH ₂ CH ₃	1.4231	1.3997
CH ₂ F ₂	1.3705 ^a	1.355 ^a
CH ₃ CHF ₂	1.3808 ^a	1.3629 ^a
CH ₃ CH ₂ CHF ₂	1.3810 ^a	1.3635 ^a
CH ₃ CF ₂ CH ₃	1.3914 ^a	1.3716 ^a
CHF ₃	1.3476 ^a	1.3336 ^a
CH ₃ CF ₃	1.3583 ^a	1.3425 ^a
CH ₃ CH ₂ CF ₃	1.3591 ^a	1.3433 ^a
CF ₄	1.3329 ^a	1.3329 ^a
(CH ₃) ₃ CF	1.4335	1.4068

^a Average of all C—F bonds in the molecule. ^b B3LYP/6-31+G(d,p). ^c QCISD/6-311G(d,p).

2.3.3 Enthalpies of Formation of C2-C4 Target Molecules

Isodesmic reaction schemes were used to determine enthalpy of formation of C2-C4 fluorinated hydrocarbons. The work reactions are chosen to have similar bonding on the reactant and product sides in order to have good cancellation of calculation error across the reactions. Table 2.4 lists the method average, the selected average, and the overall average enthalpies for each target molecule. The B3LYP/6-31+G(d,p) and G4(MP2)-6X are consistently a factor of two higher in standard deviation in standard heat of reaction, and were excluded from the selected method.

Table 2.4 also compares the literature enthalpy values for each of the fluorinated hydrocarbons. The recommended values in this work, for CH₃CH₂F, CH₂F₂, CH₃CHF₂, CH₃CH₂CHF₂, CHF₃, CH₃CF₃, CH₃CH₂CF₃, and CF₄ agree with reference data within

their uncertainty, when uncertainty was reported. There are several species with a larger difference from the literature values. The enthalpy of formation of $\text{CH}_3\text{CHFCH}_3$ in this work gives a $5.11 \text{ kcal mol}^{-1}$ lower enthalpy than the value recommended by Pedley⁴⁴. The suggestion enthalpy of $\text{CH}_3\text{CH}_2\text{CH}_2\text{F}$ in this work is near $2.60 \text{ kcal mol}^{-1}$ lower energy than Stull⁵⁰, Frenkel⁵¹ and Yamada's^{6, 8} values. The determination enthalpy of $\text{CH}_3\text{CF}_2\text{CH}_3$ in this work shows a $3.45 \text{ kcal mol}^{-1}$ lower enthalpy than the value presented by Williamson⁵². The evaluation of $(\text{CH}_3)_3\text{CF}$ in this work is $7.31 \text{ kcal mol}^{-1}$ lower energy than Yamada⁶.

Table 2.4 The Method Average under Each Calculation Level and the Overall Average of Enthalpy of Formation of 14 Fluorinated Hydrocarbons and the Differences Between This Calculation with Experimental Reference Values or Literature Reference Values

	$\Delta H_{f,298}^a$								
	B3LYP	CBS-QB3	CBS-APNO	M06	M06-2X	ω B97X	W1U	G4	G4(MP2)-
CH₃CH₂F									
Selected Avg	-65.42 ± 1.11 [0.25] ^b (27) ^c								
Overall Avg	-65.46 [0.36] (35)								
Method Avg	-65.68 (4)	-65.04 (4)	-65.04 (4)	-65.44 (4)	-65.18 (4)	-65.52 (4)	-65.08 (3)	-64.97 (4)	-65.01 (4)
Std. ^b	0.51	0.09	0.09	0.15	0.25	0.23	0.18	0.12	0.55
Literature	-62.90 ± 0.40 ^d , -62.5 ^e , -64.51 ^f , -66.10 ± 1.00 ^g , -65.70 (G3) ^h , -65.20 (G3[MP2(full)]) ^h , -65.06 ⁱ , -65.20 ^j , -66.5 ± 0.4								
CH₃CH₂CH₂F									
Selected Avg	-70.24 ± 1.30 [0.21] ^b (41) ^c								
Overall Avg	-70.19 [0.32] (53)								
Method Avg	-70.08 (6)	-70.07 (6)	-69.93 (6)	-70.16 (6)	-70.00 (6)	-70.15 (6)	-69.89 (5)	-69.76 (6)	-69.51 (6)
Std.	0.41	0.07	0.07	0.11	0.20	0.20	0.14	0.10	0.48
Literature	-68.33 ± 0.55 ^j , -67.20 ^c , -67.83 ^k , -67.37 ^l								
CH₃CHFCH₃									
Selected Avg	-75.26 ± 1.30 [0.20] ^b (41) ^c								
Overall Avg	-75.13 [0.45] (53)								
Method Avg	-74.96 (6)	-75.02 (6)	-74.93 (6)	-75.35 (6)	-74.96 (6)	-75.25 (6)	-74.77 (5)	-74.89 (6)	-73.83 (6)
Std.	0.41	0.07	0.07	0.11	0.20	0.20	0.14	0.10	0.48
Literature	-70.15 ± 0.36 ^j , -75.4 ± 0.5 ^v								
CH₃CH₂CH₂CH₂F									
Selected Avg	-75.17 ± 1.28 [0.21] ^b (54) ^c								
Overall Avg	-75.10 [0.32] (72)								
Method Avg	-74.80 (9)	-75.05 (9)	-74.92 (9)	-74.95 (9)	-74.85 (9)	-74.95 (9)		-74.99 (9)	-74.43 (9)
Std.	0.34	0.09	0.08	0.08	0.18	0.18		0.13	0.32
CH₃CHFCH₂CH₃									
Selected Avg	-80.25 ± 1.28 [0.22] ^b (66) ^c								
Overall Avg	-79.99 [0.49] (88)								
Method Avg	-79.42 (11)	-80.16 (11)	-79.95 (11)	-80.24 (11)	-79.86 (11)	-79.94 (11)		-80.03 (11)	-78.48 (11)
Std.	0.48	0.08	0.08	0.12	0.20	0.22		0.11	0.49
CH₂F₂									
Selected Avg	-108.07 ± 1.46 [0.52] ^b (47) ^c								
Overall Avg	-107.97 [0.72] (61)								
Method Avg	-106.64 (7)	-107.46 (7)	-108.09 (7)	-107.16 (7)	-107.50 (7)	-107.39 (7)	-107.78 (5)	-107.77 (7)	-107.72 (7)
Std.	0.30	0.04	0.04	0.06	0.12	0.15	0.07	0.07	0.26
Literature	-108.08 ± 0.22 ^j , -107.71 ^m , -108.40 (G3) ^h , -107.90 (G3[MP2(full)]) ^h , -107.67 ± 0.48 ⁿ								
CH₃CHF₂									
Selected Avg	-120.87 ± 1.62 [0.30] ^b (68) ^c								
Overall Avg	-120.68 [0.50] (88)								
Method Avg	-119.61 (10)	-120.25 (10)	-120.68 (10)	-120.47 (10)	-120.46 (10)	-120.42 (10)	-120.27 (8)	-120.21 (10)	-119.45 (10)
Std.	0.40	0.05	0.05	0.11	0.16	0.18	0.11	0.08	0.40
Literature	-118.79 ± 2.01 ^j , -119.70 ± 0.07 ^d , -118.80 ^e , -119.29 ^f , -121.30 (G3) ^h , -120.90 (G3[MP2(full)]) ^h , -120.22 ± 0.76 ⁿ , -120.77 ± 1.05 ^o								
CH₃CH₂CHF₂									
Selected Avg	-125.82 ± 1.65 [0.47] ^b (78) ^c								
Overall Avg	-125.51 [0.66] (104)								
Method Avg	-124.07 (13)	-125.18 (13)	-125.47 (13)	-125.30 (13)	-125.23 (13)	-125.07 (13)		-125.93 (13)	-124.01 (13)
Std.	0.40	0.05	0.05	0.11	0.16	0.18		0.08	0.43
Literature	-123.66 ^l								
CH₃CF₂CH₃									
Selected Avg	-133.25 ± 1.65 [0.34] ^b (78) ^c								
Overall Avg	-132.72 [0.87] (104)								
Method Avg	-131.10 (13)	-132.73 (13)	-132.89 (13)	-133.34 (13)	-132.77 (13)	-132.62 (13)		-132.47 (13)	-130.06 (13)
Std.	0.40	0.05	0.05	0.11	0.16	0.18		0.08	0.43
Literature	-129.80 ± 3.00 ^p								

CHF₃									
Selected Avg	-166.71 ± 1.97 [0.73] ^b (93) ^c								
Overall Avg	-166.24 [1.03] (121)								
Method Avg	-162.81	-165.61	-167.36	-165.43	-165.59	-165.09	-166.53	-166.40	-165.30
	(14)	(14)	(14)	(14)	(14)	(14)	(9)	(14)	(14)
Std.	0.27	0.04	0.03	0.06	0.11	0.14	0.06	0.06	0.21
Literature	-166.20 ± 0.65 ^d , -166.72 ± 0.64 ^q , -166.60 ^m , -165.10 ^r , -167.10 (G3) ^h , -166.90 (G3[MP2(full)]) ^h , -166.09 ± 0.48 ^u								
CH₃CF₃									
Selected Avg	-180.51 ± 2.05 [0.51] ^b (119) ^c								
Overall Avg	-179.87 [0.89] (155)								
Method Avg	-176.43	-179.61	-180.85	-179.92	-179.76	-179.03	-179.75	-179.81	-177.58
	(18)	(18)	(18)	(18)	(18)	(18)	(11)	(18)	(18)
Std.	0.33	0.05	0.04	0.08	0.15	0.16	0.10	0.07	0.32
Literature	-177.96 ± 0.41 ^j , -178.20 ± 0.38 ^d , -178.94 ± 0.76 ^s , -178.20 ^e , -178.47 ^j , -181.30 (G3) ^h , -181.00 (G3[MP2(full)]) ^h , -179.61 ± 0.76 ⁿ								
CH₃CH₂CF₃									
Selected Avg	-185.48 ± 2.15 [0.56] ^b (138) ^c								
Overall Avg	-184.73 [0.95] (184)								
Method Avg	-180.96	-184.80	-185.76	-184.92	-184.59	-183.76		-184.89	-182.34
	(23)	(23)	(23)	(23)	(23)	(23)		(23)	(23)
Std.	0.29	0.04	0.04	0.08	0.13	0.14		0.06	0.32
Literature	-183.09 ^l								
CF₄									
Selected Avg	-223.15 ± 2.52 [0.94] ^b (189) ^c								
Overall Avg	-222.12 [1.31] (247)								
Method Avg	-215.77	-221.67	-224.78	-221.40	-221.48	-220.05	-223.12	-223.03	-220.14
	(29)	(29)	(29)	(29)	(29)	(29)	(15)	(29)	(29)
Std.	0.21	0.03	0.03	0.04	0.09	0.11	0.05	0.05	0.16
Literature	-223.14 ± 0.33 ^j , -223.00 ± 0.40 ^q , -221.00 ± 6.00 ^m , -223.10 ± 1.10 ^s , -223.90 (G3) ^h , -223.70 (G3[MP2(full)]) ^h , -223.18 ± 0.31 ^u								
(CH₃)₃CF									
Selected Avg	-85.75 ± 1.71 [0.11] ^b (4) ^c								
Overall Avg	-85.75 [0.11] (4)								
Method Avg		-85.83 (4)	-85.75 (4)					-85.6 (4)	
Std.		0.10	0.11					0.07	
Literature	-81.2, -78.2 ^l , -86.0 ± 2.0 ^v								

^a Units in kcal mol⁻¹. ^b Standard deviation in square brackets. ^c Number of isodesmic reactions used in method average in brackets. ^d Chen⁵³. ^e Stull⁵⁰, ^f Berry⁵⁴, ^g Luo⁵⁵, ^h Haworth⁴, ⁱ Bakowies⁵⁶, ^j Pedley⁴⁴, ^k Frenkel⁵⁷, ^l Yamada⁷, ^m Chase¹¹, ⁿ Nagy⁵, ^o Zachariah⁹, ^p Williamson⁵², ^q Kolesov⁵⁸, ^r Lord⁵⁹, ^s Kolesov⁶⁰, ^t Yamada⁶ (calculated value -81.2, revised to -78.2, see re-revised below). ^u Csontos¹². ^v Kormos¹⁴.

(Selected and Overall values are shown to two decimal places for comparisons; they should be rounded to one decimal for application)

Table 2.5 illustrates the trends in adding carbon atom and separately adding fluorine atoms.

Table 2.5 Change in the Enthalpy of Formation by Inserting One CH₂ Group in the Carbon Chain, and in Replacing An H Atom with A Fluorine Atom

Compound (# of C)	ΔH_{f298}° ^a	$\Delta^{a,b}$	Compound (# of F)	ΔH_{f298}° ^a	$\Delta^{a,b}$
CH ₃ CH ₂ F (2)	-65.42		CH ₂ F ₂ (2)	-108.07	
CH ₃ CH ₂ CH ₂ F (3)	-70.24	4.82	CHF ₃ (3)	-166.71	58.64 ^c
CH ₃ CH ₂ CH ₂ CH ₂ F (4)	-75.17	4.93	CF ₄ (4)	-223.15	56.44 ^c
CH ₃ CHFCH ₃ (3)	-75.26		CH ₃ CH ₂ F (1)	-65.42	
CH ₃ CHFCH ₂ CH ₃ (4)	-80.25	4.99	CH ₃ CHF ₂ (2)	-120.87	55.45 ^c
CH ₃ CHF ₂ (2)	-120.87		CH ₃ CF ₃ (3)	-180.51	59.64 ^c
CH ₃ CH ₂ CHF ₂ (3)	-125.82	4.95	CH ₃ CH ₂ CH ₂ F (1)	-70.24	
CH ₃ CF ₃ (2)	-180.51		CH ₃ CH ₂ CHF ₂ (2)	-125.82	55.58 ^c
CH ₃ CH ₂ CF ₃ (3)	-185.48	4.97	CH ₃ CH ₂ CF ₃ (3)	-185.48	59.66 ^c
			CH ₃ CHFCH ₃ (1)	-75.26	
			CH ₃ CF ₂ CH ₃ (2)	-133.25	57.99 ^d

^aUnits in kcal mol⁻¹. ^bDifference rows. ^c Adding one more fluorine atom to a Primary carbon. ^d To a Secondary carbon.

In the C_xH_(2x+1)F, C_xH_(2x)F₂, and C_xH_(2x-1)F₃ (x ≥ 2) systems, adding one more -CH₂- group lowers the enthalpy of formation approximately 4.9 kcal mol⁻¹, as is the case throughout hydrocarbon group additivity.

The following enthalpy changes are observed for substitution of a fluorine atom for a hydrogen atom on a normal C₂ and higher mono- and di- fluoro carbons. Substitution on a primary fluoro-methyl group, where the fluorine atoms are on the same carbon: (i) the enthalpy of formation decreases 55.5 kcal mol⁻¹ from monofluorocarbon to difluorocarbon; (ii) from difluorocarbon to trifluorocarbon, the enthalpy of formation decreases 59.7 kcal mol⁻¹. Substitution of a fluorine atom for a hydrogen atom on a

secondary carbon group (conversion of a CHF group to a difluorocarbon CF₂ group) lowers the enthalpy 58.0 kcal mol⁻¹. For methane converting from a trifluorocarbon to tetrafluorocarbon, the enthalpy of formation decreases 56.4 kcal mol⁻¹. This study utilizes and discusses these trends further below, where this study develops and revises groups for use in fluorocarbon group estimation for thermochemical properties. Specifically, this study use these -CH₂- insertion and F/H substitution trends to estimate the enthalpy of formation values for several fluoroalkanes: 1-fluoropentane, 2-fluoropentane, 1,1-difluorobutane, 1,1,1-trifluorobutane, 1,1-difluoropentane, 1,1,1-trifluoropentane, 2,2-difluorobutane, and 2,2-difluoropentane in Table 2.6. This study compares the data from these trends to values from group additivity.

This study recommends use of group additivity for thermochemical property estimation, as these trend values are limited to normal alkyl fluorocarbons and cannot be used when the fluorine atoms are on adjacent carbon groups (see group additivity below).

Table 2.6 Enthalpy of Formation for C5 Fluorinated Hydrocarbons Estimated Using the CH₂ Insertion and F/H Substitution Trends, and Comparison to Group Additivity (kcal mol⁻¹)

Molecules	Based on Trend	Group Additivity
CH ₃ CH ₂ CH ₂ CH ₂ CH ₂ F	-80.07	-80.28
CH ₃ CHFCH ₂ CH ₂ CH ₃	-85.25	-85.26
CH ₃ CH ₂ CH ₂ CHF ₂	-130.82	-130.70
CH ₃ CH ₂ CH ₂ CF ₃	-190.48	-190.50
CH ₃ CH ₂ CH ₂ CH ₂ CHF ₂	-135.82	-135.70
CH ₃ CH ₂ CH ₂ CH ₂ CF ₃	-195.48	-195.50
CH ₃ CF ₂ CH ₂ CH ₃	-138.25	-138.25
CH ₃ CF ₂ CH ₂ CH ₂ CH ₃	-143.25	-143.25

2.3.4 Internal Rotor Potential Energy Diagrams

Potential energy profiles for internal rotations in each molecule are calculated at the B3LYP/6-31+G(d,p) density functional level. The potential energy as a function of dihedral angle is calculated by scanning the torsion angles from 0° to 360° at 10° intervals, while allowing the molecule's remaining structural parameters to be optimized. Ten-parameter Fourier series expansions to represent the energy versus rotation angle have been calculated for each of the internal rotors, according to Eq 2.1.

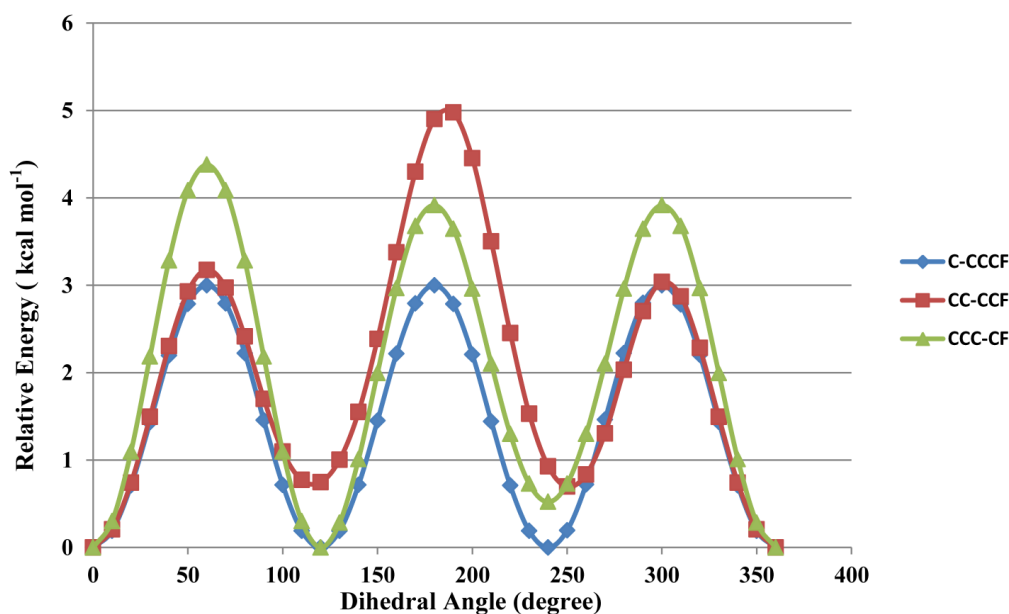


Figure 2.2 Potential energy profiles of the C-CCCF, CC-CCF, and CCC-CF internal rotors for 1-fluorobutane (symbols). The solid line is the fit of the Fourier series expansions.

Figure 2.2 shows the potential energy profiles of the three C–C internal rotors in 1-fluorobutane. The nonuniformity in foldness is due to different gauche interactions, c-c—c-cf and cc-c—c-f. The energy profiles for all target molecules with internal rotors are included in Figures G.1-G.11 of the Appendix G.

2.3.5 Entropy and Heat Capacity

The entropy and heat capacity results using the B3LYP/6-31+G(d,p) geometries (Table B) and frequencies (Table C) are summarized in the Appendix. TVR represents the sum of the contributions from translations, vibrations, and external rotations. IR indicates the contribution from hindered internal rotation, which replaces the torsion frequency contributions for these internal rotors in the TVR heat capacity and entropy data. Table 2.7 lists the entropies and heat capacities compared with literature. The values in this work agree well with the literature data.

Table 2.7 Ideal Gas Phase Entropy and Heat Capacity Obtained by B3LYP/6-31+G(d,p) Calculation, Comparison with Literature

		S_{298}° ^b	C_{p300} ^b	C_{p400}	C_{p500}	C_{p600}	C_{p800}	C_{p1000}	C_{p1500}
CH ₃ F	TVR ^a	53.25	8.97	10.50	12.17	13.72	16.28	18.25	21.37
	Rodgers ^e	53.25	8.99	10.56	12.26	13.84	16.46	18.45	21.56
	Csontos ^l	53.18±0.36							
CH ₃ CH ₂ F	TVR	59.21	12.00	15.22	18.38	21.17	25.66	29.02	34.30
	Internal rotor ^c	4.20	2.06	2.15	2.09	1.97	1.73	1.54	1.28
	total ^d	63.41	14.06	17.37	20.46	23.14	27.38	30.56	35.58
	Stull ^f	63.22	14.17	17.57	20.72	23.44	27.76	30.98	
	Chen ^g	63.34	14.28	17.71	20.86	23.56	27.82	31.00	35.90
	Yamada ^h	63.23	14.23	17.69	20.92	23.69	28.06	31.27	36.16
	CH ₃ CH ₂ CH ₂ F	TVR	63.60	14.84	19.68	24.34	28.41	34.88	39.70
Internal rotor	9.10	4.25	4.10	3.79	3.47	3.00	2.70	2.34	
total	72.70	19.09	23.78	28.12	31.88	37.88	42.41	49.53	
Stull ^f	72.84	19.83	24.55	28.99	32.82	38.88	43.37		
Frenkel ⁱ	72.84	19.71	24.65	29.18	33.02	39.04	43.42		
Yamada ^l	73.39	19.70	24.74	29.35	33.27	39.38	43.82	50.57	
CH ₃ CHFCH ₃	TVR	61.97	15.77	20.51	25.01	28.94	35.21	39.91	47.26
	Internal rotor	8.68	4.19	4.26	4.07	3.80	3.31	2.95	2.48
	total	70.65	19.97	24.78	29.08	32.75	38.52	42.86	49.75
	Yamada ^k	70.24	20.18	25.31	29.85	33.68	39.61	43.96	50.61
	Stull ^f	69.82	19.68	24.72	29.27	33.14	39.14	43.55	
	Frenkel ⁱ	70.03	20.00	25.19	29.71	33.51	39.39	43.81	
	CH ₃ CH ₂ CH ₂ CH ₂ F	TVR	67.59	17.77	24.17	30.29	35.63	44.10	50.38
Internal rotor	16.75	6.90	6.69	6.29	5.85	5.08	4.54	3.80	
total	84.34	25.67	30.85	36.58	41.48	49.18	54.92	63.88	
CH ₃ CHFCH ₂ CH ₃	TVR	65.94	18.73	25.02	30.99	36.18	44.44	50.59	60.15
	Internal rotor	14.55	7.35	6.99	6.48	5.97	5.12	4.54	3.79

	total	80.49	26.07	32.01	37.47	42.15	49.56	55.13	63.94
CH ₂ F ₂	TVR	57.65	10.34	12.26	14.12	15.71	18.14	19.87	22.42
	Rodgers ^e	58.94	10.28	12.22	14.10	15.72	18.22	19.98	22.54
	Csontos ^l	58.87±0.36							
CH ₃ CHF ₂	TVR	63.31	14.22	17.73	20.93	23.64	27.82	30.83	35.42
	Internal rotor	4.25	2.07	2.15	2.09	1.97	1.72	1.54	1.28
	total	67.55	16.29	19.88	23.01	25.61	29.54	32.37	36.69
	Stull ^f	67.52	16.31	19.93	23.07	25.68	29.69	32.56	
	Chen ^g	67.50	16.31	19.93	23.08	25.70	29.70	32.57	36.90
	Yamada ^h	67.34	16.37	20.07	23.32	26.01	30.06	32.92	37.16
CH ₃ CH ₂ CHF ₂	TVR	67.43	17.17	22.22	26.88	30.85	37.01	41.48	48.29
	Internal rotor	10.55	4.38	4.38	4.18	3.91	3.41	3.04	2.53
	total	77.98	21.54	26.60	31.05	34.76	40.42	44.52	50.82
	Yamada ^j	77.51	21.64	26.89	31.51	35.35	41.18	45.33	51.47
CH ₃ CF ₂ CH ₃	TVR	64.17	18.56	23.55	28.01	31.77	37.59	41.85	48.42
	Internal rotor	8.82	4.20	4.22	4.00	3.73	3.24	2.90	2.45
	total	72.99	22.75	27.77	32.01	35.49	40.83	44.74	50.87
	Frenkel ⁱ	72.38	22.87	28.22	32.52	36.34	41.76	45.64	51.42
CHF ₃	TVR	62.20	12.38	14.69	16.65	18.19	20.34	21.73	23.59
	Rodgers ^e	62.04	12.27	14.61	16.59	18.16	20.35	21.76	23.63
	Csontos ^l	61.95±0.36							
CH ₃ CF ₃	TVR	64.53	16.82	20.63	23.82	26.40	30.18	32.79	36.62
	Internal rotor	4.31	2.09	2.14	2.06	1.93	1.69	1.51	1.26
	total	68.84	18.91	22.77	25.89	28.33	31.86	34.29	37.87
	Stull ^f	68.66	18.83	22.75	25.90	28.38	31.98	34.45	
	Chen ^g	68.67	18.84	22.75	25.90	28.38	31.98	34.44	38.00
	Yamada ^h	68.59	18.94	22.89	26.11	28.65	32.29	34.75	38.26
CH ₃ CH ₂ CF ₃	TVR	68.34	19.77	25.11	29.76	33.59	39.35	43.42	49.47
	Internal rotor	10.72	4.38	4.37	4.16	3.88	3.37	3.00	2.51
	total	79.06	24.16	29.48	33.91	37.47	42.72	46.41	51.98
	Yamada ^j	78.79	24.32	29.77	34.32	37.99	43.41	47.15	52.55
CF ₄	TVR	62.73	14.92	17.56	19.52	20.93	22.72	23.71	24.83
	Rodgers ^e	62.46	14.59	14.65	17.30	20.74	22.58	23.61	24.78
	Csontos ^l	62.36±0.36							
(CH ₃) ₃ CF	TVR	67.54	25.39	31.85	37.73	42.79	50.81	65.80	66.20
	Internal rotor	13.29	6.32	6.29	5.92	5.49	4.76	4.26	3.63
	total	80.83	31.71	38.14	43.65	48.28	55.56	61.06	69.83
	Yamada ^j	74.32	26.53	32.87	39.10	44.02	51.47	56.89	65.20

^a Sum of contributions from translations, vibrations, and external rotations. ^b Units in cal mol⁻¹ K⁻¹. ^c Contributions from internal rotors. ^d Sum of TVR and internal rotors. ^e Rodgers⁶¹. ^f Stull⁵⁰. ^g Chen⁵³. ^h Yamada⁸. ⁱ Frenke⁵⁷. ^j Yamada⁶. ^k Yamada⁷. ^l Csontos¹².

2.3.6 Group Additivity

Group Additivity is particularly useful for large molecules where high-level ab initio or density functional calculations are not practical. It represents a molecule's thermochemical properties as the sum of the thermochemical properties of a series of groups. The groups for each target molecule are shown in Table 2.8. The group additivity contributions for 1-fluoropropane are



The additivity contributions for groups C/C/H₃ and C/C₂/H₂ are known as -10.00 and -5.00 kcal mol⁻¹, respectively. The group C/C/F/H₂ is less well-known, however, and has been calculated here, with the results provided in Table 2.9.

$$(-70.24) = (-10.00) + (-5.00) + (\text{C/C/F/H}_2) \quad (\text{Eq. 3.9})$$

Thus, the group additivity contribution of

$$\text{C/C/F/H}_2 = (-70.24) - (-10.00) - (-5.00) = -55.24 \text{ kcal mol}^{-1}$$

On the basis of the estimation of each fluorinated groups, this study estimates up to C₅ fluorinated hydrocarbon system which is illustrated in Table 2.8.

Table 2.8 Composition of Groups for Ten C₂-C₄ Fluorocarbons

	$\text{CH}_3\text{CH}_2\text{F}$	$\text{CH}_3\text{CH}_2\text{CH}_2\text{F}$	$\text{CH}_3\text{CHFCH}_3$	$\text{CH}_3\text{CH}_2\text{CH}_2\text{CH}_2\text{F}$	$\text{CH}_3\text{CHFCH}_2\text{CH}_3$
Group 1	C/C/H ₃	C/C/H ₃	C/C/H ₃	C/C/H ₃	C/C/H ₃
Group 2	C/C/F/H ₂	C/C ₂ /H ₂	C/C ₂ /F/H	C/C ₂ /H ₂	C/C ₂ /F/H
Group 3		C/C/F/H ₂	C/C/H ₃	C/C ₂ /H ₂	C/C ₂ /H ₂
Group 4				C/C/F/H ₂	C/C/H ₃
	CH_3CHF_2	$\text{CH}_3\text{CH}_2\text{CHF}_2$	$\text{CH}_3\text{CF}_2\text{CH}_3$	CH_3CF_3	$\text{CH}_3\text{CH}_2\text{CF}_3$
Group 1	C/C/H ₃	C/C/H ₃	C/C/H ₃	C/C/H ₃	C/C/H ₃
Group 2	C/C/F ₂ /H	C/C ₂ /H ₂	C/C ₂ /F ₂	C/C/F ₃	C/C ₂ /H ₂
Group 3		C/C/F ₂ /H	C/C/H ₃		C/C/F ₃

Table 2.9 Thermodynamic Properties of Related Groups

	ΔH_f° ^a	S_{298}° ^b	C_{p300} ^b	C_{p400}	C_{p500}	C_{p600}	C_{p800}	C_{p1000}	C_{p1500}
C/C/H ₃ ^c	-10.00	30.30	6.19	7.84	9.40	10.79	13.02	14.77	17.58
C/C ₂ /H ₂ ^c	-5.00	9.40	5.50	6.95	8.25	9.35	11.07	12.34	14.20
C/C/F/H ₂ ^d	-55.42	35.23	7.77	9.37	10.90	12.20	14.25	15.71	17.97
C/C/F/H ₂ ^e	-55.24	35.06	7.27	8.81	10.28	11.56	13.65	15.19	17.70
C/C/F/H ₂ ^f	-55.17	37.30	7.32	8.90	10.45	11.78	13.86	15.35	17.84
Avg	-55.28	34.86	7.45	9.03	10.54	11.85	13.92	15.42	17.84
C/C/F/H ₂ ⁿ	-52.90	35.00	8.04	9.85	11.52	12.90	15.04	16.50	18.58
C/C ₂ /F/H ^g	-55.26	12.17	7.49	8.94	10.12	11.01	12.36	13.23	14.54
C/C ₂ /F/H ^h	-55.25	12.57	8.07	9.21	10.23	11.04	12.31	13.14	14.52
Avg	-55.26	12.37	7.78	9.08	10.18	11.03	12.34	13.19	14.53
C/C ₂ /F/H ⁿ	-50.20	13.58	7.62	9.51	10.91	11.93	13.35	14.27	15.52
C/C/F ₂ /H ⁱ	-110.87	39.34	9.95	11.83	13.40	14.62	16.37	17.49	19.07
C/C/F ₂ /H ^j	-110.52	40.31	9.67	11.57	13.16	14.40	16.16	17.29	18.98
Avg	-110.70	39.83	9.81	11.70	13.28	14.51	16.27	17.39	19.03
C/C/F ₂ /H ⁿ	-109.70	39.11	10.18	12.23	13.92	15.22	17.04	18.15	19.58
C/C₂/F₂^k	-113.25	14.50	10.24	11.92	13.03	13.74	14.65	15.10	15.66
C/C ₂ /F ₂ ⁿ	-104.90	17.30	10.49	12.54	13.72	14.76	15.72	16.10	16.26
C/C/F ₃ ^l	-170.51	40.61	12.55	14.72	16.26	17.33	18.69	19.40	20.23
C/C/F ₃ ^m	-170.48	41.37	12.27	14.45	16.02	17.10	18.46	19.18	20.13
Avg	-170.50	40.99	12.41	14.59	16.14	17.22	18.58	19.29	20.18
C/C/F ₃ ⁿ	-168.20	42.55	12.75	15.05	16.71	17.86	19.27	19.98	20.68

^a Units in kcal mol⁻¹. ^b Units in cal mol⁻¹ K⁻¹. ^c Cohen⁶². ^d Derived from fluoroethane. ^e Derived from fluoropropane. ^f Derived from fluorobutane. ^g Derived from 2-fluoropropane. ^h Derived from 2-fluorobutane. ⁱ Derived from 1,1-difluoroethane. ^j Derived from 1,1-difluoropropane. ^k Derived from 2,2-difluoropropane. ^l Derived from 1,1,1-trifluoroethane. ^m Derived from 1,1,1-trifluoropropane. ⁿ Yamada⁶.

2.3.7 Monofluoro to Pentafluoro Ethanes Comparisons and Revaluation of Groups for Fluorocarbons with Fluorine Atoms on Adjacent Carbons

Yamada et al.⁶⁻⁸ used isodesmic work reactions in an earlier study to determine standard enthalpies of monofluoro- to pentafluoro- ethanes. At that time, accurate data for the reference species was limited. This study revisits their work reaction analysis using reference values from this study and the previously reported, "calculated thermal reaction enthalpies", to re-evaluate the heat of formation of the higher multifluoro ethanes. This study compares and tries to improve the accuracy of their data in previous studies^{6, 8}. Current values (this study) are compared with the reported values for their previous paper⁶

and recalculated values from Yamada et al. using reference species data from this study with the previous "calculated thermal reaction enthalpies". Table 2.10 illustrates the re-evaluations of fluoroethane, 1-fluoropropane, and 2-fluoropropane. Heats of formation for these three molecules show agreement with current study, where the differences in standard enthalpies between the revised values and data of the current study are less than 1 kcal mol⁻¹.

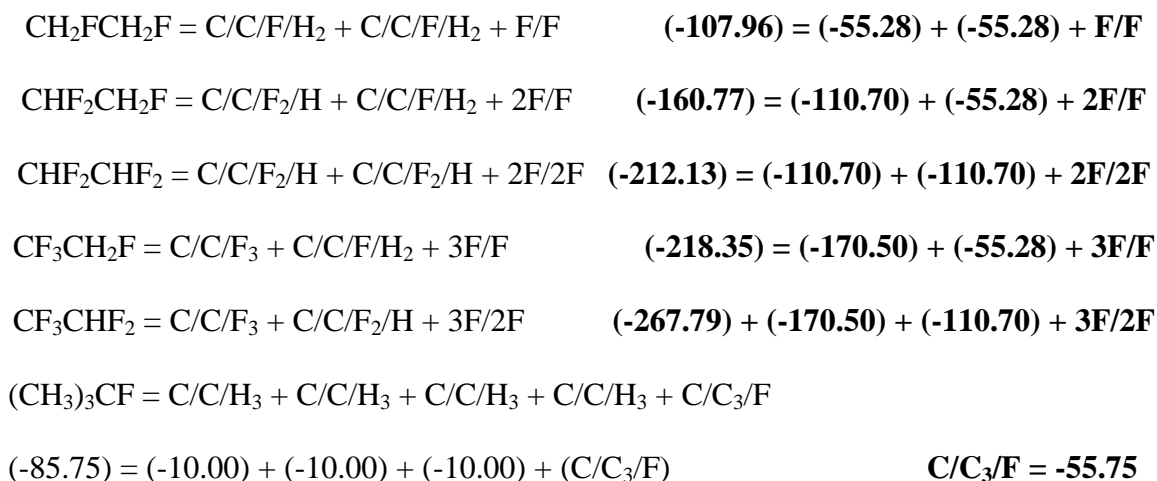
Table 2.10 Re-evaluation of the Enthalpy of Formation from Previous Study

Isodesmic reaction ^a	$\Delta H_{f,298}^b$		
	Revised ^c	Yamada 1999 ^d	this study ^e
$\text{CH}_3\text{CH}_2\text{CH}_2\text{F} + \text{CH}_3\text{CH}_3 = \text{CH}_3\text{CH}_2\text{CH}_3 + \text{CH}_3\text{CH}_2\text{F}$	-70.39	-67.46	-70.24
$\text{CH}_3\text{CH}_2\text{F} + \text{CH}_4 = \text{CH}_3\text{F} + \text{CH}_3\text{CH}_3$	-66.37	-65.61	-65.42
$\text{CH}_3\text{CHFCH}_3 + \text{CH}_3\text{CH}_3 = \text{CH}_3\text{CH}_2\text{CH}_3 + \text{CH}_3\text{CH}_2\text{F}$	-75.48	-72.55	-75.26
$(\text{CH}_3)_3\text{CF} + \text{CH}_3\text{CH}_2\text{CH}_3 = (\text{CH}_3)_3\text{CH} + \text{CH}_3\text{CHFCH}_3$	-85.80	-78.20	-85.75

^a Isodesmic reaction from Yamada⁶. ^b Units in kcal mol⁻¹. Bold (target species) ^c Heat of formation of target molecules calculated with Yamada's⁶ calculated thermal energy and values for reference species from this current study. ^d Yamada⁶. ^e Heat of formation of target molecules selected in this study.

This study further estimates the standard enthalpy for five multifluorinated ethanes in the Yamada et al. articles that were not included in this study but were reported previously using work reaction analysis⁶. The thermal energy of the reactions from the previous study [G2(MP2)] was used to calculate the enthalpy of isodesmic reaction, and the enthalpies of formation for reference species are from this study. This study reinforces the need for fluorine-fluorine non-nearest neighbor interaction (NNi) groups described previously^{6, 8} to be included in the group additivity estimation of fluorocarbons when fluorines are present on adjacent central atoms. This study uses the group values in Table

2.8 and the re-evaluation of the heat of formation of the target molecules in Table 2.11 to re-evaluate the fluorine/fluorine interaction terms. All enthalpies are in kcal mol⁻¹.



Enthalpies of formation for the five multifluoro-ethanes are shown and compared with previously reported values in Table 2.11. The re-evaluated F/F enthalpy interaction terms are presented in Table 2.12 and are compared with previous studies. C/C₃F group is reviewed as of -55.75 kcal mol⁻¹, which present significant different value comparing with Yamada's paper (-48.2 kcal mol⁻¹).

Table 2.11 Enthalpies of Formation: Difluoro- to Pentafluoro- Ethanes

Isodesmic reaction ^a	$\Delta H_{f,298}^b$				
	this study ^c	Yamad a 1999 ^d	Yamad a 1998 ^e	Berry 1998 ^f	Haworth 2000 ^g
CH₂FCH₂F + CH ₃ CH ₃ = CH ₃ CH ₂ F + CH ₃ CH ₂ F	-107.96	-102.7	-106.6	-105.9	-107.3
CHF₂CH₂F + CH ₃ CH ₃ = CH ₃ CHF ₂ + CH ₃ CH ₂ F	-160.77	-156.9	-157.8	-158.5	-161.1
CHF₂CHF₂ + CH ₃ CH ₃ = CH ₃ CHF ₂ + CH ₃ CHF ₂	-212.13	-209.6	-210.1	-209.1	-212.5
CF₃CH₂F + CH ₃ CH ₃ = CF ₃ CH ₃ + CH ₃ CH ₂ F	-218.35	-213.3	-214.1	-215.6	-219.0
CF₃CHF₂ + CH ₃ CH ₃ = CF ₃ CH ₃ + CH ₃ CHF ₂	-267.79	-264.1	-264.0	-264.3	-268.2 ^h

^a Isodesmic reaction from Yamada⁶, reference species this study. ^b Units in kcal mol⁻¹. ^c Heat of formation of target molecules calculated with Yamada's⁶ total energy and reference species values from this study. ^d Yamada⁶. ^e Yamada⁸. ^f Berry² ^g Haworth⁴, G3 calculation method. ^h Haworth⁴, G3[MP2(full)] calculation method. Bold – target molecule, values of this study, recommended.

2.4 Summary

Thermodynamic properties of 14 C1 to C4 fluorocarbons with one to three fluorine atoms on a carbon atom of the molecule are calculated using density functional and ab initio methods with isodesmic reaction schemes for cancellation of calculation errors. Standard enthalpies of formation are determined from the average of CBS-QB3, CBS-APNO, M06, M06-2X, ω B97X, G4, and W1U calculation levels and multiple work reactions. Entropies and heat capacities are determined with B3LYP/6-31+G(d,p) optimized geometries and frequencies. Hindered internal rotation contributions to entropy and heat capacity are calculated by intramolecular torsion potential curves at the B3LYP/6-31+G(d,p) level, with an entropy correction for mixing of rotational conformers. For C2 and higher compounds, adding the second fluorine atom to the primary carbon site leads to about 55 kcal mol⁻¹ energy decrease, whereas adding the third fluorine atom to the primary carbon site reduces the standard enthalpy 59 kcal mol⁻¹. Adding the second fluorine atom to the secondary carbon site lowers the enthalpy 58 kcal mol⁻¹. All calculation methods in the SELECTED appear to work well for work reaction analysis methods for enthalpies of formation of fluorinated hydrocarbons.

CHAPTER 3

THERMOCHEMICAL PROPERTIES ($\Delta_f H^\circ(298\text{ K})$, $S^\circ(298\text{ K})$, $C_p(T)$) AND BOND DISSOCIATION ENERGIES FOR C1-C4 NORMAL HYDROPEROXIDES AND PEROXY RADICALS

3.1 Overview

Several research groups⁶³⁻⁶⁵ have developed molecular beam, mass spectrometry as a direct sampling analytical method for intermediate species from flow reactors studying combustion and oxidation of hydrocarbons relative to ignition and combustion conditions. The resulting analytical measurements in these studies are showing the formation of hydrocarbon radical reactions with oxygen that result in two or three oxygen addition reactions to the hydrocarbon backbone. Intermediate oxygenated hydrocarbons containing several hydroperoxide groups and a ketone moiety have been observed by Crouse et al.⁶⁶ and Di Tommaso et al.⁶⁷ have also observed the intermediates and final products of several oxygen molecule addition reactions to ketone radical under atmospheric conditions. Thermochemical properties, enthalpy, entropy, and heat capacity, for these multi-hydroperoxide, hydrocarbons, ketones, and aldehydes, are needed for the development of the kinetics and reaction mechanisms to understand the chemistry and model these processes.

There are a number of calculated values for the enthalpy of formation data on smaller (C_1 - C_6) alkyl peroxides and the corresponding peroxy radicals, and these values are widely used and applied in modeling combustion⁶⁸⁻⁶⁹, and in atmospheric chemistry⁷⁰. They are also used in understanding oxidation chemistry of organic chemicals to form hydroperoxides for synthesis⁷¹.

They are also used as references to generate Benson¹⁰ group contribution values, which are used to estimate thermochemical data on larger peroxides and peroxy radicals. Accurate formation enthalpies for C₁-C₄ normal hydroperoxides are required to understand reaction paths and assist in the development of detailed chemical kinetic mechanisms, which can be applied to model the oxidation of hydrocarbon species in a variety of environments, particularly for atmospheric and combustion chemistries.

There is, however, a limited set of experimental data on the enthalpy of formation data for these smaller peroxide molecules; to the best knowledge, there are only experimental data on CH₃OOCH₃⁷² and CH₃CH₂OOCH₂CH₃⁷²⁻⁷³. In addition, there is little or no comparison of the experimental data with current theoretical values that are widely used. One objective of this study is to use these reported experimental standard enthalpies as reference values, in calculations using work reactions with similar bonding groups on both sides of the reactions, for both smaller and larger hydroperoxides and compare results with the calculation data in the literature⁷⁴. The good agreement indicates that the experiment data for these peroxides and alkyl hydroperoxy radical (HOO•) as reference species. Enthalpies of formation and bond dissociation energies are among the most useful and widely referenced thermodynamic properties of chemical compounds in the study of gas-phase hydrocarbon chemical oxidation, such as those occurring in atmospheric and combustion conditions.

A number of researchers have worked at the calculating and improving accuracy values on alkyl peroxides and their peroxy radicals over the past several decades. Pedley⁴⁴ suggested -47.54 ± 14.03 kcal mol⁻¹ as enthalpy of formation for CH₃CH₂OOH, which was derived from two reported experimental values: -57.85 ± 14.00 kcal mol⁻¹ in liquid phase

from a study by Stathis⁷⁵, and -47.55 ± 14.04 kcal mol⁻¹ in the gas phase from Egerton⁷⁶. The enthalpy of formation of n-propyl hydroperoxide (CH₃CH₂CH₂OOH) was reported as -76.01 ± 15.00 kcal mol⁻¹ (liquid phase) by Stathis⁷⁵. Burke et al.⁷⁷, have recently published a review on standard enthalpies of formation and standard entropy data on C₁-C₄ species and included C₂-C₄ alkyl peroxide species, however, thermochemistry on methyl peroxide was not discussed.

Current literature values and values calculated in this study for ethyl and propyl hydroperoxides are near -39.0 and -44.0 kcal mol⁻¹ respectively, very different from the data recommended by Pedley⁴⁴.

Recent publications using calculation methods generally show relatively small discrepancies. In Burke et al.'s⁷⁷ review, standard enthalpy values from calculation methods for the enthalpy of formation of CH₃CH₂OOH are (in kcal mol⁻¹): -39.9^{74} , -44.8^{78} , -39.4^{79} , -38.8^{80} , -39.3^{81} , -38.0^{82} , -39.1^{83} , -39.0^{84} ; the enthalpy of formation values for CH₃CH₂CH₂OOH are (in kcal mol⁻¹): -44.8^{78} , -44.1^{81} , -44.8^{83} , -43.3^{84} . (This study further notes here that the value of -44.8 kcal mol⁻¹ for ethyl hydroperoxide CH₃CH₂OOH, was taken from the values of propyl hydroperoxide CH₃CH₂CH₂OOH in error). The uncertainty of the enthalpy of formation for CH₃CH₂OOH and CH₃CH₂CH₂OOH are reported as 14 and 15 kcal mol⁻¹ by Pedley⁴⁴.

The standard enthalpy of formation of methyl hydroperoxide was reported as -31.31 kcal mol⁻¹ from Khursan et al.⁸⁵ and -30.55 ± 0.22 from ATcT. Matthews et al.⁸⁶ determined an enthalpy of formation of -31.0 ± 1 kcal mol⁻¹ based on vibrational overtone excitation experiment. Enthalpy of methyl hydroperoxide from other studies is: -30.7 ± 0.9 by Goldsmith et al.⁸⁴, -30.95 ± 0.22 by Simmie et al.⁸³, -31.8 by Lay et al.⁷⁴, -30.67 by

Sheng et al.⁷⁹, -30.9 ± 0.7 by Blanksby et al.⁸⁷, and -33.0 by Khachatryan et al.⁸⁸, (all in kcal mol^{-1}). Overall the standard enthalpy data, between the respective stable molecules and radicals for the C2 to C4 hydroperoxides and radicals, shows better agreement.

In 2012, Goldsmith et al.⁸⁴, performed calculations on several C₁-C₃ oxy hydrocarbons and has reported standard enthalpies for the radicals: methyl peroxy as 3.3 ± 0.6 , ethyl peroxy as -5.0 ± 0.9 , n-propyl peroxy as -9.8 ± 0.9 kcal mol^{-1} . Older data sources report the enthalpy of formation of methyl peroxy radical ranging from 1.2 kcal mol^{-1} to 6.2 kcal mol^{-1} : 1.2 ⁷⁹ (2002), 2.0 ⁸¹ (2004), 2.1 ⁸⁷ (2001), 2.2 ⁸⁹ (1998), 2.7 ⁹⁰ (1985), 2.9 ⁶² (1996), 2.9 ⁸³ (2008), 5.5 ⁹¹ (1964), 6.2 ⁹² (1979). Standard enthalpy of formation of methyl peroxy in kcal mol^{-1} was reported by Benson⁹¹ as 5.5 ± 3.0 (1964), by Nangia et al.⁹², as 6.2 (1979), by Slagle et al.⁹⁰, as 2.7 ± 0.8 (1985), by Cohen⁶² as 2.9 ± 1.5 (1996), Knyazev et al.⁸⁹, as 2.15 ± 1.22 (1998), by Blanksby et al.⁸⁷, as 2.7 ± 0.7 (2001), by Sebbar et al.⁸¹, as 2.02 ± 0.1 (2004), by Simmie et al.⁸³, as 2.92 ± 0.22 (2008).

In the present work, the formation enthalpies, entropies, and heat capacities of C₁-C₄ normal hydroperoxides and their peroxy radicals based on their most stable rotation conformers have been evaluated using multilevel and single DFT computational chemistry methods. Both Complete Basis set and Gaussian Composite Calculation methods have been used. These methods employ a variety of different geometries, frequency determinations, and higher order energy corrections. Work reactions that employ experimental values for the heat of formation of CH_3OOCH_3 and $\text{CH}_3\text{CH}_2\text{OOCH}_2\text{CH}_3$ as the reference species have been used in order to compute values for the alkyl hydroperoxides and the alkyl hydroperoxy radical. These values were then compared to

literature values computed using atomization energies using work reactions with hydrocarbons and alcohols as reference species.

3.2 Computational Methods

All values reported in this paper are for a standard state of 298 K and 1 atm unless otherwise states. The absence of imaginary frequencies in the computed vibrational frequencies in the optimized geometries verified that all stable structures were true minima at their respective levels of theory. All calculations were performed using the Gaussian 09²⁸ Program. A “j” represents location of radical in this paper. A number of different calculation methods were used.

B3LYP combined the three-parameter Becke exchange functional, B3³³, with LYP Lee-Yang-Parr correlation functional was used with the 6-31+G(d,p) basis set because it has moderate cost and capability of calculating larger molecules. M06-2X³⁷ as a currently popular hybrid meta exchange-correlation functional DFT method was applied with 6-311+G(2d,d,p) basis set. The multilevel calculation Gaussian-4 theory⁴¹, (G4), applied an initial geometry optimization and frequency calculation at the B3LYP/6-31G(2df,p) level. A series of single point correlation energy calculations starting from CCSD(T), then MP4SDTQ, and MP2-Full were employed for higher accuracy. CBS-QB3³⁵ utilized B3LYP/6-311G(2d,d,p) level of theory to optimize geometries and to calculate frequencies, and continually applies CCSD(T), MP4(SDQ), and MP2 level to calculate single point energies. Another composite calculation method, CBS-APNO³⁶ method determines the initial optimized geometry and variational frequencies at the HF/6-311G(d,p) level, followed by a higher-level QCISD/6-311G(d,p) geometry

optimization. A single point energy calculation is then performed at the QCISD(T)/6-311++G(2df,p) level, followed by a procedure that extrapolates the energy to the complete basis set limit.

3.2.1 Enthalpy of Formation

Work reactions are hypothetical reactions for the determination of the enthalpy of formation for target molecules. In this study, each species is optimized at the selected level of calculation, and the energy obtained is used to calculate the enthalpy of reaction of the work reaction. The calculated enthalpy of formation of each work reaction is then used to calculate the enthalpy of formation of the target molecules, where the two products and one reactant are the reference species that have known, evaluated enthalpy of formation from literature.

Enthalpies of formation and bond dissociation energies were determined by averaging selected methods as described below. The standard enthalpies of formation for the species CH_3OOCH_3 and $\text{CH}_3\text{CH}_2\text{OOCH}_2\text{CH}_3$ which are derived using experimental measurements were considered as core reference species, the values are then used to compute values in order to compare with previous published calculated values for C1 and C2 hydroperoxides. This study then uses these recommended values to calculate higher carbon number hydroperoxide targets. For example, the determined value for CH_3OOH ($-30.96\text{kcal mol}^{-1}$) was then used as a reference species in work reactions to calculate $\text{CH}_3\text{CH}_2\text{OOH}$. In the same pattern, CH_3OOH and $\text{CH}_3\text{CH}_2\text{OOH}$ were considered as reference species in work reactions to calculate $\text{CH}_3\text{CH}_2\text{CH}_2\text{OOH}$. C1-C3 peroxide

molecules have been considered in the work reaction analysis for CH₃CH₂CH₂CH₂OOH. The standard enthalpies of formation for the parent molecules from different sets of work reactions are compared and are shown to be consistent. The ethyl peroxy radical, CH₃CH₂OOj, was selected as a core radical in the isodesmic reactions in this study since, based on uniformity of data for its enthalpy of formation throughout the literature.

Table 3.1 illustrates the very small calculated $\Delta_{\text{rxn}}H$ (298 K), consistently less than 1 kcal mol⁻¹, from the work reactions in this study with group balance: a hydroperoxide and a peroxy radical are on each side. This data can also be used to calculate Benson¹⁰ Group increments. The reactions in Table 3.1 involve C1 to C4 carbon peroxy radicals and corresponding hydroperoxides. The small $\Delta_{\text{rxn}}H$ (298 K) indicates that the bond types and energies across each reaction, are similar and consistent with -CH₂- group increases in the carbon chain.

Table 3.1 Calculated $\Delta_{\text{rxn}}H_{298}$ from Work Reactions: Hydroperoxides and Peroxy Radicals

Work reactions	$\Delta_{\text{rxn}}H_{a,b}$
1. CH₃OOj + CH ₃ CH ₂ OOH = CH ₃ OOH + CH₃CH₂OOj	-0.6
2. CH₃CH₂OOj + CH ₃ CH ₂ CH ₂ OOH = CH ₃ CH ₂ OOH + CH₃CH₂CH₂OOj	0.1
3. CH₃CH₂CH₂OOj + CH ₃ CH ₂ CH ₂ CH ₂ OOH = CH ₃ CH ₂ CH ₂ OOH + CH₃CH₂CH₂CH₂OOj	-0.2
4. CH₃CH₂OOj + CH ₃ CH ₂ CH ₂ CH ₂ OOH = CH ₃ CH ₂ OOH + CH₃CH₂CH₂CH₂OOj	-0.1

^a Units in kcal mol⁻¹. ^b Enthalpy of reaction under CBS-APNO calculation level.

Hess's law describes the enthalpy of reaction as below:

$$\Delta_f H_{\text{rxn},298}^\circ = \sum \Delta_f H_{298}^\circ (\text{products}) - \sum \Delta_f H_{298}^\circ (\text{reactants}) \quad (\text{Eq. 3.1})$$

From the first work reaction in Table 3.1,

$$\Delta_f H_{rxn,298}^{\circ}(\text{reaction 1}) = -0.6 = [\Delta_f H_{298}^{\circ}(\text{CH}_3\text{OOH}) + \Delta_f H_{298}^{\circ}(\text{CH}_3\text{CH}_2\text{OOj})] -$$

$$[\Delta_f H_{298}^{\circ}(\text{CH}_3\text{OOj}) + \Delta_f H_{298}^{\circ}(\text{CH}_3\text{CH}_2\text{OOH})] \quad (\text{Eq. 3.2})$$

$$\Delta_1 = [\Delta_f H_{298}^{\circ}(\text{CH}_3\text{OOj}) + \Delta_f H_{298}^{\circ}(\text{CH}_3\text{CH}_2\text{OOj})] = [\Delta_f H_{298}^{\circ}(\text{CH}_3\text{OOH}) -$$

$$\Delta_f H_{298}^{\circ}(\text{CH}_3\text{CH}_2\text{OOH}) - \Delta_f H_{rxn,298}^{\circ}(\text{reaction 1})] = (-30.96) - (-38.94) -$$

$$(-0.6) = 8.85 \text{ kcal/mol} \quad (\text{Eq. 3.3})$$

Δ_1 in equation 3.3 shows the calculated enthalpy difference between methyl peroxy and ethyl peroxy radicals as 8.85 kcal mol⁻¹. This is similar but not equal to the difference between CH₃OH and CH₃CH₂OH 8.5 kcal mol⁻¹. Enthalpies of formation for CH₃OOH and CH₃CH₂OOH are calculated from this study and represent the average value from up to 10 work reactions and three composite calculation methods; see enthalpy data below.

Equation 3.4 uses the enthalpy of formation for CH₃CH₂OOH and CH₃CH₂CH₂OOH calculated from this study (Table 3.5) and the calculated $\Delta_{rxn}H$ above, to calculate Δ_2 , which describes the enthalpy of formation difference between the ethyl peroxy CH₃CH₂OOj and propyl peroxy radicals CH₃CH₂CH₂OOj as 4.99 kcal mol⁻¹. This indicates that the difference of one -CH₂- group is 5 kcal mol⁻¹, which in good agreement with the Benson¹⁰ group values.

By this analogy:

$$\Delta_2 = [\Delta_f H_{298}^{\circ}(\text{CH}_3\text{CH}_2\text{OOj}) - \Delta_f H_{298}^{\circ}(\text{CH}_3\text{CH}_2\text{CH}_2\text{OOj})] = [\Delta_f H_{298}^{\circ}(\text{CH}_3\text{CH}_2\text{OOH}) -$$

$$\Delta_f H_{298}^{\circ}(\text{CH}_3\text{CH}_2\text{CH}_2\text{OOH}) - \Delta_f H_{rxn,298}^{\circ}(\text{reaction 2})] = (-38.94) - (-44.03) -$$

$$(0.1) = 4.99 \text{ kcal/mol} \quad (\text{Eq. 3.4})$$

Equation 3.5 uses the calculated enthalpy of formation for CH₃CH₂CH₂OOH and CH₃CH₂CH₂CH₂OOH (Table 3.5) and $\Delta_{rxn}H$ above for Δ_3 , which describes the enthalpy of formation difference between the propyl peroxy, CH₃CH₂CH₂OOj, and the butyl peroxy

radicals $\text{CH}_3\text{CH}_2\text{CH}_2\text{CH}_2\text{OOj}$ is $5.01 \text{ kcal mol}^{-1}$. This again supports the difference for insertion of one $-\text{CH}_2-$ group as near 5 kcal mol^{-1} .

$$\begin{aligned}\Delta_3 &= [\Delta_f H_{298}^\circ(\text{CH}_3\text{CH}_2\text{CH}_2\text{OOj}) - \Delta_f H_{298}^\circ(\text{CH}_3\text{CH}_2\text{CH}_2\text{CH}_2\text{OOj})] \\ &= [\Delta_f H_{298}^\circ(\text{CH}_3\text{CH}_2\text{CH}_2\text{OOH}) - \Delta_f H_{298}^\circ(\text{CH}_3\text{CH}_2\text{CH}_2\text{CH}_2\text{OOH}) \\ &\quad - \Delta_f H_{rxn,298}^\circ(\text{reaction 3})] \\ &= (-44.03) - (-48.85) - (-0.2) = 5.02 \text{ kcal/mol} \quad (\text{Eq. 3.5})\end{aligned}$$

Δ_4 in equation 3.6 describes the enthalpy of formation difference between the two carbon peroxy radical $\text{CH}_3\text{CH}_2\text{OOj}$ and four carbon peroxy radical $\text{CH}_3\text{CH}_2\text{CH}_2\text{CH}_2\text{OOj}$ as $10.01 \text{ kcal mol}^{-1}$. This indicates that the difference for insertion of two $-\text{CH}_2-$ group is near $10.0 \text{ kcal mol}^{-1}$, two $-\text{CH}_2-$ groups which agrees with the Benson's group values.

$$\begin{aligned}\Delta_4 &= [\Delta_f H_{298}^\circ(\text{CH}_3\text{CH}_2\text{OOj}) - \Delta_f H_{298}^\circ(\text{CH}_3\text{CH}_2\text{CH}_2\text{CH}_2\text{OOj})] = \\ &[\Delta_f H_{298}^\circ(\text{CH}_3\text{CH}_2\text{OOH}) - \Delta_f H_{298}^\circ(\text{CH}_3\text{CH}_2\text{CH}_2\text{CH}_2\text{OOH}) - \Delta_f H_{rxn,298}^\circ(\text{reaction 4})] = \\ &(-38.94) - (-48.85) - (-0.1) = 10.01 \text{ kcal/mol} \quad (\text{Eq. 3.6})\end{aligned}$$

The enthalpies of formation for stable molecules were established from up to ten work reactions where the enthalpies of reaction were calculated from total energies with the CBS-APNO calculation method.

The enthalpy of formation differences were calculated between sets of two radicals as shown below:

CH_3OOj and $\text{CH}_3\text{CH}_2\text{OOj}$	$\Delta_1 = 8.85 \text{ kcal mol}^{-1}$
$\text{CH}_3\text{CH}_2\text{OOj}$ and $\text{CH}_3\text{CH}_2\text{CH}_2\text{OOj}$	$\Delta_2 = 4.99 \text{ kcal mol}^{-1}$
$\text{CH}_3\text{CH}_2\text{CH}_2\text{OOj}$ and $\text{CH}_3\text{CH}_2\text{CH}_2\text{CH}_2\text{OOj}$	$\Delta_3 = 5.02 \text{ kcal mol}^{-1}$
$\text{CH}_3\text{CH}_2\text{OOj}$ and $\text{CH}_3\text{CH}_2\text{CH}_2\text{CH}_2\text{OOj}$	$\Delta_4 = 10.01 \text{ kcal mol}^{-1}$

The enthalpy relationships between each radical set were observed using these differences while the absolute value of each radical was omitted.

The consistent differences corresponding to difference in number of carbons atoms between the carbon sequence delta enthalpy values implied accuracy for the energy calculation and enthalpy of formation of both the stable molecules and the peroxy radicals. The homolytic bond dissociation energies determined from a parent molecule and the corresponding radical were determined as follows:

$$D(ROO - H) = \Delta_f H^\circ(ROOj) + \Delta_f H^\circ(H) - \Delta_f H^\circ(ROOH) \quad (\text{Eq. 3.7})$$

$$D(RO - OH) = \Delta_f H^\circ(ROj) + \Delta_f H^\circ(OH) - \Delta_f H^\circ(ROOH) \quad (\text{Eq. 3.8})$$

$$D(R - OOH) = \Delta_f H^\circ(Rj) + \Delta_f H^\circ(OOH) - \Delta_f H^\circ(ROOH) \quad (\text{Eq. 3.9})$$

$$D(RO - Oj) = \Delta_f H^\circ(ROj) + \Delta_f H^\circ(O) - \Delta_f H^\circ(ROOj) \quad (\text{Eq. 3.10})$$

$$D(R - OOj) = \Delta_f H^\circ(Rj) + \Delta_f H^\circ(O_2) - \Delta_f H^\circ(ROOj) \quad (\text{Eq. 3.11})$$

The uncertainty for the target molecules incorporated:

- (i) the uncertainty of the work reaction calculation method,
- (ii) the number of work reactions,
- (iii) the uncertainty of the reference species.

Uncertainty of the work reaction computational method was derived from analysis of calculated $\Delta_f H_{\text{rxn}}$ for a series of 16 work reactions versus $\Delta_f H_{\text{rxn}}$ of evaluated literature data. The uncertainty method is fully described in a previous study. Appendix Table E.17 shows the root-mean-square for the 16 work reactions was $0.44 \text{ kcal mol}^{-1}$. The Student's t-test was applied to values from sets of work reactions to determine the 95% confidence limits. The uncertainty for each species in each work reaction have been included to

determine the uncertainty for target species in each reaction. The average values of these uncertainties have been reported as the uncertainty for that species.

3.2.2 Entropy and Heat Capacity

Potential energy profiles for internal rotors to determine the lowest energy conformer were obtained by scanning the torsion angles from 0° to 360° at 10° intervals. In this work, rotational conformers related to RC-OOR', RO-OR', RC-CR' are studied to find the lowest energy conformer and to use the internal rotor potential for calculation of entropy and heat capacity contributions from internal rotors. Zero point vibration energies are scaled by a factor of 0.964⁴⁸ for the B3LYP/6-31+G(d,p) calculation method for the use in calculation of standard entropy and heat capacity. All rotors are re-scanned once a lower energy conformer is found, relative to the initial low energy conformer, until the lowest energy structure is found. S°_{298} and $C_p(T)$ values for each molecule are calculated using the program SMCPS⁴⁶; S°_{298} and $C_p(T)$ values contributions from all internal rotors are explicitly evaluated using the program Rotator⁴⁷. Entropy and heat capacity as a function of temperature are determined from the lowest energy conformer structure, moments of inertia, vibration frequencies, internal rotor potentials, symmetry, electron degeneracy, number of optical isomers and molecular mass. The SMCPS program uses the rigid-rotor-harmonic approximation from the frequencies along with moments of inertia from the optimized B3LYP/6-31+G(d,p) level. Rotator employs ten-parameter Fourier series expansions to represent the energy versus rotation dihedral angles in following form:

$$V(\phi) = a_0 + \sum_{i=1}^{10} a_i \cos(i\phi) + \sum_{j=1}^{10} b_j \cos(j\phi) \quad (\text{Eq. 3.12})$$

$$a_0 = \frac{\sum_{i=1}^m f_i}{m} \quad (\text{Eq. 3.13})$$

$$a_i = \frac{\sum_{i=1}^m f_i \cos(n\theta)}{m} \quad (\text{Eq. 3.14})$$

$$b_j = \frac{\sum_{i=1}^m f_i \sin(n\theta)}{m} \quad (\text{Eq. 3.15})$$

The value of a_i and b_j are calculated to provide the minima and maxima of the torsional potentials with allowance for a shift of the theoretical extreme angular positions. Internal rotor torsion frequencies are omitted from the SMCPS frequency sets and contributions are added separately.

3.3 Results and Discussion

3.3.1 Geometries

The optimized geometries at the B3LYP/6-31+G(d,p) density functional calculation level for each of the target molecules are in Appendix. The Cartesian coordinates are listed in Appendix Table B, vibrational frequencies in Appendix Table C, moments of inertia in Appendix Table D. The structures are shown in Figures F.15-F.22 of the Appendix F. The HOMO (Highest Occupied Molecular Orbital) demonstration of C1-C4 peroxide molecule and their peroxy radicals are shown in Figure H.1-H.4 of the Appendix H.

Data for reference species in work reactions are listed in Appendix Table A.

Table 3.2 Comparison of Major Bond Lengths and Dihedral Angles Between Each Target

ROOH	CH ₃ OOH	CH ₃ CH ₂ OOH	CH ₃ CH ₂ CH ₂ OOH	CH ₃ CH ₂ CH ₂ CH ₂ OOH
B(R-O) ^a	1.41970	1.42951	1.43011	1.42842
B(O-O)	1.46163	1.46283	1.46342	1.46070
B(O-H)	0.97095	0.97060	0.97068	0.97096
D(RO-OH) ^b	128.6	126.1	124.1	123.6

ROOj	CH₃OOj	CH₃CH₂OOj	CH₃CH₂CH₂OOj	CH₃CH₂CH₂CH₂OOj
B(R-O)	1.45124	1.46474	1.46561	1.46592
B(O-O)	1.32336	1.32365	1.32393	1.32379
D(OO-CC)		74.9	73.8	74.2

^a "B" stand for bond length in Å. ^b "D" stands for dihedral angle in degree.

Table 3.2 summarizes the important geometry information. Removing one hydrogen to get the peroxy radical makes R-O bond 3% longer and decreases O-O bond by 10%. Typical dihedral angle of RO-OH is ~125 degrees.

3.3.2 Enthalpies of Formation for C1-C4 Stable Molecules

Enthalpies of formation for CH₃OOH, CH₃CH₂OOH, CH₃CH₂CH₂OOH, CH₃CH₂CH₂CH₂OOH were evaluated using the sets of work reactions listed in Table 3.3. Values in bold are the recommendations for each target compound in this study and consist of the average of enthalpies of formation calculated with CBS-QB3, CBS-APNO, and G4 methods. M06-2X/6-311+G(2d,d,p) has been excluded based on its consistent, relatively high standard deviations, which were two or more times higher than three composite method calculations.

Enthalpies of formation for the C2-C4 hydroperoxides were further calculated using a second set of work reactions in order to further examine accuracy and consistency of this study's calculations. The data are presented in Table 3.5. The calculations used the compounds listed in Table 3.4 as reference species data from this second set of calculations are compared with the first work reaction results in Table 3.3 and the available literature. The enthalpy of formation of CH₃OOH was determined as -30.96 kcal mol⁻¹ which was in a good agreement with experimental analysis -31.0 kcal mol⁻¹. The standard enthalpy

values of target compounds from two sets of work reactions are identical. Enthalpies of formation along with uncertainty of all four compound are in good agreement with available literature. See Table 3.5.

Table 3.3 Work Reactions and Heat of Formation for C1-C4 Alkyl Hydroperoxides

Work reactions	$\Delta_f H^\circ_{298}$ ^a			
	CBS-QB3	M06-2X	G4	CBS-AP NO
CH₃OOH + CH ₄ = HOOH + CH ₃ CH ₃	-31.23	-31.36	-31.00	-30.67
CH₃OOH + CH ₃ CH ₃ = HOOH + CH ₃ CH ₂ CH ₃	-31.28	-32.03	-30.97	-30.74
CH₃OOH + CH ₃ CH ₂ CH ₃ = HOOH + CH ₃ CH ₂ CH ₂ CH ₃	-31.18	-31.17	-30.90	-30.66
CH₃OOH + CH ₃ CH ₂ CH ₂ CH ₃ = HOOH + CH ₃ CH ₂ CH ₂ CH ₂ CH ₃	-31.28	-32.60	-30.82	-30.76
CH₃OOH + CH ₃ CH ₂ CH ₃ = CH ₃ OOCH ₃ + CH ₃ CH ₃	-30.53	-29.89	-31.09	-31.24
CH₃OOH + CH ₃ CH ₂ CH ₂ CH ₃ = CH ₃ OOCH ₃ + CH ₃ CH ₂ CH ₃	-30.62	-30.76	-31.16	-31.32
CH₃OOH + CH ₃ CH ₂ CH ₂ CH ₃ = CH ₃ CH ₂ OOCH ₂ CH ₃ + CH ₄	-30.62	-31.36	-30.95	-31.18
CH₃OOH + CH ₃ CH ₂ CH ₂ CH ₂ CH ₃ = CH ₃ CH ₂ OOCH ₂ CH ₃ + CH ₃ CH ₃	-30.57	-30.11	-31.13	-31.09
Average by method	-30.91	-31.16	-31.00	-30.96
Method Average of Three ^b		-30.96		
Method Average of Four ^c		-31.01		
Standard Deviation	0.35	0.91	0.12	0.28
CH₃CH₂OOH + CH ₄ = HOOH + CH ₃ CH ₂ CH ₃	-39.19	-39.72	-39.20	-38.61
CH₃CH₂OOH + CH ₃ CH ₃ = HOOH + CH ₃ CH ₂ CH ₂ CH ₃	-39.15	-39.53	-39.10	-38.60
CH₃CH₂OOH + CH ₃ CH ₂ CH ₃ = HOOH + CH ₃ CH ₂ CH ₂ CH ₂ CH ₃	-39.15	-40.10	-38.96	-38.62
CH₃CH₂OOH = CH ₃ OOCH ₃	-38.49	-38.26	-39.29	-39.18
CH₃CH₂OOH + CH ₃ CH ₂ CH ₃ = CH ₃ CH ₂ OOCH ₂ CH ₃ + CH ₄	-38.49	-38.86	-39.09	-39.04
CH₃CH₂OOH + CH ₃ CH ₂ CH ₂ CH ₃ = CH ₃ CH ₂ OOCH ₂ CH ₃ + CH ₃ CH ₃	-38.53	-39.05	-39.19	-39.05
CH₃CH₂OOH + CH ₃ CH ₂ CH ₂ CH ₂ CH ₃ = CH ₃ CH ₂ OOCH ₂ CH ₃ + CH ₃ CH ₂ CH ₃	-38.53	-38.48	-39.33	-39.03
Average by method	-38.79	-39.14	-39.17	-38.87
Method Average of Three ^b		-38.94		
Method Average of Four ^c		-38.99		
Standard Deviation	0.35	0.67	0.13	0.25
CH₃CH₂CH₂OOH + CH ₄ = HOOH + CH ₃ CH ₂ CH ₂ CH ₃	-44.42	-44.60	-43.96	-43.71
CH₃CH₂CH₂OOH + CH ₃ CH ₃ = HOOH + CH ₃ CH ₂ CH ₂ CH ₂ CH ₃	-44.48	-45.85	-43.79	-43.80

$\text{CH}_3\text{CH}_2\text{CH}_2\text{OOH} + \text{CH}_4 = \text{CH}_3\text{OOCH}_3 + \text{CH}_3\text{CH}_3$	-43.77	-43.32	-44.15	-44.29
$\text{CH}_3\text{CH}_2\text{CH}_2\text{OOH} + \text{CH}_3\text{CH}_3 = \text{CH}_3\text{OOCH}_3 + \text{CH}_3\text{CH}_2\text{CH}_3$	-43.82	-44.00	-44.12	-44.37
$\text{CH}_3\text{CH}_2\text{CH}_2\text{OOH} + \text{CH}_3\text{CH}_2\text{CH}_3 = \text{CH}_3\text{OOCH}_3 + \text{CH}_3\text{CH}_2\text{CH}_2\text{CH}_3$	-43.73	-43.13	-44.06	-44.28
$\text{CH}_3\text{CH}_2\text{CH}_2\text{OOH} + \text{CH}_3\text{CH}_2\text{CH}_2\text{CH}_3 = \text{CH}_3\text{OOCH}_3 + \text{CH}_3\text{CH}_2\text{CH}_2\text{CH}_2\text{CH}_3$	-43.82	-44.57	-43.98	-44.38
$\text{CH}_3\text{CH}_2\text{CH}_2\text{OOH} + \text{CH}_3\text{CH}_3 = \text{CH}_3\text{CH}_2\text{OOCH}_2\text{CH}_3 + \text{CH}_4$	-43.82	-44.60	-43.92	-44.22
$\text{CH}_3\text{CH}_2\text{CH}_2\text{OOH} + \text{CH}_3\text{CH}_2\text{CH}_3 = \text{CH}_3\text{CH}_2\text{OOCH}_2\text{CH}_3 + \text{CH}_3\text{CH}_3$	-43.77	-43.93	-43.95	-44.15
$\text{CH}_3\text{CH}_2\text{CH}_2\text{OOH} + \text{CH}_3\text{CH}_2\text{CH}_2\text{CH}_3 = \text{CH}_3\text{CH}_2\text{OOCH}_2\text{CH}_3 + \text{CH}_3\text{CH}_2\text{CH}_3$	-43.86	-44.79	-44.02	-44.23
$\text{CH}_3\text{CH}_2\text{CH}_2\text{OOH} + \text{CH}_3\text{CH}_2\text{CH}_2\text{CH}_2\text{CH}_3 = \text{CH}_3\text{CH}_2\text{OOCH}_2\text{CH}_3 + \text{CH}_3\text{CH}_2\text{CH}_2\text{CH}_3$	-43.76	-43.36	-44.10	-44.13
Average by method	-43.92	-44.22	-44.00	-44.16
Method Average of Three ^b			-44.03	
Method Average of Four ^c			-44.08	
Standard Deviation	0.28	0.83	0.11	0.23
$\text{CH}_3\text{CH}_2\text{CH}_2\text{CH}_2\text{OOH} + \text{CH}_4 = \text{HOOH} + \text{CH}_3\text{CH}_2\text{CH}_2\text{CH}_2\text{CH}_3$	-49.27	-49.90	-48.66	-48.58
$\text{CH}_3\text{CH}_2\text{CH}_2\text{CH}_2\text{OOH} + \text{CH}_4 = \text{CH}_3\text{OOCH}_3 + \text{CH}_3\text{CH}_2\text{CH}_3$	-48.62	-48.06	-49.00	-49.15
$\text{CH}_3\text{CH}_2\text{CH}_2\text{CH}_2\text{OOH} + \text{CH}_3\text{CH}_3 = \text{CH}_3\text{OOCH}_3 + \text{CH}_3\text{CH}_2\text{CH}_2\text{CH}_3$	-48.57	-47.87	-48.90	-49.14
$\text{CH}_3\text{CH}_2\text{CH}_2\text{CH}_2\text{OOH} + \text{CH}_3\text{CH}_2\text{CH}_3 = \text{CH}_3\text{OOCH}_3 + \text{CH}_3\text{CH}_2\text{CH}_2\text{CH}_2\text{CH}_3$	-48.57	-48.44	-48.75	-49.16
$\text{CH}_3\text{CH}_2\text{CH}_2\text{CH}_2\text{OOH} = \text{CH}_3\text{CH}_2\text{OOCH}_2\text{CH}_3$	-48.61	-48.66	-48.79	-49.01
Average by method	-48.73	-48.59	-48.82	-49.01
Method Average of Three ^b			-48.85	
Method Average of Four ^c			-48.79	
Standard Deviation	0.30	0.80	0.13	0.24

^a Units in kcal mol⁻¹. ^b Calculation levels include CBS-QB3, G4, CBS-APNO, and the recommended values in this study. ^c The four calculation levels.

Table 3.4 Work Reactions and Heat of Formation Using Enthalpy Values of CH₃OOH, CH₃CH₂OOH from Above as Reference Species

Isodesmic reactions	$\Delta_f H^\circ_{298}$ ^a			
	CBS-QB3	M06-2X	G4	CBS-APNO
$\text{CH}_3\text{CH}_2\text{OOH} + \text{CH}_4 = \text{CH}_3\text{OOH} + \text{CH}_3\text{CH}_3$	-38.87	-38.64	-39.19	-38.83
$\text{CH}_3\text{CH}_2\text{OOH} + \text{CH}_3\text{CH}_3 = \text{CH}_3\text{OOH} + \text{CH}_3\text{CH}_2\text{CH}_3$	-38.92	-39.32	-39.16	-38.90
$\text{CH}_3\text{CH}_2\text{OOH} + \text{CH}_3\text{CH}_2\text{CH}_3 = \text{CH}_3\text{OOH} + \text{CH}_3\text{CH}_2\text{CH}_2\text{CH}_3$	-38.83	-38.45	-39.10	-38.82
$\text{CH}_3\text{CH}_2\text{OOH} + \text{CH}_3\text{CH}_2\text{CH}_2\text{CH}_3 = \text{CH}_3\text{OOH} + \text{CH}_3\text{CH}_2\text{CH}_2\text{CH}_2\text{CH}_3$	-38.92	-39.89	-39.02	-38.92
$\text{CH}_3\text{CH}_2\text{OOH} + \text{HOOH} = 2 \text{CH}_3\text{OOH}$	-38.60	-38.25	-39.15	-39.12

Average by method	-38.83	-38.91	-39.12	-38.92
Method Average of Three ^b			-38.96	
Method Average of Four ^c			-38.95	
Standard Deviation	0.05	0.66	0.08	0.05
CH₃CH₂CH₂OOH + HOOH = CH ₃ OOH + CH ₃ CH ₂ OOH	-43.96	-43.62	-43.77	-44.35
CH₃CH₂CH₂OOH + CH ₄ = CH ₃ OOH + CH ₃ CH ₂ CH ₃	-44.20	-44.39	-44.02	-44.01
CH₃CH₂CH₂OOH + CH ₃ CH ₃ = CH ₃ OOH + CH ₃ CH ₂ CH ₂ CH ₃	-44.16	-44.20	-43.93	-44.01
CH₃CH₂CH₂OOH + CH ₃ CH ₂ CH ₃ = CH ₃ OOH + CH ₃ CH ₂ CH ₂ CH ₃	-44.16	-44.77	-43.78	-44.02
CH₃CH₂CH₂OOH + CH ₄ = CH ₃ CH ₂ OOH + CH ₃ CH ₃	-44.22	-44.01	-43.80	-44.05
CH₃CH₂CH₂OOH + CH ₃ CH ₃ = CH ₃ CH ₂ OOH + CH ₃ CH ₂ CH ₃	-44.27	-44.69	-43.77	-44.13
CH₃CH₂CH₂OOH + CH ₃ CH ₂ CH ₃ = CH ₃ CH ₂ OOH + CH ₃ CH ₂ CH ₂ CH ₃	-44.18	-43.82	-43.71	-44.05
CH₃CH₂CH₂OOH + CH ₃ CH ₂ CH ₂ CH ₃ = CH ₃ CH ₂ OOH + CH ₃ CH ₂ CH ₂ CH ₂ CH ₃	-44.28	-45.26	-43.63	-44.15
Average by method	-44.18	-44.35	-43.80	-44.10
Method Average of Three ^b			-44.02	
Method Average of Four ^c			-44.11	
Standard Deviation	0.10	0.54	0.12	0.11
CH₃CH₂CH₂CH₂OOH + HOOH = 2 CH ₃ CH ₂ OOH	-48.82	-47.97	-48.39	-49.25
CH₃CH₂CH₂CH₂OOH + CH ₄ = CH ₃ OOH + CH ₃ CH ₂ CH ₂ CH ₃	-48.95	-48.26	-48.80	-48.79
CH₃CH₂CH₂CH₂OOH + CH ₃ CH ₃ = CH ₃ OOH + CH ₃ CH ₂ CH ₂ CH ₂ CH ₃	-49.00	-49.51	-48.62	-48.88
CH₃CH₂CH₂CH₂OOH + CH ₄ = CH ₃ CH ₂ OOH + CH ₃ CH ₂ CH ₂ CH ₃	-49.07	-48.75	-48.65	-48.91
CH₃CH₂CH₂CH₂OOH + CH ₃ CH ₃ = CH ₃ CH ₂ OOH + CH ₃ CH ₂ CH ₂ CH ₃	-49.02	-48.56	-48.55	-48.90
CH₃CH₂CH₂CH₂OOH + CH ₃ CH ₂ CH ₃ = CH ₃ CH ₂ OOH + CH ₃ CH ₂ CH ₂ CH ₂ CH ₃	-49.03	-49.13	-48.40	-48.92
CH₃CH₂CH₂CH₂OOH + CH ₄ = CH ₃ CH ₂ CH ₂ OOH + CH ₃ CH ₃	-48.83	-48.09	-48.91	-48.81
CH₃CH₂CH₂CH₂OOH + CH ₃ CH ₃ = CH ₃ CH ₂ CH ₂ OOH + CH ₃ CH ₂ CH ₃	-48.88	-48.77	-48.88	-48.89
CH₃CH₂CH₂CH₂OOH + CH ₃ CH ₂ CH ₃ = CH ₃ CH ₂ CH ₂ OOH + CH ₃ CH ₂ CH ₂ CH ₃	-48.78	-47.90	-48.81	-48.81
CH₃CH₂CH₂CH₂OOH + CH ₃ CH ₂ CH ₂ CH ₃ = CH ₃ CH ₂ CH ₂ OOH + CH ₃ CH ₂ CH ₂ CH ₂ CH ₃	-48.88	-49.34	-48.73	-48.91
Average by method	-48.93	-48.63	-48.67	-48.91
Method Average of Three ^b			-48.84	
Method Average of Four ^c			-48.78	
Standard Deviation	0.10	0.57	0.18	0.13

^a Units in kcal mol⁻¹. ^b Calculation levels include CBS-QB3, G4, CBS-APNO. ^c All four calculation levels.

Table 3.5 Comparison of Calculated $\Delta_f H_{298}^\circ$ Values for C1-C4 Alkyl Hydroperoxides to Available Literature Data

	$\Delta_f H_{298}^\circ$ ^a		
	This study from Table 4 ^b	This study from Table 5	Reference data
CH₃OOH	-30.96±0.67		-30.95±0.22 ^{c,m} -30.1±1.0 ^{d,n} -31.8 ^{e,m} -30.67 ^{f,m} -30.9±0.7 ^{g,n} -33.0 ^{h,n} -30.7±0.9 ^{i,m}
CH₃CH₂OOH	-38.94±0.81	-38.96	-39.13±0.22 ^{c,m} -39.9 ^{e,m} -39.5±0.7 ^{g,n} -40.0 ^{h,n} -39.28±0.01 ^{j,m} -39.81 ^{k,o}
CH₃CH₂CH₂OOH	-44.03±0.67	-44.02	-43.87 ^{k,o} -43.30±0.90 ^{i,m} -44.05±0.14 ^{j,m} -44.77±0.41 ^l -43.83±0.26 ^{c,m}
CH₃CH₂CH₂CH₂OOH	-48.85±0.96	-48.84	-48.37±0.24 ^{c,m} -49.06 ^{k,o}

^a Units in kcal mol⁻¹. ^b Recommendation in this study. ^c Simmie⁸³. ^d Matthews⁸⁶. ^e Lay⁷⁴. ^f Sheng⁷⁹. ^g Blanksby⁸⁷. ^h Khachatryan⁸⁸. ⁱ Goldsmith⁸⁴. ^j Sebbar⁸¹. ^k Burke⁷⁷. ^l Chen⁹³. ^m Calculation work. ⁿ Experimental work. ^o Review paper.

3.3.3 Enthalpies of Formation for C1-C4 Peroxy Radicals

This study starts their calculations with the ethyl peroxy radical (CH₃CH₂OOj) in order to compare their data with literature where there is only a small discrepancy in the reported values. Recently, in 2015, Burke et al.⁷⁷ suggested -6.09 kcal mol⁻¹ for ethyl peroxy which was taken from reference data on a number of evaluations. The calculation in this study at -6.19 kcal mol⁻¹ agrees with the Burke et al.'s⁷⁷ evaluation. Goldsmith et al.⁸⁴ (in 2012) calculated -5.0±0.9 using atomization, Simmie et al.⁸³ (in 2008) determined -5.62±0.17

using alcohols as reference species, Sebbar et al.⁸¹ (in 2004), reported -5.75 ± 0.1 , Blanksby et al.⁸⁷ (2001), presented -6.8 ± 0.7 , and Knyazev et al.⁸⁹ experiments (in 1998), reported -6.5 ± 2.4 , all values in kcal mol^{-1} . Work reactions that are used to calculate ethyl peroxy radicals are listed in Table 3.6. Enthalpies of formation on alkyl hydroperoxy molecules as reference species are from Table 3.3. The recommended value in this study is based on the first two work reactions because the reactions use hydroperoxy radical as a reference and the small enthalpies of reaction (indicated in Table 3.6, footnote a). The small enthalpies of reaction, less than 2 kcal mol^{-1} in the first work reactions, show that there are only small differences in bonding and structure between the reactants and the products and suggest good cancellation of the calculation error. The enthalpy value of the ethyl peroxy radical, was then used as an added reference species for the calculation of methyl peroxy, n-propyl peroxy, and n-butyl peroxy radicals in Table 3.7. Values from M06-2X/6-311+G(2d,d,p) calculations were excluded from average as noted above.

Table 3.8 provides a second set of work reactions which use small molecules and do not involve any peroxy radicals as reference species and this study notes that this reduces the error cancellation in the work reaction calculation. The results still show good agreement between the work reaction calculation methods. All calculation levels were included in the average here.

Table 3.9 uses small hydroperoxy and alkyl peroxy radicals in the work reaction calculations. This study used lower carbon number compounds to determine higher carbon number compounds. Ethyl peroxy radical was determined only from work reactions that included methyl peroxy radical species. N-propyl peroxy radical was determined from work reactions that included ethyl peroxy and methyl peroxy radical species. N-butyl

peroxy radical was determined from work reactions that included C1-3 radical species. M06-2X/6-311+G(2d,d,p) has been excluded for the same concern as before. These calculated enthalpy of formation values also show good agreement with the work reaction sets of Table 3.7 and Table 3.8. Results from Table 3.7 - Table 3.9 are summarized in Table 3.10 along with a comparison with available literature and the uncertainty that calculated in this work.

Methyl peroxy radical has been reported by Slagle et al.⁹⁰ as 2.7 ± 0.8 kcal mol⁻¹ which was from experimental data and equilibrium calculation. Knyazev et al. reported 2.30 kcal mol⁻¹ which was calculated from experimental data as well. The recommended value, 2.37 kcal mol⁻¹ is in good agreement with Knyazev et al.⁸⁹. The calculated values of n-propyl peroxy and n-butyl peroxy compounds in this study are about 1 kcal mol⁻¹ lower than Burke et al.'s⁷⁷ determination. The value of n-propyl peroxy in this study is about 2 kcal mol⁻¹ lower than Goldsmith et al.'s⁸⁴ evaluation.

Table 3.6 Work Reactions for Peroxy Radical

Isodesmic reactions	$\Delta_f H^\circ_{298}$ ^a			
	CBS-QB3	M06-2X	G4	CBS-APN O
1. CH ₃ CH ₂ OOj + HOOH = CH ₃ CH ₂ OOH + HOOj	-6.09 (2)	-6.08 (2)	-6.16 (2)	-6.09 (2)
2. CH ₃ CH ₂ OOj + CH ₃ CH ₂ OOH = CH ₃ CH ₂ OOCH ₂ CH ₃ + HOOj	-5.88 (2)	-6.77 (3)	-6.56 (2)	-5.85 (2)
3. CH ₃ CH ₂ OOj + CH ₄ = CH ₃ OOH + CH ₃ CH ₂ j	-5.98 (22)	-6.31 (22)	-6.34 (22)	-7.09 (23)
4. CH ₃ CH ₂ OOj + CH ₃ CH ₃ = CH ₃ OOH + CH ₃ CH ₂ CH ₂ j	-6.01 (19)	-6.67 (20)	-6.02 (19)	-7.21 (21)
5. CH ₃ CH ₂ OOj + CH ₄ = CH ₃ CH ₂ OOH + CH ₃ j	-5.80 (20)	-6.54 (21)	-5.95 (20)	-6.87 (21)
6. CH ₃ CH ₂ OOj = CH ₃ CH ₃ = CH ₃ CH ₂ OOH + CH ₃ CH ₂ j	-6.05 (16)	-6.61 (17)	-6.09 (16)	-7.21 (17)
7. CH ₃ CH ₂ OOj + CH ₃ CH ₂ CH ₃ = CH ₃ CH ₂ OOH + CH ₃ CH ₂ CH ₂ j	-6.03 (16)	-6.29 (17)	-5.80 (16)	-7.25 (18)
8. CH ₃ CH ₂ OOj + CH ₄ = CH ₃ OOCH ₃ + CH ₃ j	-5.35 (28)	-5.85 (29)	-6.30 (29)	-7.10 (30)

9. $\text{CH}_3\text{CH}_2\text{OOj} = \text{CH}_3\text{CH}_3 =$ $\text{CH}_3\text{OOCH}_3 + \text{CH}_3\text{CH}_2\text{j}$	-5.60 (25)	-5.92 (25)	-6.44 (25)	-7.45 (26)
10. $\text{CH}_3\text{CH}_2\text{OOj} + \text{CH}_3\text{CH}_2\text{CH}_3 =$ $\text{CH}_3\text{OOCH}_3 + \text{CH}_3\text{CH}_2\text{CH}_2\text{j}$	-5.58 (25)	-5.60 (25)	-6.15 (25)	-7.48 (27)
11. $\text{CH}_3\text{CH}_2\text{OOj} + \text{CH}_3\text{CH}_2\text{CH}_3 =$ $\text{CH}_3\text{CH}_2\text{OOCH}_2\text{CH}_3 + \text{CH}_3\text{j}$	-5.34 (19)	-6.45 (21)	-6.10 (20)	-6.96 (21)
Average by method	-5.79	-6.28	-6.18	-6.96
Total Average ^b			-6.30	
Average of first two work reactions ^c			-6.19	
Average of reaction 3 to 11 ^d			-6.33	
Standard Deviation	0.28	0.38	0.22	0.52

^a Units in kcal mol⁻¹. Values in parenthesis are enthalpies of reaction. ^b Average of heat of formation under four calculation levels considering 11 work reactions. ^c Average of heat of formation under four calculation levels considering work reactions 1 and 2. ^d Average of heat of formation under four calculation levels considering work reactions 3 to 11.

Table 3.7 Isodesmic Reactions for Peroxy Radicals : CH_3OOj , $\text{CH}_3\text{CH}_2\text{CH}_2\text{OOj}$, and $\text{CH}_3\text{CH}_2\text{CH}_2\text{CH}_2\text{OOj}$. $\text{CH}_3\text{CH}_2\text{OOj}$ is Used as A Reference Species

Isodesmic reactions	$\Delta_f\text{H}^\circ_{298}$ ^a			
	CBS-QB3	M06-2X	G4	CBS-A PNO
$\text{CH}_3\text{OOj} + \text{CH}_3\text{CH}_3 = \text{CH}_3\text{CH}_2\text{OOj} + \text{CH}_4$	2.36	1.97	2.53	2.25
$\text{CH}_3\text{OOj} + \text{CH}_3\text{CH}_2\text{CH}_3 = \text{CH}_3\text{CH}_2\text{OOj} +$ $\text{CH}_3\text{CH}_2\text{CH}_2\text{j}$	2.41	2.65	2.50	2.33
$\text{CH}_3\text{OOj} + \text{CH}_3\text{CH}_2\text{CH}_2\text{CH}_3 = \text{CH}_3\text{CH}_2\text{OOj} +$ $\text{CH}_3\text{CH}_2\text{CH}_2\text{CH}_2\text{j}$	2.31	1.78	2.44	2.24
$\text{CH}_3\text{OOj} + \text{CH}_3\text{CH}_2\text{CH}_2\text{CH}_2\text{CH}_3 = \text{CH}_3\text{CH}_2\text{OOj}$ $+ \text{CH}_3\text{CH}_2\text{CH}_2\text{CH}_2\text{CH}_2\text{j}$	2.41	3.22	2.36	2.34
Average by method	2.37	2.40	2.46	2.29
Method Average of Three ^b		2.37		
Method Average of Four ^c		2.38		
Standard Deviation	0.05	0.66	0.08	0.05
$\text{CH}_3\text{CH}_2\text{CH}_2\text{OOj} + \text{CH}_4 = \text{CH}_3\text{CH}_2\text{OOj} +$ CH_3CH_3	-11.31	-10.99	-11.60	-11.16
$\text{CH}_3\text{CH}_2\text{CH}_2\text{OOj} + \text{CH}_3\text{CH}_3 = \text{CH}_3\text{CH}_2\text{OOj} +$ $\text{CH}_3\text{CH}_2\text{CH}_3$	-11.36	-11.67	-11.57	-11.24
$\text{CH}_3\text{CH}_2\text{CH}_2\text{OOj} + \text{CH}_3\text{CH}_2\text{CH}_3 = \text{CH}_3\text{CH}_2\text{OOj}$ $+ \text{CH}_3\text{CH}_2\text{CH}_2\text{CH}_3$	-11.27	-10.80	-11.50	-11.16
$\text{CH}_3\text{CH}_2\text{CH}_2\text{OOj} + \text{CH}_3\text{CH}_2\text{CH}_2\text{CH}_3 =$ $\text{CH}_3\text{CH}_2\text{OOj} + \text{CH}_3\text{CH}_2\text{CH}_2\text{CH}_2\text{CH}_3$	-11.36	-12.23	-11.42	-11.25
Average by method	-11.33	-11.42	-11.52	-11.20
Method Average of Three ^b		-11.35		
Method Average of Four ^c		-11.37		
Standard Deviation	0.05	0.66	0.08	0.05
$\text{CH}_3\text{CH}_2\text{CH}_2\text{CH}_2\text{OOj} + \text{CH}_4 = \text{CH}_3\text{CH}_2\text{OOj} +$ $\text{CH}_3\text{CH}_2\text{CH}_3$	-16.47	-16.30	-17.14	-16.26
$\text{CH}_3\text{CH}_2\text{CH}_2\text{CH}_2\text{OOj} + \text{CH}_3\text{CH}_3 = \text{CH}_3\text{CH}_2\text{OOj}$ $+ \text{CH}_3\text{CH}_2\text{CH}_2\text{CH}_3$	-16.43	-16.11	-17.04	-16.25
$\text{CH}_3\text{CH}_2\text{CH}_2\text{CH}_2\text{OOj} + \text{CH}_3\text{CH}_2\text{CH}_3 =$	-16.43	-16.68	-16.89	-16.27

$\text{CH}_3\text{CH}_2\text{OOj} + \text{CH}_3\text{CH}_2\text{CH}_2\text{CH}_2\text{CH}_3$				
Average by method	-16.45	-16.36	-17.02	-16.26
Method Average of Three ^b		-16.58		
Method Average of Four ^c		-16.52		
Standard Deviation	0.02	0.29	0.12	0.01

a Units in kcal mol⁻¹. ^b Calculation levels include CBS-QB3, G4, CBS-APNO. The recommendation, this study. ^c All four calculation levels.

Table 3.8 Isodesmic Reactions and Enthalpy of Formation for C1-C4 Peroxy Radicals

Isodesmic reactions	$\Delta_f H^\circ_{298}$ ^a			
	CBS-QB3	M06-2X	G4	CBS-AP NO
$\text{CH}_3\text{OOj} + \text{HOOH} = \text{CH}_3\text{OOH} + \text{HOOj}$	2.53	2.37	2.31	2.46
$\text{CH}_3\text{OOj} + \text{CH}_3\text{OOH} = \text{CH}_3\text{OOCH}_3 + \text{HOOj}$	2.63	2.35	2.16	2.39
$\text{CH}_3\text{OOj} + \text{CH}_4 = \text{CH}_3\text{OOH} + \text{CH}_3\text{j}$	2.63	1.73	2.33	1.50
$\text{CH}_3\text{OOj} + \text{CH}_3\text{CH}_3 = \text{CH}_3\text{OOH} + \text{CH}_3\text{CH}_2\text{j}$	2.57	1.85	2.38	1.34
$\text{CH}_3\text{OOj} + \text{CH}_3\text{CH}_2\text{CH}_3 = \text{CH}_3\text{OOH} + \text{CH}_3\text{CH}_2\text{CH}_2\text{j}$	2.59	2.17	2.67	1.31
$\text{CH}_3\text{OOj} + \text{CH}_3\text{CH}_3 = \text{CH}_3\text{OOCH}_3 + \text{CH}_3\text{j}$	3.00	2.10	2.22	1.13
Average by method	2.66	2.10	2.34	1.69
Total Average ^b		2.20		
Standard Deviation	0.17	0.26	0.18	0.58
$\text{CH}_3\text{CH}_2\text{OOj} + \text{HOOH} = \text{CH}_3\text{CH}_2\text{OOH} + \text{HOOj}$	-6.09	-6.08	-6.16	-6.09
$\text{CH}_3\text{CH}_2\text{OOj} + \text{CH}_3\text{CH}_2\text{OOH} = \text{CH}_3\text{CH}_2\text{OOCH}_2\text{CH}_3 + \text{HOOj}$	-5.88	-6.77	-6.56	-5.85
$\text{CH}_3\text{CH}_2\text{OOj} + \text{CH}_4 = \text{CH}_3\text{CH}_2\text{OOH} + \text{CH}_3\text{j}$	-5.80	-6.54	-5.95	-6.87
$\text{CH}_3\text{CH}_2\text{OOj} + \text{CH}_3\text{CH}_3 = \text{CH}_3\text{CH}_2\text{OOH} + \text{CH}_3\text{CH}_2\text{j}$	-6.05	-6.61	-6.09	-7.21
$\text{CH}_3\text{CH}_2\text{OOj} + \text{CH}_3\text{CH}_2\text{CH}_3 = \text{CH}_3\text{CH}_2\text{OOH} + \text{CH}_3\text{CH}_2\text{CH}_2\text{j}$	-6.03	-6.29	-5.80	-7.25
$\text{CH}_3\text{CH}_2\text{OOj} + \text{CH}_3\text{CH}_2\text{CH}_3 = \text{CH}_3\text{CH}_2\text{OOCH}_2\text{CH}_3 + \text{CH}_3\text{j}$	-5.34	-6.45	-6.10	-6.96
Average by method	-5.87	-6.46	-6.11	-6.71
Total Average ^b		-6.29		
Standard Deviation	0.28	0.24	0.26	0.59
$\text{CH}_3\text{CH}_2\text{CH}_2\text{OOj} + \text{HOOH} = \text{CH}_3\text{CH}_2\text{CH}_2\text{OOH} + \text{HOOj}$	-11.02	-10.90	-11.79	-11.04
$\text{CH}_3\text{CH}_2\text{CH}_2\text{OOj} + \text{CH}_3\text{OOH} = \text{CH}_3\text{CH}_2\text{OOCH}_2\text{CH}_3 + \text{HOOj}$	-11.08	-11.87	-11.72	-10.94
$\text{CH}_3\text{CH}_2\text{CH}_2\text{OOj} + \text{CH}_4 = \text{CH}_3\text{CH}_2\text{CH}_2\text{OOH} + \text{CH}_3\text{j}$	-10.91	-11.54	-11.77	-12.00
$\text{CH}_3\text{CH}_2\text{CH}_2\text{OOj} + \text{CH}_3\text{CH}_3 = \text{CH}_3\text{CH}_2\text{CH}_2\text{OOH} + \text{CH}_3\text{CH}_2\text{j}$	-10.98	-11.42	-11.72	-12.16
$\text{CH}_3\text{CH}_2\text{CH}_2\text{OOj} + \text{CH}_3\text{CH}_2\text{CH}_3 = \text{CH}_3\text{CH}_2\text{CH}_2\text{OOH} + \text{CH}_3\text{CH}_2\text{CH}_2\text{j}$	-10.95	-11.10	-11.43	-12.19
$\text{CH}_3\text{CH}_2\text{CH}_2\text{OOj} + \text{CH}_4 = \text{CH}_3\text{OOCH}_3 + \text{CH}_3\text{CH}_2\text{j}$	-10.73	-10.73	-11.86	-12.43

CH₃CH₂CH₂OOj + CH ₃ CH ₃ =	-10.71	-12.12	-11.67	-12.20
CH ₃ CH ₂ OOCH ₂ CH ₃ + CH ₃ j				
Average by method	-10.91	-11.38	-11.71	-11.85
Total Average ^b		-11.46		
Standard Deviation	0.12	0.43	0.15	0.64
CH₃CH₂CH₂CH₂OOj + HOOH =	-16.17	-16.31	-17.32	-16.11
CH ₃ CH ₂ CH ₂ CH ₂ OOH + HOOj				
CH₃CH₂CH₂CH₂OOj + CH ₄ =	-16.06	-16.96	-17.30	-17.08
CH ₃ CH ₂ CH ₂ CH ₂ OOH + CH ₃ j				
CH₃CH₂CH₂CH₂OOj + CH ₃ CH ₃ =	-16.13	-16.83	-17.25	-17.23
CH ₃ CH ₂ CH ₂ CH ₂ OOH + CH ₃ CH ₂ j				
CH₃CH₂CH₂CH₂OOj + CH ₃ CH ₂ CH ₃ =	-16.11	-16.51	-16.96	-17.26
CH ₃ CH ₂ CH ₂ CH ₂ OOH + CH ₃ CH ₂ CH ₂ j				
CH₃CH₂CH₂CH₂OOj + CH ₄ = CH ₃ OOCH ₃ +	-15.87	-15.72	-17.11	-17.56
CH ₃ CH ₂ CH ₂ j				
CH₃CH₂CH₂CH₂OOj + CH ₄ =	-15.82	-16.76	-17.24	-17.22
CH ₃ CH ₂ OOCH ₂ CH ₃ + CH ₃ j				
Average by method	-16.02	-16.51	-17.19	-17.07
Total Average ^b		-16.70		
Standard Deviation	0.15	0.45	0.14	0.50

^a Units in kcal mol⁻¹. ^b All four calculation levels.

Table 3.9 Work Reactions and Enthalpy of Formation Including Target CH₃OOj, CH₃CH₂OOj, and CH₃CH₂CH₂OOj as Reference Species for C2-C4 Peroxy Radicals

Isodesmic reactions	$\Delta_f H_{298}^\circ$ ^a			
	CBS-QB3	M06-2X	G4	CBS-AP NO
CH₃CH₂OOj + CH ₄ = CH ₃ OOj + CH ₃ CH ₃	-6.17	-5.78	-6.35	-6.06
CH₃CH₂OOj + CH ₃ CH ₃ = CH ₃ OOj +	-6.22	-6.46	-6.32	-6.14
CH ₃ CH ₂ CH ₃				
CH₃CH₂OOj + CH ₃ CH ₂ CH ₃ = CH ₃ OOj +	-6.13	-5.59	-6.25	-6.06
CH ₃ CH ₂ CH ₂ CH ₃				
CH₃CH₂OOj + CH ₃ CH ₂ CH ₂ CH ₃ = CH ₃ OOj +	-6.23	-7.03	-6.17	-6.16
CH ₃ CH ₂ CH ₂ CH ₂ CH ₃				
Average by method	-6.19	-6.22	-6.27	-6.10
Method Average of Three ^b		-6.19		
Method Average of Four ^c		-6.19		
Standard Deviation	0.05	0.66	0.08	0.05
CH₃CH₂CH₂OOj + CH ₄ = CH ₃ OOj +	-11.35	-11.26	-11.73	-11.12
CH ₃ CH ₂ CH ₃				
CH₃CH₂CH₂OOj + CH ₃ CH ₃ = CH ₃ OOj +	-11.30	-11.07	-11.63	-11.11
CH ₃ CH ₂ CH ₂ CH ₃				
CH₃CH₂CH₂OOj + CH ₃ CH ₂ CH ₃ = CH ₃ OOj +	-11.31	-11.64	-11.48	-11.12
CH ₃ CH ₂ CH ₂ CH ₂ CH ₃				
CH₃CH₂CH₂OOj + CH ₄ = CH ₃ CH ₂ OOj +	-11.31	-10.99	-11.60	-11.16
CH ₃ CH ₃				
CH₃CH₂CH₂OOj + CH ₃ CH ₃ = CH ₃ CH ₂ OOj +	-11.36	-11.67	-11.57	-11.24
CH ₃ CH ₂ CH ₃				
CH₃CH₂CH₂OOj + CH ₃ CH ₂ CH ₃ =	-11.27	-10.80	-11.50	-11.16
CH ₃ CH ₂ OOj + CH ₃ CH ₂ CH ₂ CH ₃				
CH₃CH₂CH₂OOj + CH ₃ CH ₂ CH ₂ CH ₃ =	-11.36	-12.23	-11.42	-11.25

$\text{CH}_3\text{CH}_2\text{OOj} + \text{CH}_3\text{CH}_2\text{CH}_2\text{CH}_2\text{CH}_3$				
$\text{CH}_3\text{CH}_2\text{CH}_2\text{OOj} + \text{CH}_3\text{OOj} = 2 \text{CH}_3\text{CH}_2\text{OOj}$	-11.33	-11.39	-11.44	-11.29
Average by method	-11.32	-11.38	-11.54	-11.18
Method Average of Three ^b		-11.35		
Method Average of Four ^c		-11.36		
Standard Deviation	0.04	0.50	0.10	0.06
$\text{CH}_3\text{CH}_2\text{CH}_2\text{CH}_2\text{OOj} + \text{CH}_4 = \text{CH}_3\text{OOj} +$	-16.41	-15.71	-17.20	-16.13
$\text{CH}_3\text{CH}_2\text{CH}_2\text{CH}_3$				
$\text{CH}_3\text{CH}_2\text{CH}_2\text{CH}_2\text{OOj} + \text{CH}_3\text{CH}_3 = \text{CH}_3\text{OOj} +$	-16.47	-16.95	-17.02	-16.22
$\text{CH}_3\text{CH}_2\text{CH}_2\text{CH}_2\text{CH}_3$				
$\text{CH}_3\text{CH}_2\text{CH}_2\text{CH}_2\text{OOj} + \text{CH}_4 = \text{CH}_3\text{CH}_2\text{OOj} +$	-16.47	-16.30	-17.14	-16.26
$\text{CH}_3\text{CH}_2\text{CH}_3$				
$\text{CH}_3\text{CH}_2\text{CH}_2\text{CH}_2\text{OOj} + \text{CH}_3\text{CH}_3 =$	-16.43	-16.11	-17.04	-16.25
$\text{CH}_3\text{CH}_2\text{OOj} + \text{CH}_3\text{CH}_2\text{CH}_2\text{CH}_3$				
$\text{CH}_3\text{CH}_2\text{CH}_2\text{CH}_2\text{OOj} + \text{CH}_3\text{CH}_2\text{CH}_3 =$	-16.43	-16.68	-16.89	-16.27
$\text{CH}_3\text{CH}_2\text{OOj} + \text{CH}_3\text{CH}_2\text{CH}_2\text{CH}_2\text{CH}_3$				
$\text{CH}_3\text{CH}_2\text{CH}_2\text{CH}_2\text{OOj} + \text{CH}_4 =$	-16.46	-15.98	-16.92	-16.37
$\text{CH}_3\text{CH}_2\text{CH}_2\text{OOj} + \text{CH}_3\text{CH}_3$				
$\text{CH}_3\text{CH}_2\text{CH}_2\text{CH}_2\text{OOj} + \text{CH}_3\text{CH}_3 =$	-16.51	-16.66	-16.89	-16.45
$\text{CH}_3\text{CH}_2\text{CH}_2\text{OOj} + \text{CH}_3\text{CH}_2\text{CH}_3$				
$\text{CH}_3\text{CH}_2\text{CH}_2\text{CH}_2\text{OOj} + \text{CH}_3\text{CH}_2\text{CH}_3 =$	-16.42	-15.79	-16.82	-16.36
$\text{CH}_3\text{CH}_2\text{CH}_2\text{OOj} + \text{CH}_3\text{CH}_2\text{CH}_2\text{CH}_3$				
$\text{CH}_3\text{CH}_2\text{CH}_2\text{CH}_2\text{OOj} + \text{CH}_3\text{CH}_2\text{CH}_2\text{CH}_3 =$	-16.52	-17.23	-16.74	-16.46
$\text{CH}_3\text{CH}_2\text{CH}_2\text{OOj} + \text{CH}_3\text{CH}_2\text{CH}_2\text{CH}_2\text{CH}_3$				
$\text{CH}_3\text{CH}_2\text{CH}_2\text{OOj} + \text{CH}_3\text{CH}_2\text{OOj} = 2$	-16.50	-16.35	-16.67	-16.56
$\text{CH}_3\text{CH}_2\text{CH}_2\text{OOj}$				
Average by method	-16.46	-16.38	-16.93	-16.33
Method Average of Three ^b		-16.58		
Method Average of Four ^c		-16.53		
Standard Deviation	0.04	0.50	0.17	0.13

^a Units in kcal mol⁻¹. ^b Calculation levels include CBS-QB3, G4, CBS-APNO. ^c All four calculation levels.

Table 3.10 Comparison of Calculated $\Delta_f H_{298}^\circ$ Values for C1-C4 Peroxy Radicals to Available Literature Data

	$\Delta_f H_{298}^\circ$ ^a			Reference data
	This study Table 3.7 ^c	This study Table 3.8	This study Table 3.9	
CH₃OOj	2.37±1.24	2.20	2.37 ^d	1.2 ^f 2.7±0.8 ^g 2.9±1.5 ⁱ 2.2±1.2 ^j 2.92±0.22 ^l 2.07±0.7 ^k 2.02±0.1 ^m 3.3±0.6 ⁿ 5.5±3.0 ^o 6.2 ^h 2.0 ^p
CH₃CH₂OOj	-6.19±0.92^b	-6.29	-6.19	-6.09 ^e -6.5±2.4 ^j -6.8±0.7 ^k -5.75±0.1 ^m -5.62±0.17 ^l -5.0±0.9 ⁿ -6.0 ^p
CH₃CH₂CH₂OOj	-11.35±1.24	-11.46	-11.35	-10.42 ^e -9.8±0.9 ⁿ -10.54±0.26 ^l -11.0 ^p
CH₃CH₂CH₂CH₂OOj	-16.58±1.64	-16.70	-16.58	-15.70 ^e -15.01±0.24 ^l -16.0 ^p

^a Units in kcal mol⁻¹. ^b Table 3.6. ^c The recommendation in this study. ^d Table 3.7. ^e Burke⁷⁷. ^f Sheng⁷⁹. ^g Slagle⁹⁰. ^h Nangia⁹². ⁱ Cohen⁶². ^j Knyazev⁸⁹. ^k Blanksby⁸⁷. ^l Simmie⁸³. ^m Sebbar⁸¹. ⁿ Goldsmith⁸⁴. ^o Benson⁹¹. ^p Sharma⁶.

3.3.4 Internal Rotor Potential Energy Diagrams

Figure 3.1 shows the potential energy profiles of the 4 internal rotors in propyl hydroperoxide. The RO-OH rotor and the RC-OOH rotor have barrier about 7 kcal mol⁻¹. The C-C potential barriers are near 3 kcal mol⁻¹ which is approximately one half the

barriers of peroxide RO-OH and R-OOH groups. The potential energy profiles for all target molecules with internal rotors are included in Figure G.12- G.18 of the Appendix G.

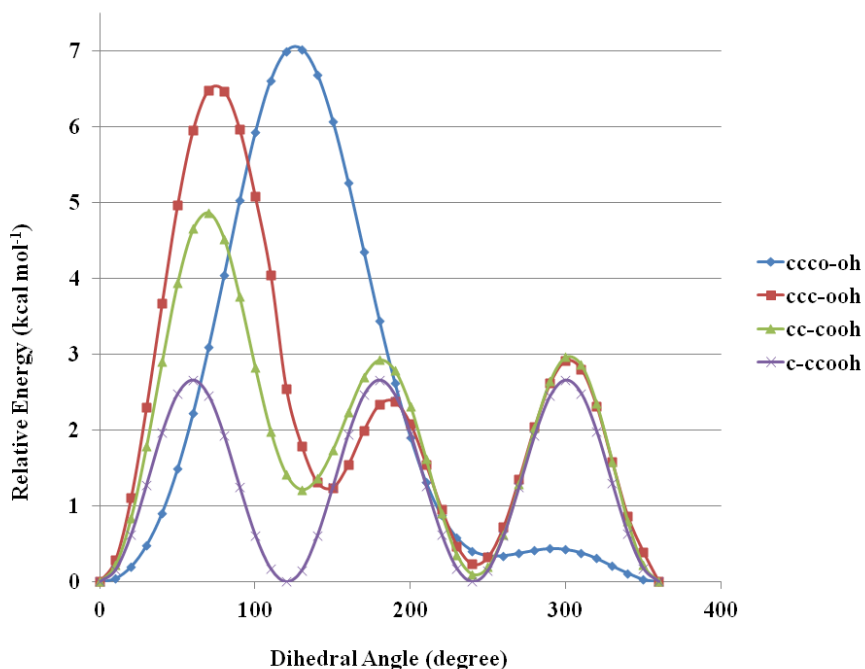


Figure 3.1 Potential energy profiles of the CCCO-OH, CCC-OOH, CC-COOH, and C-CCOOH internal rotors for propyl peroxide (symbols). The solid line is the fit of the Fourier series expansions.

3.3.5 Entropy and Heat Capacity

Table 3.11 lists the standard entropies and heat capacities at 300 K, 400 K, 500 K, 600 K, 800 K, 1000 K, 1500 K, along with available literature data. TVR represents the sum of the contributions from translations, vibrations, and external rotations. Internal rotor indicates the contribution from hindered internal rotation, which replaces the torsion frequency contributions in the TVR heat capacity and entropy data summations. The standard entropy values (298 K) for methyl hydroperoxide, ethyl hydroperoxide, and propyl hydroperoxide

agree with the data in the literature; for butyl hydroperoxide however, this study finds a standard entropy value about $4 \text{ cal mol}^{-1} \text{ K}^{-1}$ higher than the literature value. This study notes the standard entropy values for methyl, ethyl, propyl, and butyl hydroperoxides are 66.27, 77.08, 87.35, and 97.71 ($\text{cal mol}^{-1} \text{ K}^{-1}$) where Goos et al., have reported the values of 66.22 for methyl peroxide, 87.86 $\text{cal mol}^{-1} \text{ K}^{-1}$ for propyl hydroerpxide, and 91.19 $\text{cal mol}^{-1} \text{ K}^{-1}$ for butyl hydroperoxide. Based on Benson's group additivity, the standard entropy of a hydrocarbon -CH₂- group is $9.42 \text{ cal mol}^{-1} \text{ K}^{-1}$. Calculating the butyl hydroperoxide entropy from propyl hydroperoxide and the established group value results in the standard entropy of butyl hydroperoxide as $97.28 \text{ cal mol}^{-1} \text{ K}^{-1}$, which is in agreement with the values from calculations in the present study. This study reports the calculated standard entropy of butyl peroxy are $\sim 3 \text{ cal mol}^{-1} \text{ K}^{-1}$ higher than the literature.

Goldsmith et al., reported the standard entropy of methanol, ethanol, and n-propanol as (in $\text{cal mol}^{-1} \text{ K}^{-1}$) 57.2 ± 0.4 , 66.8 ± 0.9 , and 76.3, respectively, which follow group additivity. Goldsmith et al., also reported the standard entropy of methoxy, ethoxy, and n-propoxy radicals as (in $\text{cal mol}^{-1} \text{ K}^{-1}$) 54.4 ± 0.3 , 66.8 ± 1.0 , and 75.7 ± 1.5 , respectively, which also agree with group additivity calculation. Burke et al., recommended $66.11 \text{ cal mol}^{-1} \text{ K}^{-1}$ as the standard entropy for ethoxy radical, and suggested $74.5 \text{ cal mol}^{-1} \text{ K}^{-1}$ for n-propoxy radical; they calculated $75.29 \text{ cal mol}^{-1} \text{ K}^{-1}$ for n-propoxy radical based on group additivity. This study reports the standard entropy of methyl hydroperoxide, ethyl hydroperoxide, n-propyl hydroperoxide, and n-butyl hydroperoxide as (in $\text{cal mol}^{-1} \text{ K}^{-1}$) 66.27, 77.08, 87.35, and 97.71, respectively, which also follow group additivity. This study reports the standard entropy of methyl peroxy, ethyl peroxy, n-propyl peroxy, and n-butyl

peroxy radicals as (in $\text{cal mol}^{-1} \text{K}^{-1}$) 64.70, 75.43, 86.18, and 96.11, respectively, which also follow group additivity.

The frequency scaling factor that in this study used for entropy and heat capacity calculations is 0.964 at the B3LYP/6-31+G(d,p) level of calculation; this is lower than previous factor 0.98 used in this group. This will account for some increase in the standard entropy for the hydroperoxides and peroxy radicals by with increased contributions from the vibrations.

The heat capacity data over the temperature range of 300 K to 1500 K all show agreement with the literature.

Table 3.11 Ideal Gas Phase Entropy and Heat Capacity Obtained by B3LYP/6-31+G(d,p) Calculation, Comparison with Available Literature

		S_{298}° ^b	C_{p300} ^b	C_{p400}	C_{p500}	C_{p600}	C_{p800}	C_{p1000}	C_{p1500}
CH₃OOH ^h symmetry = 3	TVR ^a	58.44	11.03	13.43	15.79	17.86	21.18	23.69	27.72
	Internal rotors	7.83	3.51	3.53	3.44	3.32	3.11	2.94	2.63
optical isomer = 1	Total	66.27	14.53	16.96	19.23	21.19	24.29	26.62	30.34
	Literature	67.1±0.8 ^c	14.6±0.7	17.1±0.9	19.4±1.0	21.4±1.0	24.5±1.0	26.8±0.9	30.5±0.7
CH₃CH₂OOH ^h symmetry = 3	TVR	63.03	14.10	18.11	21.93	25.24	30.49	34.41	40.61
	Internal rotors	14.05	5.63	5.55	5.34	5.12	4.72	4.41	3.89
optical isomer = 1	Total	77.08	19.73	23.66	27.27	30.36	35.21	38.82	44.50
	Literature	75.2±1.4 ^c	20.2±1.2	24.1±1.5	27.8±1.5	30.8±1.5	35.6±1.5	39.2±1.4	44.8±1.0
CH₃CH₂CH₂OOH ^h symmetry = 3	TVR	66.68	16.89	22.60	27.94	32.54	39.78	45.13	53.52
	Internal rotors	20.68	8.48	8.04	7.54	7.11	6.43	5.95	5.21
optical isomer = 1	Total	87.35	25.37	30.64	35.49	39.65	46.20	51.08	58.73
	Literature	84.2±2.0 ^c	25.7±1.6	31.2±1.9	36.1±2.0	40.2±2.0	46.7±2.0	51.5±1.9	59.0±1.4
CH₃CH₂CH₂CH₂OOH ^h symmetry = 3	TVR	70.32	19.81	27.08	33.90	39.77	48.99	55.81	66.41
	Internal rotors	27.38	11.53	10.72	9.91	9.24	8.23	7.54	6.53
optical isomer = 1	Total	97.71	31.34	37.80	43.81	49.00	57.23	63.35	72.94
	Literature	92.82 ^g							
CH₃OOj ⁱ symmetry = 3	TVR	59.20	10.67	12.85	14.96	16.80	19.70	21.84	25.16
	Internal rotor	5.50	1.30	1.19	1.12	1.09	1.05	1.03	1.01
optical isomer = 0	Total	64.70	11.98	14.03	16.08	17.88	20.75	22.87	26.17
	Literature	64.4±0.5 ^c	12.1±0.5	14.2±0.8	16.2±0.9	18.0±1.0	20.9±1.0	23.0±0.9	26.3±0.7
CH₃CH₂OOj ⁱ symmetry = 3	TVR	64.00	13.81	17.57	21.12	24.19	29.02	32.58	38.06
	Internal rotors	11.44	3.71	3.47	3.20	2.97	2.65	2.45	2.22
optical isomer = 0	Total	75.43	17.52	21.04	24.32	27.17	31.67	35.03	40.28
	Literature	74.2±1.1 ^c	17.6±1.1	21.3±1.4	24.7±1.4	27.6±1.4	32.1±1.4	35.4±1.3	40.5±1.0
CH₃CH₂CH₂OOj ⁱ symmetry = 3	TVR	68.05	16.63	21.99	27.04	31.40	38.22	43.23	50.94
	Internal rotors	18.13	5.86	5.67	5.34	4.99	4.43	4.04	3.53
optical isomer = 0	Total	86.18	22.49	27.66	32.38	36.39	42.65	47.28	54.47
	Literature	83.5±1.7 ^c	23.0±1.5	28.2±1.8	32.9±2.0	36.9±2.0	43.1±1.9	47.7±1.8	54.7±1.4
CH₃CH₂CH₂CH₂OOj ⁱ symmetry = 3	TVR	71.53	19.52	26.50	33.04	38.67	47.78	53.94	63.84
	Internal rotors	24.58	9.15	8.55	7.87	7.25	6.31	5.69	4.87
optical isomer = 0	Total	96.11	28.67	35.05	40.91	45.92	53.79	56.92	68.72
	Literature	93.55 ^g							
		92.39 ^f							

^a Sum of contributions from translations, vibrations, and external rotations. ^b Units in cal mol⁻¹ K⁻¹. ^c Goldsmith⁸⁴. ^d Lay⁴⁷. ^e Goos¹³. ^f Burke⁷⁷. ^g Zhu⁶⁹. ^h Symmetry number is 3. Optical isomer number is 2. ⁱ Symmetry number is 3. Optical isomer number is 1.

3.3.6 Bond Dissociation Energies at 298 K

ROO-H, RO-OH, R-OOH, RO-Oj, and R-OOj bond strengths are listed and compared with available literature in Table 3.12. ROO-H bond dissociation energies steadily decrease with increasing carbon number in the normal alkyl hydroperoxides from 85.3 in CH₃OO-H to 84.2 in CH₃CH₂CH₂CH₂OO-H (kcal mol⁻¹). RO-OH bond dissociation energies steadily increase with increasing the carbon number from 44.0 in CH₃O-OH to 45.9 in CH₃CH₂CH₂CH₂O-OH. R-OOH bond dissociation energies steadily increase with increasing carbon number from 68.1 in CH₃-OOH to 71.1 in CH₃CH₂CH₂CH₂-OOH. Table 3.11 shows that the RO-Oj and R-OOj bond dissociation energies also steadily increase with increasing carbon chain length.

Removing one hydrogen atom from terminal oxygen results in a RO-O Π bond formation: it increases the bond energy of O-O by ~18 kcal mol⁻¹ and decreases the R-OO bond energy by ~35 kcal mol⁻¹, respectively. As noted in the geometry section, removing one hydrogen from the peroxy oxygen decreases O-O bond distance by 10% and increases R-O bond distance by 3%.

Table 3.12 Bond Dissociation Energies of ROO-H, RO-OH, R-OOH, RO-Oj, and R-OOj. Comparison with Available Literature

	CH₃OOH	CH₃CH₂OOH	CH₃(CH₂)₂OOH	CH₃(CH₂)₃OOH
ROO-H	85.3	84.8	84.7	84.2
Literature	88±1 ^c , 86.6 ^d , 86.04±0.24 ^e , 88.43±0.48 ^f , 87.24 ^g , 85.56 ^h	86.1 ^d , 85.56±0.24 ^e , 84.85±2.2 ⁱ , 86.76 ^g	85.33±0.48 ^e , 80.07 ^j	85.56±0.24 ^e
RO-OH	44.0	45.8	45.1	45.9
Literature	44.96(G2) ^a , 44.68(CBSQ) ^a , 44.6 ^b , 44.93±0.48 ^e , 45.65 ^k , 45.17±0.96 ^l	44.93±0.48 ^e , 46.37 ^k	44.93±0.48 ^e	45.41±0.48 ^e
R-OOH	68.9	70.9	71.3	71.1
Literature	68.83±0.24 ^e , 71.80±3.01 ^l	70.75±0.24 ^e , 79.40±5.00 ^l	70.98±0.48 ^e , 87.09 ^l	70.98±0.96 ^e
RO-Oj	61.3	62.7	63.0	64.2
Literature	61.66±0.48 ^e	62.14±0.48 ^e	62.14±0.48 ^e	62.62±0.48 ^e
R-OOj	32.6	35.2	35.6	35.9
Literature	32.03±0.24 ^e , 32.74±0.96 ^m , 32.98 ⁿ , 32.4±0.7 ^o	34.18±0.24 ^e , 35.61±1.90 ^m , 35.34 ⁿ	34.66±0.48 ^e , 36.09 ⁿ	34.66±0.96 ^e

^a Bach⁹⁴. ^b Barker⁹⁵. ^c Blanksby⁹⁶. ^d Lay⁷⁴. ^e Simmie⁸³. ^f Kondo⁹⁷. ^g Jonsson⁹⁸. ^h Fu⁹⁹. ⁱ Blanksby⁸⁷. ^j Mitov¹⁰⁰. ^k Wijaya¹⁰¹. ^l Luo¹⁰². ^m Knyazev⁸⁹. ⁿ Merle¹⁰³. ^o Slagle⁹⁰.

3.4 Summary

Experimental data on CH_3OOCH_3 and $\text{CH}_3\text{CH}_2\text{OOCH}_2\text{CH}_3$ peroxides have been used as reference species in work reactions to calculate standard enthalpy of formation of $\text{C}_1\text{-C}_4$ normal alkyl hydroperoxide compounds, where previously accepted data was from computational methods. The M06-2X/6-311+G(2d,d,p), CBS-QB3, CBS-APNO, and G4 calculation methods were used. Comparison of available literature with data several different work reactions sets show very good agreement. The agreement of the literature enthalpy values with use of the experimental formation enthalpy data of the di-methyl and di-ethyl peroxies suggests that the published enthalpy data of molecules are suitable for use as reference species in work reactions to calculate branched peroxides, hydroperoxides, and corresponding radicals. Standard enthalpy of formation of methyl peroxy, n-propyl peroxy, and n-butyl peroxy radicals have been determined using work reactions involving the above peroxides with hydroperoxy and ethyl peroxy radicals as reference species and show good agreement with current computational literature. Entropies and heat capacities are determined with B3LYP/6-31+G(d,p) optimized structures and frequencies. Internal rotors have been investigated by intramolecular torsion potential curves at the B3LYP/6-31+G(d,p) level. Bond dissociation energies for R-OOH, RO-OH, ROO-H, R-OOj, and RO-Oj have been determined and compare with literature. Recommended entropy values for propyl hydroperoxide and butyl hydroperoxide are updated.

CHAPTER 4

THERMOCHEMICAL PROPERTIES ($\Delta_F H^\circ(298\text{ K})$), $S^\circ(298\text{ K})$, $C_P(T)$) AND BOND DISSOCIATION ENERGIES FOR FLUORINATED METHANOL AND FLUORINATED METHYL HYDROPEROXIDES: $\text{CH}_{3-x}\text{F}_x\text{OH}$, AND $\text{CH}_{3-x}\text{F}_x\text{OOH}$

4.1 Overview

Halogenated compounds address critical attention because of their wide applications in industry ¹ and for fluorocarbons their high stability and persistence in the environment. HFC-134a, mono- to tri- fluorinated methyl hydroperoxides and their corresponding radicals are intermediates in the atmospheric degradation of hydrofluorocarbons are important to understanding the oxidation and reduction reactions ¹⁰⁴.

A review on synthesis and decomposition of the saturated and unsaturated fluorinated peroxide has been published in 1996 by Sawada ¹⁰⁵. Hayman et al. ¹⁰⁶ described the degradation of the fluorinated hydrocarbons and indicated that the fluorinated hydroperoxides and their radicals are important intermediates in the fluorocarbon degradation cycle. Schneider et al. ¹⁰⁴ focused on trifluoromethyl compounds and concluded that substituting hydrogen atoms in methyl group by fluorine atoms shortened C-O and O-O bonds, whereas substituting fluorine atoms by chlorine atoms increased the C-O and O-O bond lengths. El-Taher ¹⁰⁷ calculated the thermochemical properties on fluorinated methyl peroxides with B3LYP, MP2(FULL), and MP4(SDTQ) methods and showed the stabilizing influence of fluorine-substituted methyl groups.

In Reints et al 108.'s work, bond dissociation energy of CF₃O-H was reported as 118.8 kcal mol⁻¹, and which is similar to the O-H bond in water and suggests the CF₃O radical may be quite reactive.

Kosmas et al. 109, investigated the geometry and R-OOH bond dissociation energy of halogenated methyl peroxides (CH_{n+1}X_{2-n}OOX, X=F, Cl, Br, I) and concluded that increasing the halogen substitutions on the methyl group stabilized and molecular system and increased the R-C bond energy. However, while they addressed the stability of the fluorinated hydroperoxide system they did not discuss the weakest O-O bond which is the most likely to react in a thermal environment.

As enthalpy of formation of hydrocarbon hydroperoxide and fluorinated hydrocarbons 110 have been re-evaluated in this group's previous studies, in this paper, this study employs updated enthalpy value of C1-C4 hydroperoxides and fluorinated hydrocarbons as reference species in work reaction to determine the enthalpy of formation of fluorinated methyl peroxides and their derivative radicals, consequently, calculated the stability of peroxides and alcohols with fluorine substitution on methyl group.

4.2 Computational Methods

4.2.1 Enthalpy of Formation

All values reported in this paper are for a standard state of 298 K and 1 atm. The absence of imaginary frequencies verified that all stable structures were true minima at their

respective levels of theory. All calculations were performed using the Gaussian 09²⁸ program.

The Gaussian-n family calculation, Gaussian-4 theory⁴¹, optimized geometry and calculated frequency at the B3LYP/6-31G(2df,p) level, followed by a series of single point correlation energy calculations started from CCSD(T), MP4SDTQ, until MP2-Full were employed.

A well-developed composite calculation method, CBS-QB3³⁵, utilized B3LYP/6-311G(2d,d,p) level of theory to optimize geometries and to calculate frequencies, and continually applies CCSD(T), MP4(SDQ), and MP2 level to calculate single point energies.

To compare and to provide accurate calculation, CBS-APNO³⁶, another composite calculation method was also used. It determines the initial geometry optimization and frequency calculation at the HF/6-311G(d,p) level, followed by a higher-level QCISD/6-311G(d,p) geometry optimization. A single point energy calculation was then performed at the QCISD(T)/6-311++G(2df,p) level, followed by extrapolation to the complete basis set limit.

Enthalpies of formation and bond dissociation energies were determined by averaging the use of isodesmic work reactions and the CBS-QB3, CBS-APNO, and G4 calculation methods. Table A of the Appendix shows the standard enthalpy of formation for each reference species in the isodesmic reactions along with the available uncertainties. The enthalpy of formation of fluorohydrocarbons and hydroperoxides are taken from their recent publications which renewed and updated the thermochemistry properties. The enthalpy of formation of small alkanes and their alkyl radicals are taken from Ruscic's¹¹¹

latest publication which update the thermochemical properties with high quality uncertainty calculation.

4.2.2 Entropy and Heat Capacity

Entropy and heat capacity contributions for the 298 K - 1500 K temperature range are determined from the calculated structures, moments of inertia, vibrational frequencies, electron degeneracy, number of optical isomers, and the known mass of each molecule. Vibrational frequencies are scaled by a factor of 0.964⁴⁸ for calculation of standard entropy and heat capacity at B3LYP/6-31+G(d,p) level of calculation. As one of the most popular DFT methods, B3LYP, combined the three-parameter Becke exchange functional, B3³³, with Lee-Yang-Parr correlation functional, LYP³⁴, was used with the 6-31+G(d,p) basis set because its economic cost and its capability of calculating larger molecules.

The "SMCPS"⁴⁶ program employed the rigid-rotor-harmonic oscillator approximation from the frequencies along with moments of inertia from the optimized structure was used to determine the contributions of translation, external rotation, and vibrations.

The "Rotator"⁴⁷ program developed by Krasnoperov, Lay, Venanzi, Bozzelli, and Shokhirev determined the contributions from internal rotors from the corresponding internal rotor torsion frequencies. In this work, a ten-parameter Fourier series function are presented as torsional potential curve to calculate the contribution of free internal rotation.

4.2.3 Bond Dissociation Energies

A variety of homolytic bond dissociation energies determined from a parent molecule and the corresponding radical were determined:

$$D(\text{ROO} - \text{H}) = \Delta_f H^\circ(\text{ROO} \bullet) + \Delta_f H^\circ(\text{H}) - \Delta_f H^\circ(\text{ROOH}) \quad (\text{Eq.4.1})$$

$$D(\text{RO} - \text{OH}) = \Delta_f H^\circ(\text{RO} \bullet) + \Delta_f H^\circ(\text{OH}) - \Delta_f H^\circ(\text{ROOH}) \quad (\text{Eq.4.2})$$

$$D(\text{R} - \text{OOH}) = \Delta_f H^\circ(\text{R} \bullet) + \Delta_f H^\circ(\text{OOH}) - \Delta_f H^\circ(\text{ROOH}) \quad (\text{Eq.4.3})$$

$$D(\text{RO} - \text{O} \bullet) = \Delta_f H^\circ(\text{RO} \bullet) + \Delta_f H^\circ(\text{O}) - \Delta_f H^\circ(\text{ROO} \bullet) \quad (\text{Eq.4.4})$$

$$D(\text{R} - \text{OO} \bullet) = \Delta_f H^\circ(\text{R} \bullet) + \Delta_f H^\circ(\text{O}_2) - \Delta_f H^\circ(\text{ROO} \bullet) \quad (\text{Eq.4.5})$$

$$D(\text{RO} - \text{H}) = \Delta_f H^\circ(\text{RO} \bullet) + \Delta_f H^\circ(\text{H}) - \Delta_f H^\circ(\text{ROH}) \quad (\text{Eq.4.6})$$

$$D(\text{R} - \text{OH}) = \Delta_f H^\circ(\text{R} \bullet) + \Delta_f H^\circ(\text{OH}) - \Delta_f H^\circ(\text{ROH}) \quad (\text{Eq.4.7})$$

$$D(\text{R} - \text{O} \bullet) = \Delta_f H^\circ(\text{R} \bullet) + \Delta_f H^\circ(\text{O}) - \Delta_f H^\circ(\text{RO} \bullet) \quad (\text{Eq.4.8})$$

$$D(\text{R} - \text{H}) = \Delta_f H^\circ(\text{R} \bullet) + \Delta_f H^\circ(\text{H}) - \Delta_f H^\circ(\text{RH}) \quad (\text{Eq.4.9})$$

RO-OH bond is compared with RO-O• bond, R-OOH bond is compared with R-OO• bond, R-OH bond is compared with R-O• bond, ROO-H is compared with RO-H.

4.3 Results and Discussion

4.3.1 Geometries

The optimized geometries at the B3LYP/6-31+G(d,p) for CH₂FOOH, CHF₂OOH, CF₃OOH, CH₂FOO•, CHF₂OO•, CF₃OO•, CH₂FOH, CHF₂OH, CF₃OH, CH₂FO•, CHF₂O•, CF₃O•, CH₂F•, CHF₂•, CF₃• are presented in the Figure F.23-37 of the Appendix.

The Cartesian coordinates, vibrational frequencies, and moments of inertia are also presented as Table A-C of the Appendix, respectively.

Figure 4.1 shows the important geometry parameters of methyl peroxide and mono- to tri- fluoro peroxide molecules. Comparison see Table 4.1. Substituting a F atom for a H atom reduces the C-X bond length from 1.37658 Å (CH_2FOOH) to 1.32148 Å (CF_3OOH). Substituting a F atom for a H atom reduces the C-O bond length from 1.43989 Å (CH_3OOH) to 1.43157 Å (CF_3OOH). From CH_3OOH to CH_2FOOH , the CO-OH dihedral angle is reduced from 118 degree to 94 degree. The F atom attached to the methyl group attracts the H atom in the -OOH group. From CH_2FOOH to CHF_2OOH , two F atoms push the H in -OOH group away about only 2 degree. From CHF_2OOH to CF_3OOH , the CF_3 - group pushes the H in the -OOH group away by another 10 degree. This is a result of the F atoms electron withdrawing effects. The HC-OO dihedral angle remains ~ 180 degree. Overall, the substitution of F atoms strengthens the C-F and C-O bonds.

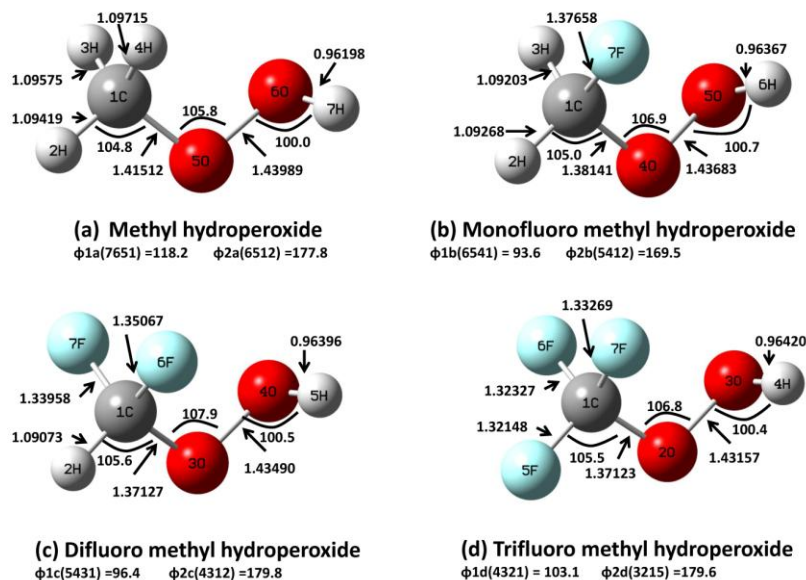
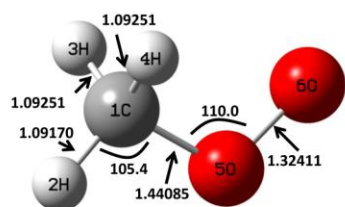


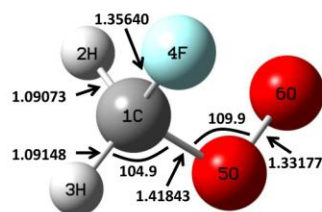
Figure 4.1 Geometry of methyl hydroperoxide and mono- to tri- fluoro methyl hydroperoxide molecules calculated by CBS-APNO method. Bond lengths in Å, bond angles in degree, dihedral angles in degree.

Table 4.1 Important Geometry Parameters of Methyl Hydroperoxide and Mono- to Tri-Fluoro Methyl Hydroperoxides. Bond Lengths in Å, Dihedral Angles in Degree

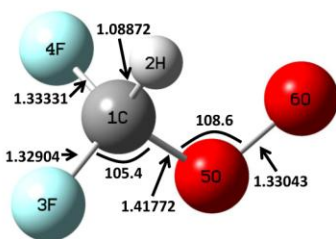
	B(C-F)	B(C-O)	B(O-O)	B(O-H)	$\Phi_1(\text{HO-OC})$	$\Phi_2(\text{OO-CH})$
CH₃OOH		1.41512	1.43989	0.96198	118.2	177.8
CH₂FOOH	1.37658	1.38141	1.43683	0.96367	93.6	169.5
CHF₂OOH	1.35067	1.37127	1.43490	0.96396	96.4	179.8
	1.33958					
CF₃OOH	1.33269	1.37123	1.43157	0.96420	96.4	179.6
	1.32327					
	1.32148					



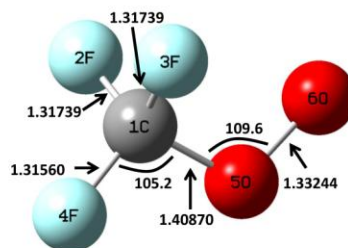
(e) Methyl hydroperoxy radical
 $\phi_{1e}(6512) = 180.0$



(f) Monofluoro methyl hydroperoxy radical
 $\phi_{1f}(6513) = 164.2$



(g) Difluoro methyl hydroperoxy radical
 $\phi_{1g}(6513) = 163.9$



(h) Trifluoro methyl hydroperoxy radical
 $\phi_{1h}(6514) = 180.0$

Figure 4.2 Geometry of methyl hydroperoxy and mono- to tri- fluoro methyl hydroperoxy molecules calculated by CBS-APNO method. Bond Lengths in Å, bond angles in degree, dihedral angles in degree.

Table 4.2 Important Geometry Parameters of Methyl Hydroperoxy and Mono- to Tri-Fluoro Methyl Hydroperoxy. Bond Lengths in Å, Dihedral Angles in Degree

	B(C-F)	B(C-O)	B(O-O)	$\Phi_1(\text{OO-CH})$
CH₃OO•		1.44085	1.32411	180.0
CH₂FOO•	1.35640	1.41843	1.33177	164.2
CHF₂OO•	1.33331	1.41772	1.33043	163.9
	1.32904			
CF₃OO•	1.31739	1.40870	1.33244	180.0
	1.31739			
	1.31560			

Figure 4.2 shows the important geometry parameters of methyl hydroperoxy and mono- to tri- fluoro hydroperoxy radicals. Comparison see Table 4.2.

Substituting a F atom for a H atom reduces the C-X bond length from 1.35640 Å ($\text{CH}_2\text{FOO}\bullet$) to 1.31560 Å ($\text{CF}_3\text{OO}\bullet$). Substituting a F atom for a H atom reduces the C-O bond length from 1.44085 Å ($\text{CH}_3\text{OO}\bullet$) to 1.40870 Å ($\text{CF}_3\text{OO}\bullet$). From CH_3OOj to CH_2FOOj , the HC-OO dihedral angle is narrowed down from 180 degree to 164 degree. The F atom attached to the methyl group pushes the O atom in the -OOj group away. From CH_2FOOj to CHF_2OOj , the C-O torsion angle remains the same. From CHF_2OOj to CF_3OOj , the C-O torsion angle goes back to 180 degree because of the symmetric property.

Overall, the substitution of F atoms strengthens the C-F and C-O bond.

From CH_3OOH to CH_3OOj , abstracting the H atom from the -OOH group shortens the O-O bond from 1.43989 Å to 1.32411 Å, whereas lengthens the C-O bond from 1.41512 Å to 1.44085 Å. From CH_2FOOH to CH_2FOOj , abstracting the H atom from the -OOH group shortens the O-O bond from 1.43683 Å to 1.33177 Å, whereas lengthens the C-O bond from 1.38141 Å to 1.41843 Å. From CHF_2OOH to CHF_2OOj , abstracting the H atom from the -OOH group shortens the O-O bond from 1.43490 Å to 1.33043 Å, whereas lengthens the C-O bond from 1.37127 Å to 1.41772 Å. From CF_3OOH to CF_3OOj , abstracting the H atom from the -OOH group shortens the O-O bond from 1.43157 Å to 1.33244 Å, whereas lengthens the C-O bond from 1.37123 Å to 1.40870 Å.

In summary, eliminating the H from the peroxide group strengthens the O-O bond but weakens the C-O bond.

Figure 4.3 shows the important geometry parameters of methanol and mono- to tri- fluoro methanol molecules. Comparison see Table 4.3.

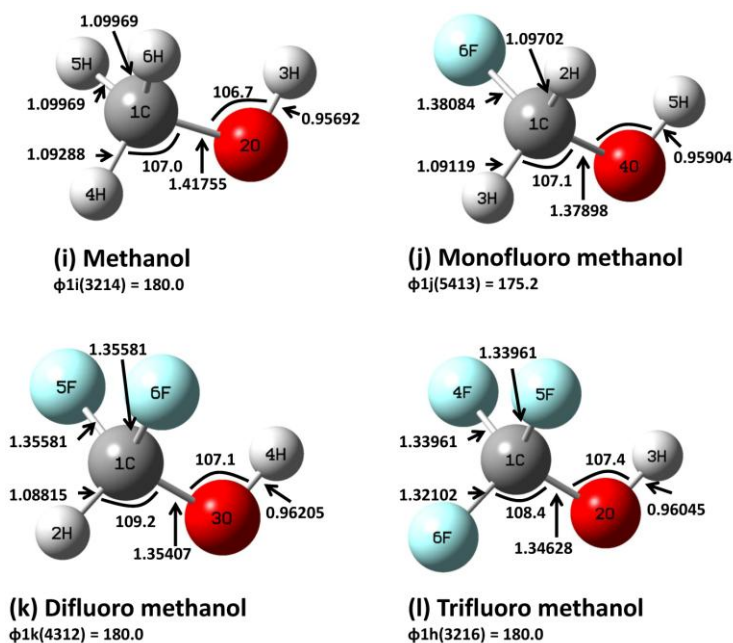


Figure 4.3 Geometry of methanol and mono- to tri- fluoro methanol molecules calculated by CBS-APNO method. Bond lengths in Å, bond angles in degree, dihedral angles in degree.

Table 4.3 Important Geometry Parameters of Methanol and Mono- to Tri-Fluoro Methanol. Bond Lengths in Å, Dihedral Angles in Degree

	B(C-F)	B(C-O)	B(O-H)	$\Phi_{1}(\text{HO-CH})$
CH₃OH		1.41755	0.95692	180.0
CH₂FOH	1.38084	1.37898	0.95904	175.2
CHF₂OH	1.35581	1.35407	0.96205	180.0
	1.35581			
CF₃OH	1.33961	1.34628	0.96045	180.0
	1.33961			
	1.32102			

Substituting a F atom for a H atom reduces the C-X bond length from 1.38084 Å (CH₂FOH) to 1.32102 Å (CF₃OH). Substituting a F atom for a H atom reduces the C-O bond length from 1.41755 Å (CH₃OH) to 1.34628 Å (CF₃OH). Substituting a F atom for a H atom lengthens the O-H bond length from 0.95692 Å (CH₃OH) to 0.96045 Å (CF₃OH). The dihedral angle HO-CH remains ~180 degree.

In summary, the substitution of F atoms strengthens the C-F and C-O bond.

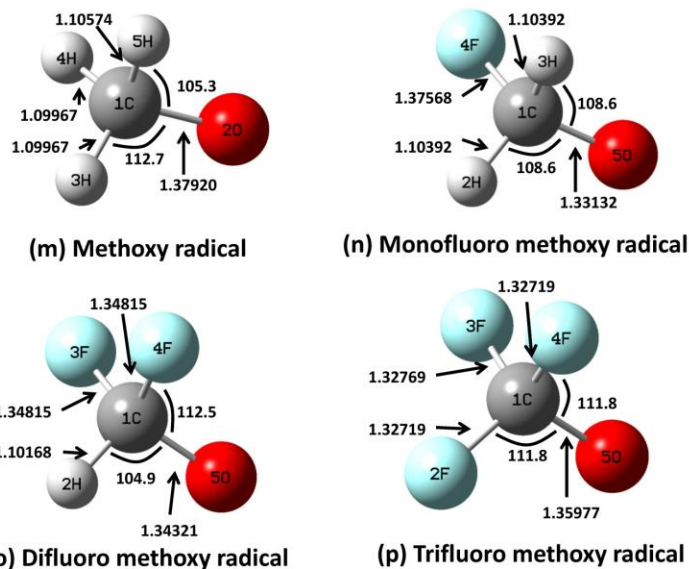


Figure 4.4 Geometry of methoxy and mono- to tri- fluoro methoxy calculated by CBS-APNO method. Bond lengths in Å, bond angles in degree, dihedral angles in degree.

Figure 4.4 shows the important geometry parameters of methoxy and mono- to tri-fluoro methoxy radicals. Comparison see Table 4.4.

Table 4.4 Important Geometry Parameters of Methoxy and Mono- to Tri-Fluoro Methoxy. Bond Lengths in Å, Dihedral Angles in Degree

	B(C-F)	B (C-O)
CH₃O•		1.37920
CH₂FO•	1.37568	1.33132
CHF₂O•	1.34815	1.34321
	1.34815	
CF₃O•	1.32769	1.35977
	1.32719	
	1.32719	

Substituting one F atom for a H atom shortens the C-F bond. Substituting a F atom for a H atom reduces the C-X bond length from 1.37568 Å (CH₂FO•) to 1.32719 Å (CF₃O•). Substituting a F atom for a H atom reduces the C-O bond from 1.37920 Å (CH₃O•) to 1.33132 Å (CH₂FO•), whereas lengthens the C-O bond from 1.33132

Å(CH₂FO•) to 1.34321 Å(CHF₂O•) and then to 1.35977 Å(CF₃O•). From CH₃OH to CH₃O•, abstracting the H atom from the -OH group shortens the C-O bond from 1.41755 Å(CH₃OH) to 1.37920 Å(CF₃OH). From CH₂FOH to CH₂FOj, abstracting the H atom from the -OH group shortens the C-O bond from 1.37898 Å(CH₂FOH) to 1.33132 Å(CH₂FO•). From CHF₂OH to CHF₂O•, abstracting the H atom from the -OH group shortens the C-O bond from 1.35407 Å(CHF₂OH) to 1.34321 Å(CHF₂O•). However, from CF₃OH to CF₃O•, abstracting the H atom from the -OH group lengthens the C-O bond from 1.34628 Å(CF₃OH) to 1.35977Å(CF₃O•).

4.3.2 Enthalpy of Formation

Table 4.5 shows the isodesmic reactions that used to determine the enthalpy of formation of each target species with three difference calculation methods. The average in bold are taken from three calculation methods with up to eight isodesmic reactions.

Table 4.5 Isodesmic Reactions and Heat of Formation for Fluoro Methyl Hydroperoxides. (All in kcal mol⁻¹)

Isodesmic reactions	$\Delta_f H^\circ_{298}$		
	CBS-QB3	CBS-APNO	G4
CH₂FOOH + CH ₄ = CH ₃ OOH + CH ₃ F	-83.52	-83.83	-83.57
CH₂FOOH + CH ₃ CH ₃ = CH ₃ OOH + CH ₃ CH ₂ F	-83.69	-84.02	-83.79
CH₂FOOH + CH ₃ CH ₂ CH ₃ = CH ₃ OOH + CH ₃ CH ₂ CH ₂ F	-83.46	-83.93	-83.85
CH₂FOOH + CH ₃ CH ₃ = CH ₃ CH ₂ OOH + CH ₃ F	-83.59	-83.95	-83.33
CH₂FOOH + CH ₃ CH ₂ CH ₃ = CH ₃ CH ₂ OOH + CH ₃ CH ₂ F	-83.73	-84.08	-83.59
CH₂FOOH + CH ₃ CH ₂ CH ₂ CH ₃ = CH ₃ CH ₂ OOH + CH ₃ CH ₂ CH ₂ F	-83.57	-84.05	-83.70
CH₂FOOH + CH ₃ CH ₂ CH ₃ = CH ₃ CH ₂ CH ₂ OOH + CH ₃ F	-83.38	-83.87	-83.61
CH₂FOOH + CH ₃ CH ₂ CH ₂ CH ₃ = CH ₃ CH ₂ CH ₂ OOH + CH ₃ CH ₂ F	-83.58	-84.07	-83.92
Method Average	-83.56	-83.98	-83.67
Average		-83.74	
Standard Deviation for the work reaction set	0.12	0.09	0.19

$\text{CHF}_2\text{OOH} + \text{CH}_4 = \text{CH}_3\text{OOH} + \text{CH}_2\text{F}_2$	-137.77	-138.36	-137.92
$\text{CHF}_2\text{OOH} + \text{CH}_3\text{CH}_3 = \text{CH}_3\text{OOH} + \text{CH}_3\text{CHF}_2$	-137.84	-138.65	-138.30
$\text{CHF}_2\text{OOH} + \text{CH}_3\text{CH}_2\text{CH}_3 = \text{CH}_3\text{OOH} + \text{CH}_3\text{CH}_2\text{CHF}_2$	-137.83	-138.78	-137.54
$\text{CHF}_2\text{OOH} + \text{CH}_3\text{CH}_3 = \text{CH}_3\text{CH}_2\text{OOH} + \text{CH}_2\text{F}_2$	-137.85	-138.48	-137.67
$\text{CHF}_2\text{OOH} + \text{CH}_3\text{CH}_2\text{CH}_3 = \text{CH}_3\text{CH}_2\text{OOH} + \text{CH}_3\text{CHF}_2$	-137.87	-138.71	-138.10
$\text{CHF}_2\text{OOH} + \text{CH}_3\text{CH}_2\text{CH}_2\text{CH}_3 = \text{CH}_3\text{CH}_2\text{OOH} +$ $\text{CH}_3\text{CH}_2\text{CHF}_2$	-137.94	-138.90	-137.39
$\text{CHF}_2\text{OOH} + \text{CH}_3\text{CH}_2\text{CH}_3 = \text{CH}_3\text{CH}_2\text{CH}_2\text{OOH} + \text{CH}_2\text{F}_2$	-137.63	-138.41	-137.95
$\text{CHF}_2\text{OOH} + \text{CH}_3\text{CH}_2\text{CH}_2\text{CH}_3 = \text{CH}_3\text{CH}_2\text{CH}_2\text{OOH} +$ CH_3CHF_2	-137.73	-138.69	-138.43
Method Average	-137.81	-138.62	-137.91
Average		-138.11	
Standard Deviation for the work reaction set	0.10	0.19	0.36
$\text{CF}_3\text{OOH} + \text{CH}_4 = \text{CH}_3\text{OOH} + \text{CHF}_3$	-193.09	-193.81	-193.31
$\text{CF}_3\text{OOH} + \text{CH}_3\text{CH}_3 = \text{CH}_3\text{OOH} + \text{CH}_3\text{CF}_3$	-192.93	-194.19	-193.71
$\text{CF}_3\text{OOH} + \text{CH}_3\text{CH}_2\text{CH}_3 = \text{CH}_3\text{OOH} + \text{CH}_3\text{CH}_2\text{CF}_3$	-192.69	-194.19	-193.71
$\text{CF}_3\text{OOH} + \text{CH}_3\text{CH}_3 = \text{CH}_3\text{CH}_2\text{OOH} + \text{CHF}_3$	-193.17	-193.93	-193.07
$\text{CF}_3\text{OOH} + \text{CH}_3\text{CH}_2\text{CH}_3 = \text{CH}_3\text{CH}_2\text{OOH} + \text{CH}_3\text{CF}_3$	-194.24	-194.24	-193.51
$\text{CF}_3\text{OOH} + \text{CH}_3\text{CH}_2\text{CH}_2\text{CH}_3 = \text{CH}_3\text{CH}_2\text{OOH} +$ $\text{CH}_3\text{CH}_2\text{CF}_3$	-192.80	-194.34	-193.45
$\text{CF}_3\text{OOH} + \text{CH}_3\text{CH}_2\text{CH}_3 = \text{CH}_3\text{CH}_2\text{CH}_2\text{OOH} + \text{CHF}_3$	-192.95	-193.85	-193.35
$\text{CF}_3\text{OOH} + \text{CH}_3\text{CH}_2\text{CH}_2\text{CH}_3 = \text{CH}_3\text{CH}_2\text{CH}_2\text{OOH} +$ CH_3CF_3	-192.82	-194.23	-193.84
Method Average	-193.09	-194.10	-193.49
Average		-193.56	
Standard Deviation for the work reaction set	0.49	0.20	0.25
$\text{CH}_2\text{FOO}\cdot + \text{HOOH} = \text{CH}_2\text{FOOH} + \text{HOOj}$	-44.38	-44.61	-45.08
$\text{CH}_2\text{FOO}\cdot + \text{CH}_4 = \text{CH}_2\text{FOOH} + \text{CH}_3\text{j}$	-44.27	-45.57	-45.06
$\text{CH}_2\text{FOO}\cdot + \text{CH}_3\text{CH}_3 = \text{CH}_2\text{FOOH} + \text{CH}_3\text{CH}_2\text{j}$	-44.66	-46.05	-45.34
$\text{CH}_2\text{FOO}\cdot + \text{CH}_3\text{CH}_2\text{CH}_3 = \text{CH}_2\text{FOOH} + \text{CH}_3\text{CH}_2\text{CH}_2\text{j}$	-44.40	-45.85	-44.81
$\text{CH}_2\text{FOO}\cdot + \text{CH}_3\text{OOH} = \text{CH}_2\text{FOOH} + \text{CH}_3\text{OOj}$	-44.53	-44.70	-45.02
$\text{CH}_2\text{FOO}\cdot + \text{CH}_3\text{CH}_2\text{OOH} = \text{CH}_2\text{FOOH} + \text{CH}_3\text{CH}_2\text{OOj}$	-44.48	-44.71	-45.11
$\text{CH}_2\text{FOO}\cdot + \text{CH}_3\text{CH}_2\text{CH}_2\text{OOH} = \text{CH}_2\text{FOOH} +$ $\text{CH}_3\text{CH}_2\text{CH}_2\text{OOj}$	-44.70	-44.91	-44.63
Method Average	-44.49	-45.20	-45.01
Average		-44.90	
Standard Deviation for the work reaction set	0.16	0.61	0.23
$\text{CHF}_2\text{OO}\cdot + \text{HOOH} = \text{CHF}_2\text{OOH} + \text{HOOj}$	-98.35	-98.63	-100.16
$\text{CHF}_2\text{OO}\cdot + \text{CH}_4 = \text{CHF}_2\text{OOH} + \text{CH}_3\text{j}$	-98.25	-99.59	-100.15
$\text{CHF}_2\text{OO}\cdot + \text{CH}_3\text{CH}_3 = \text{CHF}_2\text{OOH} + \text{CH}_3\text{CH}_2\text{j}$	-98.64	-100.08	-100.43
$\text{CHF}_2\text{OO}\cdot + \text{CH}_3\text{CH}_2\text{CH}_3 = \text{CHF}_2\text{OOH} + \text{CH}_3\text{CH}_2\text{CH}_2\text{j}$	-98.38	-99.87	-99.89
$\text{CHF}_2\text{OO}\cdot + \text{CH}_3\text{OOH} = \text{CHF}_2\text{OOH} + \text{CH}_3\text{OOj}$	-98.51	-98.72	-100.10
$\text{CHF}_2\text{OO}\cdot + \text{CH}_3\text{CH}_2\text{OOH} = \text{CHF}_2\text{OOH} + \text{CH}_3\text{CH}_2\text{OOj}$	-98.45	-98.73	-100.20
$\text{CHF}_2\text{OO}\cdot + \text{CH}_3\text{CH}_2\text{CH}_2\text{OOH} = \text{CHF}_2\text{OOH} +$ $\text{CH}_3\text{CH}_2\text{CH}_2\text{OOj}$	-98.68	-98.93	-99.72
Method Average	-98.47	-99.22	-100.09
Average		-99.26	
Standard Deviation for the work reaction set	0.16	0.61	0.23
$\text{CF}_3\text{OO}\cdot + \text{HOOH} = \text{CF}_3\text{OOH} + \text{HOOj}$	-152.72	-152.96	-154.97

$\text{CF}_3\text{OO}\bullet + \text{CH}_4 = \text{CF}_3\text{OOH} + \text{CH}_3\text{j}$	-152.61	-153.92	-154.96
$\text{CF}_3\text{OO}\bullet + \text{CH}_3\text{CH}_3 = \text{CF}_3\text{OOH} + \text{CH}_3\text{CH}_2\text{j}$	-153.00	-154.41	-155.24
$\text{CF}_3\text{OO}\bullet + \text{CH}_3\text{CH}_2\text{CH}_3 = \text{CF}_3\text{OOH} + \text{CH}_3\text{CH}_2\text{CH}_2\text{j}$	-152.74	-154.20	-154.70
$\text{CF}_3\text{OO}\bullet + \text{CH}_3\text{OOH} = \text{CF}_3\text{OOH} + \text{CH}_3\text{OOj}$	-152.87	-153.05	-154.91
$\text{CF}_3\text{OO}\bullet + \text{CH}_3\text{CH}_2\text{OOH} = \text{CF}_3\text{OOH} + \text{CH}_3\text{CH}_2\text{OOj}$	-152.82	-153.06	-155.01
$\text{CF}_3\text{OO}\bullet + \text{CH}_3\text{CH}_2\text{CH}_2\text{OOH} = \text{CF}_3\text{OOH} + \text{CH}_3\text{CH}_2\text{CH}_2\text{OOj}$	-153.04	-153.26	-154.53
Method Average	-152.83	-153.55	-154.90
Average		-153.76	
Standard Deviation for the work reaction set	0.16	0.61	0.23
$\text{CH}_2\text{FOH} + \text{CH}_4 = \text{CH}_3\text{OH} + \text{CH}_3\text{F}$	-101.48	-101.84	-101.61
$\text{CH}_2\text{FOH} + \text{CH}_3\text{CH}_3 = \text{CH}_3\text{OH} + \text{CH}_3\text{CH}_2\text{F}$	-101.65	-102.04	-101.83
$\text{CH}_2\text{FOH} + \text{CH}_3\text{CH}_2\text{CH}_3 = \text{CH}_3\text{OH} + \text{CH}_3\text{CH}_2\text{CH}_2\text{F}$	-101.42	-101.94	-101.90
$\text{CH}_2\text{FOH} + \text{CH}_3\text{CH}_3 = \text{CH}_3\text{CH}_2\text{OH} + \text{CH}_3\text{F}$	-101.84	-102.22	-102.00
$\text{CH}_2\text{FOH} + \text{CH}_3\text{CH}_2\text{CH}_3 = \text{CH}_3\text{CH}_2\text{OH} + \text{CH}_3\text{CH}_2\text{F}$	-101.97	-102.35	-102.26
$\text{CH}_2\text{FOH} + \text{CH}_3\text{CH}_2\text{CH}_2\text{CH}_3 = \text{CH}_3\text{CH}_2\text{OH} + \text{CH}_3\text{CH}_2\text{CH}_2\text{F}$	-101.81	-102.32	-102.37
Method Average	-101.69	-102.12	-102.00
Average		-101.94	
Standard Deviation for the work reaction set	0.22	0.21	0.28
$\text{CHF}_2\text{OH} + \text{CH}_4 = \text{CH}_3\text{OH} + \text{CH}_2\text{F}_2$	-161.09	-161.64	-161.17
$\text{CHF}_2\text{OH} + \text{CH}_3\text{CH}_3 = \text{CH}_3\text{OH} + \text{CH}_3\text{CHF}_2$	-161.16	-161.92	-161.56
$\text{CHF}_2\text{OH} + \text{CH}_3\text{CH}_2\text{CH}_3 = \text{CH}_3\text{OH} + \text{CH}_3\text{CH}_2\text{CHF}_2$	-161.15	-162.06	-160.80
$\text{CHF}_2\text{OH} + \text{CH}_3\text{CH}_3 = \text{CH}_3\text{CH}_2\text{OH} + \text{CH}_2\text{F}_2$	-161.45	-162.02	-161.56
$\text{CHF}_2\text{OH} + \text{CH}_3\text{CH}_2\text{CH}_3 = \text{CH}_3\text{CH}_2\text{OH} + \text{CH}_3\text{CHF}_2$	-161.47	-162.24	-161.99
$\text{CHF}_2\text{OH} + \text{CH}_3\text{CH}_2\text{CH}_2\text{CH}_3 = \text{CH}_3\text{CH}_2\text{OH} + \text{CH}_3\text{CH}_2\text{CHF}_2$	-161.55	-162.44	-161.28
Method Average	-161.31	-162.05	-161.40
Average		-161.59	
Standard Deviation for the work reaction set	0.18	0.25	0.33
$\text{CF}_3\text{OH} + \text{CH}_4 = \text{CH}_3\text{OH} + \text{CHF}_3$	-217.53	-218.21	-217.70
$\text{CF}_3\text{OH} + \text{CH}_3\text{CH}_3 = \text{CH}_3\text{OH} + \text{CH}_3\text{CF}_3$	-217.37	-218.59	-218.11
$\text{CF}_3\text{OH} + \text{CH}_3\text{CH}_2\text{CH}_3 = \text{CH}_3\text{OH} + \text{CH}_3\text{CH}_2\text{CF}_3$	-217.13	-218.62	-218.00
$\text{CF}_3\text{OH} + \text{CH}_3\text{CH}_3 = \text{CH}_3\text{CH}_2\text{OH} + \text{CHF}_3$	-217.89	-218.59	-218.09
$\text{CF}_3\text{OH} + \text{CH}_3\text{CH}_2\text{CH}_3 = \text{CH}_3\text{CH}_2\text{OH} + \text{CH}_3\text{CF}_3$	-217.68	-218.90	-218.54
$\text{CF}_3\text{OH} + \text{CH}_3\text{CH}_2\text{CH}_2\text{CH}_3 = \text{CH}_3\text{CH}_2\text{OH} + \text{CH}_3\text{CH}_2\text{CF}_3$	-217.52	-219.00	-218.48
Method Average	-217.52	-218.65	-218.15
Average		-218.11	
Standard Deviation for the work reaction set	0.26	0.28	0.31
$\text{CH}_2\text{FO}\bullet + \text{CH}_3\text{OH} = \text{CH}_2\text{FOH} + \text{CH}_3\text{Oj}$	-49.30	-49.12	-49.66
$\text{CH}_2\text{FO}\bullet + \text{CH}_3\text{CH}_2\text{OH} = \text{CH}_2\text{FOH} + \text{CH}_3\text{CH}_2\text{Oj}$	-49.13	-48.89	-48.56
Method Average	-49.22	-49.00	-49.11
Average		-49.11	
Standard Deviation for the work reaction set	0.12	0.16	0.77
$\text{CHF}_2\text{O}\bullet + \text{CH}_3\text{OH} = \text{CHF}_2\text{OH} + \text{CH}_3\text{Oj}$	-97.59	-97.86	-98.75
$\text{CHF}_2\text{O}\bullet + \text{CH}_3\text{CH}_2\text{OH} = \text{CHF}_2\text{OH} + \text{CH}_3\text{CH}_2\text{Oj}$	-97.41	-97.63	-97.65
Method Average	-97.50	-97.75	-98.20
Average		-97.82	

Standard Deviation for the work reaction set	0.12	0.16	0.77
$\text{CF}_3\text{O}\cdot + \text{CH}_3\text{OH} = \text{CF}_3\text{OH} + \text{CH}_3\text{Oj}$	-149.93	-150.63	-151.66
$\text{CF}_3\text{O}\cdot + \text{CH}_3\text{CH}_2\text{OH} = \text{CF}_3\text{OH} + \text{CH}_3\text{CH}_2\text{Oj}$	-149.76	-150.40	-150.56
Method Average	-149.84	-150.51	-151.11
Average		-150.49	
Standard Deviation for the work reaction set	0.12	0.16	0.77
$\text{CH}_2\text{F}\cdot + \text{CH}_4 = \text{CH}_3\text{j} + \text{CH}_3\text{F}$	-7.26	-7.55	-7.38
$\text{CH}_2\text{F}\cdot + \text{CH}_3\text{CH}_3 = \text{CH}_3\text{CH}_2\text{j} + \text{CH}_3\text{F}$	-7.65	-8.03	-7.66
$\text{CH}_2\text{F}\cdot + \text{CH}_3\text{CH}_2\text{CH}_3 = \text{CH}_3\text{CH}_2\text{CH}_2\text{j} + \text{CH}_3\text{F}$	-7.39	-7.82	-7.13
$\text{CH}_2\text{F}\cdot + \text{CH}_3\text{CH}_3 = \text{CH}_3\text{j} + \text{CH}_3\text{F}$	-7.43	-7.74	-7.60
$\text{CH}_2\text{F}\cdot + \text{CH}_3\text{CH}_2\text{CH}_3 = \text{CH}_3\text{CH}_2\text{j} + \text{CH}_3\text{CH}_2\text{F}$	-7.78	-8.16	-7.92
$\text{CH}_2\text{F}\cdot + \text{CH}_3\text{CH}_2\text{CH}_3 = \text{CH}_3\text{j} + \text{CH}_3\text{CH}_2\text{CH}_2\text{F}$	-7.20	-7.65	-7.67
Method Average	-7.45	-7.79	-7.52
Average		-7.61	
Standard Deviation for the work reaction set	0.28	0.34	0.20
$\text{CHF}_2\cdot + \text{CH}_4 = \text{CH}_3\text{j} + \text{CH}_2\text{F}_2$	-58.26	-58.89	-58.64
$\text{CHF}_2\cdot + \text{CH}_3\text{CH}_3 = \text{CH}_3\text{CH}_2\text{j} + \text{CH}_2\text{F}_2$	-58.65	-59.37	-58.92
$\text{CHF}_2\cdot + \text{CH}_3\text{CH}_2\text{CH}_3 = \text{CH}_3\text{CH}_2\text{CH}_2\text{j} + \text{CH}_2\text{F}_2$	-58.39	-59.16	-58.38
$\text{CHF}_2\cdot + \text{CH}_3\text{CH}_3 = \text{CH}_3\text{j} + \text{CH}_3\text{CHF}_2$	-58.33	-59.17	-59.02
$\text{CHF}_2\cdot + \text{CH}_3\text{CH}_2\text{CH}_3 = \text{CH}_3\text{CH}_2\text{j} + \text{CH}_3\text{CHF}_2$	-58.68	-59.59	-59.34
$\text{CHF}_2\cdot + \text{CH}_3\text{CH}_2\text{CH}_3 = \text{CH}_3\text{j} + \text{CH}_3\text{CH}_2\text{CHF}_2$	-58.32	-59.31	-58.26
Method Average	-58.45	-59.13	-58.78
Average		-58.82	
Standard Deviation for the work reaction set	0.28	0.34	0.20
$\text{CF}_3\cdot + \text{CH}_4 = \text{CH}_3\text{j} + \text{CHF}_3$	-111.87	-112.58	-112.60
$\text{CF}_3\cdot + \text{CH}_3\text{CH}_3 = \text{CH}_3\text{CH}_2\text{j} + \text{CHF}_3$	-112.26	-113.08	-112.88
$\text{CF}_3\cdot + \text{CH}_3\text{CH}_2\text{CH}_3 = \text{CH}_3\text{CH}_2\text{CH}_2\text{j} + \text{CHF}_3$	-112.00	-112.86	-112.35
$\text{CF}_3\cdot + \text{CH}_3\text{CH}_3 = \text{CH}_3\text{j} + \text{CH}_3\text{CF}_3$	-111.70	-112.96	-113.01
$\text{CF}_3\cdot + \text{CH}_3\text{CH}_2\text{CH}_3 = \text{CH}_3\text{CH}_2\text{j} + \text{CH}_3\text{CF}_3$	-112.05	-113.38	-113.32
$\text{CF}_3\cdot + \text{CH}_3\text{CH}_2\text{CH}_3 = \text{CH}_3\text{j} + \text{CH}_3\text{CH}_2\text{CF}_3$	-111.47	-112.99	-112.90
Method Average	-112.06	-112.82	-112.74
Average		-112.57	
Standard Deviation for the work reaction set	0.28	0.34	0.20

Table 4.6 summarizes the enthalpy of formation for each target species and compares with available literature data.

Table 4.6 Enthalpy of Formation of Each Target Molecules in this Study Compare to Available Literatures (All in kcal mol⁻¹)

Species	$\Delta\text{H}_{\text{f},298}^{\circ}$ ^a	Diff. ^a	Literature ^a
CH_3OOH	-30.96 ^b		
CH_2FOOH	-83.7	52.8	-86.7 ^{d,e} , -84.0 ^{d,f} , -86.1 ^{d,g} , -83.9 ^{d,h} , -82.5 ^k ,
CHF_2OOH	-138.1	54.4	-144.0 ^{d,e} , -139.1 ^{d,f} , -142.6 ^{d,g} , -138.3 ^{d,h} , -136.9 ^k ,

CF₃OOH	-193.6	55.5	-199.8 ^{d,e} , -194.3 ^{d,f} , -197.4 ^{d,g} , -192.4 ^{d,h} , -191.0 ^d , -191.9 ^k
CH₃OO•	2.37 ^b		
CH₂FOO•	-44.9	47.3	
CHF₂OO•	-99.6	54.4	
CF₃OO•	-153.8	54.5	
CH₃OH	-47.97 ^c		
CH₂FOH	-101.9	53.8	
CHF₂OH	-161.6	59.7	
CF₃OH	-218.1	56.5	-217.7 ⁱ , -213.5 ^j
CH₃O•	5.15±0.08 ^c		
CH₂FO•	-49.1	54.3	
CHF₂O•	-97.8	48.7	
CF₃O•	-150.5	52.7	-156.7 ^j , -150.4 ⁱ
CH₃•	34.98 ^c		
CH₂F•	-7.6	42.6	-6.9 ^k
CHF₂•	-58.8	51.2	-57.6 ^k
CF₃•	-112.6	53.8	-110.8 ⁱ , -111.3 ^k

^a Units in kcal mol⁻¹. ^b Wang¹¹⁰. ^c Ruscic¹¹¹. ^d El-Taher. ^e MP2(FULL)/6-31G(d,p). ^f MP4(SDTQ)/6-311+G(d,p). ^g B3LYP/6-31G(d,p). ^h B3LYP/6-311+G(2df,2p). ⁱ Schneider¹⁰⁴. ^j Batt¹¹². ^k Kosmas¹⁰⁹.

This study's standard enthalpies of fluoro hydroperoxide molecules, CH₂FOOH, CHF₂OOH, and CF₃OOH, agree with El-Taher's¹⁰⁷ determination calculated by the B3LYP/6-311+G(2df,2p) method.

This study's standard enthalpies of CF₃OH and CF₃O• agree with Schneider et al.'s¹⁰⁴ determination. However, this study's values of CF₃OH is ~5 kcal mol⁻¹ lower than Batt et al.¹¹², and this study's values of CF₃O• is ~6 kcal mol⁻¹ higher than Batt et al.¹¹²

This study's standard enthalpies of CH₂F•, CHF₂•, and CF₃•, agree with Kosmas et al.'s¹⁰⁹ determination.

Substituting one F atom for a H atom on the methyl group of methyl hydroperoxide, methyl hydroperoxy, methanol, methoxy, and methane molecules results in stabilization of the system by ranging from 43 kcal mol⁻¹ to 60 kcal mol⁻¹ energy.

4.3.3 Internal Rotor Potential Energy Diagrams

Figure 4.5 shows the potential energy profiles of the 2 internal rotors in the methyl hydroperoxide and mono- to tri-fluoro hydroperoxide molecules. Table 4.7 summaries the internal rotor energy barriers for methyl hydroperoxide and mono- to tri-fluoro hydroperoxides.

Table 4.7 Energy Barrier for Each Internal Rotor in Methyl Hydroperoxide and Mono- to Tri-Fluoro Methyl Hydroperoxides (Units in kcal mol⁻¹)

	R-OOH (diamond symbol)	RO-OH (square symbol)
CH₃OOH	2.9	6.8
CH₂FOOH	12.8	7.9
CHF₂OOH	7.6	5.1
CF₃OOH	4.7	6.6

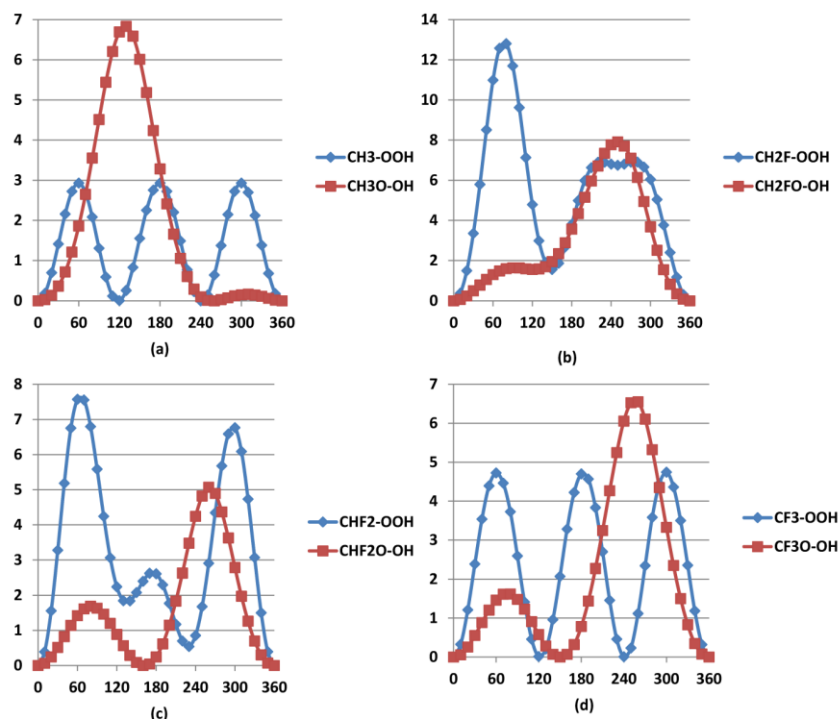


Figure 4.5 Potential Energy Profiles of the Internal Rotors of the Methyl Hydroperoxide and Mono- to Tri- Fluoro Hydroperoxides (a-d). The Solid Lines are the Fit of the Fourier Series Expansions.

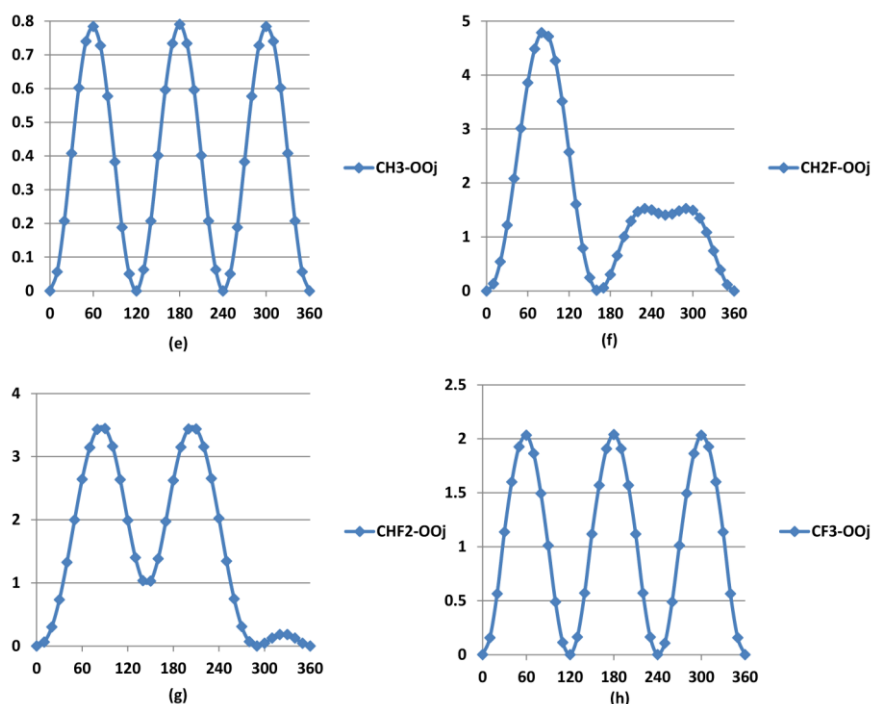


Figure 4.6 Potential Energy Profiles of the Internal Rotors of the Methyl Hydroperoxy and Mono- to Tri- Fluoro Hydroperoxy Radicals (e-h). The Solid Lines are the Fit of the Fourier Series Expansions.

Table 4.8 Energy Barrier for Each Internal Rotor in Methyl Hydroperoxy and Mono- to Tri-Fluoro Methyl Hydroperoxy Radicals (Units in kcal mol⁻¹)

	R-OO• (diamond symbol)
CH₃OO•	0.8
CH₂FOO•	4.8
CHF₂OO•	3.4
CF₃OO•	2.0

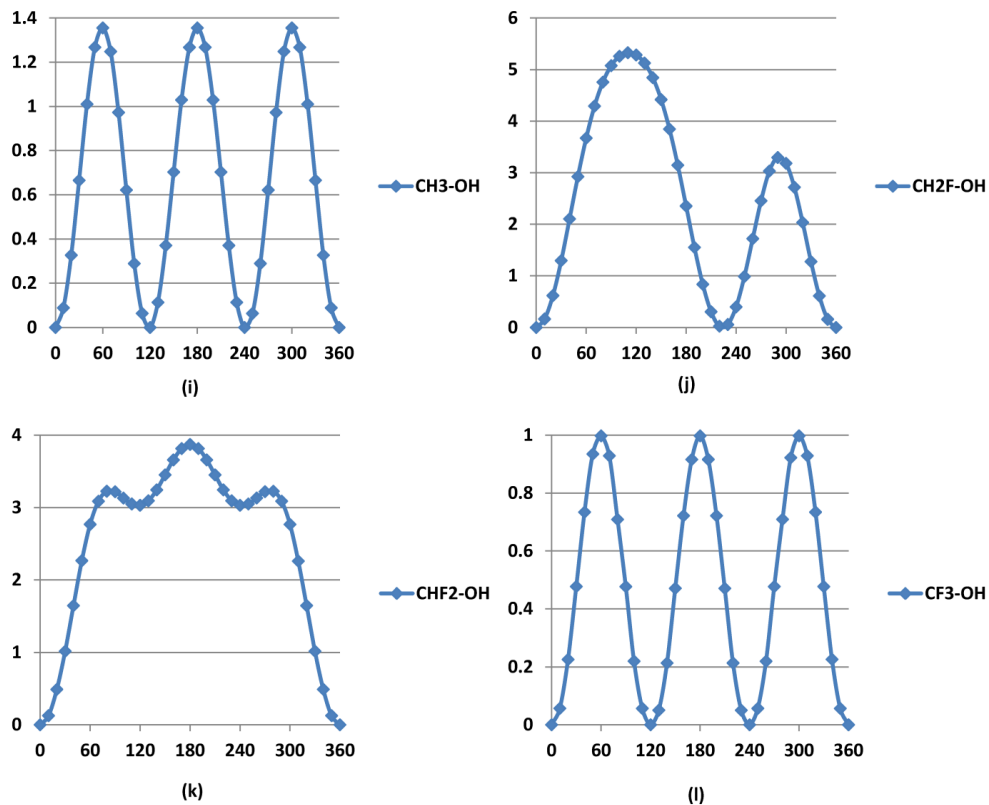


Figure 4.7 Potential Energy Profiles of the Internal Rotors of the Methanol and Mono- to Tri- Fluoro Methanol (i-l). The solid Lines are the Fit of the Fourier Series Expansions.

Table 4.9 Energy Barrier for Each Internal Rotor in Methanol and Mono- to Tri-Fluoro Methanol. (Units in kcal mol⁻¹).

	R-OH (diamond symbol)
CH₃OH	1.4
CH₂FOH	5.3
CHF₂OH	3.9
CF₃OH	1.0

4.3.4 Entropy and Heat Capacity

Table 4.10 lists the standard entropy and heat capacities at 300 K, 400 K, 500 K, 600 K, 800 K, 1000 K, and 1500 K. TVR represents the sum of the contributions from translations, vibrations, and external rotations. Internal rotor indicates the contribution from hindered internal rotation, which replaces the torsion frequency contributions in the TVR heat capacity and entropy data summations.

Table 4.10 Ideal Gas Phase Entropy and Heat Capacity Obtained by B3LYP/6-31+G(d,p) Calculation, Comparison with available Literature

		S°_{298}	C_{p300}	C_{p400}	C_{p500}	C_{p600}	C_{p800}	C_{p1000}	C_{p1500}
CH ₂ FOOH	TVR	64.28	12.38	15.22	17.78	19.91	23.08	25.33	28.77
	Internal rotor	6.73	5.67	5.12	4.78	4.59	4.36	4.14	3.56
	Total	71.01	18.05	20.34	22.56	24.50	27.44	29.47	32.33
CHF ₂ OOH	TVR	67.82	14.52	17.66	20.28	22.35	25.24	27.16	29.92
	Internal rotor	8.60	4.90	4.58	4.27	4.02	3.64	3.35	2.86
	Total	76.42	19.42	22.24	24.55	26.36	28.89	30.51	32.78
CF ₃ OOH	TVR	68.78	17.18	20.57	23.16	25.08	27.59	29.12	31.14
	Internal rotor	9.09	3.96	4.03	4.01	3.93	3.65	3.36	2.84
	Total	77.87	21.14	24.61	27.17	29.00	31.24	32.48	33.98
CH ₂ FOH	TVR	60.42	10.57	12.80	14.93	16.76	19.60	21.68	24.93
	Internal rotor	2.62	1.82	2.07	2.15	2.14	1.99	1.81	1.48
	Total	63.04	12.39	14.86	17.08	18.90	21.59	23.48	26.41
CHF ₂ OH	TVR	64.35	12.65	15.28	17.51	19.29	21.83	23.55	26.10
	Internal rotor	4.53	3.40	3.66	3.41	2.99	2.27	1.83	1.36
	Total	68.87	16.04	18.94	20.92	22.28	24.10	25.38	27.45
CF ₃ OH	TVR	65.46	15.20	18.16	20.40	22.06	24.22	25.55	27.34
	Internal rotor	4.40	1.35	1.24	1.17	1.12	1.07	1.05	1.02

	Total	69.86	16.55	19.40	21.57	23.18	25.30	26.59	28.36
CH ₂ FOO•	TVR	65.34	12.09	14.64	16.93	18.81	21.59	23.48	26.22
	Internal rotor	5.99	2.35	2.06	1.86	1.72	1.53	1.40	1.23
	Total	71.33	14.44	16.70	18.78	20.53	23.11	24.89	27.46
CHF ₂ OO•	TVR	69.10	14.40	17.20	19.51	21.31	23.79	25.34	27.39
	Internal rotor	6.09	2.05	2.09	2.02	1.91	1.68	1.51	1.27
	Total	75.20	16.45	19.29	21.53	23.22	25.47	26.85	28.66
CF ₃ OO•	TVR	70.10	17.02	20.11	22.40	24.07	26.16	27.33	28.63
	Internal rotor	6.64	2.22	1.95	1.71	1.54	1.33	1.22	1.10
	Total	76.74	19.24	22.05	24.12	15.61	27.50	28.55	29.73
CH ₂ FO•	TVR	61.57	10.96	13.13	15.04	16.60	18.91	20.52	22.85
CHF ₂ O•	TVR	65.86	12.95	15.37	17.31	18.81	20.85	22.14	23.85
CF ₃ O•	TVR	68.03	15.66	18.16	20.00	21.33	22.99	23.90	24.92
CH ₂ F•	TVR	54.99	9.64	10.77	11.81	12.70	14.12	15.22	17.05
CHF ₂ •	TVR	59.89	10.13	11.66	13.00	14.07	15.60	16.61	18.04
CF ₃ •	TVR	63.37	12.05	13.86	15.25	16.27	17.58	18.31	19.13

4.3.5 Bond Dissociation Energies at 298 K

Table 4.11 shows the summary and comparison of bond dissociation energies with available literature.

Table 4.11 Summary and Comparison of Bond Dissociation Energies with Available Literature (All in kcal mol⁻¹)

	R = CH ₃	R = CH ₂ F	R = CHF ₂	R = CF ₃
ROO-H	85.3 87.6 ^{a,b} , 86.7 ^{a,c} , 86.9 ^{a,d} , 86.1 ^{a,e}	90.9 95.0 ^{a,b} , 93.8 ^{a,c} , 94.2 ^{a,d} , 93.3 ^{a,e}	91.0 94.1 ^{a,b} , 90.2 ^{a,c} , 93.8 ^{a,d} , 93.4 ^{a,e}	91.9 94.5 ^{a,b} , 93.4 ^{a,c} , 94.1 ^{a,d} , 93.5 ^{a,e} , 95.1 ^f ,
RO-OH	44.0 48.2 ^{a,b} , 47.7 ^{a,c} , 42.9 ^{a,d} , 42.7 ^{a,e}	43.6 47.9 ^{a,b} , 46.8 ^{a,c} , 40.5 ^{a,d} , 39.9 ^{a,e}	49.3 52.2 ^{a,b} , 48.6 ^{a,c} , 46.5 ^{a,d} , 46.3 ^{a,e}	52.0 49.5 ^{a,b} , 53.2 ^{a,c} , 48.9 ^{a,d} , 49.5 ^{a,e} , 49.7 ^f , 49.4 ^h ,
R-OOH	68.9 72.1 ^{a,b} , 66.8 ^{a,c} , 63.0 ^{a,d} , 61.0 ^{a,e}	79.1 83.8 ^{a,b} , 77.2 ^{a,c} , 72.3 ^{a,d} , 69.9 ^{a,e} , 72.9 ^g ,	82.2 88.3 ^{a,b} , 77.6 ^{a,c} , 75.5 ^{a,d} , 71.6 ^{a,e} , 74.8 ^g ,	83.9 87.7 ^{a,b} , 82.3 ^{a,c} , 77.0 ^{a,d} , 72.2 ^{a,e} , 83.5 ^f , 75.8 ^g ,
RO-Oj	61.3^k	55.4	61.0	62.8 57.0 ^f ,
R-OOj	32.6^k	37.3	40.4	41.2 37.0 ^f ,
R-OH	91.9^l	103.3	111.7	114.5 116.2 ^f ,
RO-H	105.3^l	104.9	115.9	119.7 119.4 ^f , 118.8 ^h , 124.7 ⁱ , 117.5 ^j ,
R-Oj	89.4^l	101.1	98.6	97.5 99.2 ^f
R-H	104.9^l	100.8	101.4	106.2

^a El-Taher ¹⁰⁷. ^b MP2(FULL)/6-31G(d,p). ^c MP4(SDTQ)/6-311+G(d,p). ^d B3LYP/6-31G(d,p). ^e B3LYP/6-311+G(2df,2p). ^f Schneider. ^g Kosmas. ^h Reints. ⁱ Huey. ^j Asher. ^k Wang. ^l Ruscic.

The ROO-H bond is the strongest, about 90 kcal mol⁻¹, which is about two times of the RO-OH bond, and is about 10 kcal mol⁻¹ higher than the R-OOH bond. Fluorine substitution stabilizes each kind of bond. The first F atom substitution contributes more in the R-O and O-H bonds than the second and the third F atom. The second F atom substitution contributes more in the O-O bond than the first and the third F atom.

Eliminating the terminal H atom in the peroxide group switches the O-O bond from the weakest to the strongest. The R-OO• bonds are about one half of the R-OOH bonds.

R-OH bonds are $\sim 25\text{-}30 \text{ kcal mol}^{-1}$ stronger than the R-OOH bonds, and are about three times stronger than the R-OO• bonds. RO-H bonds are $\sim 15\text{-}20 \text{ kcal mol}^{-1}$ stronger than the ROO-H bonds.

The R-OH bonds are $\sim 2 \text{ kcal mol}^{-1}$ stronger than the R-O• bonds in methanol, mono- and di-fluoro methanol, and the R-OH bond is $\sim 17 \text{ kcal mol}^{-1}$ stronger than the R-O• in tri-fluoro methanol.

4.4 Summary

Standard enthalpy of formation of fluoro methyl hydroperoxide, $\text{CH}_3\text{-xFxOOH}$ ($1 \leq x \leq 3$), fluoro methyl hydroperoxy, $\text{CH}_3\text{-xFxOO}\cdot$ ($1 \leq x \leq 3$), and fluoro methanol, $\text{CH}_3\text{-xFxOH}$, are determined by CBS-QB3, CBS-APNO, and G4 methods. Small standard deviations show good error cancellation of isodesmic reactions. Standard entropy and heat capacity as a function of temperature are determined with B3LYP/6-31+G(d,p) optimized structure and frequencies. Internal rotors have been investigated by intramolecular torsion potential curves at the B3LYP/6-31+G(d,p) level. Bond dissociation energy between R-OOH, RO-OH, ROO-H, R-OO•, RO-O•, R-OH, RO-H, R-O•, and R-H have been determined and compared with literature.

CHAPTER 5

THERMOCHEMISTRY AND KINETIC ANALYSIS OF UNIMOLECULAR OXIRANYL RADICAL DISSOCIATION REACTION: A THEORETICAL STUDY

5.1 Overview

In the chemistry of hydrocarbons, a number of experiment studies on the formation of cyclic ethers under ambient conditions and in the early stages of combustion have been reported¹¹³⁻¹¹⁶. The earliest experiment that this study is aware of is that of Baldwin et al.¹¹⁷, who observed the formation of oxirane from a reaction between an ethyl radical and O₂. Several more recent experimental results showing the formation of cyclic ethers in significant concentrations from the oxidation of hydrocarbons over a low-to moderate temperature range of combustion, have been reported by Battin-Leclerc et al.¹¹³, Dagaut et al.¹¹⁴⁻¹¹⁵, and Yahyaoui et al.¹¹⁶. There are also computational studies that show the pathways of the formation of three-membered to five- membered cyclic ethers from the corresponding hydroperoxy alkyl radicals, of which Wijaya et al.¹⁰¹ and Zador et al.¹¹⁸ have given overviews. The pathway to cyclic ethers starts with the association of an alkyl hydrocarbon radical with molecular oxygen to form a peroxy radical. The peroxy radical then undergoes an intramolecular hydrogen transfer to form a hydroperoxide alkyl radical. The radical site on this alkyl radical then attacks the peroxide oxygen atom, which is bonded to a carbon atom and cleaves the weak RO-OH bond to form a cyclic ether. Sun and Bozzelli¹¹⁹, reported calculations on the association reaction of hydroperoxy neopentyl radicals with molecular oxygen, which forms cyclic ethers and OH radical as products. Bugler et al.¹²⁰. updated the kinetics of the formation of cyclic ethers to better fit their experimental data on the parent hydrocarbon conversion profiles versus temperature, in the

negative temperature regime. Auzmendi-Murua and Bozzelli¹²¹ used isopentanol as an example to illustrate the formation of cyclic ethers through the oxidation of an alcohol under combustion conditions. They also represented a pathway for the formation of cyclic ethers from an α,β unsaturated hydrocarbon reaction with a OH radical and O₃, which occurred under ambient conditions.

The formed cyclic ethers undergo abstraction reactions with the radical pool to form cyclic ether radicals through combustion and oxidation under ambient conditions. The unimolecular dissociation reactions of the three-membered cyclic ether radical (oxiranyl radical) are the focus of this study. The parent oxiranyl radical and radicals formed from its dissociation reaction paths can undergo further unimolecular dissociation or a chemical activation reaction with ³O₂ to form energized peroxy radicals. The chemical activation reactions with O₂ form the second part of the investigation on oxiranyl radical chemistry and are considered in a separate publication.

The thermochemical properties of oxirane and the oxiranyl radical have been determined in previous studies¹²¹⁻¹²² together with the bond-dissociation energies, which are needed to further understand the dissociation and oxidation kinetics. Abstraction reactions via the radical pool species will cleave the 104.5 kcal mol⁻¹ carbon-hydrogen bond of oxirane and form a carbon-centered oxiranyl radical.

Joshi et al.¹²³ reported that the enthalpy of formation for an oxiranyl radical is somewhat uncertain; they reexamined the thermochemistry of the oxiranyl radical by using isodesmic reactions, and thus, determined the enthalpy of formation to be 39.6 kcal mol⁻¹, by taking an average of the G3B3 and CBS-APNO calculations. By using this value, they calculated a 13.5 kcal mol⁻¹ energy barrier for the ring opening of the asymmetric oxiranyl

radical to form a vinoxyl radical. Auzmendi-Murua and Bozzelli ¹²¹ determined the enthalpy of formation for an oxiranyl radical as 39.7 kcal mol⁻¹, which is close to the value of Joshi et al. ¹²³. Initially, this study determined the enthalpy of transition state (TS1), which corresponds to the ring-opening pathway, as 54.97 kcal mol⁻¹ at the CBS-APNO level. This results in an energy barrier for ring opening of 15.28 kcal mol⁻¹, which is 1.78 kcal mol⁻¹ higher than the value determined by Joshi et al. This suggested that this study needs to perform additional calculations for the transition-state energy, as the ring-opening step is significant in this unimolecular dissociation system. Notably, the activation energy of this step affects the overall rate determination for products of this ring-opening path.

Figure 5.1 shows the three-membered cyclic ether, oxirane, and the oxiranyl radical structures, along with the geometry parameters.

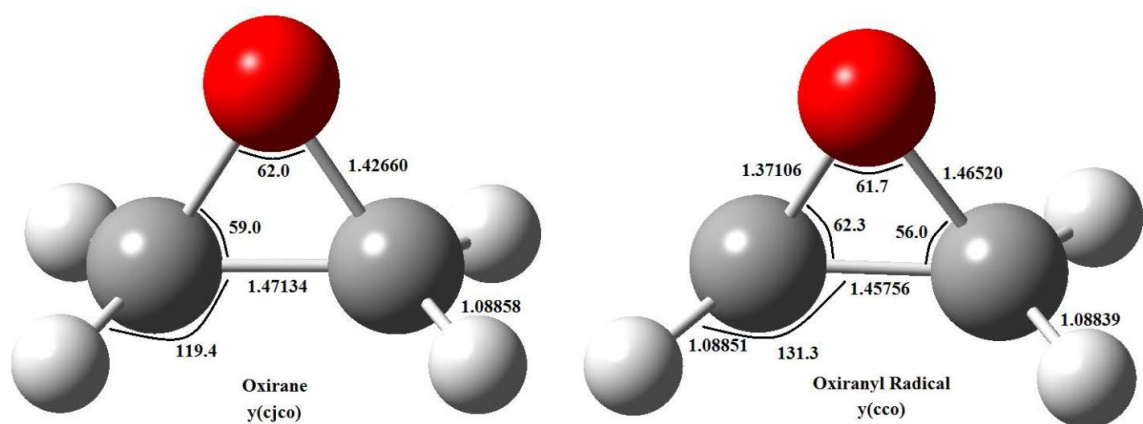


Figure 5.1. Nomenclature and figures of the oxirane (left) and oxiranyl radical (right) with detailed geometry parameters. Bond length in Å, bond angle in degree.

5.2 Computational Methods

5.2.1 Enthalpy of Formation

All calculations were performed using the Gaussian 09²⁸ program suite. The total energy of the oxiranyl radicals, vinoxyl radicals, and TS1 were calculated using six popular DFT methods, B3LYP³³⁻³⁴, B2PLYP¹²⁴, M06³⁷, M06-2X³⁷, ω B97X³⁸, and ω B97XD¹²⁵, in conjunction with the 6-31G(d,p), 6-31G+(d,p), and 6-311+G(2d,d,p) basis sets, calculations were also performed with the higher level composite methods, G3¹²⁶, G4⁴¹, CBS-QB3³⁵, CBS-APNO³⁶, W1U³⁹, and CCSD(T)¹²⁷⁻¹³⁰/aug-cc-pVTZ¹³¹⁻¹³². The enthalpy value of TS1 is taken as an average from the energy difference between the TS1 and the reactant (oxiranyl radical) and the energy difference between the TS1 and the product (vinoxy radical). Enthalpies of the acetyl radical, methyl radical, ketene, TS2, TS3, TS4, and TS5 were calculated using the same methods as for the ring-opening pathway except for G4 and W1U. The enthalpies of formation for the TS structures in the isomerization pathways are calculated with the same methods and basis sets as for the ring opening. The enthalpies of formation for the TS structures in dissociation or elimination reactions are calculated from that of the corresponding reactant and the energy difference between TS structure and the reactant.

In a previous study¹¹⁰, the authors tested B3LYP³³⁻³⁴, M06³⁷, M06-2X³⁷, ω B97X³⁸, G4¹²⁶, CBS-QB3³⁵, CBS-APNO³⁶, W1U³⁹ by using work reactions for fluorinated hydrocarbons and showed that the calculations were in close agreement and had good accuracy. The B3LYP method, which combines the three parameter Becke exchange functional, B3, with the Lee-Yang-Parr (LYP) correlation functional, has been widely used

for stable molecules, transition states, and radicals. The fourth series of the Gaussian-n family calculations, G4 can be used to perform an initial geometry optimization and frequency calculation at the B3LYP/6-31G(2df,p) level, followed a series of single-point correlation energy calculations starting from CCSD(T), MP4SDTQ to MP2-Full. CBS-QB3 uses the B3LYP/6-311G(2d,d,p) level to calculate geometries and frequencies followed by several single-point energy calculations at the MP2, MP4SDQ, and CCSD(T) levels. The final energies are determined with a CBS extrapolation. The CBS-APNO composite method can be used to perform an initial geometry optimization and frequency calculation at the HF/6-311G(d,p) level, followed by a higher-level QCISD/6-311G(d,p) geometry optimization. A single point energy calculation can then be performed at the QCISD(T)/6-311++G(2df,p) level with a subsequent extrapolation to the complete basis-set limit. Two newer hybrid meta-exchange-correlation functional methods, M06 and M06-2X, were reported by Truhlar Group. The M06 functional is parameterized for both transition metals and nonmetals, whereas the M06-2X functional is a highly nonlocal functional with double the amount of nonlocal exchange (2X) and is parameterized only for nonmetals. ω B97X includes a mixture of 100% long-range exact exchange and 16% of exact short-range exchange. W1U theory, as a modification of W1, is an unrestricted coupled-cluster spin-contamination-corrected [UCSR(T)] method. Owing to the computational requirements of the CCSD(T)-FC\AugH-cc-pVTZ+2df and CCSD-FC\AugH-cc-pVTZ+2df energy calculations in the W1U method, this method was only used in evaluation of the β -scission ring-opening pathway. B2PLYP is based on mixing standard generalized gradient approximations (GGAs) for exchange by Becke (B) and for correlation by LYP with HF exchange and a perturbative second-order correlation

part (PT2), which is obtained from the Kohn-Sham (GGA) orbitals and eigenvalues. ω B97XD is a modified version of ω B97X that uses the Grimme's¹²⁴ D2 dispersion model. The G3 method is the third series of the Gaussian-n family and was also applied to each pathway to allow comparison with the G3B3 evaluation of Joshi et al.¹²³.

5.2.2 Entropy and Heat Capacity

Entropy and heat capacity contributions as a function of temperature were determined from the calculated structures, moments of inertia, vibration frequencies, symmetry, electron degeneracy, number of optical isomers, and the known mass of each molecule. The calculations used standard formulas from statistical mechanics for the contributions of translation, external rotation, and vibrations by using the SMCPS⁴⁶ program. Contributions from internal rotors using Rotator⁴⁷ were substituted for contributions from the corresponding internal rotor torsion frequencies. Rotator⁴⁷ is a program for the calculation of thermodynamic functions from hindered rotations with arbitrary potentials based on a method developed by Krasnoperov, Lay, Shokhirev, and co-workers. This technique employs the expansion of the hindrance potential in the Fourier series, calculation of the Hamiltonian matrix on the basis of the wave functions of free internal rotation, and subsequent calculation of energy levels by direct diagonalization of the Hamiltonian matrix.

5.2.3 Rate Constants

The potential energy plots, thermochemical properties, and forward and reverse rate constants (high-pressure limit) were calculated for each elementary reaction step. Unimolecular dissociation reactions were treated with QRRK for $k(E)$ and Master Equation analysis for fall-off with the Chemaster⁷⁹ Code, where temperature and pressure dependence of the rate constants were calculated. The Chemkin¹³³ Code was used to solve a set of differential equations to provide an overall mechanism of the reaction system. Reverse reaction rate constants were determined from the thermochemistry and the forward rate constant, and were thermodynamically consistent. The QRRK calculation of rate constants utilized a reduced set of three vibration frequencies for densities of states, which accurately reproduce the molecules' heat capacity and include one external rotation in the calculation of the density of states. The Master Equation analysis used an exponential-down model for the energy transfer function with $(\Delta E^\circ_{\text{down}})$ 900 cal mol⁻¹ for N₂ as the third body. Rate constants, $k(E)$, were evaluated by using incremental energy increase of 0.25 kcal mol⁻¹ up to 70 kcal mol⁻¹ above the highest barrier. Lennard-Jones parameters¹³⁴, $\sigma(\text{\AA})$, and ϵ/k (K) were obtained from tabulations and from an estimation method based on molar volumes and compressibility. For nitrogen gas¹³⁵, σ is 3.798 Å, ϵ/k is 71.4 K; for oxiranyl radical¹³⁵, σ is 4.807 Å, ϵ/k is 248.9 K (from cyclopropane). High-pressure-limit elementary-rate parameters were used as input data to the QRRK calculations, and the results plotted against pressure and temperature are presented in details.

5.3 Results and Discussion

Table 5.1 lists the standard enthalpy of formation values for reference species used in the work reactions: ketene, carbon monoxide, and the oxiranyl, vinoxyl, acetyl, and methyl radicals. The table also shows literature values for comparison.

The enthalpy of formation of a vinoxyl radical was taken as 2.76 kcal mol⁻¹, as reported by Zhu et al.¹³⁶, who took an average from the results of B3LYP/6-31G(d,p), B3LYP/6-311++G(3df,2p), QCISD(T)/6-31G(d,p), and CBS-QB3 calculations. The enthalpy of formation of an acetyl radical was taken as -2.76 kcal mol⁻¹, as determined from the six available values in the literature: -2.5 (1992), -2.9±0.7 (1996), -3.4±2.0 (2002), -2.46 (2005), -3.0 (2006), and -2.3 (2012) kcal mol⁻¹.

Table 5.1 Standard Enthalpy of Formation at 298.15 K of Reference Species and Comparison with Available Literature

		$\Delta H_{f,298}^{\circ a,b}$	$\Delta H_{f,298}^{\circ a,c}$	Literature
oxiranyl radical	y(cjco)	39.69^d	39.6	39.6 ^k , 35.8±1.5 ^q
vinoxyl radical	cjcho	2.76±2^u	3.1	3.1 ^l , 3.52±0.38 ^h , 3.85 ^r , 3.6 ^s , 4.4 ^t
acetyl radical	ccj=o	-2.76^w	-2.5	-2.5 ^m , -3.0 ^s , -2.9±0.7 ⁿ , -3.43±2 ^u , -2.46 ⁱ , -2.3 ^t
Ketene	c=c=o	-11.35±0.38^j		
methyl radical	ch3j	35.01±0.02^e	35.1	35.1 ⁿ
carbon monoxide	co	-26.3^g	-26.4	-26.4 ^o , -26.417±0.041 ^f
hydrogen	h	52.103±0.001^f	52.1	52.1 ^p

^a Units in kcal mol⁻¹. ^b This study. ^c Taken in Joshi's¹²³ paper. ^d Auzmendi-Murua¹²¹. ^e Goos¹³. ^f Cox¹³⁷. ^g Asatryan¹³⁸. ^h Lee¹³⁹. ⁱ Ruscic¹⁴⁰. ^j Pedley⁴⁴. ^k Joshi¹²³. ^l Bouchoux¹⁴¹. ^m Niiranen¹⁴². ⁿ Tsang¹⁴³. ^o Chase11. ^p JANAF¹⁴⁴. ^q Luo¹⁰². ^r Tabor¹⁴⁵. ^s da Silva¹⁴⁶. ^t Goldsmith⁸⁴. ^u Zhu¹³⁶. ^v Melius. ^w Average of six available literature (Niiranen¹⁴², da Silva¹⁴⁶, Tsang¹⁴³, Zhu¹³⁶, Ruscic¹⁴⁰, Goldsmith⁸⁴.)

5.3.1 Potential Energy Diagrams

Figure 5.2 shows the potential energy diagram of the unimolecular oxiranyl radical dissociation reaction; the enthalpies of formation of the reactants, transition states, and products were determined from the calculations at the CBS-APNO level. One exception is the TS1 value; this is an average value from CBS-APNO and CCSD(T)/aug-cc-pVTZ calculations. The values in parenthesis are energy barriers for the respective pathway.

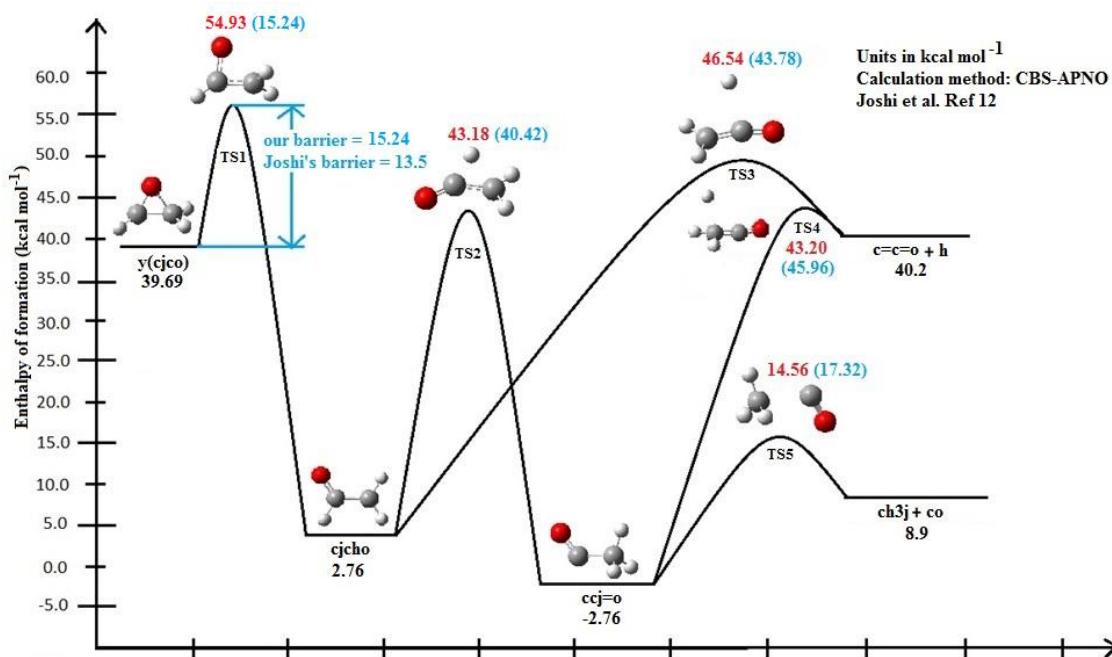


Figure 5.2 Potential energy diagram for unimolecular dissociation reaction of oxiranyl radical (energy barriers in parenthesis). Enthalpy of formation for TS1 are taken average of CBS-APNO and CCSD(T)/aug-cc-pVTZ.

5.3.2 Enthalpy of Formation for the Transition States

Table 5.2 summarizes and compares the enthalpy of formation calculations for each transition state, which were obtained by using twelve calculation methods.

The reactions were separated into four reaction classes:

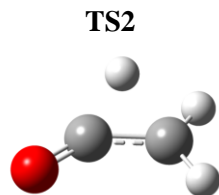
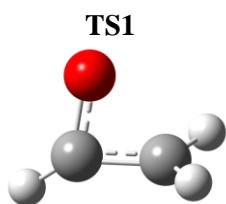
- 1) β -scission ring opening.
- 2) Intramolecular hydrogen transfer.
- 3) β -scission hydrogen elimination.
- 4) β -scission CH_3 elimination.

The optimized lowest-energy structures (Figure H.38-H. 45), coordinates (Appendix Table B), vibration frequencies (Appendix Table C), and moments of inertia (Appendix Table D) for all structures are available in the Appendix. The transition states are characterized as having only one negative eigenvalue of Hessian (force constant) matrices. The absence of imaginary frequencies verifies that the structures are true minima at the respective levels of theory. Intrinsic reaction coordinate (IRC) calculations were performed at the B3LYP/6-31+G(d,p) level to ensure connectivity of stationary points.

The values calculated with the larger 6-311+G(2d,d,p) basis set for each DFT method are used in the comparisons, G3, G4, CBS-QB3, CBS-APNO, and W1U, if applicable. This study analyzes the performance of each DFT calculation method below, and discusses the details for each type of reaction.

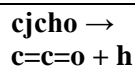
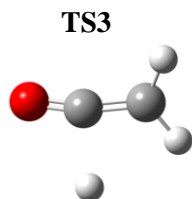
Table 5.2 Calculated standard enthalpy of the transition state structures at 298 K for the oxiranyl radical β -scission ring opening reaction system (Data recommended in this study are indicated by *)

Species	Reaction	Enthalpy of formation (kcal mol ⁻¹)		
β-scission ring opening				
	y(cjco) → cjcho	B3LYP		
		6-31G(d,p)	6-31+G(d,p)	6-311+G(2d,d,p)
		53.65	52.90	52.84
		B2PLYP		
		6-31G(d,p)	6-31+G(d,p)	6-311+G(2d,d,p)
		54.32	53.14	53.17
		M06		
		6-31G(d,p)	6-31+G(d,p)	6-311+G(2d,d,p)
		55.27	54.45	54.59
		M06-2X		
		6-31G(d,p)	6-31+G(d,p)	6-311+G(2d,d,p)
		57.38	56.75	56.88
		ωB97X		
		6-31G(d,p)	6-31+G(d,p)	6-311+G(2d,d,p)
		56.93	56.31	56.22
		ωB97XD		
		6-31G(d,p)	6-31+G(d,p)	6-311+G(2d,d,p)
		55.64	55.00	54.92
		CBS-QB3		53.19
		CBS-APNO		54.97
		G3		57.22
		G4		52.95
		W1U		53.32
		CCSD(T)/aug-cc-pVTZ		54.89
		Recommend^a		54.93*
Intramolecular hydrogen transfer				
	cjcho → ccj=o	B3LYP		
		6-31G(d,p)	6-31+G(d,p)	6-311+G(2d,d,p)
		42.66	42.14	41.35
		B2PLYP		
		6-31G(d,p)	6-31+G(d,p)	6-311+G(2d,d,p)
		44.80	44.01	42.82
		M06		
		6-31G(d,p)	6-31+G(d,p)	6-311+G(2d,d,p)
		41.43	41.02	40.23
		M06-2X		
		6-31G(d,p)	6-31+G(d,p)	6-311+G(2d,d,p)

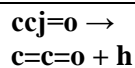
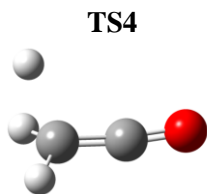


	44.04	43.59	42.95
	ωB97X		
	6-31G(d,p)	6-31+G(d,p)	6-311+G(2d,d,p)
	45.21	44.79	43.79
	ωB97XD		
	6-31G(d,p)	6-31+G(d,p)	6-311+G(2d,d,p)
	43.80	43.36	42.35
	CBS-QB3		
	CBS-APNO		
	G3		
			43.89
			43.18*
			42.63

β -scission hydrogen elimination

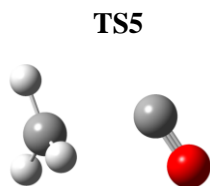


	B3LYP		
	6-31G(d,p)	6-31+G(d,p)	6-311+G(2d,d,p)
	46.92	47.77	44.74
	B2PLYP		
	6-31G(d,p)	6-31+G(d,p)	6-311+G(2d,d,p)
	46.53	47.29	44.18
	M06		
	6-31G(d,p)	6-31+G(d,p)	6-311+G(2d,d,p)
	46.76	47.53	44.75
	M06-2X		
	6-31G(d,p)	6-31+G(d,p)	6-311+G(2d,d,p)
	46.96	47.48	45.58
	ωB97X		
	6-31G(d,p)	6-31+G(d,p)	6-311+G(2d,d,p)
	51.70	52.58	49.76
	ωB97XD		
	6-31G(d,p)	6-31+G(d,p)	6-311+G(2d,d,p)
	50.06	50.81	47.85
	CBS-QB3		
	CBS-APNO		
	G3		
			45.95
			46.54*
			45.13



	B3LYP		
	6-31G(d,p)	6-31+G(d,p)	6-311+G(2d,d,p)
	41.87	42.98	40.36
	B2PLYP		
	6-31G(d,p)	6-31+G(d,p)	6-311+G(2d,d,p)
	43.40	44.36	41.88
	M06		
	6-31G(d,p)	6-31+G(d,p)	6-311+G(2d,d,p)
	41.21	42.30	40.01
	M06-2X		

	6-31G(d,p)	6-31+G(d,p)	6-311+G(2d,d,p)
	43.26	43.74	42.10
	ωB97X		
	6-31G(d,p)	6-31+G(d,p)	6-311+G(2d,d,p)
	47.65	48.44	46.16
	ωB97XD		
	6-31G(d,p)	6-31+G(d,p)	6-311+G(2d,d,p)
	45.72	46.47	44.03
	CBS-QB3		42.34
	CBS-APNO		43.20*
	G3		41.26
β-scission dissociation			
	ccj=o \rightarrow co +		B3LYP
	cj		
	6-31G(d,p)	6-31+G(d,p)	6-311+G(2d,d,p)
	15.19	15.56	14.68
	B2PLYP		
	6-31G(d,p)	6-31+G(d,p)	6-311+G(2d,d,p)
	14.95	15.40	14.61
	M06		
	6-31G(d,p)	6-31+G(d,p)	6-311+G(2d,d,p)
	14.44	14.41	14.14
	M06-2X		
	6-31G(d,p)	6-31+G(d,p)	6-311+G(2d,d,p)
	14.12	14.43	13.72
	ωB97X		
	6-31G(d,p)	6-31+G(d,p)	6-311+G(2d,d,p)
	16.73	17.27	16.48
	ωB97XD		
	6-31G(d,p)	6-31+G(d,p)	6-311+G(2d,d,p)
	15.80	16.29	15.54
	CBS-QB3		14.15
	CBS-APNO		14.56*
	G3		14.17



The cyclic oxiranyl radical initially cleaves a C-O bond and the CH₂ group rotates about 75 degrees to form a resonantly stabilized vinoxyl radical (\cdot). The CBS-APNO calculated enthalpy of formation for TS1 is 54.97 kcal mol⁻¹, resulting in a barrier of 15.3 kcal mol⁻¹, this value is close to the enthalpy value determined by using CCSD(T) (54.89 kcal mol⁻¹). Table 5.2 shows that these values are lower than the values obtained from G3,

M06-2X, and ω B97X calculations, close to the values obtained from M06 (54.59 kcal mol⁻¹) and ω B97XD (54.92 kcal mol⁻¹) calculations, and higher than the values given by the B3LYP, B2PLYP, CBS-QB3, G4, and W1U methods. The average value from the composite calculation methods is 54.42 kcal mol⁻¹. In this study, the value 54.93 kcal mol⁻¹ was selected, which is the calculated average from CBS-APNO and CCSD(T)/aug-cc-pVTZ. The CBS-APNO method was selected as the benchmark and was used to determine barriers in the subsequent reaction steps.

The calculated energy barrier for the ring-opening pathway is 15.2 kcal mol⁻¹ through the APNO and CCSD(T), as noted above. Joshi et al. calculated the enthalpy of formation for oxiranyl radical as 39.6 kcal mol⁻¹, and determined the energy barrier of ring-opening step as 13.5 kcal mol⁻¹. The enthalpy of formation of TS1 was calculated as 53.1 kcal mol⁻¹ at the G3B3 calculation level. This study performed additional calculations for the enthalpy of the TS1 to obtain values of: 52.84 (B3LYP), 53.17 (B2PLYP), 54.59 (M06), 56.88 (M06-2X), 56.22 (ω 97X), 54.92 (ω B97XD), 53.19 (CBS-QB3), 54.97 (CBS-APNO), 57.22 (G3), 52.95 (G4), 53.32 (W1U), and 54.89 (CCSD(T)) kcal mol⁻¹. There is an overall discrepancy of 4.38 kcal mol⁻¹, between the calculation methods, with values ranging from 52.84 (B3LYP) to 57.22 (G3) kcal mol⁻¹.

There are two possible pathways with similar barriers to further reactions of the initially formed vinoxyl radical. The lowest-energy pathway (TS2) is through an intra-molecular hydrogen transfer reaction over a 40.42 kcal mol⁻¹ energy barrier to an acetyl radical. The second pathway is β -scission of a hydrogen atom (H-elimination reaction; TS3) over a 43.78 kcal mol⁻¹ energy barrier to a ketene and a hydrogen atom (C=C=O + H).

There are two pathways for further reaction of the acetyl radical: the lowest-energy pathway is a β -scission dissociation to a methyl radical plus carbon monoxide ($\text{CH}_3\cdot + \text{CO}$; TS5) over a $17.32 \text{ kcal mol}^{-1}$ energy barrier; the second channel is a β -scission hydrogen-elimination reaction (TS4) over a $45.96 \text{ kcal mol}^{-1}$ energy barrier to a ketene.

The enthalpy of formation for the intramolecular hydrogen transfer reaction was determined to be $43.18 \text{ kcal mol}^{-1}$ at CBS-APNO level, which is in agreement with the CBS-QB3 and G3 results and is 1.5 and 3 kcal mol^{-1} higher than the values obtained by the B3LYP and M06-2X methods, respectively.

TS3 and TS4 are both transition states of β -scission hydrogen-elimination reaction pathways. The CBS-APNO enthalpy values of TS3 and TS4 are higher than those determined from B3LYP, B2PLYP, M06, M06-2X, CBS-QB3, and G3 methods, and are lower than the values from the ω B97X and ω B97XD methods. The results from CBS-QB3 and M06-2X show good agreement with CBS-APNO, whereas values obtained from B3LYP, M06, and ω B97XD show a larger discrepancy; they are higher by about 2 kcal mol^{-1} . TS3 and TS4 enthalpy values determined by using B2PLYP and G3 are about 2 kcal mol^{-1} lower than that determined through CBS-APNO.

The enthalpy of formation data for the beta-scission methyl radical elimination barrier TS5, show that the B3LYP, B2PLYP, M06, M06-2X, ω B97XD, CBS-QB3, and G3 results are all in agreement with that of CBS-APNO, whereas the ω B97X result is about 2 kcal mol^{-1} higher.

A summary of the comparison of the DFT-calculated barrier values with the CBS-APNO values shows:

1) The M06 and ω B97XD DFT calculation methods compare well with CBS-APNO for the β -scission ring opening reaction.

2) M06-2X and ω B97XD show good agreement for the intramolecular hydrogen transfer reaction.

3) M06-2X performs reasonably well for the two hydrogen elimination reactions.

4) All tested DFT calculation methods, except for ω B97X, show good agreement with the CBS-APNO values for the methyl radical elimination reaction.

Figure 5.3 summarizes the differences between the enthalpy of formation calculations for each method and basis set with the recommended values for each transition state.

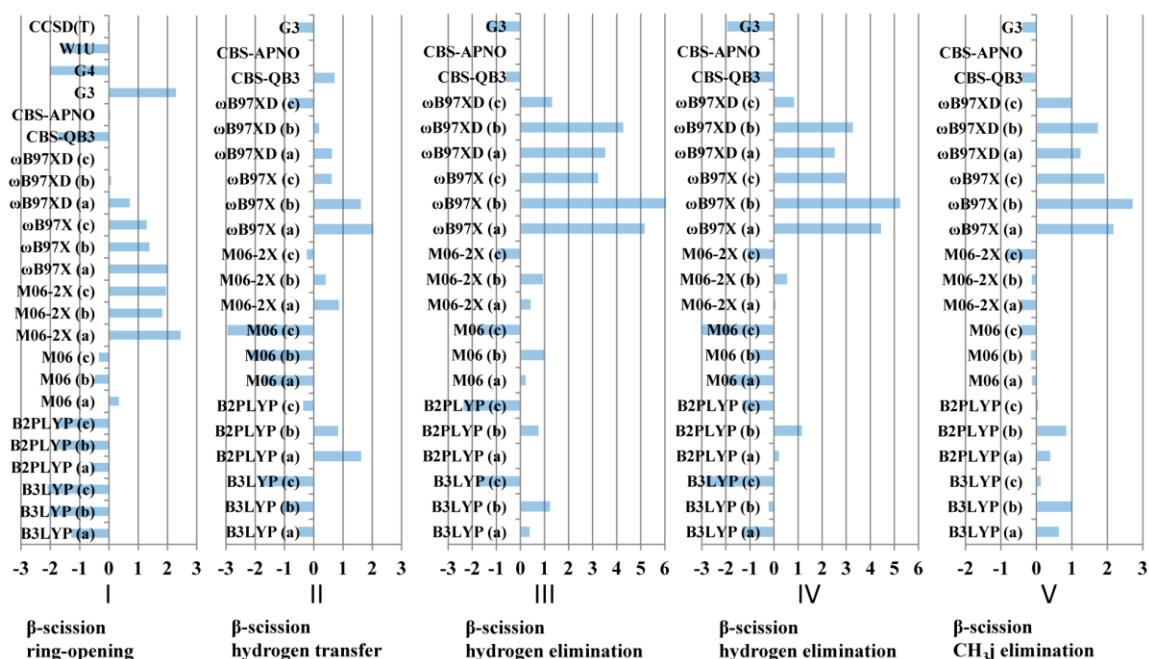


Figure 5.3 Enthalpy differences (kcal mol^{-1}) between each method from the recommended enthalpy for each transition state. Transition state 1(I) to transition state 5 (V), (a), (b), and (c) indicate 6-31G(d,p), 6-31+G(d,p), and 6-311+G(2d,d,p), respectively, for each DFT method.

5.3.3 Entropy and Heat Capacity

Entropy and heat capacity calculations were performed by using B3LYP/6-31+G(d,p) geometries and harmonic frequencies. The data are summarized in Table 5.3 with comparison to available literature data.

Table 5.3 Ideal Gas Phase Entropy and Heat Capacity Obtained by B3LYP/6-31+G(d,p) Calculation, Comparison with available Literature

	S_{298}° ^a	C_{p300} ^b	C_{p400}	C_{p500}	C_{p600}	C_{p800}	C_{p1000}	C_{p1500}
y(cjco) ^c	60.36	11.08	13.95	16.50	18.58	21.66	23.84	27.16
Lit. ^d	60.4±0.5	11.2±0.9	14.2±1.1	16.7±1.1	18.8±1.1	21.8±1.0	24.0±0.9	27.3±0.7
cjc=0	62.23	12.87	15.34	17.51	19.33	22.16	24.23	27.36
Lit. ^d	61.9±0.6	12.7±0.8	15.3±1.0	17.5±1.0	19.3±1.0	22.1±1.0	24.2±0.9	27.4±0.7
Lit. ^e	64.0							

ccj=O	64.28	12.08	14.09	16.03	17.76	20.57	22.72	26.08
Lit. ^d	63.7±0.5	12.1±0.6	14.1±0.8	16.1±0.9	17.8±1.0	20.7±1.0	22.8±0.9	26.2±0.7
Lit. ^{ef}	63.9							
c=c=O	57.74	12.30	14.08	15.52	16.72	18.61	20.05	22.39
Lit. ^d	57.6±0.6	12.3±0.6	14.1±0.6	15.6±0.7	16.8±0.7	18.7±0.7	20.1±0.6	22.4±0.5
H	52.1	27.39	4.97	4.97	4.97	4.97	4.97	4.97
CO	47.23	6.96	7.00	7.10	7.24	7.57	7.87	8.34
Lit. ^d	47.1±0.1	7.0±0.0	7.0±0.0	7.1±0.1	7.2±0.1	7.6±0.1	7.9±0.1	8.3±0.1
CJ	46.50	9.36	10.09	10.81	11.50	12.78	13.94	16.13
Lit. ^d	46.4±0.3	9.4±0.2	10.1±0.3	10.9±0.4	11.6±0.4	12.9±0.5	14.0±0.5	16.2±0.5
TS1	60.83	11.18	13.63	15.79	17.57	20.28	22.26	25.35
TS2	61.19	11.82	14.12	16.20	17.99	20.79	22.81	25.81
TS3	63.72	15.04	17.29	19.00	20.36	22.42	23.94	26.34
TS4	64.95	15.47	17.55	19.16	20.45	22.45	23.94	26.32
TS5	69.15	15.24	16.69	17.94	19.05	20.98	22.59	25.39

^{a,b} Units in cal mol⁻¹ K⁻¹. ^c This study. ^d Goldsmith⁸⁴. ^e Baulch¹⁴⁷. ^f PrIme¹⁴⁸.

5.3.4 Beta-Scission Ring-Opening Reaction Kinetics

Table 5.4 lists the high-pressure-limit elementary rate parameters used as input data for the QRRK calculations.

Table 5.4 High Pressure Limit Elementary Rate Parameters for the Unimolecular Dissociation Reaction of Oxiranyl Radical

Reaction	$k = A(T)^n \exp(-E/RT)$		
	A	n	E _{fit} (kcal mol ⁻¹)
y(cjco) → cjcho	2.1788E+12	0.37352	15.79
cjcho → y(cjco)	2.8932E+12	0.06169	52.79
cjcho → ccj=O	6.6366E+11	0.30922	40.86
ccj=O → cjcho	3.1435E+09	1.04750	45.90
cjcho → c=c=O + h	8.9465E+09	1.19224	43.92
c=c=O + h → cjcho	2.1608E+09	1.36696	6.08
ccj=O → c=c=O + h	6.6144E+07	1.96420	45.63
c=c=O + h → ccj=O	3.3728E+09	1.40063	2.75
ccj=O → ch3j + CO	4.1083E+10	1.33465	17.43
ch3j + CO → ccj=O	5.6358E+05	2.24288	5.56

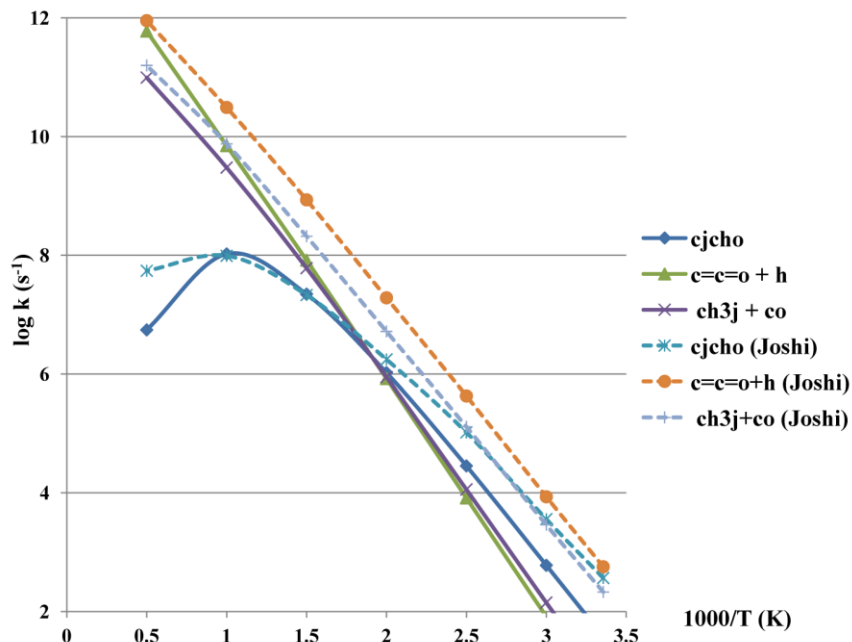


Figure 5.4 Rate constant plot as a function of $1000/T$ (K) ranging from 298 K to 2000 K at 2 atm for comparison of this study with Joshi et al.¹²³.

The calculated rate constants for the different channels versus temperature at 2 atm pressure are illustrated in Figure 5.4 for comparison with previous work. The primary difference in the two studies is the slightly higher, ($1.8 \text{ kcal mol}^{-1}$) energy barrier in this study. At the high temperatures, above 1000 K, the $\text{C}=\text{C}=\text{O} + \text{H}$ channel dominates, with the $\text{CH}_3\text{j} + \text{CO}$ channel being slightly lower. At temperatures close to 500 K and below the dissociation reaction to $\text{C}=\text{C}=\text{O} + \text{H}$ and the dissociation reaction to $\text{CH}_3\text{j} + \text{CO}$ compete.

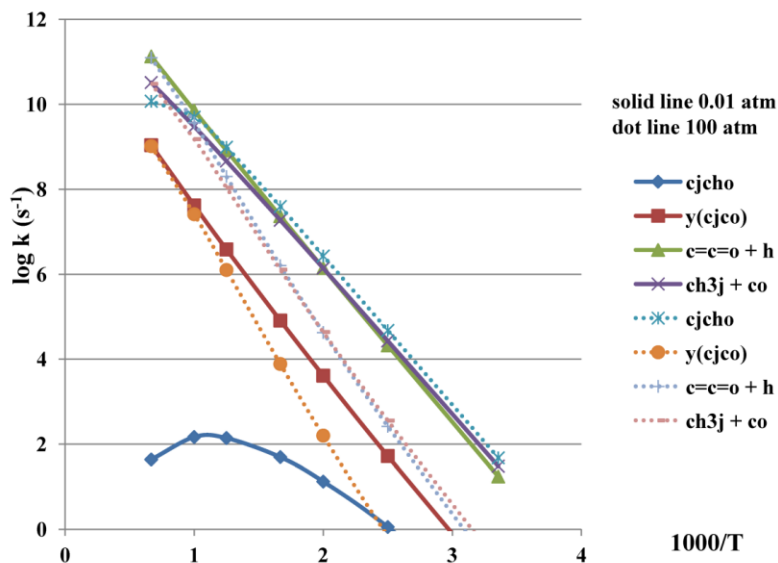


Figure 5.5 Rate constant plot as a function of temperature ranging from 298 K to 2000K under 0.01 atm and 100 atm.

Figure 5.5 shows the rate constants plotted versus $1000/T$ (K) at pressure of 0.01 and 100 atm. Increasing the pressure increases the rate constant of the initially formed vinoxyl radical channel ($\text{CH}_2\text{j}-\text{CH}=\text{O}$), relative to the remaining dissociation channels: $\text{C}=\text{C}=\text{O} + \text{H}$, $\text{CH}_3\text{j} + \text{CO}$, and back to the reactant.

Figure 5.5 illustrates that at low pressure, 0.01 atm, the reaction back to oxiranyl radical is less important. The kinetic parameters for the dissociation reaction to $\text{C}=\text{C}=\text{O} + \text{H}$ and the dissociation reaction to $\text{CH}_3\text{j} + \text{CO}$ are similar and are the two important channels.

At high temperature (100 atm; Figure 5.5), the kinetic parameters of the $\text{C}=\text{C}=\text{O} + \text{H}$ and $\text{CH}_3\text{j} + \text{CO}$ channels are similar. However, $\text{CH}_2\text{j}-\text{CH}=\text{O}$ becomes the major product under high pressure in the low-temperature range.

This study reports a slight difference in the rate constant compared with that obtained by Joshi et al, owing to the different ($1.7 \text{ kcal mol}^{-1}$ higher) activation energy for the oxiranyl ring opening pathway. This study's rate constants are about ten times lower than those calculated by Joshi et al. at 2000 K. They reported that the $\text{CH}_2\text{j}-\text{CH}=\text{O}$ channel

competes with the CH₃j + CO channel at about 360 K and 2 atm pressure, whereas this study sees this competition at 500 K and 2 atm. Joshi et al. reported that the CH₃j + CO and C=C=O + H channels are near parallel over the entire temperature range, whereas this study observed a crossing at 500 K.

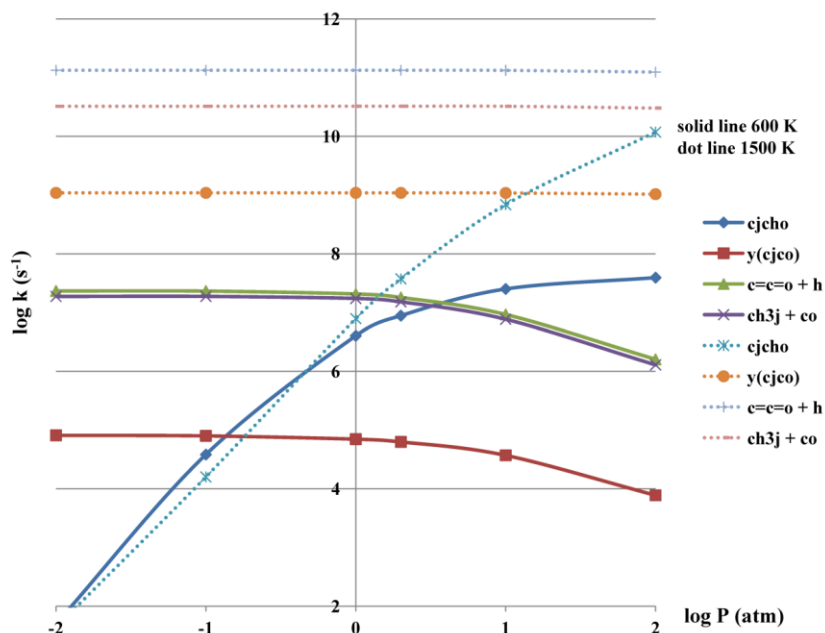


Figure 5.6 Rate constant plot as a function of pressure ranging from 0.01 atm to 100 atm under 600 K and 1500 K.

Figure 5.6 shows the plot of rate constants versus pressure from 0.01 to 100 atm at 600 K (solid lines) and 1500 K (dotted lines). At 600 K, C=C=O + H is the dominant product channel at low pressures, whereas the CH₂j-CH=O is dominant at high pressures. At 1500 K, the major product is C=C=O + H, and the kinetics are independent of pressure.

The Chemkin program has been used to simulate the overall reaction system and treats all channels as reversible with reverse system and treats all channels as reversible with reverse rate constants calculated from the thermochemistry. Table 5.5 lists the kinetic parameters for each pathway.

Table 5.5 Reversible Elementary Rate Parameters for the Unimolecular Dissociation Reaction of Oxiranyl Radical

Reaction	$k = A(T)^n \exp(-E_a/RT)$		
	A	n	$E_{fit}(\text{kcal mol}^{-1})$
$y(\text{cjco}) \rightleftharpoons \text{cjcho}$	9.23E+49	-12.43	24.27
$y(\text{cjco}) \rightleftharpoons \text{c=c=O} + \text{h}$	3.64E+14	-0.26	17.92
$y(\text{cjco}) \rightleftharpoons \text{ccj=O}$	7.59E-01	-2.42	15.86
$y(\text{cjco}) \rightleftharpoons \text{ch3j} + \text{CO}$	4.60E+18	-1.74	18.15
$\text{cjcho} \rightleftharpoons \text{ccj=O}$	6.05E+29	-5.49	46.14
$\text{cjcho} \rightleftharpoons \text{c=c=O} + \text{h}$	9.30E+30	-5.71	49.27
$\text{ccj=O} \rightleftharpoons \text{c=c=O} + \text{h}$	3.58E+07	-4.34	46.26
$\text{ccj=O} \rightleftharpoons \text{ch3j} + \text{CO}$	5.25E+28	-5.76	19.48

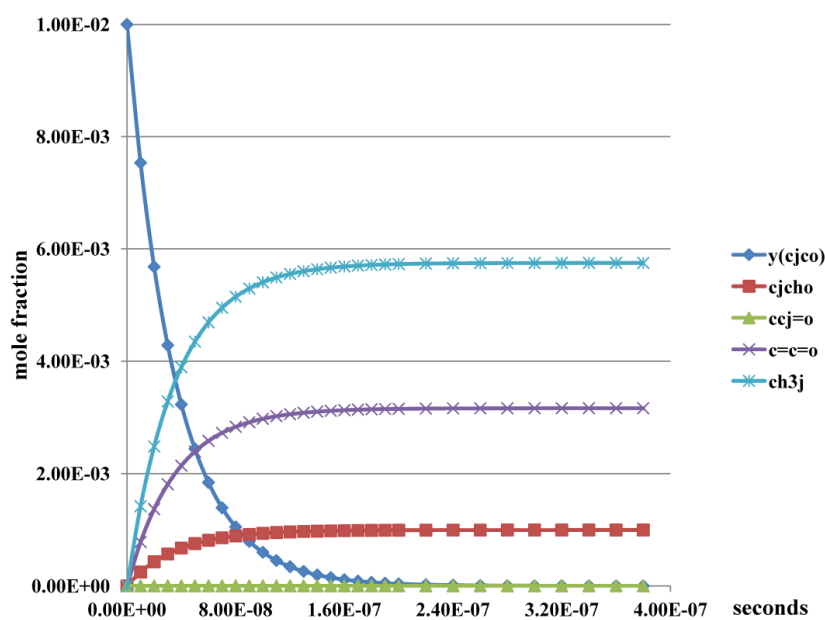


Figure 5.7 Chemkin modeling of β -scission ring opening reaction of oxiranyl radical at 1 atm, 600 K, 1% of oxiranyl radical with 99% of N_2 .

Figure 5.7 shows the Chemkin simulation for the dissociation of an oxiranyl radical versus time at 1 atm and 600 K. The reaction reaches equilibrium at about 2.4×10^{-7} s. The major product is $\text{CH}_3\text{j} + \text{CO}$.

Figure 5.8 shows the Chemkin run at a higher temperature of 800 K, where the major products switch to $\text{C}=\text{C}=\text{O} + \text{H}$. $\text{CH}_3\text{j} + \text{CO}$ becomes the second important channel. The reaction reaches near completion at about 2.6×10^{-9} s at this temperature.

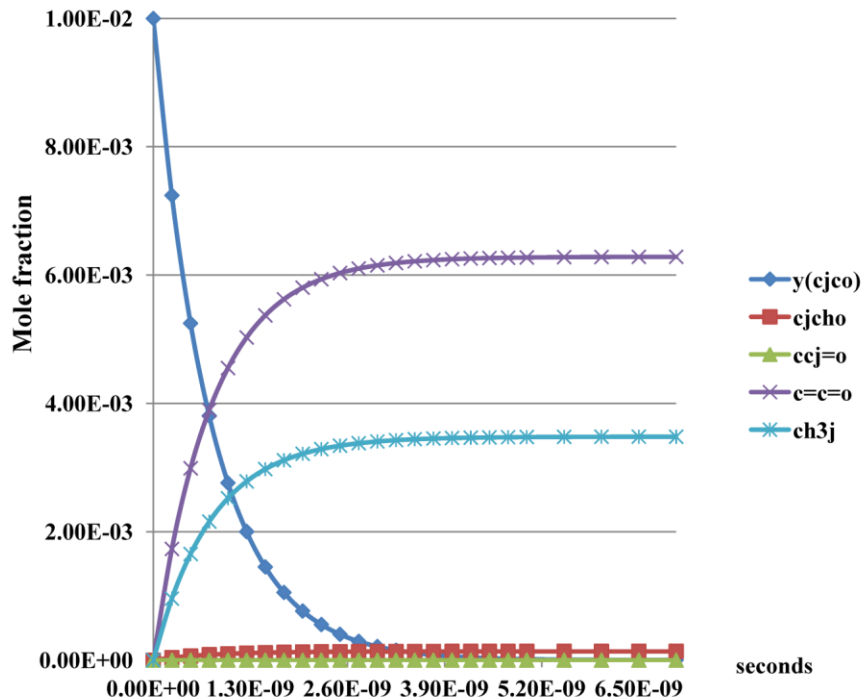


Figure 5.8 Chemkin modeling of β -scission ring opening reaction of oxiranyl radical at 1 atm, 800 K, 1% of oxiranyl radical with 99% of N_2 .

At the lower temperature of 600 K, the oxiranyl radical dissociates to $CH_2j-CH=O$ via TS1 then via TS2 through an intramolecular H transfer and dissociates via TS5 to form $CH_3j + CO$. At the higher temperature of 800 K, the energized $CH_2j-CH=O$ undergoes direct H atom elimination (TS3) to form $C=C=O + H$. TS3 is favored at 800 K, because at this higher temperature, the preexponential factor is about two orders of magnitude higher, than that for the H atom transfer (TS2).

5.4 Summary

The thermochemical properties, including standard enthalpies, of five transition-state structures of the oxiranyl radical β -scission ring-opening system were determined, and the data obtained by using twelve DFT and ab initio composite calculation methods were compared. Herein, the ring opening barrier was determined to be $15.28 \text{ kcal mol}^{-1}$, which is $1.8 \text{ kcal mol}^{-1}$ higher than the value obtained in a previous study by Joshi et al. This energy difference resulted in a slightly slower rate constant for each reaction channel in this β -scission ring opening system. Under low pressure, the ketene + hydrogen pathway competed with the methyl radical + carbon monoxide pathway, whereas under high pressure, the initially formed vinoxyl radical was the major product. At high temperatures, the ketene + hydrogen path was the dominant path and was independent of pressure. The performance of the B3LYP, B2PLYP, M06, M06-2X, ω B97X, and ω B97XD DFT methods were compared for each of the five different reaction transition-state barriers.

CHAPTER 6

THERMOCHEMISTRY AND KINETIC ANALYSIS ON MOLECULAR OXYGEN ASSOCIATION REACTION OF OXIRANYL RADICAL: A THEORETICAL STUDY

6.1 Overview

Cyclic ethers are important intermediate formed in the oxidation process of hydrocarbons under both atmospheric and combustion conditions. A number of experimental studies^{114-117, 149-152} show the formation of 3 to 5 member ring cyclic ethers in the combustion chemistry and atmospheric chemistry. Experimental studies by Baldwin, Walker, and co-workers^{117, 149-151} in the 1980s and more recently by Dagaut and co-workers^{114-116, 152} have shown that cyclic ethers are important, low barrier reaction products in the oxidation of linear and branched hydrocarbons.

Calculation studies^{78-79, 101, 138} have described the reaction steps relative to the formation of the cyclic ethers. Auzmendi-Murua et al.¹²¹ described the important initial reaction paths in oxidation of isooctane to form 3 to 5 member cyclic ethers, and also showed the initial reaction paths in oxidation of isopentanol to form 3 to 5 member ring cyclic ethers. And under atmospheric conditions, the oxidation of isoprene forms 3 to 4 member ring cyclic ethers. Wijaya et al.¹⁰¹ performed a calculation study on the formation of 3 to 5 member ring cyclic ethers from primary, secondary, and tertiary hydroperoxyalkyl radicals and addressed the importance of formation of cyclic ethers in the low-temperature oxidation process of hydrocarbons. Chen et al.⁷⁸ presented the important reaction pathways for tert-butyl radical oxidation including the formation of cyclic ethers. Asatryan et al.¹³⁸ performed a calculation study on the 2-pentyl radical oxidation reactions including the formation of 3 to 4 member ring cyclic ethers. Snirsiriwat et al.¹⁵³ have also calculated

the formation kinetics from oxidation of tert-isooctane. Zádor et al.¹¹⁸ reviewed on the elementary reaction kinetics relate to the modeling and prediction of low-temperature combustion and auto-ignition starting from alkylperoxy and hydroperoxyalkyl radicals.

Under both combustion and atmospheric chemistry conditions, the formed cyclic ethers will undergo abstraction reactions with the radical pool to form cyclic ether radicals in combustion and atmosphere. Under combustion conditions, these radicals can undergo unimolecular dissociation. The ring opening reaction has been studied and compared with available literature, however, to the best knowledge, there are very limited studies on the oxidation reaction of cyclic ether systems. But under atmospheric condition, these radicals will chemically activate with $^3\text{O}_2$ to form peroxy radicals, which further react to form reactive oxygenated intermediates.

The thermochemical properties and reaction paths are reported for the species resulting from reactions in the oxiranyl radical + O_2 system in this study. Transition state structures and intermediates that result from the isomerization and dissociation reactions of oxiranyl radicals with molecular oxygen to form the R- O_2 chemically activated from variational transition state theory. The competition between unimolecular ring opening reaction of oxiranyl radical and association reaction over 300 K to 800 K at 1 atm is also reported, and shows that the dominating products change with temperature.

6.2 Computational Methods

6.2.1 Enthalpy of Formation

All calculations were performed using the Gaussian 09²⁸ program. The total energy of the oxiranyl radicals and its derived peroxy radicals, and transition states have been calculated using B3LYP/6-311+G(2d,d,p), B2PLYP/6-311+G(2d,d,p), M06/6-311+G(2d,d,p), M06-2X/6-311+G(2d,d,p), ω B97X/6-311+G(2d,d,p), ω 97XD/6-311+G(2d,d,p), G4, CBS-QB3 methods. CBS-APNO method is applied to some of the species.

The study on the unimolecular dissociation reaction of oxiranyl radical applied the same DFT methods and compared each DFT method with CBS-APNO calculation. This study takes the average of six DFT methods above and compare with the average of available composite calculation methods. B3LYP, as one of the most popular and reliable¹⁵⁴ DFT methods, combines the three parameter Becke exchange functional, B3³³, with the Lee-Yang-Parr (LYP)³⁴ correlation functional, has been widely used because of its economic cost. B2PLYP¹²⁴, another combination of Becke³³ and LYP³⁴, which mixes the standard generalized gradient approximations (GGAs) for exchange by Becke and applies the HF exchange and a perturbative second-order correlation part (PT2) by Lee-Yang-Parr. M06 and M06-2X are two hybrid meta-exchange-correlation functional methods which have been developed by Truhlar's³⁷ Group. ω B97X³⁸ mixes 100% of long-range exact exchange and 16% of exact short-range exchange, whereas the modified ω B97XD¹²⁵ applies the Grimme's¹²⁴ D2 dispersion model. G4⁴¹, initially performs geometry optimization and frequency calculation by B3LYP/6-31G(2df,p) method, then applies a

series of single-point correlation energy calculations including CCSD(T), MP4SDTQ, MP2-Full. CBS-QB3³⁵, a well-known composite calculation method, calculates the geometry and frequency by B3LYP/6-31G(2d,d,p) method, followed by a series of single-point energy calculations at the MP2, MP4SDQ, and CCSD(T) levels. Another composite calculation method, CBS-APNO³⁶, initially uses HF/6-311G(d,p) to calculate the geometry and frequency, followed by QCISD/6-311G(d,p) optimization of geometry. Then it calculates the single point energy by QCISD/6-311++G(2df,p) method with a subsequent extrapolation to the complete basis set limit.

6.2.2 Entropy and Heat Capacity

Entropy and heat capacity contributions as a functional of temperature are determined from the calculated structure, moments of inertia, vibration frequencies, symmetry, electron degeneracy, number of optical isomers, and the known mass of each molecule. The SMCPS⁴⁶ program uses the standard formulas from statistical mechanics for the contributions of translation, external rotation, and vibrations. The Rotator⁴⁷ program is used to consider the contributions of internal rotors of species separately from the corresponding internal rotor torsion frequencies. Lay, Krasnoperov, Shokhirev, and co-workers, developed a technique to calculate the thermodynamic functions from hindered rotations with arbitrary potentials. This technique employs expansion of the hinderance potential in the Fourier series, calculation of the Hamiltonian matrix in the basis of the wave functions of free internal rotation, and subsequent calculation of energy levels by direct diagonalization of the Hamiltonian matrix.

6.2.3 Rate Constants

The potential energy surface, thermochemical properties, and forward and reverse constants (high-pressure limit) are calculated for each elementary reaction step. Multifrequency quantum Rice Ramsperger Kassel (QRRK) analysis is used for $k(E)$ and Master Equation analysis is used for fall-off with the Chemaster⁷⁹ Code, where temperature and pressure dependence of the rate constants were calculated.

The QRRK calculation of rate constants utilizes a reduced set of three vibration frequencies for densities of states which accurately reproduce the molecules' heat capacity and include one external rotation in calculation in the density of states. The Master Equation analysis uses an exponential-down model for the energy transfer function with $(\Delta E_{\text{down}}^\circ)$ 900 cal mol⁻¹ for N₂ as the third body. Rate constants, $k(E)$ were evaluated using energy of 0.25 kcal mol⁻¹ increments up to 70 kcal mol⁻¹ above the highest barrier. Lennard-Jones parameters, $\sigma(\text{\AA})$ and ϵ/k (K) are obtained from tabulations and from an estimation method based on molar volumes and compressibility. For N₂¹³⁴, $\sigma(\text{\AA})$ is 3.798, ϵ/k (K) is 71.4; for oxiranyl radical¹³⁴, $\sigma(\text{\AA})$ is 4.807, ϵ/k (K) is 248.9 (from cyclopropane).

The Chemkin¹³³ Code is used to solve a set of differential equations to provide an overall mechanism of the reaction system. Reverse reaction rate constants are determined from the thermochemistry and the forward rate constant, and are thermodynamically consistent.


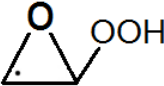
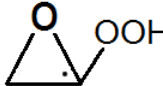
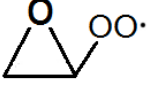
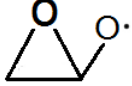

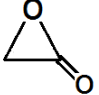

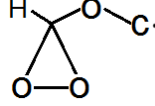
6.3 Results and Discussion

Table 6.1 shows the nomenclature and figures of the oxiranyl radical and the derivative compounds in this study. The optimized geometries from the B3LYP/6-311G(2d,d,p) calculations in the CBS-QB3 calculation method, for the target molecules are presented in Figure F.46-76 of the Appendix. Optimized geometry coordinates, vibration frequencies, and moments of inertia for all structures are available in Table A.-C. of the Appendix.

Table A of the Appendix lists the standard enthalpy of formation values for reference species used in the work reactions and their literature source.

The enthalpy of formation of the $y(coc-cco)$, $y(cjoo)$, and $y(coo)-ocj$ obtained from the use of the reaction schemes are shown in Table E.17 of Appendix.

Table 6.1 Nomenclature and Figures of the Oxiranyl Radical and Its Derivative Compounds

 y(cjoc) $y(CH\cdot OCH_2)$ Oxiranyl Radical	 y(cjoc)-q $y(CH\cdot OCH)-OOH$ Oxiranyl Hydroperoxide	 y(cocj)-q $y(CHOCH\cdot)-OOH$ Oxiranyl Hydroperoxide
 y(coc)-qj $y(CH_2OCH)-OO\cdot$ Oxirane Hydroperoxy Radical	 y(coc)-oj $y(CH_2OCH)-O\cdot$ Oxirane Alkoxy Radical	 y(cdco) $y(CHCHO)$ Oxirene
 y(coc)-do $y(CH_2OC)=O$ Oxiranone	 y(cjoo) $y(CH\cdot OO)$ Dioxiranyl Radical	 y(coo)-ocj $y(CHOO)-O-CH_2\cdot$ Dioxirane Methyl Ether Radical

$\begin{array}{c} \text{O} \\ \parallel \\ \bullet\text{C}-\text{OH} \\ \text{cjdo-oh} \\ \text{C}=\text{O}-\text{OH} \\ \text{Formic Acid Radical} \end{array}$	$\begin{array}{c} \text{O}\bullet \quad \text{O} \\ \quad \parallel \\ \text{CH}_2-\text{C}-\text{H} \\ \text{ojc-cho} \\ \bullet\text{O}-\text{CH}_2-\text{CHO} \\ \text{Dioxiranyl Radical} \end{array}$	$\begin{array}{c} \text{O} \quad \quad \text{O} \\ \quad \quad \parallel \\ \bullet\text{CH}_2-\text{O}-\text{C}-\text{H} \\ \text{cjocho} \\ \text{C}\cdot\text{H}_2-\text{O}-\text{CHO} \\ \text{Ether Radical} \end{array}$
$\begin{array}{c} \text{O} \quad \quad \text{O} \\ \diagdown \quad \diagup \\ \text{y}(\text{cco-cco}) \\ \text{y}[\text{CHCHO}]-\text{y}[\text{CHCHO}] \\ \text{2,4-Dioxabicyclo[1.1.0]butane} \end{array}$		

6.3.1 Potential Energy Diagrams

Figure 6.1 shows the potential energy diagram of the oxidation reaction of oxiranyl radical; the enthalpies of formation of the reactants, transition states, and products were determined from the recommendation values in this study. The values in parenthesis are energy barriers for the respective pathway.

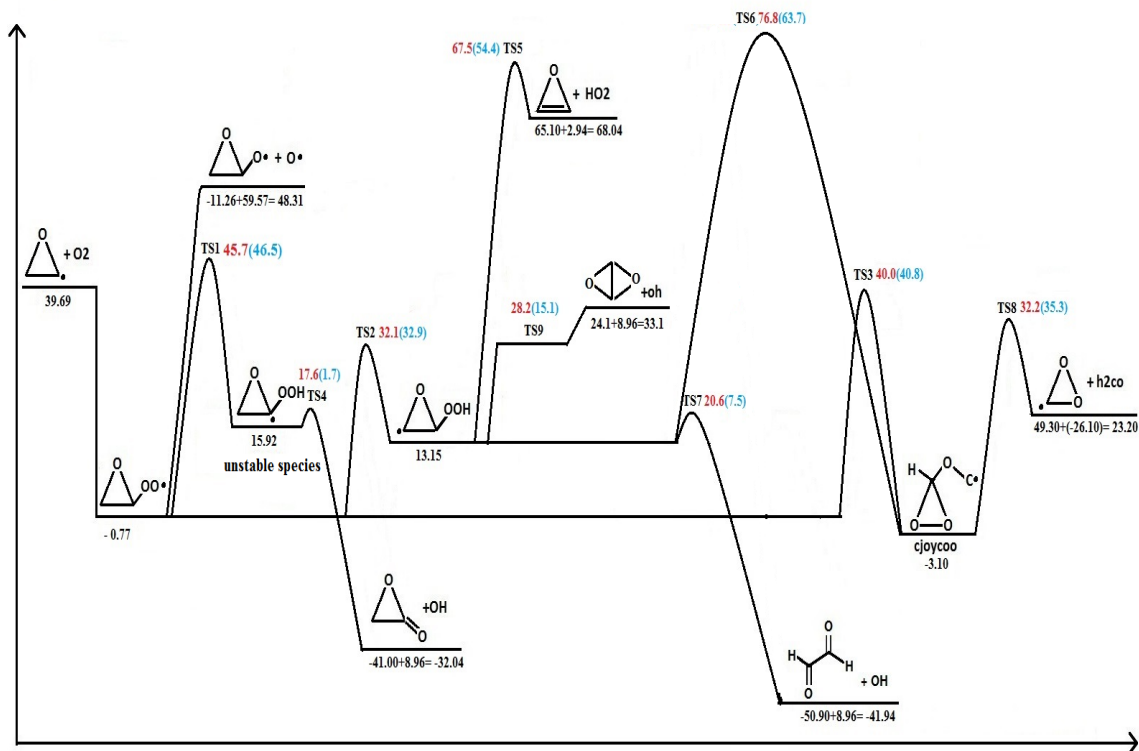


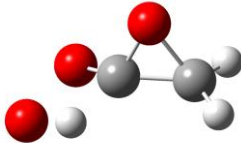
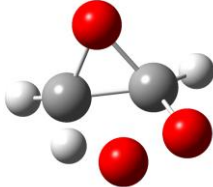
Figure 6.1 Potential energy diagram for oxidation reaction of oxiranyl radical. Enthalpy of formation for each TS (energy barrier in parenthesis). Data are taken from Table 6.2. Units in kcal mol^{-1} .

6.3.2 Enthalpy of Formation for the Transition States

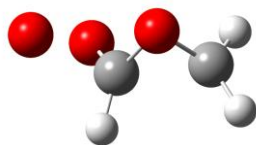
Table 6.2 summarizes and compares the enthalpy of formation calculations for each transition state in Figure 6.1. Transition states with barrier are characterized as having only one negative frequency. The absence of imaginary frequencies verifies that structures are true minima at the respective levels of theory. Intrinsic Reaction (IRC) calculations are performed at the B3LYP/6-31+G(d,p) level to ensure connectivity of stationary points. The final point geometries at both sides of the TS are re-optimized to proper minima. The enthalpy of formation of TS1, TS2, TS3, TS10, TS11, TS12 and TS13 are taken as an average from the energy difference between the TS and the reactant and the energy

difference between the TS and the product. Enthalpy of formation of TS4, TS5, TS6, TS7, TS8, TS9, TS14, and TS15 are calculated from the energy difference between TS structure and the reactant. The enthalpies of the transition state structures in oxidation reaction of oxiranyl radical with O₂ system calculated using B3LYP, B2PLYP, M06, M06-2X, ω B97X, ω B97XD, G4, CBS-QB3, and CBS-APNO are shown in Table 6.2.

Table 6.2 Calculated Standard Enthalpy of Formation of the Transition State Structures at 298 K for the Oxiranyl Radical Oxidation Reaction System. See Figure 6.1. (Data Recommended in This Study are Indicated by *)

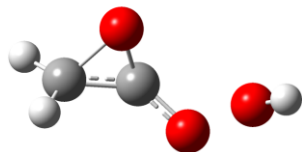
Species	Reaction	$\Delta_f H^\circ_{298}$ (Ea) ^{a,e}
	y(coc)-qj → y(cocj)-q	B3LYP/6-311+G(2d,d,p)
TS1  Hydrogen atom transfers from peroxy the carbon to the peroxy oxygen radical. First step in two-step reaction with second barrier very low, 1.7 kcal mol ⁻¹ – see TS4. *b Average of G4 and CBS-QB3.		45.0 (45.8)
		B2PLYP/6-311+G(2d,d,p)
		46.5 (47.3)
		M06/6-311+G(2d,d,p)
		47.4 (48.2)
		M06-2X/6-311+G(2d,d,p)
		49.2 (50.0)
		ω B97X/6-311+G(2d,d,p)
		48.7 (49.5)
		ω B97XD/6-311+G(2d,d,p)
		47.0 (47.8)
		CBS-QB3
		44.6 (45.4)
		CBS-APNO
	NA	
	G4	
	46.8 (47.6)	
	45.7*^b (46.5)	
	v(coc)-qj → v(cioc)-q	B3LYP/6-311+G(2d,d,p)
TS2  Hydrogen transfers from the methylene carbon to the peroxy oxygen radical forming C•H radical and hydroperoxide. *b Average of G4 and CBS-QB3.		30.3 (31.1)
		B2PLYP/6-311+G(2d,d,p)
		32.0 (32.8)
		M06/6-311+G(2d,d,p)
		31.0 (31.8)
		M06-2X/6-311+G(2d,d,p)
		33.4 (34.2)
		ω B97X/6-311+G(2d,d,p)
		33.6 (34.4)
		ω B97XD/6-311+G(2d,d,p)

		32.0 (32.8)
		CBS-QB3
		30.1 (30.9)
		CBS-APNO
		NA
		G4
		32.0 (32.8)
		31.1*^b (31.9)
	y(coc)-qj → y(coo)-ocj	B3LYP/6-311+G(2d,d,p)
TS3		40.5 (41.3)
		B2PLYP/6-311+G(2d,d,p)
		42.1 (42.9)
		M06/6-311+G(2d,d,p)
		41.5 (42.3)
		M06-2X/6-311+G(2d,d,p)
		43.0 (43.8)
		ωB97X/6-311+G(2d,d,p)
		45.0 (45.8)
		ωB97XD/6-311+G(2d,d,p)
		42.5 (43.3)
		CBS-QB3
		38.5 (39.3)
		CBS-APNO
		NA
		G4
		41.6 (42.4)
		40.1*^b (40.9)
	y(cocj)-q → y(coc)-do + oh	B3LYP/6-311+G(2d,d,p)
TS4		15.8 (-0.1)
		B2PLYP/6-311+G(2d,d,p)
		18.4 (2.5)
		M06/6-311+G(2d,d,p)
		16.9 (1.0)
		M06-2X/6-311+G(2d,d,p)
		20.5 (4.6)
		ωB97X/6-311+G(2d,d,p)
		19.1 (3.2)
		ωB97XD/6-311+G(2d,d,p)
		18.1 (2.2)
		CBS-QB3
		17.3 (1.4)
		CBS-APNO
		17.9 (2.0)
		G4
		19.3 (3.4)
		17.6*^d (1.7)
	y(cjoc)-q → y(cdco) + ho2	B3LYP/6-311+G(2d,d,p)



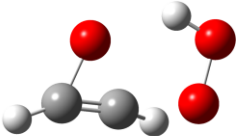
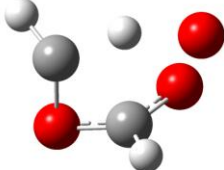
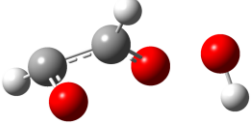
Ring Opening - Dioxygen Oxirane ring formation
 The carbon-carbon bond initiates ring opening, then the peroxy oxygen radical attacks the ipso carbon of the C•OOH group forming a dioxirane ring on the peroxy carbon site. The initial ether oxygen and attached new carbon radical are single bonded to the ipso carbon.

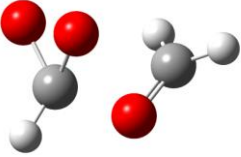
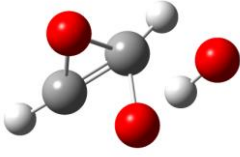
*b Average of G4 and CBS-QB3.



OH elimination from the oxiranyl hydroperoxide, y(coci)-q, to form the oxiranone crossing over a small energy barrier, 1.7 kcal mol⁻¹.

*d Average of CBS-QB3 and CBS-APNO.

<p>TS5</p>  <p>HO2 unimolecular elimination from the oxiranyl peroxide, y(cjoc)-q, to form an oxirene ring structure.</p> <p style="text-align: right;">*b Average of G4 and CBS-QB3.</p>	61.5 (48.4)
	B2PLYP/6-311+G(2d,d,p)
	66.5 (53.4)
	M06/6-311+G(2d,d,p)
	64.5 (51.4)
	M06-2X/6-311+G(2d,d,p)
	68.5 (55.4)
	ω B97X/6-311+G(2d,d,p)
	67.2 (54.1)
	ω B97XD/6-311+G(2d,d,p)
	66.3 (53.2)
	CBS-QB3
	66.6 (53.5)
	CBS-APNO
	NA
G4	
68.4 (55.3)	
67.5*^b (54.4)	
y(cjoc)-q → hco + hco + oh	B3LYP/6-311+G(2d,d,p)
<p>TS6</p>  <p>The carbon-carbon bond starts cleaving toward forming two C•H radicals while the methylene carbon starts c-o π bond formation and the ether oxygen starts cleaving the bond to the hydroperoxide carbon. The c•o-oh carbon starts c=O π bond formation with simultaneous c=O—oh cleavage (beta scission). Overall formation of HC•O + HC•O + OH.</p> <p style="text-align: right;">*c Average of G4, CBS-QB3 and CBS-APNO.</p>	75.8 (62.7)
	B2PLYP/6-311+G(2d,d,p)
	77.7 (64.6)
	M06/6-311+G(2d,d,p)
	76.6 (63.5)
	M06-2X/6-311+G(2d,d,p)
	79.6 (66.5)
	ω B97X/6-311+G(2d,d,p)
	79.9 (66.8)
	ω B97XD/6-311+G(2d,d,p)
	77.6 (64.5)
	CBS-QB3
	77.5 (64.4)
	CBS-APNO
	77.6 (64.5)
G4	
77.2 (64.1)	
76.8*^c (63.7)	
y(cjoc)-q → cho-cho + oh	B3LYP/6-311+G(2d,d,p)
<p>TS7</p>  <p>Similar to TS6 without carbon – carbon bond cleavage. The</p>	15.4 (2.3)
	B2PLYP/6-311+G(2d,d,p)
	18.0 (4.9)
	M06/6-311+G(2d,d,p)
	19.7 (6.6)
	M06-2X/6-311+G(2d,d,p)
30.2 (17.1)	

<p>oxiranyl hydroperoxide, y(cjoc)-q, with the radical site on the non-hydroperoxide carbon starts to undergo β-scission ring opening. The carbon radical - ring oxygen bond starts to close to form a new π bond, while the peroxide carbon-ring oxygen bond opens forming a radical on the peroxide carbon. This peroxide carbon then start a β-scission forming a C=O π bond and cleaving the OH group. The final products are glyoxal + OH. The overall products are HCO-HCO plus OH.</p> <p style="text-align: center;">*c Average of G4, CBS-QB3 and CBS-APNO.</p>	ω B97X/6-311+G(2d,d,p)	28.7 (15.6)	
	ω B97XD/6-311+G(2d,d,p)	25.5 (12.4)	
	CBS-QB3	20.9 (7.8)	
	CBS-APNO	20.7 (7.6)	
	G4	20.1 (7.0)	
		20.6* ^c (7.5)	
	y(coo)-ocj \rightarrow y(cjoo) + h2co		
	<p>TS8</p>  <p>The C•H2-O—Y(COO) radical site undergoes β-scission to form the C=O π bond of formaldehyde and a dioxiranyl radical by cleaving the ring carbon C—OC•H2 bond.</p> <p style="text-align: center;">*d Average of CBS-QB3 and CBS-APNO</p>	B3LYP/6-311+G(2d,d,p)	26.6 (29.7)
		B2PLYP/6-311+G(2d,d,p)	29.7 (32.8)
		M06/6-311+G(2d,d,p)	28.4 (31.5)
M06-2X/6-311+G(2d,d,p)		34.2 (37.3)	
ω B97X/6-311+G(2d,d,p)		33.0 (36.1)	
ω B97XD/6-311+G(2d,d,p)		31.1 (35.2)	
CBS-QB3		31.9 (35.0)	
CBS-APNO		32.4 (35.5)	
G4		34.4 (37.5)	
		32.2* ^d (35.3)	
y(cjoc)-q \rightarrow y(cco-cco) + oh			
<p>TS9</p>  <p>The C•H carbon radical (y(cjoc)-q) attacks the O atom bonded to the carbon of the hydroperoxide group (inserts). This insertion cleaves the RO-OH bond and forms a second, merged</p>		B3LYP/6-311+G(2d,d,p)	NA
		B2PLYP/6-311+G(2d,d,p)	27.0 (13.9)
		M06/6-311+G(2d,d,p)	25.0 (11.9)
	M06-2X/6-311+G(2d,d,p)	28.3 (13.2)	
	ω B97X/6-311+G(2d,d,p)	27.5 (14.4)	

oxirane ring molecule, 2,4-Dioxabicyclo[1.1.0]butane plus OH radical. The stability of this bicyclic is low and it falls apart with a low barrier to trans c=O π bond formation / trans c—O ring opening to glyoxal + the OH. *b Average of G4 and CBS-QB3.	ω B97XD/6-311+G(2d,d,p)
	28.3 (15.2)
	CBS-QB3
	28.5 (15.4)
	CBS-APNO
	NA
	G4
	28.0 (14.9)
	28.2*^b (15.1)

Units in kcal mol⁻¹. ^b Recommended value for the TS. Average of G4 and CBS-QB3. ^c Recommended value for the TS. Average of G4, CBS-QB3 and CBS-APNO. ^d Recommended value for the TS. Average of CBS-QB3 and CBS-APNO. ^e Energy Barrier in the parenthesis.

TS1: Six DFT methods (B3LYP, B2PLYP, M06, M06-2X, ω B97X, ω B97XD) in conjunction with the 6-311+G(2d,d,p) basis set are used to calculate the enthalpy of formation of TS1, the intramolecular hydrogen transfer reaction from the ipso carbon to the peroxy radical group, y(coc)-qj, and the alkyl radical, y(cocj)-q. TS1 is a four-member ring transition state. The average of six DFT calculation methods determines the barrier as 48.1 kcal mol⁻¹. The average of two higher level calculation methods, G4 and CBS-QB3, results in a barrier of 46.5 kcal mol⁻¹, which is 1.6 kcal mol⁻¹ lower than the average of the DFT methods. G4 calculates the energy barrier for this pathway as 47.6 kcal mol⁻¹, and this is 2.2 kcal mol⁻¹ higher than the calculation by CBS-QB3 (45.4 kcal mol⁻¹). An average barrier is recommended at 46.5 kcal mol⁻¹. This carbon radical of a hydroperoxide group has a small barrier (1.7 kcal mol⁻¹) for highly exothermic beta scission of the OH radical - carbonyl formation, where normal non cyclic alkyl hydroperoxides have much smaller or zero barrier for this OH elimination, see TS4 below.

TS2: TS2 is a five-member ring transition state which corresponds to the intramolecular hydrogen transfer reaction between the hydrogen on the non-peroxy carbon to the peroxy radical, forming the alkyl radical hydroperoxide, y(cjoc)-q. The average of

six DFT calculation methods result in an barrier as $32.9 \text{ kcal mol}^{-1}$, whereas the average of two composite calculation methods, G4 and CBS-QB3, result in an barrier as $31.9 \text{ kcal mol}^{-1}$, $1.0 \text{ kcal mol}^{-1}$ lower than the average of DFT methods. G4 calculates the barrier as $32.8 \text{ kcal mol}^{-1}$, and this is $1.9 \text{ kcal mol}^{-1}$ higher than the calculation by CBS-QB3. The energy barrier is assigned as $31.9 \text{ kcal mol}^{-1}$.

TS3: The carbon-carbon bond initiates ring opening, then the peroxy oxygen radical attacks the ipso carbon of the $\text{C}\cdot\text{OOH}$ group forming a dioxirane ring (ycoo)-ocj on the peroxy carbon site. The initial ether oxygen and attached new carbon radical are single bonded to the ipso carbon. Ring Opening - Dioxygen Oxirane ring formation via TS3. The average of six DFT calculation methods determines the barrier as $43.2 \text{ kcal mol}^{-1}$, whereas the average of two composite calculation methods is $40.9 \text{ kcal mol}^{-1}$, this is $2.3 \text{ kcal mol}^{-1}$ lower determination than the average of DFT methods. G4 calculates the barrier as $42.4 \text{ kcal mol}^{-1}$, and this is $3.1 \text{ kcal mol}^{-1}$ higher than the calculation by CBS-QB3. The energy barrier is assigned as $40.9 \text{ kcal mol}^{-1}$.

TS4: The radical formed from reaction through TS1 undergoes beta scission (carbonyl formation and OH elimination) from the iso hydroperoxide alkyl radical. The average of six DFT calculation methods determines a barrier of $2.2 \text{ kcal mol}^{-1}$. The three higher level calculation methods, G4, CBS-QB3, and CBS-APNO calculate an average barrier of $2.3 \text{ kcal mol}^{-1}$, which agrees well with DFT average. However, the average of CBS-QB3 and CBS-APNO calculation methods results in a of $1.7 \text{ kcal mol}^{-1}$. G4 calculates the barrier as $3.4 \text{ kcal mol}^{-1}$, which is $2.0 \text{ kcal mol}^{-1}$ higher than the calculation by CBS-QB3, and this is $1.4 \text{ kcal mol}^{-1}$ higher than the calculation by CBS-APNO. The energy barrier is assigned as $1.7 \text{ kcal mol}^{-1}$. As noted above, unlike the more common typical OH elimination from an

iso alkyl radical hydroperoxide, in this ring system, there is a small energy barrier, 1.7 kcal mol⁻¹, perhaps resulting from ring strain.

TS5: This transition state is unimolecular elimination reaction to form oxirene plus HO₂ from the alkyl radical, y(cjoc)-q. The average of six DFT calculation methods determines the barrier as 52.7 kcal mol⁻¹. The average of G4 and CBS-QB3 calculation methods is 54.4 kcal mol⁻¹, which is 1.8 kcal mol⁻¹ higher than the average of DFT methods. G4 calculates the barrier as 55.3 kcal mol⁻¹, and this is 1.8 kcal mol⁻¹ higher than the calculation by CBS-QB3. The energy barrier is assigned as 54.4 kcal mol⁻¹.

TS6: The carbon-carbon bond starts cleaving leading toward the formation of two C•H radicals as the methylene carbon starts C=O π bond formation to the ether oxygen. The ether oxygen starts cleaving the bond to the hydroperoxide carbon. The -C•O-OH carbon starts C=O π bond formation with simultaneous C=O--OH cleavage (beta scission). Overall product set is HC•O + HC•O + OH. The average of six DFT calculation methods calculates the barrier as 64.8 kcal mol⁻¹. The average of the G4, CBS-QB3, and CBS-APNO calculations is 64.3 kcal mol⁻¹, which is 0.5 kcal mol⁻¹ lower than the average of DFT methods. The barriers calculated by G4 (64.1 kcal mol⁻¹), CBS-QB3 (64.4 kcal mol⁻¹), and CBS-APNO (64.5 kcal mol⁻¹) are in a good agreement and the energy barrier is assigned as 64.3 kcal mol⁻¹.

TS7: The oxiranyl hydroperoxide, y(cjoc)-q, radical of the non-hydroperoxide carbon starts to undergo β-scission to the ether oxygen and with the ether oxygen –cooh bond undergoing ring opening. The forming carbon radical at the ring oxygen starts form a new π bond with the oxygen of the peroxide. This peroxide carbon continues the β-scission forming a C=O π bond and cleaving the OH group. The carbon – carbon bond of the ring

remains and the final products are glyoxal + OH. This reaction is similar to TS6 without the carbon – carbon bond cleavage. The average of six DFT calculation methods determines the barrier as 9.8 kcal mol⁻¹. The average of G4, CBS-QB3, and CBS-APNO calculation methods is 7.5 kcal mol⁻¹, which is 2.3 kcal mol⁻¹ lower than the DFT method average. The barriers calculated by G4 (7.0 kcal mol⁻¹), CBS-QB3 (7.8 kcal mol⁻¹), and CBS-APNO (7.6 kcal mol⁻¹) are in agreement with each other. The energy barrier is assigned as 7.5 kcal mol⁻¹.

TS8: The C_jH₂-O—Y(COO) radical site undergoes β-scission to form the C=O π bond of formaldehyde and a dioxiranyl radical by cleaving the ring carbon C—OC•H₂ bond. H₂CO elimination from dioxirane ring, y(coo)-ocj, via TS8. The average of six DFT calculation methods results in a barrier of 33.6 kcal mol⁻¹. The average of G4, CBS-QB3, and CBS-APNO calculation methods is 36.0 kcal mol⁻¹, which is 2.4 kcal mol⁻¹ higher determination than the average of DFT methods. The average of CBS-QB3 and CBS-APNO calculation methods shows the barrier as 35.3 kcal mol⁻¹. G4 calculates the barrier as 37.5 kcal mol⁻¹, which is 2.5 kcal mol⁻¹ higher than the calculation by CBS-QB3, and 2.0 kcal mol⁻¹ higher than the calculation by CBS-APNO. The energy barrier is assigned as 35.3 kcal mol⁻¹.

TS9: The C•H carbon radical (y(cjoc)-q) attacks the O atom bonded to the carbon of the hydroperoxide group (inserts). This insertion cleaves the RO-OH bond and forms a bicyclic a second merged oxirane ring molecule, i.e. a di-oxirane structure. This is 2,4-Dioxabicyclo[1.1.0]butane plus an OH radical. The stability of this bicyclic is low and it falls apart with a low barrier to trans c=o π bond formation / trans c—o ring opening to glyoxal + the OH. The average of five DFT calculation methods determines the barrier as

14.1 kcal mol⁻¹. The average of G4 and CBS-QB3 calculation methods is 15.2 kcal mol⁻¹, which is 1.1 kcal mol⁻¹ higher than the DFT method average. G4 calculates the barrier as 14.9 kcal mol⁻¹, and this agrees with the calculation by CBS-QB3 (15.4 kcal mol⁻¹). The energy barrier is assigned as 15.2 kcal mol⁻¹.

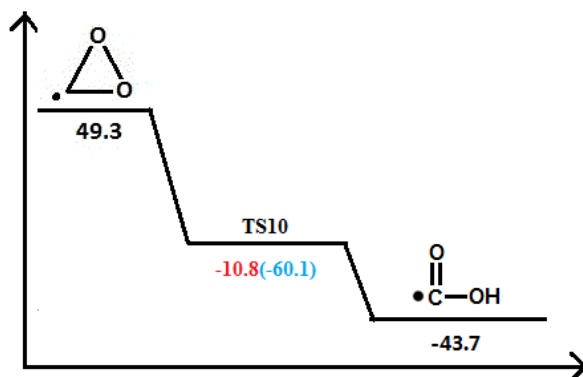


Figure 6.2 Potential energy diagram for ring opening reaction of dioxirane radical (energy barrier in parenthesis). Enthalpy of formation for each TS is taken from Table 6.3. Units in kcal mol⁻¹.

TS10: 2,4-Dioxabicyclo[1.1.0]butane is unstable and undergoes ring opening with no barrier cleaving the carbon oxygen bonds (trans) on opposite sides of the merged ring. The average of five DFT calculation methods determines the barrier as 1.2 kcal mol⁻¹. The average of G4, CBS-QB3, and CBS-APNO calculation methods is -0.5 kcal mol⁻¹, which is 1.7 kcal mol⁻¹ lower than the DFT methods average. The barriers calculated by G4 (-0.2 kcal mol⁻¹), CBS-QB3 (-0.4 kcal mol⁻¹), and CBS-APNO (-0.9 kcal mol⁻¹) are in good agreement. The energy barrier is assigned -0.5 kcal mol⁻¹

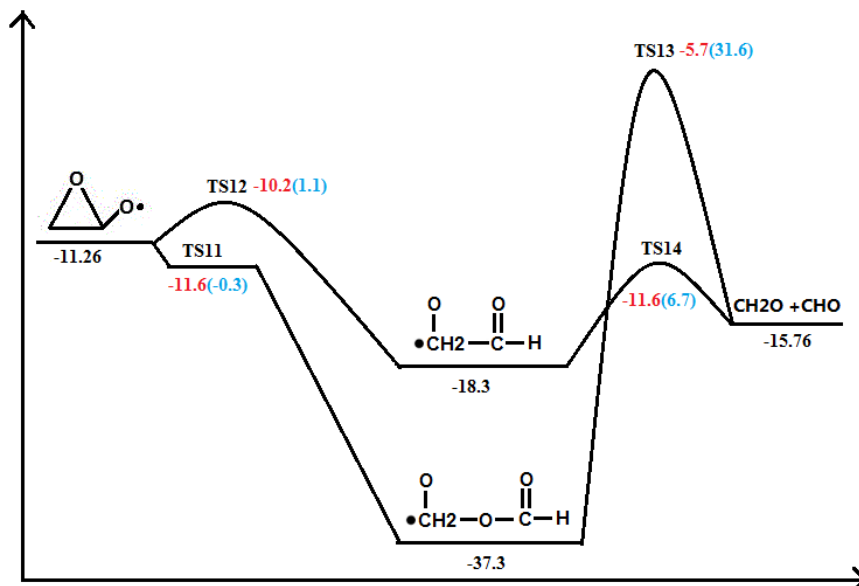
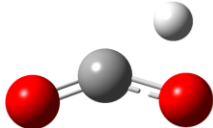
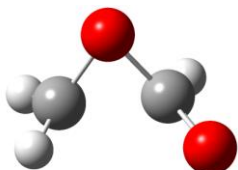
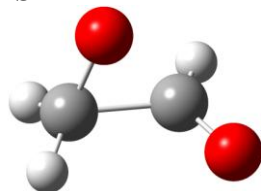


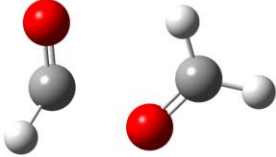
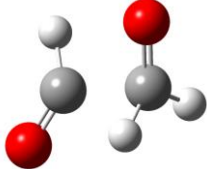
Figure 6.3 Potential energy diagram for ring opening reaction of alkoxy radical (energy barrier in parenthesis). Enthalpy of formation for each TS are taken from Table 6.3. Units in kcal mol⁻¹.

Table 6.3 Calculated Standard Enthalpy of Formation of the Transition State Structures at 298 K for the Unimolecular Dissociation Reaction of $\gamma(\text{cjoo})$ and $\gamma(\text{coc})\text{-oj}$. See Figure 6.2 and 6.3. (Data Recommended in This Study are Indicated by *)

Species	Reaction	$\Delta_f H^\circ_{298}$ ^a (Ea) ^c
	$\gamma(\text{cjoo}) \rightarrow \text{cjdo-oh}$	B3LYP/6-311+G(2d,d,p)
TS10 		-13.5 (-62.8)
		B2PLYP/6-311+G(2d,d,p)
		-13.1 (-62.4)
		M06/6-311+G(2d,d,p)
		-15.6 (-64.9)
		M06-2X/6-311+G(2d,d,p)
		-11.8 (-61.1)
		ω B97X/6-311+G(2d,d,p)
		-12.2 (-61.5)
		ω B97XD/6-311+G(2d,d,p)
		-13.1 (-62.4)
		CBS-QB3
		-11.0 (-60.3)
	CBS-APNO	
	NA	
	G4	

*b Average of G4 and CBS-QB3.

		-10.6 (-59.9)
		-10.8*^b (-60.1)
	y(coc)-oj → cjocho	B3LYP/6-311+G(2d,d,p)
TS11		-11.3 (-0.04)
		B2PLYP/6-311+G(2d,d,p)
		-10.6 (0.7)
		M06/6-311+G(2d,d,p)
		-11.9 (-0.6)
		M06-2X/6-311+G(2d,d,p)
		-11.8 (-0.5)
		ωB97X/6-311+G(2d,d,p)
		-11.4 (-0.1)
		ωB97XD/6-311+G(2d,d,p)
		-11.9 (-0.6)
		CBS-QB3
		-12.3 (-0.04)
		CBS-APNO
		NA
		G4
		-11.0 (0.3)
	-11.6*^b (-0.3)	
	*b Average of G4 and CBS-QB3.	
	y(coc)-oj → ojc-cho	B3LYP/6-311+G(2d,d,p)
TS12		-8.9 (2.4)
		B2PLYP/6-311+G(2d,d,p)
		-8.7 (2.6)
		M06/6-311+G(2d,d,p)
		-8.1 (3.2)
		M06-2X/6-311+G(2d,d,p)
		-7.8 (3.5)
		ωB97X/6-311+G(2d,d,p)
		-7.8 (3.5)
		ωB97XD/6-311+G(2d,d,p)
		-8.4 (2.9)
		CBS-QB3
		-10.7 (0.6)
		CBS-APNO
		NA
		G4
		-9.8 (1.5)
	-10.2*^b (1.1)	
	*b Average of G4 and CBS-QB3.	

		cjocho → h2co + hco	B3LYP/6-311+G(2d,d,p)			
TS13 	*b Average of G4 and CBS-QB3.		-11.0 (26.3)			
			B2PLYP/6-311+G(2d,d,p)	-7.6 (29.7)		
			M06/6-311+G(2d,d,p)	-8.4 (28.9)		
			M06-2X/6-311+G(2d,d,p)	-4.1 (33.2)		
			ωB97X/6-311+G(2d,d,p)	-4.1 (33.2)		
			ωB97XD/6-311+G(2d,d,p)	-5.9 (31.4)		
			CBS-QB3	-5.8 (31.5)		
			CBS-APNO	NA		
			G4	-5.6 (31.7)		
				-5.7*^b (31.6)		
				ojc-cho → h2co + hco	B3LYP/6-311+G(2d,d,p)	
		TS14 	*b Average of G4 and CBS-QB3.		-10.8 (7.5)	
					B2PLYP/6-311+G(2d,d,p)	-11.3 (7.0)
					M06/6-311+G(2d,d,p)	-10.4 (7.9)
					M06-2X/6-311+G(2d,d,p)	-9.5 (8.8)
	ωB97X/6-311+G(2d,d,p)			-6.9 (11.4)		
	ωB97XD/6-311+G(2d,d,p)			-8.7 (9.6)		
	CBS-QB3			-12.1 (6.2)		
	CBS-APNO			NA		
	G4			-11.1 (7.2)		
				-11.6*^b (6.7)		

^a Units in kcal mol⁻¹. ^b Recommendation value for the TS. Average of G4 and CBS-QB3. ^c Energy Barrier in the parenthesis.

TS10: 2,4-Dioxabicyclo[1.1.0]butane is unstable and undergoes ring opening with no barrier cleaving the carbon oxygen bonds (trans) on opposite sides of the merged ring. The average of five DFT calculation methods determines the barrier as $1.2 \text{ kcal mol}^{-1}$. The average of G4, CBS-QB3, and CBS-APNO calculation methods is $-0.5 \text{ kcal mol}^{-1}$, which is $1.7 \text{ kcal mol}^{-1}$ lower than the DFT methods average. The barriers calculated by G4 ($-0.2 \text{ kcal mol}^{-1}$), CBS-QB3 ($-0.4 \text{ kcal mol}^{-1}$), and CBS-APNO ($-0.9 \text{ kcal mol}^{-1}$) are in good agreement. The energy barrier is assigned $-0.5 \text{ kcal mol}^{-1}$.

TS11: The dioxirane ring undergoes ring-opening via TS11 to form the hydroxylcarbonyl $\text{HO}\dot{\text{C}}=\text{O}$ radical. The average enthalpy for the TS structure from the six DFT calculation methods is $-62.5 \text{ kcal mol}^{-1}$. The average enthalpy from G4 and CBS-QB3 calculations is $-60.1 \text{ kcal mol}^{-1}$, which is $2.4 \text{ kcal mol}^{-1}$ higher than DFT average value. G4 calculates the barrier as $-59.9 \text{ kcal mol}^{-1}$, and this agrees with the CBS-QB3 calculation $-60.3 \text{ kcal mol}^{-1}$. The energy barrier is assigned as $-60.1 \text{ kcal mol}^{-1}$.

TS12: Ring opening of the alkoxy oxirane radical $\text{y}(\text{coc})\text{-oj}$, which results from the chain branching channel is not stable; it beta scissions with a very low barrier, cleaving the C-C bond in TS12 to form an ester radical $\text{C}\cdot\text{OCH}=\text{O}$. The average of six DFT calculation methods determines the barrier as $-0.2 \text{ kcal mol}^{-1}$ in agreement with the average of G4 and CBS-QB3 calculation method values, $-0.4 \text{ kcal mol}^{-1}$. G4 calculates the barrier as $0.3 \text{ kcal mol}^{-1}$, which is $0.7 \text{ kcal mol}^{-1}$ higher than CBS-QB3 calculation ($-1.04 \text{ kcal mol}^{-1}$). The energy barrier is assigned as $-0.4 \text{ kcal mol}^{-1}$. There is also a barrier which is only $\sim 1 \text{ kcal mol}^{-1}$ higher cleaving the $\text{c}-\text{o}$ bond in the ring forming an alkoxy radical $\text{O}\cdot\text{CH}_2\text{CH}=\text{O}$.

TS13: Ring opening of the alkoxy oxiranyl radical, y(coc)-oj, can occur by beta scission cleaving a C-O bond via TS13 to form an alkoxy radical of glyoxal, ojch2-cho. The average of six DFT calculation methods results in a barrier of 3.0 kcal mol⁻¹, that is 1.9 kcal mol⁻¹ higher than the average of G4 and CBS-QB3 calculations. G4 calculates the barrier as 1.5 kcal mol⁻¹, which is 0.9 kcal mol⁻¹ higher than the determination by CBS-QB3 (0.6 kcal mol⁻¹). The energy barrier is assigned as 1.1 kcal mol⁻¹.

TS14: The methyl radical on the ether, C•H₂-O-CHO, dissociates via beta scission reaction to form H₂CO plus HC•O via TS14. The average of six DFT calculation methods determines the barrier as 30.5 kcal mol⁻¹, which is 1.1 kcal mol⁻¹ higher than the average of G4 and CBS-QB3 calculations, 31.6 kcal mol⁻¹. G4 calculates the barrier as 31.7 kcal mol⁻¹, which agrees with the determination by the CBS-QB3 calculation, 31.5 kcal mol⁻¹. The energy barrier is assigned as 31.6 kcal mol⁻¹.

TS15: The •O-CH₂-CHO alkoxy radical also dissociates via beta scission to form H₂CO and HC•O through TS15. The average of six DFT calculation methods determines the barrier as 8.7 kcal mol⁻¹, which is 2.0 kcal mol⁻¹ higher than the average of G4 and CBS-QB3 calculations, 6.7 kcal mol⁻¹. G4 calculates the barrier as 7.2 kcal mol⁻¹, which is 1.0 kcal mol⁻¹ higher than the CBS-QB3 calculation. The energy barrier is assigned as 6.7 kcal mol⁻¹.

6.3.3 Entropy and Heat Capacity

Entropy and heat capacity calculations were performed by using B3LYP/6-31+G(d,p) geometries and harmonic frequencies. The data are summarized in Table 6.4 with comparison to available literature data.

Table 6.4 Ideal Gas Phase Entropy and Heat Capacity Obtained by B3LYP/6-31+G(d,p) Calculation, Comparison with Available Literature

	S_{298}° ^a	C_{p300} ^b	C_{p400}	C_{p500}	C_{p600}	C_{p800}	C_{p1000}	C_{p1500}
y(cjoc)^c	60.36	11.08	13.95	16.50	18.58	21.66	23.84	27.16
Literature ^d	60.4±0.5	11.2±0.9	14.2±1.1	16.7±1.1	18.8±1.1	21.8±1.0	24.0±0.9	27.3±0.7
y(coc)-qj^c	74.95	17.68	21.62	24.94	27.58	31.37	33.93	37.68
Literature ^e	72.53	17.63	21.56	24.88	27.53	31.33	33.91	37.68
y(coc)-oj^c	66.07	15.09	18.52	21.39	23.70	27.08	29.44	32.96
Literature ^d	67.8±0.9	15.5±1.1	18.9±1.3	21.7±1.3	24.0±1.2	27.3±1.1	29.6±1.0	33.1±0.7
y(cocj)-q^e	75.85	20.03	24.05	27.39	29.90	33.18	35.17	37.97
y(cjoc)-q^c	75.66	20.15	24.33	27.77	30.35	33.63	35.56	38.13
Literature ^e	75.75	20.31	24.41	27.75	30.23	33.43	35.35	38.02
y(coc)-do^c	63.12	12.97	15.85	18.26	20.21	23.07	25.05	27.95
Literature ^d	63.1±0.7	13.1±0.9	16.0±1.1	18.4±1.1	20.4±1.0	23.2±0.9	25.2±0.8	28.0±0.6
y(cdco)^d	60.5±0.7	13.2±0.6	15.1±0.7	16.5±0.6	17.7±0.6	19.4±0.6	20.6±0.6	22.7±0.4
yy(cco-cco)^c	63.18	14.29	17.37	19.79	21.62	24.15	25.83	28.31
cho-cho^c	67.03	14.53	17.04	19.35	21.28	24.03	25.75	28.01
Literature ^d	64.6±0.8	14.5±0.8	17.0±1.1	19.4±1.2	21.4±1.1	24.3±0.8	26.0±0.5	28.2±0.2
oh^d	43.9±0.1	6.9±0.0	6.9±0.0	7.0±0.0	7.0±0.0	7.1±0.1	7.2±0.1	7.7±0.1
h2co^d	52.2±0.2	8.4±0.2	9.3±0.4	10.4±0.5	11.4±0.6	13.3±0.7	14.7±0.6	16.9±0.5
hco^d	53.5±0.2	8.3±0.1	8.7±0.2	9.2±0.3	9.7±0.3	10.6±0.3	11.3±0.3	12.5±0.2
ho2^d	54.6±0.2	8.3±0.1	8.8±0.2	9.4±0.3	9.9±0.3	10.7±0.3	11.3±0.3	12.3±0.2
y(cjoo)^c	59.88	9.91	11.57	12.98	14.09	15.64	16.67	18.09
y(coo)-ocj^c	76.95	21.19	25.44	28.31	30.24	32.79	34.56	37.40
ojc-cho^c	70.81	15.68	18.91	21.65	23.84	27.05	29.26	32.50
Literature ^d	70.1±0.9	15.7±1.1	19.0±1.3	21.8±1.3	24.0±1.2	27.2±1.0	29.4±0.8	32.6±0.6
cjocho^c	72.11	16.88	20.13	22.98	25.27	28.47	30.47	33.06
Literature ^d	70.1±1.1	17.2±1.0	20.2±1.3	22.9±1.4	25.1±1.3	28.4±1.0	30.6±0.8	33.3±0.3
cjdo-oh^c	61.03	11.63	12.80	13.78	14.61	15.86	16.71	17.83

Literature ^d	60.2±0.6	11.3±0.6	12.8±0.6	14.0±0.5	14.8±0.4	16.1±0.3	16.9±0.2	17.9±0.1
o2^c	48.90	7.00	7.20	7.40	7.60	8.00	8.20	8.60
n2^c	45.79	1.04	1.06	1.06	1.08	1.12	1.17	1.24
ts1^c	71.59	17.59	21.61	24.94	27.57	31.33	33.83	37.33
ts2^c	60.09	16.55	21.02	24.66	27.49	31.41	33.94	37.41
ts3^c	71.15	18.05	21.87	24.98	27.42	30.91	33.30	36.85
ts4^c	73.78	18.70	22.24	25.17	27.49	30.84	33.14	36.64
ts5^c	80.01	22.57	25.43	27.76	29.43	32.00	33.87	36.91
ts6^c	70.49	18.25	22.36	25.66	28.25	31.89	34.28	37.59
ts7^c	76.37	20.20	23.42	26.08	28.20	31.29	33.44	36.77
ts8^c	79.58	19.81	22.87	25.56	27.77	31.11	33.47	36.99
ts9^c	81.87	20.86	24.41	27.10	29.12	31.94	33.90	36.99
ts10^c	59.90	10.35	11.43	12.37	13.19	14.47	15.36	16.57
ts11^c	65.57	14.09	17.23	19.90	22.06	25.28	27.57	31.01
ts12^c	65.43	13.62	16.70	19.41	21.65	25.01	27.40	30.96
ts13^c	69.65	16.09	18.50	20.66	22.52	25.49	27.70	31.11
ts14	75.93	16.52	18.74	20.77	22.58	25.54	27.78	31.21

^{a,b} Units in cal mol⁻¹ K⁻¹. ^c This study. ^d Goldsmith⁸⁴. ^e Auzmendi-Murua¹²¹.

6.3.4 Kinetic Parameters

Variational Transition State Theory Analysis

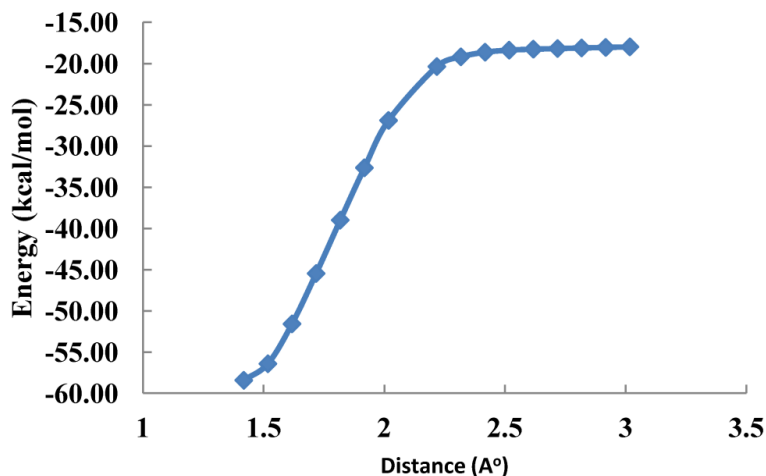


Figure 6.4 Potential energy surface for dissociation of the oxiranyl hydroperoxide, $y(\text{coc})\text{-oo}\bullet$, $\text{R-O}_2 \rightarrow \text{R}\bullet + \text{O}_2$ with $\omega\text{B97XD/6-31+G(d,p)}$ calculation method.

Figure 6.4 shows the potential energy surface for dissociation of the $y(\text{coc})\text{-oo}\bullet \rightarrow y(\text{coc}\bullet) + \text{O}_2$, where the C-O bond distance range from 1.4175 Å to 3.0175 Å, in intervals of 0.1 Å. Thermochemical properties and rate constants as a function of temperature are calculated for each point on the potential energy scans. The variational rate constant is determined from the minimum rate constant located as a function of temperature and bond distance on the curve. Rate constants are then fit to the three-parameter form of the Arrhenius equation to yield the rate parameters A' , n , and E_a . The Transition State Structure for the $\text{R}\bullet + \text{O}_2$ association reaction occurs at $\text{R-OO}\bullet$ bond lengths of 2.6 Å at 300 K, with decreases to 2.2 Å at 2000 K. Fitting the minimum rate constant as a function of temperature to the three-parameter Arrhenius equation for the association reaction results in $A' = 9.25\text{E}+04$, $n = 2.11$, $E_a = -0.40 \text{ kcal mol}^{-1}$, for a modified Arrhenius expression of $A \cdot T^n \cdot \exp(-E_a/RT)$ and for the dissociation reaction is $A' = 1.32\text{E}+13$, $n = 0.65$, $E_a = 40.80 \text{ kcal mol}^{-1}$. Variational transition state analysis is also preformed for the chain branching channel:

$y(\text{coc})\text{-oo}\bullet \rightarrow y(\text{coc})\text{-o}\bullet + \text{o}$ dissociation reaction using similar methods and step size to the peroxy system.

The potential energy surface for dissociation of the $y(\text{coc})\text{-oo}\bullet \rightarrow y(\text{coc})\text{-o}\bullet + \text{o}$, range from O-O bond distance 1.33178 Å to 3.03178 Å by the intervals of 0.1 Å is shown in figure 6. The location of the variational transition state is at RO-O bond length of 2.7 Å at 300 K, tightening to 2.0 Å at 2000 K. Fitting the minimum rate constant as a function of temperature to the three-parameter Arrhenius equation for the dissociation reaction is $A' = 4.88\text{E}+14$, $n = 0.13$, $E_a = 50.20 \text{ kcal mol}^{-1}$, and for the association reaction is $A' = 3.49\text{E}+12$, $n = -0.40$, $E_a = -0.62 \text{ kcal mol}^{-1}$.

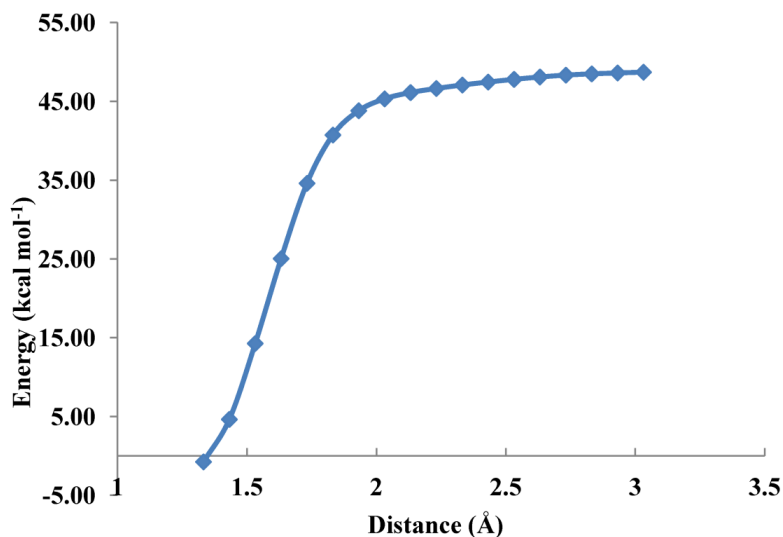


Figure 6.5 Potential energy surface for dissociation of the oxiranyl hydroperoxide, $y(\text{coc})\text{-oo}\bullet$, $\text{R-OO} \rightarrow \text{RO}\bullet + \text{O}$ with $\omega\text{B97XD/6-31+G(d,p)}$ calculation method.

Table 6.5 lists high-pressure-limit elementary rate parameters used as input data to the QRRK calculations.

Table 6.5 High Pressure Limit Elementary Rate Parameters for the Unimolecular Dissociation Reaction of Oxiranyl Radical

Reaction	$k=A(T)^n \exp(-E/RT)$		
	A	n	E_{fit} (kcal/mol)
$y(cjoc) + o_2 = y(coc)-qj$	9.25E+04	2.11	-0.40
$y(coc)-qj = y(cjoc) + o_2$	1.32E+13	0.65	40.75
$y(coc)-qj = y(coc)-oj + o$	4.88E+14	0.13	49.07
$y(coc)-oj + o = y(coc)-qj$	3.49E+12	-0.40	-0.62
$y(coc)qj = y(cocj)q$	1.86E+10	0.95	46.51
$y(cocj)q = y(coc)qj$	2.23E+12	-0.04	30.28
$y(coc)-qj = y(cjoc)-q$	5.54E+09	0.92	32.84
$y(cjoc)-q = y(coc)-qj$	6.15E+12	-0.39	19.58
$y(coc)qj = y(coo)-ocj$	4.57E+10	0.80	40.98
$y(coo)-ocj = y(coc)qj$	8.44E+11	-0.04	43.49
$y(cocj)-q = y(coc)-do + oh$	2.36E+13	-0.20	2.42
$y(coc)-do + oh = y(cocj)-q$	1.41E+04	2.24	49.39
$y(cjoc)-q = ycdco + ho_2$	6.24E+13	0.21	55.14
$ycdco + ho_2 = y(cjoc)-q$	6.12E+01	2.94	-0.92
$y(cjoc)-q = y(coo)-ocj$	1.98E+12	-0.09	64.22
$y(coo)-ocj = y(cjoc)-q$	3.29E+10	0.38	79.99
$y(cjoc)-q = cho-cho + oh$	1.52E+14	-0.24	8.33
$cho-cho + oh = y(cjoc)-q$	1.34E+05	2.01	62.52
$y(coo)-ocj = y(cjoo) + h_2co$	2.16E+13	0.14	35.70
$y(cjoo) + h_2co = y(coo)-ocj$	9.42E+01	3.08	8.19
$y(cjoc)q = yy(cco-cco) + oh$	2.88E+14	0.09	15.78
$yy(cco-cco) + oh = y(cjoc)q$	5.85E+05	2.31	-5.08

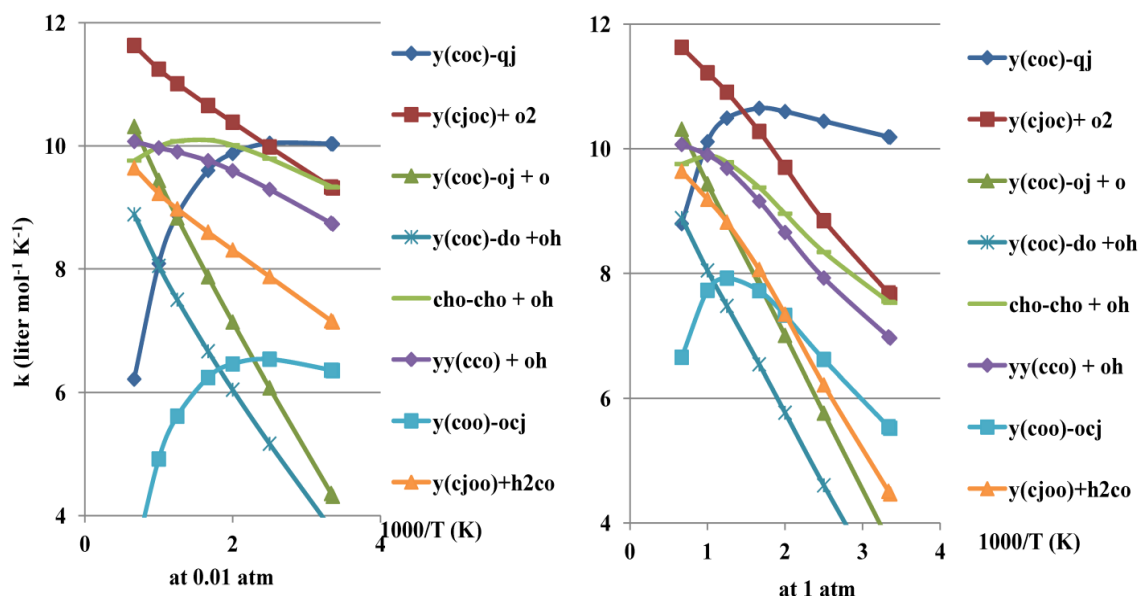


Figure 6.6 Rate constants as a function of temperature at 0.01 atm (left) and at 1 atm (right).

Rate constants to the different isomers and products versus temperature and pressure obtained by applying QRRK-Master Equation analysis for the determination of chemical activation reaction of the oxiranyl radical and O_2 are presented in Figure 6.6 and 6.7.

At low pressure 0.01 atm, high temperature range, the dominating forward channel is stabilization of the peroxy radical, reactions to glyoxal (ethanedial) plus OH radical via two different channels and chain branching to alkoxy plus oxygen atom. Other somewhat lower channels include oxirene + HO_2 , and oxiranone + OH. The dominant channel is the stabilization reaction to peroxy radical, $y(coc)-qj$ in the low temperature range.

At 1 atm, higher temperatures, the important channels are similar to those at 0.01 atm: reaction to glyoxal (ethanedial) plus OH radical (via two different channels) and chain branching to alkoxy plus oxygen atom. At Low temperatures the dominant channel is stabilization to the peroxy radical, $y(coc)-qj$. The next important channel is ethanedial plus OH radical.

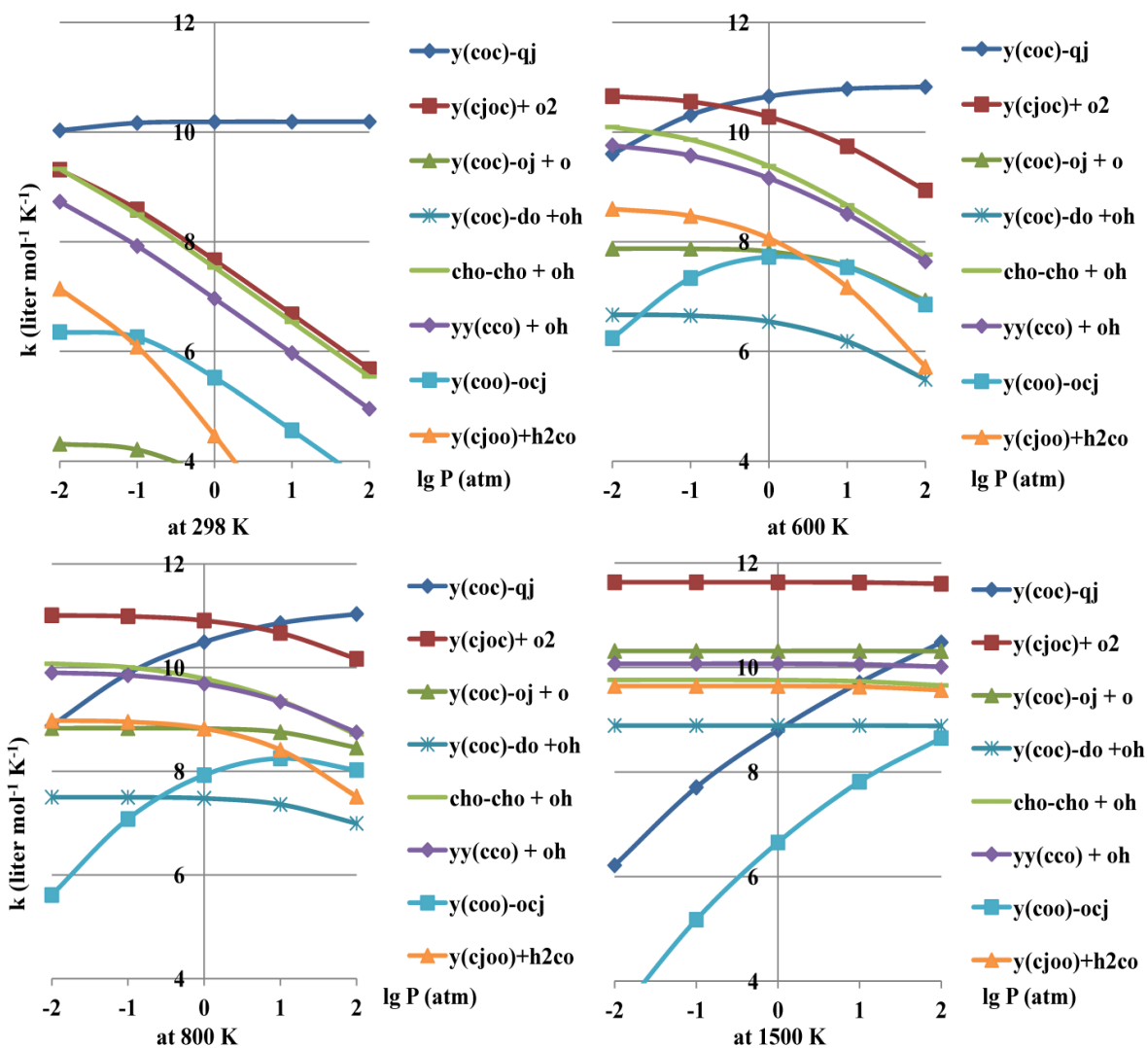


Figure 6.7 Rate constants as a function of pressure at 298 K, 600 K, 800 K, and 1500 K.

At 298 K, the dominant channel is the stabilization reaction to form peroxy radical, $y(\text{coc})\text{-qj}$, over the entire pressure range. The reaction to ethanedial + OH is next most important forward channel, via the two reaction paths.

At temperatures between 600 K and 800 K, where initiation of combustion and ignition can occur and in the low pressure range, the most important forward channel is stabilization to peroxy radical, $y(\text{coc})\text{-qj}$, with reaction to glyoxal + OH next in importance. In the temperature range of 600 – 800 K stabilization and reaction to glyoxal (ethanedial)

plus OH radical are important. Chain branching to the alkoxy radical plus O atom is also important in this range. At higher temperatures important forward channels are the chain branching to the alkoxy radical plus O atom and also two reactions to glyoxal (ethanedial) plus OH radical.

Under atmospheric conditions the stabilization to the Oxirane-peroxy radical will undergo reaction with NO to form the alkoxy radical which will immediately undergo unimolecular dissociation to $\text{O}\cdot\text{CH}_2\text{CH}=\text{O}$ and $\text{C}\cdot\text{H}_2\text{OCH}=\text{O}$. These reactive species will react with oxygen and other species in the atmosphere.

Figure 6.8 and 6.9 present Chemkin simulations for the oxidation reaction of oxiranyl radical with O_2 vs. time at 1 atm pressure and two temperatures, 600 K and 800 K. At 600 K, the dominating product is the stabilization complex, y(coc)-qj. The reaction reaches equilibrium at $1.6\text{E}-4$ second.

At 800 K, the most important product is y(coc)-qj at 50 milliseconds the second important product is 2,4-Dioxabicyclo[1.1.0]butane + OH. The dominating channel becomes to be ethanedial + OH at 3.5 milliseconds second.

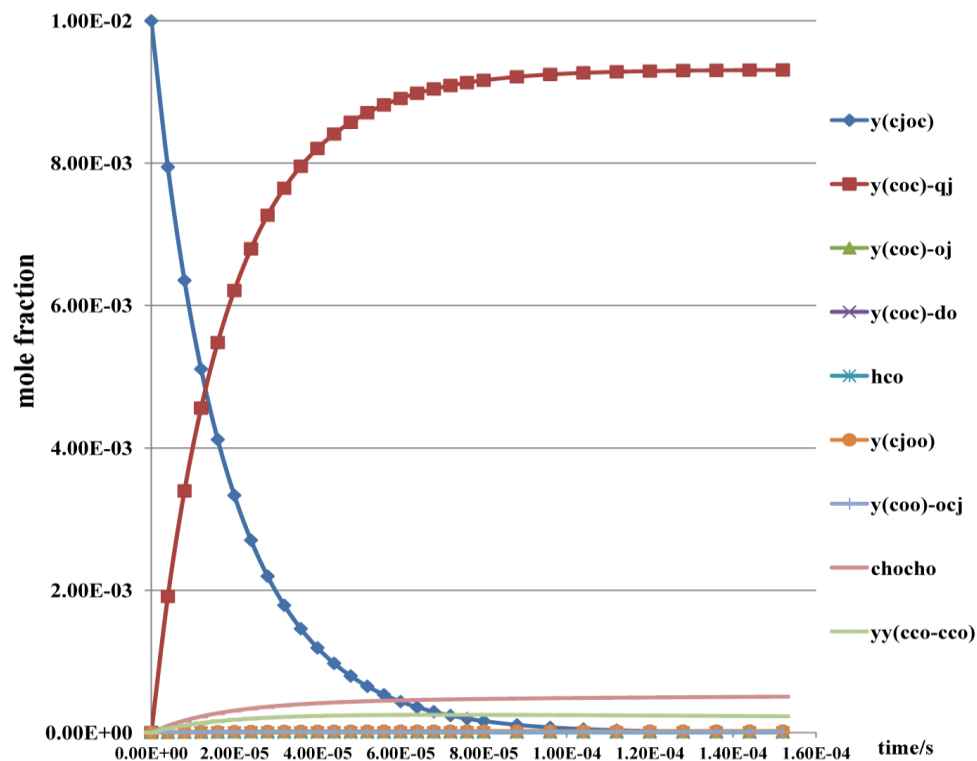


Figure 6.8 Chemkin modeling of oxidation reaction of oxiranyl radical at 1 atm, 600 K, 1% of oxiranyl radical, 6% of O₂, 93% of N₂.

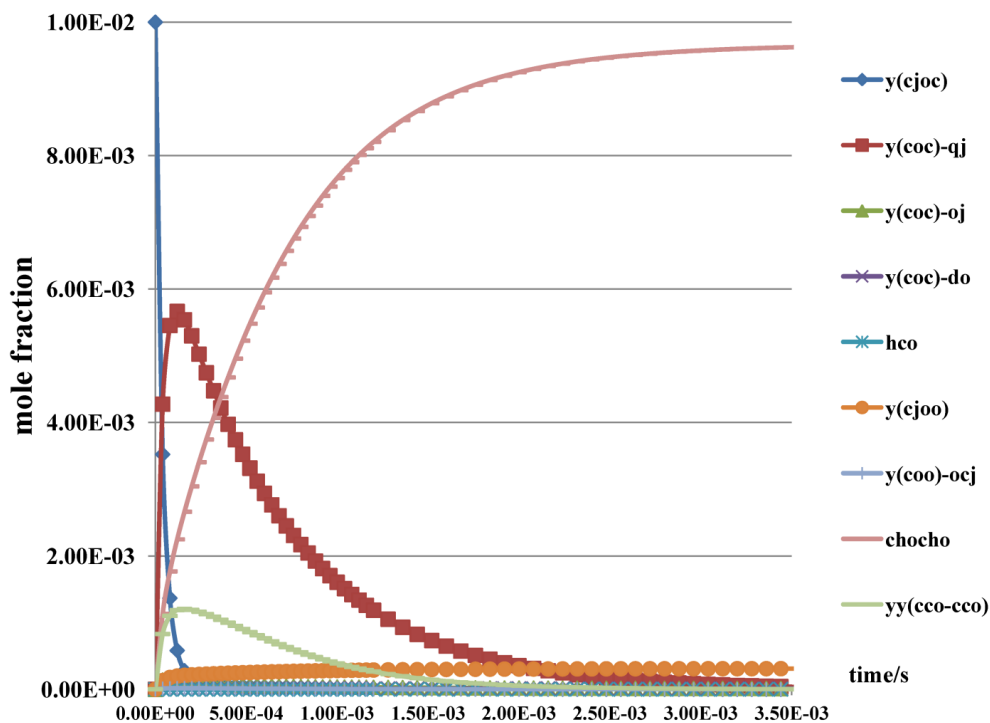


Figure 6.9 Chemkin modeling of oxidation reaction of oxiranyl radical at 1 atm, 800 K, 1% of oxiranyl radical, 6% of O₂, 93% of N₂.

6.3.5 Comparison of Dissociation and Association Reaction of Oxiranyl

Figure 6.10- 6.15 present the Chemkin simulation of the competing reaction processes: unimolecular dissociation (ring-opening) reaction and bimolecular O₂ association (oxidation) reactions of the oxiranyl radical at temperature, 298 K, 400 K, 430 K, 600 K, and 800 K.

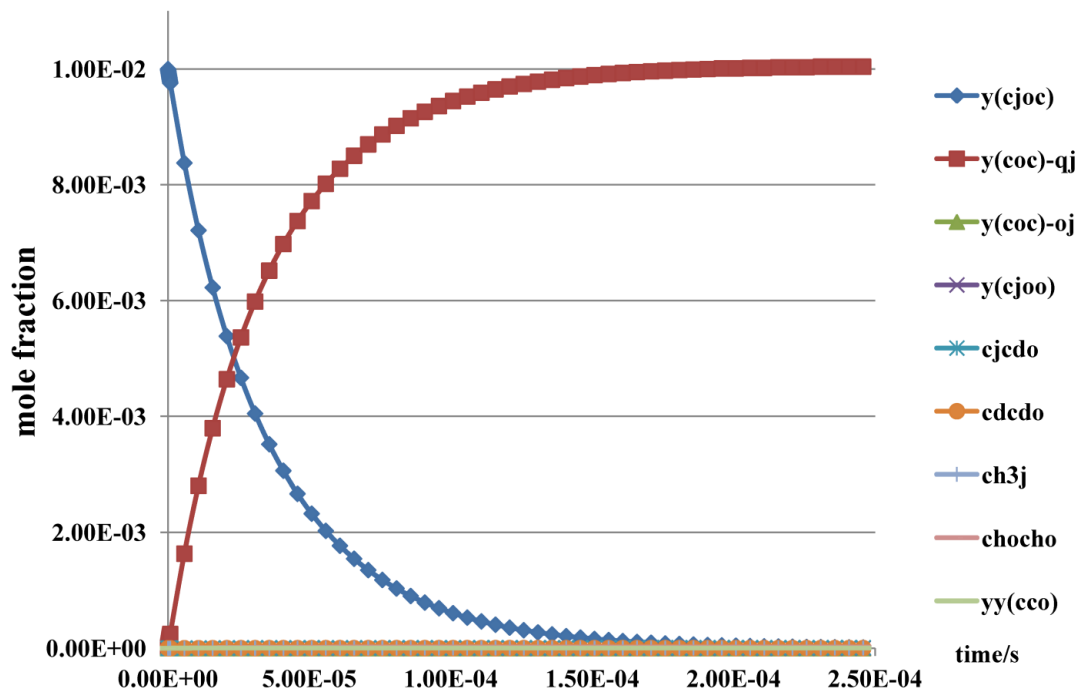


Figure 6.10 Chemkin modeling of competition between the dissociation reaction and oxidation reaction of oxiranyl radical at 1 atm, 298 K, 1% of oxiranyl radical, 6% of O₂, 93% of N₂.

At 298 K, room temperature, the dominating channel is stabilization to form peroxy radical, y(coc)-qj. The reaction reaches equilibrium at 2.5E-4 second, and the final concentration of peroxy radical equals to the initial concentration of oxiranyl radical.

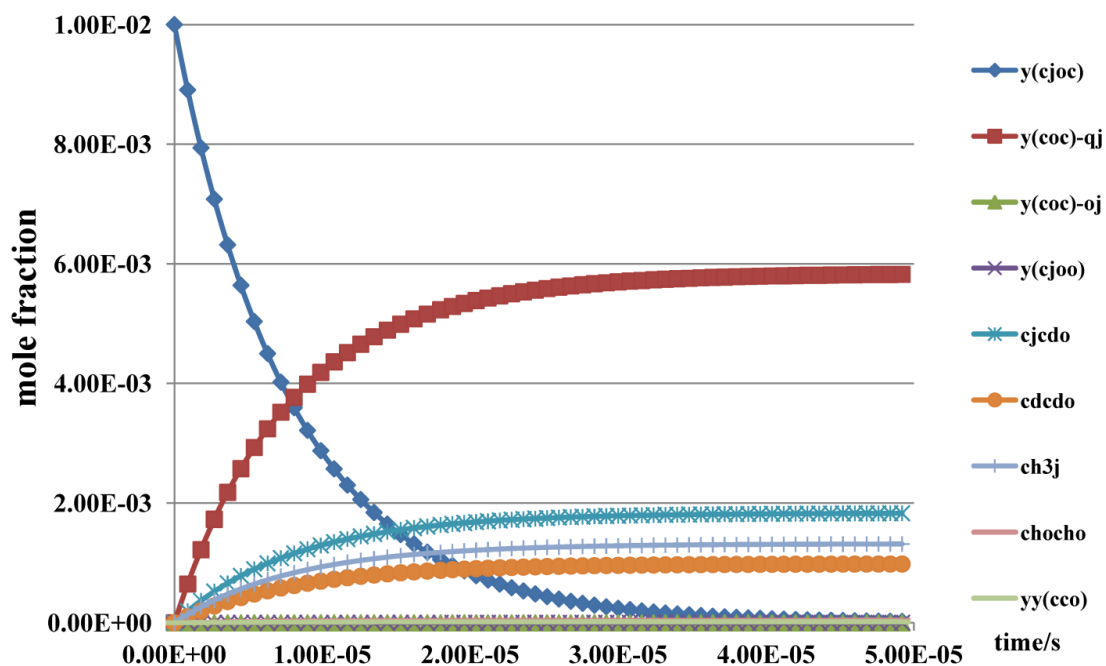


Figure 6.11 Chemkin modeling of competition between the dissociation reaction and oxidation reaction of oxiranyl radical at 1 atm, 400 K, 1% of oxiranyl radical, 6% of O₂, 93% of N₂.

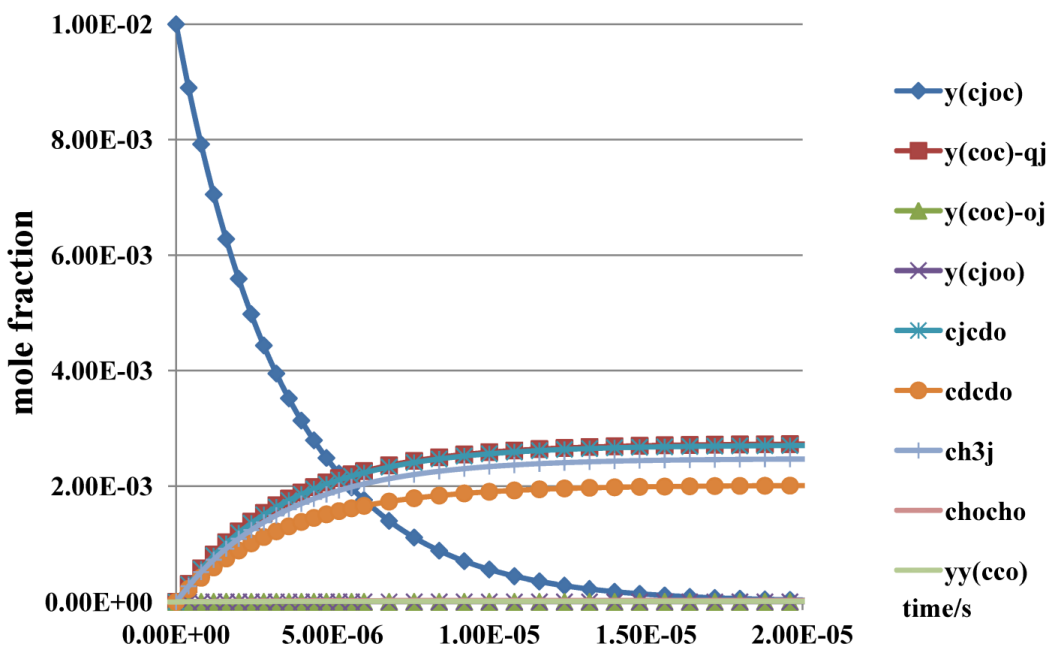


Figure 6.12 Chemkin modeling of competition between the dissociation reaction and oxidation reaction of oxiranyl radical at 1 atm, 430 K, 1% of oxiranyl radical, 6% of O₂, 93% of N₂.

At 400 K, the dominant channel remains as stabilization to form the peroxy radical, y(coc)-qj. The modeled reaction system reaches steady state at 5E-5 second. The products from unimolecular dissociation reaction system, acetyl radical, methyl radical plus carbon monoxide, and ketene plus hydrogen atom show some accumulation.

At 430 K, the stabilization channel to form peroxy radical in the oxidation reaction system is competing with the acetyl radical formation channel in the dissociation reaction system. The reaction system reaches equilibrium at 200 milliseconds. This temperature range, above 430 K, is showing a turning point where the unimolecular dissociation is competing and beginning to become the more important channel as temperature is increased.

At 500 K, there are two channels from dissociation reaction system are competing with each other, methyl radical plus carbon monoxide and ketene plus hydrogen atom. The oxidation reaction system becomes less important. The reaction equilibrium approaching 2 microseconds.

At 600 K, the dominant channels are the unimolecular dissociation reactions of oxiranyl radical, ring opening of the oxiranyl ring to form the acetyl radical, cjcdo, and further reaction of the intermediates. This reaction set reaches the equilibrium at 25 milliseconds. The second important channel is also from the unimolecular dissociation reaction of oxiranyl radical, dissociation to methyl radical plus carbon monoxide pathway. At the early reaction times, the most important channel is the ketene plus hydrogen atom channel.

At 800 K, the dominant channel is the unimolecular dissociation reaction of oxiranyl radical, and further reactions of the intermediates to methyl radical plus carbon

monoxide. The reaction reaches the equilibrium at 250 milliseconds. At early times the most important initial reaction product is ketene plus hydrogen atom from unimolecular dissociation of the ring opened intermediate. This channel is competing with the acetyl radical (methyl product) channel at 10 milliseconds.

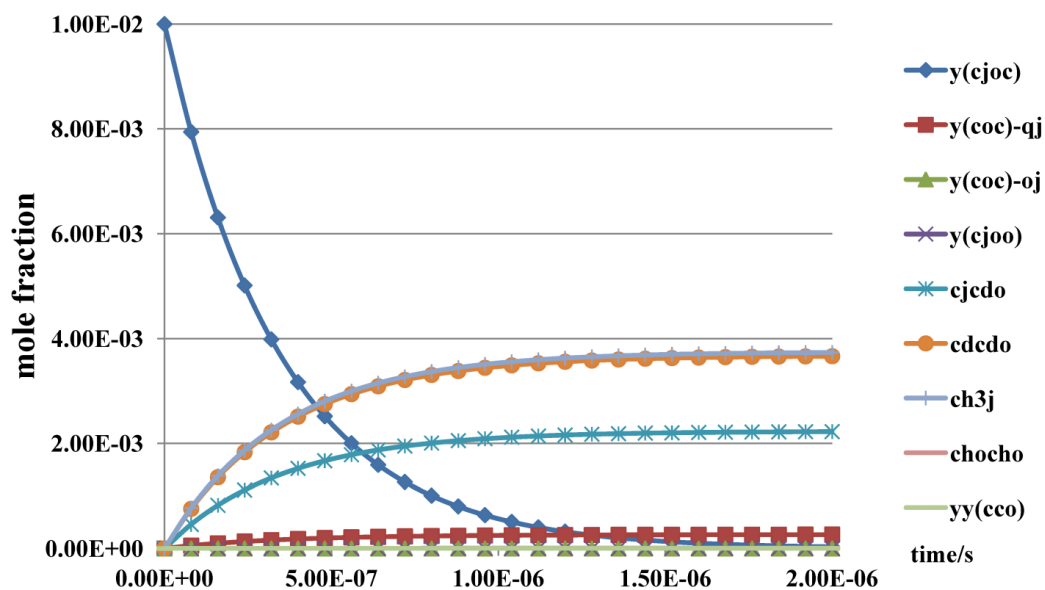


Figure 6.13 Chemkin modeling of competition between the dissociation reaction and oxidation reaction of oxiranyl radical at 1 atm, 500 K, 1% of oxiranyl radical, 6% of O₂, 93% of N₂.

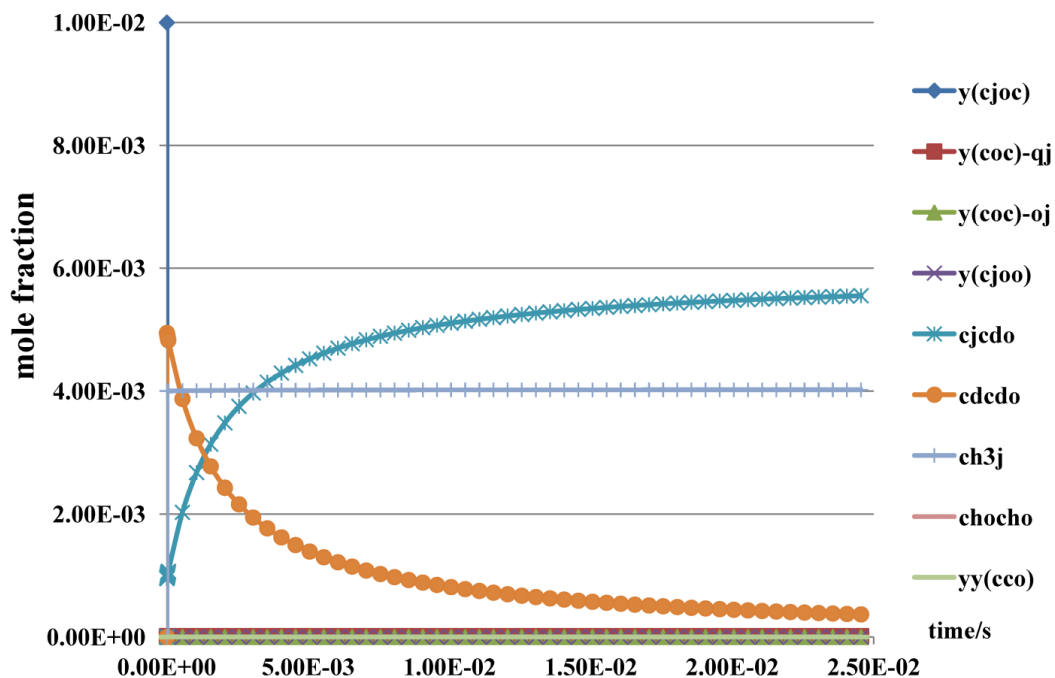


Figure 6.14 Chemkin modeling of competition between the dissociation reaction and oxidation reaction of oxiranyl radical at 1 atm, 600 K, 1% of oxiranyl radical, 6% of O₂, 93% of N₂.

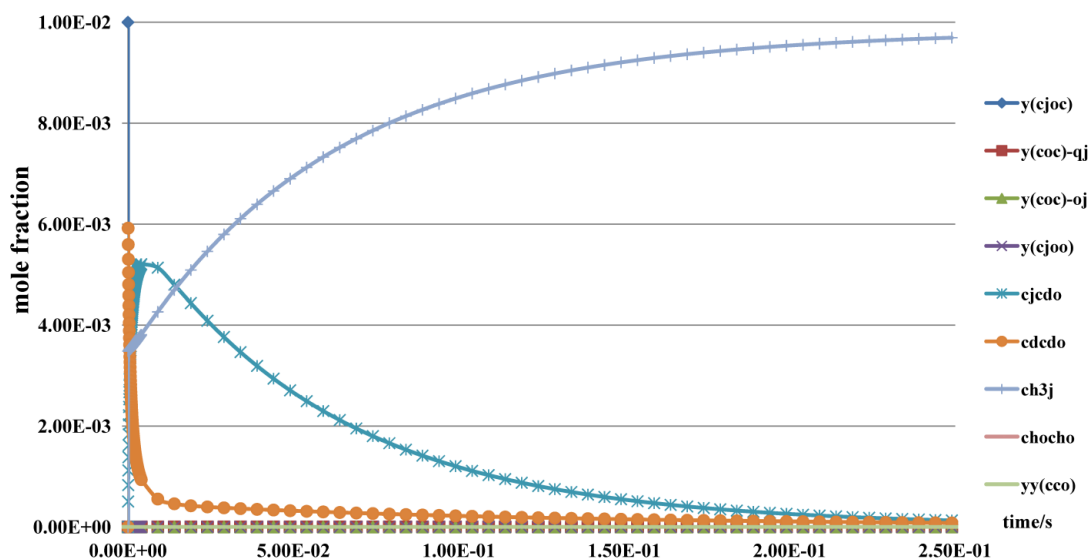


Figure 6.15 Chemkin modeling of competition between the dissociation reaction and oxidation reaction of oxiranyl radical at 1 atm, 800 K, 1% of oxiranyl radical, 6% of O₂, 93% of N₂.

6.4 Summary

Thermochemical properties including standard enthalpies of formation, standard entropy, and heat capacity as function of temperature for the oxidation reaction of oxiranyl radical with O_2 system are determined. The complete reaction mechanism of oxiranyl radical associate with O_2 is calculated with different DFT methods compare with CBS-QB3, CBS-APNO, and G4 calculation methods. Rate constants versus temperature and pressure discover that 1 atm, high temperature, association reaction of oxiranyl radical plus O_2 is not happen, low temperature, association reaction of oxiranyl radical plus O_2 tends to accumulate peroxy radical, y(cjoc)-qj. At 1 atm, below 430 K, the oxidation system is dominating, whereas above 430 K, the product sets from dissociation reaction system becomes to be most important.

CHAPTER 7

CONCLUSIONS

This work presents thermochemical properties, kinetics, and modeling results on fluoro-hydrocarbons, hydroperoxides, fluoro-hydroperoxides, and three member ring cyclic ether radical, in atmospheric and combustion environments.

Molecular geometries, vibration frequencies, internal rotor potentials and thermochemical properties ($\Delta_f H^\circ_{298}$, $S^\circ(T)$ and $C^\circ_p(T)$) for fluoro-hydrocarbons, alkyl and fluoro - hydroperoxides, and oxiranyl radical are presented using a number of different ab-initio, density functional theory (DFT) and composite calculation methods, and basis sets. Kinetic parameters for Unimolecular decomposition and oxidation of the oxiranyl radical are determined versus pressure and temperature for the chemically activated formation and unimolecular dissociation of the adducts. Kinetic calculations use multi-frequency quantum RRK analysis for the energy dependent rate constant with Master Equation analysis for fall off. The simulations for the determination of the important reaction paths, identification of main products and determination of combustion characteristics at different process conditions are evaluated.

The thermochemical and kinetic properties developed during this work illustrate the effects of fluorine substitution on C1 to C4 normal hydrocarbons C1 fluoro-hydroperoxides based on standard enthalpies of formation and bond dissociation energies. Thermochemical and kinetic calculations for the unimolecular dissociation (ring opening) and molecular oxygen oxidation reactions of oxiranyl radical show important reaction paths and their changes as function of temperature and pressure.

APPENDIX A

ENTHALPY OF FORMATION OF REFERENCE SPECIES

Appendix A includes the enthalpies of formation at 298 K of the reference species used in the isodesmic work reactions for the calculation of the enthalpies of formation of the target molecules.

Table A. Standard Enthalpy of Formation for Reference Species in the Work Reactions and Bond Dissociation Energy Calculations

Species	$\Delta_f H^\circ_{298}$ (kcal)	Reference
CH ₄	-17.78±0.10	Pedley ^{a,b}
CH ₃ CH ₃	-20.03±0.10	Pedley ^{a,b}
CH ₃ CH ₂ CH ₃	-25.02±0.12	Pedley ^{a,b}
CH ₃ CH ₂ CH ₂ CH ₃	-30.02±0.17	Pedley ^{a,b}
CH ₃ OH	-48.16±0.07	Pedley ^a
CH ₃ CH ₂ OH	-56.21±0.10	Pedley ^a
(CH ₃) ₃ CH	-32.07±0.17	Pedley ^a
CH ₃ CH(CH ₃)CH ₂ CH ₃	-36.74±0.24	Pedley ^a
CH ₃ F	-56.54±0.07	Goos ^a
CH ₃ CH ₂ CH ₂ CH ₂ CH ₃	-35.11±0.22	Pedley ^{a, b}
HOOH	-32.1±0.3	Goldsmith ^b
CH ₃ OOCH ₃	-30.05±0.30	Pedley ^b
CH ₃ CH ₂ OOCH ₂ CH ₃	-46.08±0.59	Pedley ^b
H	52.103±0.001	Cox ^{b,d}
O	59.555±0.024	Cox ^b
CH ₃ j	35.01±0.02	Goos ^{b,d}
CH ₃ CH ₂ j	29.0±0.4	Blanksby ^b
CH ₃ CH ₂ CH ₂ j	24.3±0.9	Goldsmith ^b
CH ₃ CH ₂ CH ₂ CH ₂ j	19.3±0.9	Goldsmith ^b
HOOj	2.94	Chase ^b
CH ₃ Oj	4.1±1.0	Tsang ^b
CH ₃ CH ₂ Oj	-3.01	Burke ^b
CH ₃ CH ₂ CH ₂ Oj	-9.15	Burke ^b
CH ₃ CH ₂ CH ₂ CH ₂ Oj	-11.9	Simmie ^b
OH	8.93±0.03	Ruscic ^b
y(cjco)	39.69	Auzmendi-Murua ^d
cjcho	2.76±2.00	Zhu ^d
ccj=o	-2.76	Average ^{d,f}

c=c=O	-11.35±0.38	Pedley ^d
CO	-26.3	Asatryan ^d
y(cjoc)	39.69	Auzmendi-Murua ^e
y(coc)-qj	-0.77 ^b	Auzmendi-Murua ^e
y(coc)-oj	-11.26 ^b	Auzmendi-Murua ^e
y(cocj)-q	15.92 ^b	Auzmendi-Murua ^e
y(cjoc)-q	13.15 ^b	Auzmendi-Murua ^e
y(coc)-do	-41.0 ^c	Goldsmith ^e
y(cdco)	65.1 ^c	Goldsmith ^e
yy(cco-cco)	24.1 ^d	Wang ^e
cjocho	-37.3±0.9 ^c	Goldsmith ^e
y(coc)	-12.72 ^b	Auzmendi-Murua ^e
CH ₃ OCH ₃	-44.00±0.12 ^h	Pedley ^e
Ethanedial (CHO-CHO)	-50.9±0.9 ^c	Goldsmith ^e
OH	8.96±0.01 ^e	Ruscic ^e
Formaldehyde (H ₂ CO)	-26.10±0.02 ^e	Ruscic ^e
HCO	9.99±0.02 ^e	Ruscic ^e
HO ₂	2.94 ^f	Chase ^e
y(cjoo)	49.3 ^d	Wang ^e
y(coo)-ocj	-3.10 ^d	Wang ^e
ojc-cho	-18.3±0.9 ^c	Goldsmith ^e
cjdo-oh	-43.7±0.5 ^c	Goldsmith ^e
y(coo)	-2.47 ^g	Lay ^e
CH ₃ OCH ₂ j	0.8±0.9 ^c	Goldsmith ^e

a Chapter 2. b Chapter 3. c Chapter 4. d Chapter 5. e Chapter 6.

APPENDIX B

GEOMETRIES OF STUDIED MOLECULES

Appendix B summarizes the molecular geometries of all the species.

Table B. Cartesian Coordinates for All Target Species Geometries at the B3LYP/6-31+G(d,p) Level of Theory

Compound	Atom	x	y	z
CH ₃ CH ₂ F	C	-1.19756300	-0.22496000	0.00000000
	C	0.10232600	0.55198800	0.00000000
	F	1.19389800	-0.34112500	0.00000000
	H	-2.04502900	0.47020600	0.00001800
	H	-1.27140400	-0.85885200	0.88864900
	H	-1.27142200	-0.85882700	-0.88866600
	H	0.20709500	1.17771700	0.89270700
	H	0.20709600	1.17771700	-0.89270700
CH ₃ CH ₂ CH ₂ F	C	1.54798700	-0.48238400	0.11916900
	C	0.59720400	0.64794600	-0.28933200
	C	-0.79423600	0.51781400	0.30356600
	F	-1.42067300	-0.65466000	-0.17128400
	H	2.53715600	-0.34262000	-0.32855000
	H	1.16402400	-1.45377500	-0.20595200
	H	1.67523900	-0.51800300	1.20768900
	H	0.50871300	0.69496400	-1.38179900
	H	0.99921800	1.61795600	0.03509000
	H	-1.43823000	1.35636400	0.01807200
H	-0.76579500	0.43679700	1.39658900	
CH ₃ CHFCH ₃	C	1.27754400	-0.64255600	-0.09821100
	C	0.00000000	0.03289700	0.36945400
	C	-1.27754500	-0.64255400	-0.09821100
	F	0.00000200	1.36246400	-0.13450700
	H	2.15381600	-0.07457300	0.22711700
	H	1.29526500	-0.71603000	-1.19054100
	H	1.34648800	-1.65319800	0.31894800
	H	0.00000000	0.13869000	1.46132900
	H	-1.34651700	-1.65317600	0.31899100
	H	-1.29524500	-0.71607500	-1.19053900
H	-2.15381300	-0.07453900	0.22707300	
CH ₃ CH ₂ CH ₂ CH ₂ F	C	2.39406800	-0.12276800	-0.13608300
	C	0.95649100	-0.34072500	0.34823900
	C	-0.02636900	0.69214700	-0.21881600
	C	-1.46024500	0.49727100	0.23912700
	F	-1.96058000	-0.73741900	-0.22923200

	H	3.07277700	-0.87235700	0.28436800
	H	2.76824600	0.86602700	0.15561000
	H	2.45854300	-0.19234400	-1.22839100
	H	0.92784200	-0.29960300	1.44609700
	H	0.61977800	-1.34539000	0.06775600
	H	-0.00200900	0.67250100	-1.31643000
	H	0.27969900	1.70487300	0.08263600
	H	-2.12272100	1.27477700	-0.15561300
	H	-1.54060500	0.47273600	1.33225600
CH ₃ CHFCH ₂ CH ₃	C	1.82187300	-0.61340300	-0.00131100
	C	0.48511100	0.02576300	0.33238400
	C	-0.72189800	-0.69119800	-0.25949500
	C	-2.06244600	-0.04226400	0.10076400
	F	0.50425400	1.35708000	-0.16998000
	H	1.88109300	-1.61783200	0.43178600
	H	2.64383400	-0.01526900	0.40220900
	H	1.95015800	-0.69441500	-1.08567900
	H	0.36850500	0.13157700	1.41913400
	H	-0.69976800	-1.72974900	0.09712200
	H	-0.59909400	-0.72923100	-1.34966200
	H	-2.10710100	0.98948100	-0.25931700
	H	-2.21634500	-0.02706100	1.18627800
	H	-2.89540800	-0.59461300	-0.34610100
CH ₂ F ₂	C	0.00000000	0.00000000	0.50841900
	H	-0.91662900	0.00000000	1.10369000
	H	0.91662900	0.00000000	1.10369000
	F	0.00000000	1.11234700	-0.29210500
	F	0.00000000	-1.11234700	-0.29210500
CH ₃ CHF ₂	C	-1.37712900	-0.00001300	-0.09084400
	C	0.05952800	-0.00000200	0.36039600
	F	0.71621000	1.10835700	-0.13652700
	F	0.71623700	-1.10834200	-0.13652700
	H	-1.88527900	-0.89048900	0.28869900
	H	-1.41811400	0.00040400	-1.18326200
	H	-1.88552100	0.89003400	0.28938600
	H	0.20250100	0.00000600	1.44534500
CH ₃ CH ₂ CHF ₂	C	2.00689000	0.05787300	0.10152600
	C	0.70363500	-0.66059300	-0.26593000
	C	-0.51805500	0.00171800	0.32839000
	F	-1.65593400	-0.70084800	-0.01337800
	F	-0.67317800	1.27785400	-0.17834600
	H	2.86428300	-0.46461800	-0.33232100
	H	2.15375600	0.09175600	1.18718200
	H	2.01091600	1.08523500	-0.27324500

	H	0.71822700	-1.69632700	0.09238000
	H	0.56484600	-0.69263400	-1.35250000
	H	-0.50484000	0.08955300	1.42010500
CH ₃ CF ₂ CH ₃	C	0.00000000	-0.78655700	1.29030400
	C	0.00000000	0.00469700	0.00000000
	C	0.00000000	-0.78655700	-1.29030400
	F	1.10607300	0.84877900	0.00000000
	F	-1.10607300	0.84877900	0.00000000
	H	0.00000000	-0.09706100	2.13777700
	H	0.89034700	-1.41835000	1.34260000
	H	-0.89034700	-1.41835000	1.34260000
	H	-0.89034700	-1.41835000	-1.34260000
	H	0.89034700	-1.41835000	-1.34260000
	H	0.00000000	-0.09706100	-2.13777700
CHF ₃	C	-0.00002800	-0.00003500	0.34287600
	F	0.72741300	-1.03148800	-0.12931300
	F	-1.25706600	-0.11415100	-0.12932100
	F	0.52967300	1.14565500	-0.12931500
	H	-0.00000300	0.00007000	1.43428200
CH ₃ CF ₃	C	1.48308400	0.00006200	-0.00045800
	C	-0.02180000	-0.00003400	-0.00006500
	F	-0.52972200	-1.21942300	-0.31640800
	F	-0.53009600	0.88387400	-0.89745700
	F	-0.52917700	0.33548600	1.21437200
	H	1.84427000	0.99689500	0.25919400
	H	1.84439600	-0.27337400	-0.99355100
	H	1.84458800	-0.72312500	0.73294400
CH ₃ CH ₂ CF ₃	C	-2.09598800	-0.09303100	0.00000000
	C	-0.85154800	0.80050600	-0.00001900
	C	0.44594500	0.02360400	-0.00000200
	F	1.52294100	0.85203900	-0.00024600
	F	0.56717800	-0.77869800	-1.09047200
	F	0.56737300	-0.77830200	1.09073600
	H	-2.99616600	0.52782900	0.00001100
	H	-2.12532500	-0.73258600	0.88649600
	H	-2.12534200	-0.73258800	-0.88649300
	H	-0.83052600	1.44777900	0.88251200
	H	-0.83052800	1.44774700	-0.88257300
CF ₄	C	-0.00000300	0.00002900	-0.00004500
	F	-0.32963000	-0.22252800	1.27207900
	F	0.47283500	-1.12335800	-0.53945500
	F	0.93505800	0.94818800	-0.05738600
	F	-1.07826100	0.39767800	-0.67520700
(CH ₃) ₃ CF	C	0.74631400	1.26069100	-0.43625200

	H	0.24054400	2.15148000	-0.05213100
	H	0.79017900	1.33028400	-1.52835800
	H	1.76954800	1.24837400	-0.04915800
	C	-0.00011200	0.00005000	-0.01053900
	C	-1.46514300	0.01612300	-0.43605400
	H	-1.54756800	0.01540800	-1.52807800
	H	-1.98548300	-0.86514500	-0.04924200
	H	-1.96503200	0.91018800	-0.05165100
	C	0.71854800	-1.27652600	-0.43666200
	H	1.74171600	-1.28636900	-0.04929400
	H	0.19376900	-2.15645500	-0.05293700
	H	0.76091600	-1.34673700	-1.52887800
	F	0.00041800	-0.00033900	1.42297500
CH ₃ OOH	C	-1.13428500	-0.22296900	0.02937500
	H	-1.97445000	0.47800400	0.00930200
	H	-1.15305600	-0.80792000	0.95669100
	H	-1.18658600	-0.88995300	-0.83841000
	O	0.01526000	0.60751700	-0.03680000
	O	1.16230800	-0.29728900	-0.08080000
	H	1.69925400	0.07586200	0.63696700
CH ₃ CH ₂ OOH	C	1.49029900	-0.53400400	-0.09563000
	H	1.64734800	-0.59139700	-1.17781000
	H	1.07035700	-1.48197700	0.25189700
	H	2.46537600	-0.39952400	0.38624900
	C	0.57296900	0.62872900	0.25834800
	H	0.41848300	0.70804700	1.34171200
	H	0.97822700	1.58181800	-0.10215100
	O	-0.70092000	0.57988100	-0.38842000
	O	-1.45652100	-0.50025500	0.24581900
	H	-1.69987100	-1.02232800	-0.53539400
CH ₃ CH ₂ CH ₂ OOH	C	-1.87992100	-0.61285500	-0.27565300
	H	-1.27048500	-1.41056700	-0.71043700
	H	-2.32652700	-0.04431400	-1.10051100
	H	-2.69476400	-1.07793800	0.28876700
	C	-1.03341300	0.29044400	0.62736600
	H	-1.65506400	1.08746100	1.05796900
	H	-0.63338900	-0.28321800	1.47080900
	C	0.12814000	0.96404200	-0.09966000
	H	0.67258500	1.64915300	0.56377200
	H	-0.22646100	1.52683300	-0.97340900
	O	1.05098200	0.04582900	-0.69164700
	O	1.72373500	-0.65136600	0.40513500
	H	2.64753600	-0.45290300	0.18282100
CH ₃ CH ₂ CH ₂ CH ₂ OOH	C	-2.70706000	-0.48419700	0.06407600

	H	-3.23522800	0.28845000	0.63431900
	H	-2.54489900	-1.33441400	0.73647000
	H	-3.37286800	-0.81796400	-0.73824100
	C	-1.38228100	0.04466700	-0.49226900
	H	-0.88802800	-0.73593900	-1.08332000
	H	-1.58021300	0.86934100	-1.19067700
	C	-0.42082200	0.52882200	0.59945400
	H	-0.23486900	-0.27442100	1.32308700
	H	-0.87919900	1.35205000	1.16434700
	C	0.92362800	1.01446600	0.06343100
	H	1.54989200	1.41915100	0.86824800
	H	0.78937400	1.79679700	-0.69483400
	O	1.65773600	0.01771700	-0.64892400
	O	2.12291000	-0.94774700	0.34238500
	H	1.67008200	-1.74535800	0.02475400
CH ₃ OOj	C	-1.00600800	-0.47892600	0.00000000
	H	-1.96384700	0.04382700	0.00000000
	H	-0.88672000	-1.08657500	0.89936700
	H	-0.88672000	-1.08657500	-0.89936700
	O	0.00000000	0.56704300	0.00000000
	O	1.22166700	0.05831600	0.00000000
CH ₃ CH ₂ OOj	C	-1.48095300	-0.46906000	-0.09090500
	H	-1.10742200	-1.43803800	0.25057800
	H	-1.64815000	-0.51312600	-1.17120900
	H	-2.44075100	-0.27468100	0.39942400
	C	-0.49769500	0.63231900	0.26360200
	H	-0.81231900	1.61051400	-0.11062900
	H	-0.29949300	0.68931300	1.33700800
	O	0.79196900	0.42005400	-0.39759700
	O	1.48053300	-0.55174600	0.17992700
CH ₃ CH ₂ CH ₂ OOj	C	-1.86121500	-0.60935800	-0.20186000
	H	-1.28845600	-1.49260800	-0.50053300
	H	-2.27563400	-0.15442600	-1.10917600
	H	-2.69984200	-0.94693800	0.41507300
	C	-0.98736700	0.38513600	0.57007300
	H	-1.58352800	1.25482400	0.87645400
	H	-0.60269600	-0.07064400	1.48958500
	C	0.19656900	0.91648100	-0.22746100
	H	0.77247200	1.65996700	0.32977000
	H	-0.10564500	1.32456200	-1.19720400
	O	1.12765200	-0.15461500	-0.59331300
	O	1.83427400	-0.56142000	0.44975200
CH ₃ CH ₂ CH ₂ CH ₂ OOj	C	2.70559000	-0.44257200	-0.10346200
	H	3.20670300	0.40272400	-0.59008700

	H	2.57334600	-1.22836900	-0.85612500
	H	3.38030500	-0.83069600	0.66662600
	C	1.36084800	-0.02129300	0.49916000
	H	0.89894500	-0.87894100	1.00256500
	H	1.52763200	0.73946700	1.27442000
	C	0.39015300	0.53345400	-0.55221700
	H	0.20991500	-0.21067500	-1.33789700
	H	0.83575900	1.40815600	-1.04644600
	C	-0.95614000	0.97223700	0.00768500
	H	-1.59718600	1.41970000	-0.75624400
	H	-0.85085600	1.65511900	0.85657500
	O	-1.70004300	-0.15495100	0.57775800
	O	-2.19836500	-0.93598000	-0.36780600
CH ₂ FOOH	C	-0.63181500	0.52252500	0.27074300
	H	-1.17554600	1.41531000	-0.05105600
	H	-0.49620500	0.45686800	1.35281200
	O	0.57690700	0.58102400	-0.39454900
	O	1.47210600	-0.39167000	0.21601200
	H	1.39593100	-1.13170900	-0.41106600
	F	-1.36948800	-0.59893800	-0.12076200
CHF ₂ OOH	C	-0.55423700	-0.00685400	0.42247000
	H	-1.09629500	-0.00719400	1.37198800
	O	0.77735400	-0.08038100	0.75203000
	O	1.56151400	-0.11817300	-0.46957200
	H	1.83763500	0.81299600	-0.53734700
	F	-0.83533700	1.13621900	-0.27393900
	F	-0.95653600	-1.04469100	-0.35152000
CF ₃ OOH	C	0.38450400	0.00795200	-0.00304900
	O	-0.72094400	0.82665700	-0.07770300
	O	-1.89137800	-0.02465500	-0.11764500
	H	-2.22472800	0.08487400	0.79108700
	F	1.43584100	0.83294000	0.00413200
	F	0.48187100	-0.83055400	-1.04126900
	F	0.39520700	-0.73000900	1.12491400
CH ₂ FOOj	C	-0.57325900	0.50246200	0.28704300
	H	-0.39311300	0.40185600	1.35828900
	H	-1.01044000	1.45705700	-0.01299100
	F	-1.38883800	-0.51719900	-0.13218500
	O	0.67550600	0.42537100	-0.40680800
	O	1.49232600	-0.45273200	0.17207200
CHF ₂ OOj	C	-0.38083100	0.00683400	0.30829900
	H	-0.17043300	0.03130300	1.37810800
	F	-1.35287900	-0.86507800	-0.00133900
	F	-0.73179000	1.22734200	-0.13950400

	O	0.77492900	-0.43403200	-0.41778500
	O	1.87725100	0.01744600	0.17274400
CF ₃ OOj	C	0.36051200	-0.00632900	0.00000000
	F	0.42737200	-0.76961600	-1.08609800
	F	0.42738300	-0.76959800	1.08611000
	F	1.34755600	0.88307100	-0.00001200
	O	-0.83997700	0.76823700	0.00000000
	O	-1.90800700	-0.02533000	0.00000100
CH ₂ FOH	C	0.00853600	0.51599100	0.04856000
	H	0.06788600	1.01195200	1.02456700
	H	0.06643900	1.22652600	-0.77728000
	O	-1.14816000	-0.21769200	-0.11793800
	H	-1.28086900	-0.79563400	0.64632900
	F	1.14229000	-0.31080600	-0.02683000
CHF ₂ OH	C	0.01096300	-0.00000300	0.36133000
	H	-0.05625500	-0.00000400	1.44885200
	O	1.30939000	-0.00006600	-0.02067400
	H	1.35824800	-0.00003100	-0.99025500
	F	-0.65799500	-1.09329700	-0.13673500
	F	-0.65788200	1.09336200	-0.13673000
CF ₃ OH	C	-0.00894600	0.02496800	-0.00000200
	O	-1.28420500	0.46030700	0.00003900
	H	-1.88563500	-0.29956100	0.00010500
	F	0.27642800	-0.73810900	-1.08590600
	F	0.27661900	-0.73774500	1.08610300
	F	0.80394800	1.08333200	-0.00024200
CH ₂ FOj	C	0.00000000	0.44932500	0.00000000
	H	-0.13666100	1.08523900	0.89912600
	H	-0.13666100	1.08523900	-0.89912600
	F	-1.04454200	-0.48293600	0.00000000
	O	1.20927500	-0.06500000	0.00000000
CHF ₂ Oj	C	0.08391600	-0.00117300	0.28654800
	H	0.17788700	-0.00246900	1.39346300
	F	-0.64857900	-1.08614600	-0.10639500
	F	-0.61857200	1.10344900	-0.10638200
	O	1.34037200	-0.01827700	-0.14972000
CF ₃ Oj	C	0.00587100	0.00023500	0.04158900
	F	-0.78420700	-1.08209300	-0.04466800
	F	0.89581800	-0.01005200	-0.96817100
	F	-0.78026100	1.08383800	-0.06244300
	O	0.74782800	0.00916900	1.17850100
CH ₂ Fj	C	-0.02665100	0.66264300	0.00000000
	H	0.19988300	1.10932600	0.96074200
	H	0.19988300	1.10932600	-0.96074200

	F	-0.02665100	-0.68827900	0.00000000
CHF _{2j}	C	-0.03050800	0.51381400	0.00000000
	H	0.73219500	1.29380300	0.00000000
	F	-0.03050800	-0.24314900	1.10448800
	F	-0.03050800	-0.24314900	-1.10448800
CF _{3j}	C	0.00000000	0.00000000	0.32952900
	F	0.00000000	1.26695700	-0.07322900
	F	1.09721700	-0.63347800	-0.07322900
	F	-1.09721700	-0.63347800	-0.07322900
y(cjco)	C	-0.79555900	0.19571200	0.01790500
	H	-1.29641700	0.29060900	0.98043400
	H	-1.44357100	0.11284200	-0.85162900
	C	0.59741100	0.56890100	-0.16005200
	H	1.30122000	1.10408200	0.47596700
	O	0.32845700	-0.76190100	0.03101400
cjc=o	C	1.17075400	-0.17279400	-0.00005000
	H	2.06177900	0.44778100	0.00000200
	H	1.27244200	-1.25362800	0.00012000
	C	-0.13072700	0.40954100	0.00008100
	H	-0.19123600	1.51383300	-0.00010400
	O	-1.17289300	-0.26605800	-0.00002600
ccj=o	C	-1.17055500	0.09904300	0.00000000
	H	-1.69001400	-0.28991400	0.88096700
	H	-1.69001400	-0.28989800	-0.88097400
	H	-1.18250500	1.19548100	0.00001000
	C	0.24431400	-0.43433800	0.00000000
	O	1.26499700	0.17451300	0.00000000
c=c=o	C	0.00000000	0.00000000	-1.21487100
	H	0.00000000	0.94026000	-1.75135700
	H	0.00000000	-0.94026000	-1.75135700
	C	0.00000000	0.00000000	0.10148900
	O	0.00000000	0.00000000	1.27287600
co	C	0.00000000	0.00000000	-0.64991400
	O	0.00000000	0.00000000	0.48743500
cj	C	0.00000000	0.00000000	-0.00001500
	H	0.00000000	1.08268100	0.00003000
	H	-0.93762900	-0.54134000	0.00003000
	H	0.93762900	-0.54134000	0.00003000
TS1	C	0.96161300	-0.03284100	0.02873100
	H	1.62229200	-0.12405600	-0.83255000
	H	1.22713000	-0.59349800	0.92080200
	C	-0.29316700	0.65102800	-0.05013600
	H	-0.76979600	1.55699900	0.31406100
	O	-0.76128800	-0.56857100	-0.03423500
TS2	C	-1.17902300	0.14707900	-0.01859400

	H	-1.96634200	-0.51343700	-0.36158200
	H	-1.43341500	1.16757600	0.28639200
	C	0.14579300	-0.29487200	-0.11017900
	H	-0.55283700	-0.91514500	0.77478200
	O	1.26899700	0.14347000	0.00913100
TS3	C	-1.21324000	-0.12734100	-0.02995300
	H	-1.84695500	0.57048100	-0.55661100
	H	-1.64338100	-0.91954800	0.57426800
	C	0.11377800	0.02026900	-0.01501100
	H	-0.14764700	1.86882000	0.43073000
	O	1.27934500	-0.10966500	-0.02232500
TS4	C	-1.12191600	-0.21404200	0.00003000
	H	-1.63660700	-0.37442400	-0.93849800
	H	-1.96885000	1.80743100	-0.00022800
	H	-1.63647300	-0.37387500	0.93872700
	C	0.19480500	-0.08494600	-0.00003500
	O	1.35057400	0.09185000	0.00000400
TS5	C	1.59662900	-0.09760100	0.00000100
	H	2.06475600	0.87863300	-0.00425300
	H	1.56260700	-0.65727300	-0.92817500
	H	1.56457600	-0.65002700	0.93257700
	C	-0.62662200	0.56921800	-0.00003300
	O	-1.37649800	-0.30012900	0.00000600
y(cjco)	C	0.78980800	-0.20433000	0.01762500
	H	1.28217900	-0.32206900	0.98111300
	H	1.43964500	-0.13651400	-0.85090400
	C	-0.61245500	-0.55821900	-0.16376600
	H	-1.31127600	-1.08150600	0.48637500
	O	-0.30933300	0.76442300	0.03253200
y(cjco)-ooh	C	1.60221300	-0.42100500	-0.19685700
	H	2.57664600	-0.69869000	0.19586900
	C	0.31189700	-0.23470900	0.42495900
	H	0.13114400	-0.16222500	1.49346100
	O	1.10713900	0.86341900	-0.10763500
	O	-0.78171300	-0.61107300	-0.31458300
	O	-1.86996900	0.23273100	0.11119900
	H	-1.83609600	0.91457600	-0.56978400
y(ccjo)-ooh	C	-1.62973100	-0.35665800	0.11251000
	H	-2.50168600	-0.41575500	-0.53109200
	H	-1.72436000	-0.75447000	1.12003800
	C	-0.30955100	-0.19236100	-0.47874000
	O	-0.90179500	0.92337000	0.05437700
	O	0.80847600	-0.71767100	0.10176200
	O	1.86413800	0.25088900	-0.04533800

	H	1.69519200	0.81162900	0.72202500
y(cco)-oo•	C	1.53138100	-0.48088700	0.01481900
	H	2.36304800	-0.51523200	0.71354400
	H	1.56560800	-1.16500100	-0.82897100
	C	0.22995700	0.00889500	0.45396700
	H	-0.02616600	0.32186800	1.46146800
	O	1.04114200	0.84352600	-0.30391700
	O	-0.88732700	-0.53355800	-0.22917900
	O	-1.96263000	0.21382200	0.01325200
y(cco)-o• *	C	-0.96144900	0.59116400	-0.00580000
	H	-1.59413900	0.86888200	0.83788000
	H	-0.91324200	1.27376500	-0.85066700
	C	0.40859300	-0.11467300	0.41992100
	H	0.42785900	-0.37707100	1.48110200
	O	-0.75901100	-0.74288200	-0.25821200
	O	1.43359200	0.16481700	-0.23591800
y(cdco)	C	-0.59536700	0.51470400	0.00000600
	H	-1.58573700	0.92533300	-0.00004200
	C	0.67448600	0.40872500	0.00001500
	H	1.71999900	0.64565700	-0.00006300
	O	-0.07612300	-0.88894600	-0.00000300
y(cco)-do	C	-1.03216600	-0.58561100	0.00000000
	H	-1.50577700	-0.89714400	-0.92642200
	H	-1.50577000	-0.89714900	0.92642400
	C	0.32862600	-0.06825200	-0.00000200
	O	-0.60742200	0.87520000	0.00000100
	O	1.51152000	-0.16051600	0.00000100
y(cjoo)	C	0.03639200	0.74319400	0.00000000
	H	-0.80063200	1.44925600	0.00000000
	O	0.03639200	-0.36927600	0.77352800
	O	0.03639200	-0.36927600	-0.77352800
y(coo)-ocj	C	1.59967700	-0.54096400	0.07988700
	H	2.66060100	-0.42172900	-0.09223900
	H	1.06251000	-1.44158400	-0.18928000
	C	-0.43313800	0.60328200	-0.02282300
	H	-0.83416700	1.61179000	-0.06418700
	O	0.92663900	0.66141600	-0.02852500
	O	-1.07897200	-0.30854400	0.77522400
	O	-1.08369000	-0.36816900	-0.74628400
cjdo-oh	C	-0.13309600	0.38747300	0.00000000
	O	-1.18961100	-0.13723500	0.00000000
	O	1.07313000	-0.21423600	0.00000000
	H	1.73042300	0.48692900	0.00000000
ojc-cho *	O	-1.68743200	-0.28276900	-0.20877700
	C	-0.63482500	0.47287900	0.14444000

	H	-0.48894400	1.40611400	-0.42124000
	H	-0.73075000	0.72765400	1.22384500
	C	0.68374500	-0.35467600	0.15563600
	H	0.54295400	-1.39735600	0.50280300
	O	1.73533500	0.10206500	-0.17945600
cjocho	C	-1.38375700	-0.45888000	-0.05164100
	H	-0.93425000	-1.41660000	0.17270400
	H	-2.42675900	-0.22454600	0.10457600
	O	-0.57821100	0.65784100	0.00174700
	C	0.76441200	0.44643400	0.00877000
	H	1.26566100	1.42179700	0.03530900
	O	1.30463800	-0.62108800	-0.00866700
yy(cco-cco)	C	-0.00002200	-0.68070400	0.33368400
	H	-0.00013600	-1.59273900	0.90223800
	C	0.00002200	0.68070100	0.33368600
	H	0.00013600	1.59273700	0.90224000
	O	1.07471100	-0.00003500	-0.36304400
	O	-1.07471100	0.00003700	-0.36304400
TS1*	C	-1.44221300	-0.62966500	0.17924800
	H	-1.91252300	-1.30889600	-0.52232300
	H	-1.81065800	-0.63245000	1.19938900
	C	-0.14100700	-0.04596100	-0.12088700
	H	0.78095700	-0.47823500	-0.97795200
	O	-1.20790700	0.74814600	-0.35281500
	O	0.89834500	0.31602800	0.67200700
	O	1.86475500	-0.25500700	-0.32535200
TS2*	C	-0.90103400	-0.63861000	-0.47668800
	H	-1.69199800	-1.05932400	-1.08962100
	H	0.29780400	-1.16804500	-0.26561000
	C	-0.34185000	0.69176300	-0.27229100
	H	-0.68646100	1.65405300	-0.62704600
	O	-1.20156100	0.03561600	0.70028300
	O	1.01533700	0.67407400	-0.06756900
	O	1.37846900	-0.67789000	0.17680500
TS3*	C	-1.60710900	0.33568200	0.01958300
	H	-2.34406800	0.21719100	0.80758000
	H	-1.70246900	1.11788900	-0.72504600
	C	0.03523300	-0.03207400	0.42538600
	H	0.08482900	-0.19313300	1.49648200
	O	-0.85513300	-0.77967800	-0.32728600
	O	0.88328600	0.82769300	-0.17626000
	O	1.64596800	-0.41846400	-0.02755800
TS4	C	1.67911600	-0.43213300	0.17251900
	H	2.26909600	-0.43408400	1.08474900
	H	2.09696300	-0.96164600	-0.68103800

	C	0.27374300	-0.10207900	0.21012000
	O	1.10279700	0.90110800	-0.19520000
	O	-0.78655100	-0.55546700	-0.38697600
	O	-2.03352300	0.15361000	0.30573000
	H	-2.34500100	0.60699100	-0.48797900
TS5*	C	1.64334200	-0.23309100	-0.37183100
	H	2.35864400	-0.37062900	-1.16042000
	C	0.81165100	-0.58613300	0.54000300
	H	0.45969500	-0.99947400	1.46049800
	O	0.95692000	0.90723100	0.10186500
	O	-1.26803200	-0.73600400	-0.30405700
	O	-1.73279700	0.47616000	0.09166700
	H	-1.19703400	1.10635900	-0.42491000
TS6	C	-0.99779600	0.96411600	0.04950200
	H	0.30927300	1.10710800	0.21863400
	H	-1.36311700	1.54603900	-0.79816600
	C	-0.16439300	-0.58658600	0.37105400
	H	-0.00103200	-0.70970000	1.43923500
	O	-1.40828300	-0.41922500	-0.09467100
	O	0.84891900	-0.62514100	-0.44562100
	O	1.56286500	0.51828800	0.11741200
TS7	C	-1.47993700	0.53393500	0.14811300
	H	-1.84677600	1.43272100	-0.33873100
	C	-0.17909200	0.08792100	0.42344000
	H	0.03819800	-0.64642700	1.18999800
	O	-1.71156000	-0.71707200	-0.24093100
	O	0.86336800	0.49587700	-0.29152000
	O	2.03962600	-0.25697900	0.09093800
	H	2.23128000	-0.69203900	-0.74848700
TS8	C	1.74089800	-0.48845300	-0.00955700
	H	1.93979600	-1.03008200	0.92361500
	H	1.93129300	-1.00754500	-0.95722200
	C	-0.69196600	0.63617500	0.01735800
	H	-1.08484100	1.65200100	0.04910800
	O	1.23904700	0.66401600	0.00642100
	O	-1.18017200	-0.38489000	0.75675700
	O	-1.19385600	-0.34171400	-0.77096700
TS9*	C	0.02616400	0.03469500	0.03868200
	H	0.08511000	0.03746100	1.11201700
	C	0.64111600	-0.11963800	-1.16037800
	H	1.43304600	-0.54173300	-1.75075400
	O	-0.71235000	-0.72275200	-0.88405000
	O	0.25670200	1.21378300	-0.88943500
	O	-1.02666600	1.21378300	-3.49224000

	H	-0.98264400	1.33359000	-2.52652600
TS10*	C	-0.07991300	0.24104900	-0.00000400
	H	0.99764500	1.02112900	0.00000800
	O	-1.20367000	-0.10175800	0.00000200
	O	1.13889900	-0.20667000	0.00000100
TS11*	C	-1.04669400	0.56090800	0.01425900
	H	-1.67021000	0.75103900	0.88683800
	H	-1.02239800	1.28875100	-0.79170200
	C	0.45016000	-0.14813400	0.40286800
	H	0.44466300	-0.40944900	1.46554100
	O	-0.71140500	-0.73156800	-0.28310000
	O	1.43979800	0.21819500	-0.22482900
TS12*	C	-0.91579000	0.59481800	-0.05534600
	H	-1.48146800	1.03477000	0.77360600
	H	-0.86098700	1.19841000	-0.96340400
	C	0.46952700	-0.00819300	0.44127100
	H	0.46560900	-0.24545200	1.50683400
	O	-0.88889800	-0.74568300	-0.17920000
	O	1.45820100	0.05724900	-0.27487400
TS13*	C	0.03169400	-0.01700100	-0.01012600
	H	0.06084600	-0.04794300	1.08598900
	H	0.96771000	0.03897900	-0.57401200
	O	-1.05093900	0.00401300	-0.60845100
	C	-2.51402600	0.55050200	0.44007500
	H	-3.26874100	-0.04181700	-0.10725600
	O	-2.26872100	0.59585900	1.59811900
TS14*	O	1.78016700	0.37441500	0.14358100
	C	0.98966000	-0.53921900	-0.10206400
	H	0.80702100	-0.88006600	-1.14341300
	H	0.67300200	-1.26462400	0.67212800
	C	-0.92212700	0.38352200	-0.11863800
	H	-0.75021400	1.46227300	-0.32551300
	O	-1.92204300	-0.17234000	0.12154500

APPENDIX C

VIBRATIONAL FREQUENCIES OF STUDIED MOLECULES

Appendix C includes the frequencies for all the species.

Table C. Frequencies for All Target Species at the B3LYP/6-31+G(d,p) Level of Theory (cm^{-1}).

CH ₃ CH ₂ F	252.7491	408.3686	812.9610
	879.2227	1050.0753	1120.1912
	1183.8542	1292.4143	1397.9862
	1426.5029	1486.0428	1503.8690
	1521.1318	3045.8710	3056.5380
	3101.3666	3117.3609	3135.3644
	CH ₃ CH ₂ CH ₂ F	138.4566	210.9506
	474.8449	767.0755	868.7717
	920.5848	966.8899	1071.9160
	1118.5090	1172.3592	1267.3132
	1300.4391	1380.8436	1411.8256
	1425.4820	1480.2907	1499.5378
	1512.4659	1513.8903	3029.5924
	3039.4916	3048.3062	3071.2515
	3102.1440	3107.8857	3124.2229
CH ₃ CHFCH ₃	219.1845	261.8801	352.5836
	404.7352	475.9687	814.8597
	931.6095	934.1967	942.9164
	1141.0208	1160.5867	1198.4479
	1363.3773	1375.1035	1415.6283
	1423.3330	1484.6632	1490.2413
	1495.5379	1514.2863	3043.2429
	3047.9167	3052.7533	3114.6944
	3121.5269	3127.9341	3130.5033
CH ₃ CH ₂ CH ₂ CH ₂ F	95.2634	132.0154	243.7600
	260.5666	337.0125	511.8296
	746.1274	835.1086	847.3118
	958.4457	975.9483	1033.1024
	1072.6749	1137.1648	1171.1852
	1253.4322	1275.7955	1327.3458
	1338.7226	1407.7471	1415.8645
	1421.4880	1477.5155	1499.9409
	1505.9323	1511.5664	1513.7045
	3018.5994	3025.5404	3030.9054
	3047.7089	3060.9063	3077.4593
	3099.8332	3104.0391	3104.9330

CH ₃ CHFCH ₂ CH ₃	108.3199	214.6449	224.5879
	242.7879	363.9099	455.1748
	488.3925	766.9617	824.8418
	899.4449	980.3748	1001.4957
	1037.4232	1136.0245	1147.0398
	1192.9816	1293.9403	1330.4024
	1367.9383	1407.1619	1417.9488
	1419.7617	1478.4030	1490.5424
	1501.8781	1503.4645	1513.3523
	3029.8291	3039.2163	3041.1654
3046.1035	3070.7063	3105.0309	
3118.2947	3126.4181	3128.4410	
CH ₂ F ₂	511.6660	1069.1342	1100.8787
	1172.4213	1264.1072	1453.7349
	1527.4422	3079.4389	3158.7821
CH ₃ CHF ₂	229.5347	379.9051	456.6549
	557.0879	867.4852	935.1870
	1130.8779	1132.5645	1155.8320
	1379.8702	1385.9650	1435.8938
	1488.2096	1488.6978	3063.1870
3101.2232	3145.1582	3151.1794	
CH ₃ CH ₂ CHF ₂	110.2782	214.1822	240.0498
	426.4197	462.6547	561.5331
	784.4375	893.6445	982.1736
	1040.5023	1102.5487	1136.0658
	1170.4928	1289.1684	1333.4303
	1383.8165	1420.9718	1427.2136
	1484.6297	1505.5165	1514.2602
	3045.9207	3057.0047	3086.6952
	3101.9590	3117.7077	3132.5433
CH ₃ CF ₂ CH ₃	208.5697	246.8940	327.4711
	349.5086	429.9483	510.1589
	510.4984	773.4623	890.9763
	934.7702	989.6418	1012.3189
	1204.6975	1248.1478	1279.1523
	1419.8758	1428.1912	1480.6797
	1483.5791	1497.7806	1502.0234
	3063.4956	3068.0778	3142.9067
	3149.6314	3151.7910	3152.9087
CHF ₃	490.7371	492.1143	680.9657
	1126.4985	1138.1195	1138.2750
	1383.1791	1383.2735	3162.8625
CH ₃ CF ₃	227.7109	358.3827	359.4104
	526.0975	526.8648	587.5484

	819.8720	965.9138	966.6038
	1218.4173	1218.5316	1279.5256
	1437.0281	1487.9537	1488.0515
	3079.9471	3168.5870	3168.8946
CH ₃ CH ₂ CF ₃	107.0801	203.0989	222.3506
	362.2324	403.2413	524.7397
	535.1221	611.5341	793.6093
	799.7753	988.0154	1024.4935
	1069.5608	1164.6309	1197.5566
	1262.5916	1319.6780	1401.1487
	1428.0726	1486.2721	1504.9459
	1516.3769	3058.8987	3072.7721
	3114.6616	3131.4915	3139.9607
CF ₄	419.8282	420.5134	609.3491
	609.6148	610.1771	892.1994
	1253.3903	1253.6783	1253.8550
(CH ₃) ₃ CF	189.1938	250.2208	251.6583
	332.7187	333.1638	409.6172
	456.0436	456.9076	745.0378
	877.5005	920.3387	921.4630
	965.6044	1047.0611	1047.3564
	1216.0290	1279.9173	1280.3789
	1409.1278	1410.0227	1432.6691
	1473.2123	1489.6065	1490.1244
	1500.5803	1500.7543	1523.4867
	3044.5801	3045.0832	3053.4055
	3117.6790	3118.3014	3125.0733
	3126.4343	3129.9930	3130.1813
CH ₃ OOH	157.6535	247.2572	443.7488
	875.7736	1039.0636	1171.8315
	1198.3504	1369.6975	1451.1876
	1464.0814	1514.7535	3023.4288
	3097.5111	3129.2222	3776.2201
CH ₃ CH ₂ OOH	151.0864	180.9266	233.2887
	359.2012	499.4678	791.6131
	859.5337	914.1541	1047.2746
	1105.2192	1180.6202	1303.4429
	1366.0520	1386.1798	1414.4246
	1477.2568	1489.7283	1510.3165
	3039.6216	3044.2504	3089.0091
	3112.2975	3132.5369	3777.5543
CH ₃ CH ₂ CH ₂ OOH	79.5008	164.3674	185.3262
	224.5725	279.2723	429.8362
	531.5392	764.8630	857.3880

	865.2493	923.6311	978.3032
	1067.2198	1112.0079	1177.7342
	1282.3892	1304.0338	1354.4472
	1380.2669	1396.7456	1421.2987
	1468.7226	1488.2271	1502.7590
	1512.0288	3021.0909	3034.8278
	3038.1241	3072.5034	3086.5963
	3104.6422	3123.4421	3775.7647
CH ₃ CH ₂ CH ₂ CH ₂ OOH	77.4769	100.6486	139.8770
	146.4342	176.8965	244.1784
	321.0659	371.0783	503.7478
	748.8784	821.9563	891.2707
	935.1506	960.7698	1024.2050
	1036.2478	1065.5160	1144.2731
	1189.7584	1242.6519	1295.2563
	1302.7209	1328.7304	1354.5673
	1387.5681	1414.4701	1419.7174
	1497.6498	1502.8823	1504.0768
	1514.6383	1531.2453	3013.5768
	3023.1262	3032.8426	3039.6113
	3050.7035	3057.1677	3087.3345
	3102.2864	3105.7869	3773.0726
CH ₃ OOj	132.9309	490.5137	915.9996
	1127.7787	1155.9774	1219.8060
	1444.8681	1475.4657	1486.8856
	3063.0647	3161.1396	3173.9592
CH ₃ CH ₂ OOj	106.0834	229.3836	360.9734
	523.6755	798.1467	843.2388
	995.2646	1096.6985	1154.5405
	1205.4815	1305.2427	1375.0781
	1413.8084	1485.4893	1490.3942
	1507.9842	3051.8387	3077.9247
	3122.9075	3130.5687	3149.6820
CH ₃ CH ₂ CH ₂ OOj	79.0241	139.1525	219.0807
	287.1797	430.4840	541.0463
	754.0522	853.2294	880.3616
	938.8895	1046.5925	1104.7624
	1150.9839	1190.3281	1284.2926
	1297.6739	1373.1578	1385.2702
	1425.0589	1481.2354	1484.6834
	1504.4811	1511.6105	3040.7046
	3040.9745	3069.3961	3085.3490
	3109.9102	3122.8783	3135.0210
CH ₃ CH ₂ CH ₂ CH ₂ OOj	69.2699	86.0177	141.0432

	231.8108	247.4978	312.5506
	461.8040	547.9854	741.1864
	814.1890	835.4925	907.2703
	972.0061	1015.4799	1056.6795
	1127.2287	1150.5129	1186.9491
	1264.6355	1280.8699	1331.1585
	1339.0748	1382.8599	1406.2528
	1420.3326	1480.1613	1482.7862
	1498.7935	1504.1993	1513.4699
	3024.7272	3029.8325	3033.3383
	3064.4056	3071.0728	3083.6505
	3101.6550	3107.5678	3135.1836
CH ₂ FOOH	165.3199	284.8240	418.1151
	590.2988	878.2427	995.9988
	1084.5650	1156.1698	1285.6843
	1378.0430	1418.2900	1478.5606
	3081.0869	3158.9425	3749.3200
CHF ₂ OOH	153.4315	244.5139	287.4045
	514.7047	521.9373	782.1409
	886.8217	1075.8286	1081.8976
	1133.7474	1344.3597	1384.0508
	1402.2704	3139.4541	3742.6079
CF ₃ OOH	135.3993	254.0075	280.2471
	424.3247	434.8537	569.3480
	598.8735	667.9807	866.9750
	984.1211	1188.7228	1222.4953
	1253.1700	1410.6267	3737.9075
CH ₂ FOH	397.1599	533.8530	973.8995
	1060.9698	1142.4180	1253.9429
	1382.8561	1441.5118	1530.2950
	3052.8151	3152.5870	3815.5056
CHF ₂ OH	328.1247	498.4432	538.1219
	642.7754	1006.0469	1036.7852
	1176.7681	1330.0425	1355.1487
	1427.6675	3178.5897	3780.8286
CF ₃ OH	240.4808	429.3927	440.2286
	585.4970	603.7896	616.8140
	884.8730	1090.5194	1147.4230
	1279.0576	1398.4042	3813.8475
CH ₂ FOOj	116.4793	415.2125	570.4467
	935.2934	1074.3093	1123.8548
	1183.9087	1284.6918	1420.5647
	1489.9990	3096.7584	3184.6258
CHF ₂ OOj	69.1508	341.9756	453.0518
	528.8995	634.1595	1010.1636

	1130.5489	1169.8986	1183.0424
	1347.4017	1374.9266	3171.0935
CF ₃ OOj	106.6530	274.4523	405.3090
	437.4919	561.4337	577.8415
	685.1434	853.7227	1105.2941
	1187.2663	1247.0177	1291.5041
CH ₂ FOj	540.3433	784.4738	981.7908
	1144.8151	1168.4486	1321.7886
	1350.3417	2903.0233	2932.5592
CHF ₂ Oj	466.3592	490.2382	601.4900
	944.2822	1064.8953	1133.2696
	1245.3752	1316.4938	2923.8469
CF ₃ Oj	221.4444	394.4580	560.3864
	578.1801	602.2494	882.7469
	1151.2516	1192.2102	1253.8747
CH ₂ Fj	557.0562	1163.6975	1167.3456
	1464.3749	3150.2080	3311.2675
CHF ₂ j	533.2088	999.1730	1158.4828
	1167.7594	1327.5037	3143.9904
CF ₃ j	492.5630	492.5648	683.4062
	1068.0121	1236.1114	1236.1458
y(cjco)	778.4185	803.9477	942.7245
	1041.2733	1074.3274	1127.2124
	1183.9356	1356.1578	1528.9093
	3109.5673	3148.9593	3204.1069
cjc=o	447.3715	505.9945	762.4017
	973.6514	981.4269	1164.7627
	1396.7232	1479.8354	1553.0424
	2975.3825	3158.9208	3275.1337
ccj=o	103.6461	468.0107	858.4722
	955.2937	1049.8974	1362.5106
	1458.0424	1461.7492	1925.1633
	3030.8453	3127.0082	3132.8797
c=c=o	438.4683	531.4870	601.9681
	990.3148	1170.8623	1416.5563
	2212.6752	3197.0895	3292.3122
co	2201.6461		
cj	526.3687	1412.6688	1412.6704
	3124.9628	3306.1325	3306.1335
TS1	-1122.6171	570.3509	831.0522
	880.1811	1040.1761	1093.4891
	1314.2236	1354.3747	1499.7488
	3114.6220	3178.4901	3217.1441
TS2	-1551.2333	438.1384	632.1071

	857.1098	1033.5470	1133.8052
	1215.4756	1458.1167	1823.2765
	1938.4431	3068.5842	3252.9160
TS3	-764.9804	292.4432	469.2709
	508.3923	568.1518	631.1435
	994.7479	1144.9224	1415.6143
	2136.2169	3186.0616	3302.2059
TS4	-208.3363	207.9898	382.9932
	443.1451	529.0025	683.0699
	997.2130	1157.8788	1410.5962
	2206.3469	3199.3697	3296.1928
TS5	-256.0395	18.9711	230.4079
	451.0624	490.8465	805.7191
	1416.2675	1422.7285	2089.5816
	3116.1138	3284.6165	3298.7223
y(cjco)	871.1360	924.1272	1023.3363
	1163.9136	1171.4171	1241.6145
	1308.8485	1463.1505	1655.1685
	3257.1031	3313.4907	3349.5911
y(cjco)-ooh	134.5324	303.6556	350.9666
	542.9782	641.9639	891.3072
	929.8902	1069.0088	1149.8656
	1196.3518	1286.8687	1316.8099
	1437.8351	1567.8180	1601.2127
	3330.3606	3349.0634	4121.8741
y(ccjo)-ooh	128.6781	265.4764	309.7055
	491.6210	656.3593	884.2883
	1001.9566	1117.6544	1169.2432
	1204.0956	1282.6732	1307.3069
	1526.8499	1582.9644	1669.8646
	3276.9102	3375.8128	4115.1455
y(cco)-oo•	109.1685	327.3363	511.1251
	629.6435	904.7119	991.3578
	1061.9452	1207.8623	1256.9140
	1276.3116	1281.3252	1304.7801
	1424.1730	1551.9714	1670.4292
	3273.3524	3345.7350	3371.8177
y(cco)-o• *	333.6434	437.6172	497.1030
	634.6696	796.8889	959.0008
	1080.3974	1147.2509	1206.9323
	1338.7183	1388.4405	1498.6083
	3055.1487	3067.4734	3174.5817
y(cdco)	441.4804	691.0001	820.6132
	998.5044	1095.5770	1167.3569

	1977.4955	3492.3548	3576.2804
y(cco)-do	544.8814	598.0767	845.5109
	1052.2862	1103.0609	1168.7389
	1258.7358	1343.8954	1614.9174
	2207.5144	3286.1113	3387.0480
y(cjoo)	923.9145	969.7045	1197.8471
	1208.5361	1588.3671	3267.1254
y(coo)-ocj	151.3184	217.3150	318.5045
	562.2620	726.3940	750.6888
	962.1494	974.9019	1083.8262
	1288.5243	1316.3222	1373.6207
	1492.1086	1562.4382	1640.4203
	3301.4120	3377.6542	3443.8929
cjdo-oh	533.6991	692.9526	1193.3786
	1377.1058	2117.6770	4157.0874
ojc-cho *	122.1827	348.3582	483.7335
	709.1274	742.1957	1010.2730
	1075.8828	1180.0096	1230.7786
	1352.5046	1424.3805	1832.3874
	2848.5571	2921.4770	2983.6807
cjocho	203.4145	339.0802	353.1651
	680.7143	836.6938	1081.8974
	1176.4247	1285.1696	1384.0312
	1533.8435	1572.3453	2000.7166
	3261.0898	3308.8772	3457.3203
yy(cco-cco)	598.9591	809.3729	815.5532
	846.4859	1045.6233	1053.2840
	1139.8398	1160.9899	1354.7085
	1739.8505	3465.3570	3509.3637
TS1*	-1866.3275	124.0538	355.6127
	421.3576	577.8106	778.1893
	834.7598	883.2594	941.9047
	1013.7570	1091.9213	1106.3671
	1161.1851	1428.9326	1535.8481
	1985.5851	3116.6188	3220.8841
TS2*	-1947.4889	240.2714	468.2287
	641.5394	658.6654	784.2798
	830.3169	910.8362	1024.7358
	1030.4665	1047.0693	1124.4170
	1164.7561	1264.6787	1395.8054
	1782.9311	3156.0782	3213.4767
TS3*	-1069.3399	223.7904	304.8811
	379.4301	486.1954	623.4425
	832.1448	903.2784	966.6536
	980.0933	1146.9305	1169.8796

	1238.0265	1344.6696	1486.5072
	3097.6698	3170.9335	3234.6742
TS4	-1022.2183	105.9532	193.5262
	262.8351	504.8914	586.6426
	862.1584	1020.5486	1105.1439
	1184.6130	1206.7674	1305.4451
	1350.3806	1540.2108	1675.2282
	3271.6674	3367.8886	4124.2134
TS5*	-416.5614	124.3964	167.3862
	189.8662	247.0946	266.1936
	414.8407	530.0572	620.2289
	876.6677	972.0950	1049.0332
	1134.4815	1442.3922	1692.0222
	3305.6144	3392.0912	3623.8943
TS6	-2016.2250	258.4695	333.5851
	461.6029	578.8911	645.7376
	752.2534	790.0765	919.2529
	1165.1740	1218.9074	1346.2323
	1424.1464	1483.5082	1655.4447
	1972.3125	3329.0222	3336.9384
TS7	-450.2971	164.8016	266.4648
	366.6047	490.1419	566.0303
	905.1054	946.0203	1138.6442
	1205.4546	1267.4797	1339.8166
	1417.1767	1583.0853	1593.3585
	3289.0537	3419.5430	4120.4784
TS8	-714.4458	82.4027	175.9001
	190.7731	418.1455	485.2270
	916.9497	938.3937	986.7611
	1196.7487	1231.4353	1291.5735
	1305.0695	1563.1962	1650.0167
	3206.7127	3321.3566	3329.8613
TS9*	-233.0720	56.5316	62.6407
	165.2134	296.7674	567.2888
	640.5230	711.8028	768.5661
	909.7510	926.6986	1025.5215
	1036.2369	1187.7869	1599.3329
	3289.4454	3329.1378	3628.0960
TS10*	-1872.7101	526.9650	679.3638
	1152.2008	1854.2571	2133.4907
TS11*	-355.0106	356.8098	531.2161
	604.9753	750.7285	904.0712
	1007.2056	1149.1417	1201.2534
	1347.8511	1485.4296	1496.1749

	3054.5387	3070.5771	3195.1585
TS12*	-397.9596	364.0008	481.5791
	655.4479	842.2233	945.8998
	1136.8713	1162.3158	1241.5276
	1321.2297	1511.3170	1519.9410
	3006.3480	3085.6290	3111.1810
TS13*	-603.6884	178.7950	252.4133
	355.4092	496.4257	798.3682
	1018.6667	1080.8337	1235.5564
	1430.7288	1579.5838	1820.1252
	2902.3798	3000.2228	3106.3198
TS14*	-263.7515	44.5973	205.2535
	314.7385	498.7508	707.1776
	1073.3334	1109.5383	1233.3124
	1466.6204	1609.1854	1937.6179
	2841.2172	2849.9838	2910.5432

APPENDIX D

MOMENTS OF INERTIA OF STUDIED MOLECULES

Appendix D summarizes the moments of inertia for all the species.

Table D. Moments of Inertia for All Target Species at the B3LYP/6-31+G(d,p) Level of Theory (AMU Bohr²).

CH ₃ CH ₂ F	50.14289	195.24640	222.54800
CH ₃ CH ₂ CH ₂ F	124.34260	362.81395	427.78330
CH ₃ CHFCH ₃	209.61254	225.21253	381.19860
CH ₃ CH ₂ CH ₂ CH ₂ F	143.68216	787.24170	851.14623
CH ₃ CHFCH ₂ CH ₃	223.41169	528.40376	681.90027
CH ₂ F ₂	36.94260	173.93806	198.78499
CH ₃ CHF ₂	193.85827	203.34075	354.26358
CH ₃ CH ₂ CHF ₂	209.67817	512.06328	662.26968
CH ₃ CF ₂ CH ₃	354.70018	378.82199	378.94892
CHF ₃	177.79424	177.81967	324.25764
CH ₃ CF ₃	334.46456	353.19317	353.22903
CH ₃ CH ₂ CF ₃	351.59381	666.60875	672.89445
CF ₄	321.38327	321.42051	321.43849
(CH ₃) ₃ CF	386.76791	386.83649	403.03060
CH ₃ OOH	41.72611	173.96456	200.36538
CH ₃ CH ₂ OOH	115.49261	335.52218	394.76374
CH ₃ CH ₂ CH ₂ OOH	198.58780	599.26480	638.03379
CH ₃ CH ₂ CH ₂ CH ₂ OOH	104.83963	1531.02419	1586.55026
CH ₃ OOj	34.40261	160.91472	183.67293
CH ₃ CH ₂ OOj	99.99028	328.00304	375.61793
CH ₃ CH ₂ CH ₂ OOj	182.09831	589.40874	628.07240
CH ₃ CH ₂ CH ₂ CH ₂ OOj	230.31151	1085.12308	1153.52656
CH ₂ FOOH	98.29917	323.54881	376.83523
CHF ₂ OOH	238.24709	386.45586	478.25235
CF ₃ OOH	331.71121	586.47925	592.91867
CH ₂ FOOj	81.00149	325.01608	361.49128
CHF ₂ OOj	187.54723	426.06392	566.01463
CF ₃ OOj	327.05323	561.69917	568.62898
CH ₂ FOH	39.93111	177.82069	201.37574
CHF ₂ OH	181.19340	182.17803	325.38175
CF ₃ OH	320.80315	326.01541	326.75349
CH ₂ FOj	32.30599	169.66063	190.32847
CHF ₂ Oj	170.60850	175.85078	320.08763
CF ₃ Oj	302.19360	312.74783	328.85398
CH ₂ Fj	6.92583	59.25859	65.62067
CHF ₂ j	27.19304	167.01621	191.22933

CF ₃ j	169.09626	169.09626	326.70789
y(cjco)	60.62426	76.46506	121.49837
cjc=o	27.01613	158.57899	185.59511
ccj=o	21.52870	182.17803	192.53385
c=c=o	6.36369	177.28825	183.65194
co	0.00000	31.67156	31.67156
cj	6.32813	6.32813	12.65625
TS1	51.58807	100.32644	139.78051
TS2	18.11423	176.98588	188.33601
TS3	21.02437	181.14698	196.11286
TS4	21.33621	197.51637	206.16977
TS5	31.50345	271.27254	290.31460
y(cjco)	58.63320	73.40460	116.75929
y(cjco)-ooh	101.19151	465.65352	518.23088
y(ccjo)-ooh	103.65866	457.91351	526.37762
y(cco)-oo•	101.08932	468.23045	514.92079
y(cco)-o• *	84.31044	237.36596	267.42814
y(cdco)	52.31338	65.06550	117.37886
y(cco)-do	67.32430	217.07691	272.33541
y(cjoo)	48.91291	62.38068	107.42942
y(coo)-ocj	140.30068	392.05592	411.84390
cjdo-oh	9.87316	153.37770	163.25086
ojc-cho *	49.09909	388.93470	412.00582
cjocho	74.75440	252.01892	326.04972
yy(cco-cco)	85.19366	153.48278	181.29197
TS1*	116.68234	495.62877	511.63169
TS2*	157.51133	350.49543	411.13004
TS3*	121.07493	409.32269	474.94488
TS4	99.47077	518.57827	576.64532
TS5*	132.19288	557.72048	621.03868
TS6	145.73243	360.47925	458.11376
TS7	94.78271	571.42021	616.17262
TS8	148.51946	498.70420	514.20662
TS9*	179.75738	545.70914	627.14626
TS10*	9.10286	160.71120	169.81407
TS11*	82.65025	244.51993	273.68387
TS12*	83.73812	251.63943	279.45569
TS13*	79.18936	324.81252	400.27082
TS14*	54.21622	486.31640	521.11154

APPENDIX E

WORK REACTIONS OF STUDIED MOLECULE

Table E.1 Isodesmic reactions, heat of formations, and deviations for fluoroethane

Isodesmic reactions	$\Delta H_{f,298}^a$									Average ^b	STD ^c
	CBS-QB3	M06	M06-2X	ω B97X	G4	CBS-APNO	W1U	B3LYP	G4(MP2)-6X		
$\text{CH}_3\text{CH}_2\text{F} + \text{CH}_4 = \text{CH}_3\text{F} + \text{CH}_3\text{CH}_3$	-65.23	-65.49	-65.21	-65.47	-65.19	-65.21	-65.12	-65.24	-64.43	-65.18	0.14
$\text{CH}_3\text{CH}_2\text{F} + \text{CH}_3\text{CH}_3 = \text{CH}_3\text{F} + \text{CH}_3\text{CH}_2\text{CH}_3$	-65.29	-65.84	-65.77	-65.83	-65.16	-65.29	-65.36	-66.28	-65.52	-65.59	0.29
$\text{CH}_3\text{CH}_2\text{F} + \text{CH}_3\text{CH}_2\text{CH}_3 = \text{CH}_3\text{F} + \text{CH}_3\text{CH}_2\text{CH}_2\text{CH}_3$	-65.19	-65.67	-65.30	-66.02	-65.09	-65.21		-66.33	-65.42	-65.53	0.36
$\text{CH}_3\text{CH}_2\text{F} + \text{CH}_3\text{OH} = \text{CH}_3\text{F} + \text{CH}_3\text{CH}_2\text{OH}$	-65.39	-65.71	-65.42	-65.71	-65.38	-65.39	-65.47	-65.82	-65.62	-65.55	0.15
Average ^d	-65.28	-65.68	-65.42	-65.76	-64.97	-65.28	-65.32	-65.68	-65.25	-65.42^f	
STD ^e	0.09	0.15	0.25	0.23	0.12	0.09	0.18	0.51	0.55		0.25 ^g

^a Heat of formation of target molecule, unit in kcal mol⁻¹. ^b Average of heat of formation of target molecule for each work reaction over seven calculation methods(CBS-QB3, M06, M06-2X, ω B97X, G4, CBS-APNO,W1U). ^c Standard deviation of heat of formation of target molecule for each work reaction under seven calculation levels(CBS-QB3, M06, M06-2X, ω B97X, G4, CBS-APNO,W1U). ^d Average of heat of formation of target molecule of all set of work reactions under one calculation level. ^e Standard deviation of heat of formation of target molecule of all set of work reactions under one calculation level. ^f Heat of formation of target molecule calculated from the set of work reactions and seven selected calculation levels (CBS-QB3, M06, M06-2X, ω B97X, G4, CBS-APNO,W1U). ^g Standard deviation of target molecule calculated from all set of work reaction over the seven selected calculation levels(CBS-QB3, M06, M06-2X, ω B97X, G4, CBS-APNO,W1U).

Table E.2 Isodesmic reactions, heat of formations, and deviations for 1-fluoropropane

Isodesmic reactions	$\Delta H_{f,298}^a$									Average ^b	STD ^c
	CBS-QB3	M06	M06-2X	ω B97X	G4	CBS-APNO	W1U	B3LYP	G4(MP2)-6X		
$\text{CH}_3\text{CH}_2\text{CH}_2\text{F} + \text{CH}_4 = \text{CH}_3\text{F} + \text{CH}_3\text{CH}_2\text{CH}_3$	-70.29	-70.38	-70.35	-70.22	-69.95	-70.13	-70.01	-70.06	-69.30	-70.07	0.17
$\text{CH}_3\text{CH}_2\text{CH}_2\text{F} + \text{CH}_4 = \text{CH}_3\text{CH}_2\text{F} + \text{CH}_3\text{CH}_3$	-70.46	-69.99	-70.04	-69.85	-70.25	-70.30	-70.11	-69.24	-69.23	-69.94	0.21
$\text{CH}_3\text{CH}_2\text{CH}_2\text{F} + \text{CH}_3\text{CH}_3 = \text{CH}_3\text{CH}_2\text{F} + \text{CH}_3\text{CH}_2\text{CH}_3$	-70.51	-70.35	-70.60	-70.20	-70.22	-70.38	-70.34	-70.28	-70.33	-70.36	0.15
$\text{CH}_3\text{CH}_2\text{CH}_2\text{F} + \text{CH}_3\text{CH}_2\text{CH}_3 = \text{CH}_3\text{CH}_2\text{F} + \text{CH}_3\text{CH}_2\text{CH}_2\text{CH}_3$	-70.42	-70.18	-70.13	-70.40	-70.15	-70.29		-70.33	-70.22	-70.26	0.13
$\text{CH}_3\text{CH}_2\text{CH}_2\text{F} + \text{CH}_3\text{F} = \text{CH}_3\text{CH}_2\text{F} + \text{CH}_3\text{CH}_2\text{F}$	-70.68	-69.97	-70.29	-69.84	-70.51	-70.55	-70.44	-69.46	-70.26	-70.22	0.31
$\text{CH}_3\text{CH}_2\text{CH}_2\text{F} + \text{CH}_3\text{OH} = \text{CH}_3\text{CH}_2\text{F} + \text{CH}_3\text{CH}_2\text{OH}$	-70.62	-70.22	-70.25	-70.08	-70.44	-70.48	-70.46	-69.82	-70.42	-70.31	0.18
Average ^d	-70.50	-70.18	-70.28	-70.10	-70.25	-70.35	-70.27	-69.86	-69.96	-70.24^f	
STD ^e	0.12	0.19	0.20	0.24	0.18	0.13	0.18	0.45	0.53		0.21 ^g

^a Heat of formation of target molecule, unit in kcal mol⁻¹. ^b Average of heat of formation of target molecule for each work reaction over seven calculation methods(CBS-QB3, M06, M06-2X, ω B97X, G4, CBS-APNO,W1U). ^c Standard deviation of heat of formation of target molecule for each work reaction under seven calculation levels(CBS-QB3, M06, M06-2X, ω B97X, G4, CBS-APNO,W1U). ^d Average of heat of formation of target molecule of all set of work reactions under one calculation level. ^e Standard deviation of heat of formation of target molecule of all set of work reactions under one calculation level. ^f Heat of formation of target molecule calculated from the set of work reactions and seven selected calculation levels (CBS-QB3, M06, M06-2X, ω B97X, G4, CBS-APNO,W1U). ^g

Table E.3 Isodesmic reactions, heat of formations, and deviations for 2-fluoropropane

Isodesmic reactions	$\Delta H_{f,298}^a$									Average ^b	STD ^c
	CBS-QB3	M06	M06-2X	ω B97X	G4	CBS-APNO	W1U	B3LYP	G4(MP2)-6X		
$\text{CH}_3\text{CHFCH}_3 + \text{CH}_4 = \text{CH}_3\text{F} + \text{CH}_3\text{CH}_2\text{CH}_3$	-75.24	-75.56	-75.31	-75.31	-75.08	-75.13	-74.89	-74.94	-73.37	-75.01	0.21
$\text{CH}_3\text{CHFCH}_3 + \text{CH}_4 = \text{CH}_3\text{CH}_2\text{F} + \text{CH}_3\text{CH}_3$	-75.41	-75.18	-75.00	-74.95	-75.38	-75.30	-74.98	-74.12	-73.27	-74.87	0.20
$\text{CH}_3\text{CHFCH}_3 + \text{CH}_3\text{CH}_3 = \text{CH}_3\text{CH}_2\text{F} + \text{CH}_3\text{CH}_2\text{CH}_3$	-75.46	-75.53	-75.56	-75.30	-75.35	-75.37	-75.22	-74.87	-75.15	-75.29	0.13
$\text{CH}_3\text{CHFCH}_3 + \text{CH}_3\text{CH}_2\text{CH}_3 = \text{CH}_3\text{CH}_2\text{F} + \text{CH}_3\text{CH}_2\text{CH}_3$	-75.37	-75.37	-75.09	-75.49	-75.28	-75.29		-74.93	-75.21	-75.21	0.13
$\text{CH}_3\text{CHFCH}_3 + \text{CH}_3\text{F} = \text{CH}_3\text{CH}_2\text{F} + \text{CH}_3\text{CH}_2\text{F}$	-75.64	-75.15	-75.25	-74.93	-75.65	-75.54	-75.32	-74.02	-74.43	-75.16	0.27
$\text{CH}_3\text{CHFCH}_3 + \text{CH}_3\text{OH} = \text{CH}_3\text{CH}_2\text{F} + \text{CH}_3\text{CH}_2\text{OH}$	-75.57	-75.40	-75.21	-75.18	-75.57	-75.48	-75.33	-74.42	-74.70	-75.24	0.16
Average^d	-75.45	-75.37	-75.24	-75.19	-75.38	-75.35	-75.15	-74.46	-74.00	-75.26^f	
STD^e	0.12	0.19	0.20	0.24	0.18	0.13	0.18	0.45	0.53		0.20 ^g

^a Heat of formation of target molecule, unit in kcal mol⁻¹. ^b Average of heat of formation of target molecule for each work reaction over seven calculation methods(CBS-QB3, M06, M06-2X, ω B97X, G4, CBS-APNO,W1U). ^c Standard deviation of heat of formation of target molecule for each work reaction under seven calculation levels(CBS-QB3, M06, M06-2X, ω B97X, G4, CBS-APNO,W1U). ^d Average of heat of formation of target molecule of all set of work reactions under one calculation level. ^e Standard deviation of heat of formation of target molecule of all set of work reactions under one calculation level. ^f Heat of formation of target molecule calculated from the set of work reactions and seven selected calculation levels (CBS-QB3, M06, M06-2X, ω B97X, G4, CBS-APNO,W1U). ^g Standard deviation of target molecule calculated from all set of work reaction over the seven selected calculation levels(CBS-QB3, M06, M06-2X, ω B97X, G4, CBS-APNO,W1U).

Table E.4 Isodesmic reactions, heat of formations, and deviations for 1-fluorobutane

Isodesmic reactions	$\Delta H_{f,298}^a$									Average ^b	STD ^c
	CBS-QB3	M06	M06-2X	ω B97X	G4	CBS-APNO	W1U	B3LYP	G4(MP2)-6X		
$\text{CH}_3\text{CH}_2\text{CH}_2\text{CH}_2\text{F} + \text{CH}_4 = \text{CH}_3\text{F} + \text{CH}_3\text{CH}_2\text{CH}_2\text{CH}_3$	-75.19	-75.11	-75.00	-75.19	-75.11	-75.06		-74.96	-74.23	-74.98	0.07
$\text{CH}_3\text{CH}_2\text{CH}_2\text{CH}_2\text{F} + \text{CH}_4 = \text{CH}_3\text{CH}_2\text{F} + \text{CH}_3\text{CH}_2\text{CH}_3$	-75.46	-74.89	-75.16	-74.63	-75.47	-75.31		-74.09	-74.27	-74.91	0.34
$\text{CH}_3\text{CH}_2\text{CH}_2\text{CH}_2\text{F} + \text{CH}_3\text{CH}_3 = \text{CH}_3\text{CH}_2\text{F} + \text{CH}_3\text{CH}_2\text{CH}_2\text{CH}_3$	-75.42	-75.08	-75.25	-75.17	-75.37	-75.30		-75.18	-75.26	-75.25	0.13
$\text{CH}_3\text{CH}_2\text{CH}_2\text{CH}_2\text{F} + \text{CH}_3\text{CH}_3 = \text{CH}_3\text{CH}_2\text{CH}_2\text{CH}_2\text{F} + \text{CH}_3\text{CH}_3$	-75.19	-75.09	-75.32	-74.97	-75.42	-75.20		-75.04	-75.23	-75.18	0.16
$\text{CH}_3\text{CH}_2\text{CH}_2\text{CH}_2\text{F} + \text{CH}_3\text{CH}_3 = \text{CH}_3\text{CHFCH}_3 + \text{CH}_3\text{CH}_2\text{CH}_3$	-75.18	-74.84	-75.29	-74.81	-75.22	-75.14		-75.10	-75.84	-75.18	0.20
$\text{CH}_3\text{CH}_2\text{CH}_2\text{CH}_2\text{F} + \text{CH}_3\text{CH}_2\text{CH}_3 = \text{CH}_3\text{CH}_2\text{CH}_2\text{F} + \text{CH}_3\text{CH}_2\text{CH}_2\text{CH}_3$	-75.10	-74.93	-74.84	-75.16	-75.35	-75.12		-75.09	-75.12	-75.09	0.18
$\text{CH}_3\text{CH}_2\text{CH}_2\text{CH}_2\text{F} + \text{CH}_3\text{CH}_2\text{CH}_3 = \text{CH}_3\text{CHFCH}_3 + \text{CH}_3\text{CH}_2\text{CH}_3$	-75.08	-74.68	-74.82	-75.00	-75.15	-75.06		-75.15	-75.74	-75.08	0.18
$\text{CH}_3\text{CH}_2\text{CH}_2\text{CH}_2\text{F} + \text{CH}_3\text{OH} = \text{CH}_3\text{CH}_2\text{CH}_2\text{F} + \text{CH}_3\text{CH}_2\text{OH}$	-75.30	-74.97	-74.96	-74.85	-75.64	-75.31		-74.58	-75.32	-75.12	0.30
$\text{CH}_3\text{CH}_2\text{CH}_2\text{CH}_2\text{F} + \text{CH}_3\text{OH} = \text{CH}_3\text{CHFCH}_3 + \text{CH}_3\text{CH}_2\text{OH}$	-75.28	-74.71	-74.93	-74.69	-75.44	-75.24		-74.64	-75.94	-75.11	0.32
Average^d	-75.24	-74.92	-75.06	-74.94	-75.35	-75.19		-74.87	-75.22	-75.17^f	
STD^e	0.10	0.11	0.18	0.20	0.17	0.10		0.39	0.68		0.21 ^g

^a Heat of formation of target molecule, unit in kcal mol⁻¹. ^b Average of heat of formation of target molecule for each work reaction over six calculation methods(CBS-QB3, M06, M06-2X, ω B97X, G4, CBS-APNO). ^c Standard deviation of heat of formation of target molecule for each work reaction under six calculation levels(CBS-QB3, M06, M06-2X, ω B97X, G4, CBS-APNO). ^d Average of heat of formation of target molecule of all set of work reactions under one calculation level. ^e Standard deviation of heat of formation of target molecule of all set of work reactions under one calculation level. ^f Heat of formation of target molecule calculated from the set of work reactions and six selected calculation levels (CBS-QB3, M06, M06-2X, ω B97X, G4, CBS-APNO). ^g Standard deviation of target molecule calculated from all set of work reaction over the six selected calculation levels(CBS-QB3, M06, M06-2X, ω B97X, G4, CBS-APNO).

Table E.5 Isodesmic reactions, heat of formations, and deviations for 2-fluorobutane

Isodesmic reactions	$\Delta H_{f,298}^a$									Average ^b	STD ^c
	CBS-QB3	M06	M06-2X	ω B97X	G4	CBS-APNO	W1U	B3LYP	G4(MP2)-6X		
$\text{CH}_3\text{CHFCH}_2\text{CH}_3 + \text{CH}_4 = \text{CH}_3\text{F} + \text{CH}_3\text{CH}_2\text{CH}_2\text{CH}_3$	-80.31	-80.40	-80.06	-80.24	-80.14	-80.10		-79.75	-78.45	-79.94	0.14
$\text{CH}_3\text{CHFCH}_2\text{CH}_3 + \text{CH}_4 = \text{CH}_3\text{CH}_2\text{F} + \text{CH}_3\text{CH}_2\text{CH}_3$	-80.57	-80.22	-80.22	-79.68	-80.51	-80.35		-78.87	-78.50	-79.87	0.32
$\text{CH}_3\text{CHFCH}_2\text{CH}_3 + \text{CH}_4 = \text{CH}_3\text{CH}_2\text{CH}_2\text{F} + \text{CH}_3\text{CH}_3$	-80.26	-80.07	-79.81	-79.67	-80.48	-80.17		-78.79	-78.36	-79.70	0.30
$\text{CH}_3\text{CHFCH}_2\text{CH}_3 + \text{CH}_4 = \text{CH}_3\text{CHFCH}_2\text{CH}_3 + \text{CH}_4 = \text{CH}_3\text{CHFCH}_3 + \text{CH}_3\text{CH}_3$	-80.24	-79.82	-79.79	-79.51	-80.28	-80.11		-78.85	-78.98	-79.70	0.30
$\text{CH}_3\text{CHFCH}_2\text{CH}_3 + \text{CH}_3\text{CH}_3 = \text{CH}_3\text{CH}_2\text{F} + \text{CH}_3\text{CH}_2\text{CH}_2\text{CH}_3$	-80.53	-80.41	-80.31	-80.23	-80.41	-80.34		-79.96	-79.49	-80.21	0.10
$\text{CH}_3\text{CHFCH}_2\text{CH}_3 + \text{CH}_3\text{CH}_3 = \text{CH}_3\text{CH}_2\text{CH}_2\text{F} + \text{CH}_3\text{CH}_2\text{CH}_3$	-80.31	-80.42	-80.38	-80.03	-80.45	-80.25		-79.83	-79.46	-80.14	0.16
$\text{CH}_3\text{CHFCH}_2\text{CH}_3 + \text{CH}_3\text{CH}_3 = \text{CH}_3\text{CHFCH}_3 + \text{CH}_3\text{CH}_2\text{CH}_3$	-80.29	-80.17	-80.35	-79.87	-80.25	-80.18		-79.88	-80.07	-80.13	0.17
$\text{CH}_3\text{CHFCH}_2\text{CH}_3 + \text{CH}_3\text{CH}_2\text{CH}_3 = \text{CH}_3\text{CH}_2\text{CH}_2\text{F} + \text{CH}_3\text{CH}_2\text{CH}_2\text{CH}_3$	-80.21	-80.25	-79.91	-80.22	-80.39	-80.16		-79.88	-79.35	-80.05	0.16
$\text{CH}_3\text{CHFCH}_2\text{CH}_3 + \text{CH}_3\text{CH}_2\text{CH}_3 = \text{CH}_3\text{CHFCH}_3 + \text{CH}_3\text{CH}_2\text{CH}_2\text{CH}_3$	-80.20	-80.00	-79.88	-80.06	-80.19	-80.10		-79.94	-79.97	-80.04	0.12
$\text{CH}_3\text{CHFCH}_2\text{CH}_3 + \text{CH}_3\text{OH} = \text{CH}_3\text{CH}_2\text{CH}_2\text{F} + \text{CH}_3\text{CH}_2\text{OH}$	-80.42	-80.29	-80.02	-79.91	-80.67	-80.35		-79.37	-79.55	-80.07	0.28
$\text{CH}_3\text{CHFCH}_2\text{CH}_3 + \text{CH}_3\text{OH} = \text{CH}_3\text{CHFCH}_3 + \text{CH}_3\text{CH}_2\text{OH}$	-80.40	-80.04	-80.00	-79.74	-80.47	-80.28		-79.43	-80.17	-80.07	0.28
Average^d	-80.34	-80.19	-80.07	-79.92	-80.39	-80.22		-79.50	-79.30	-80.25^f	
STD^e	0.10	0.15	0.20	0.26	0.15	0.09		0.48	0.70		0.22 ^g

^a Heat of formation of target molecule, unit in kcal mol⁻¹. ^b Average of heat of formation of target molecule for each work reaction over six calculation methods(CBS-QB3, M06, M06-2X, ω B97X, G4, CBS-APNO). ^c Standard deviation of heat of formation of target molecule for each work reaction under six calculation levels(CBS-QB3, M06, M06-2X, ω B97X, G4, CBS-APNO). ^d Average of heat of formation of target molecule of all set of work reactions under one calculation level. ^e Standard deviation of heat of formation of target molecule of all set of work reactions under one calculation level. ^f Heat of formation of target molecule calculated from the set of work reactions and six selected calculation levels (CBS-QB3, M06, M06-2X, ω B97X, G4, CBS-APNO). ^g Standard deviation of target molecule calculated from all set of work reaction over the six selected calculation levels(CBS-QB3, M06, M06-2X, ω B97X, G4, CBS-APNO).

Table E.6 Isodesmic reactions, heat of formations, and deviations for difluoromethane

Isodesmic reactions	$\Delta H_{f,298}^a$									Average ^b	STD ^c
	CBS-QB3	M06	M06-2X	ω B97X	G4	CBS-APNO	W1U	B3LYP	G4(MP2)-6X		
$\text{CH}_2\text{F}_2 + \text{CH}_4 = \text{CH}_3\text{F} + \text{CH}_3\text{F}$	-107.89	-107.59	-107.99	-107.78	-108.17	-108.52	-108.14	-106.94	-107.80	-107.87	0.30
$\text{CH}_2\text{F}_2 + \text{CH}_3\text{CH}_3 = \text{CH}_3\text{F} + \text{CH}_3\text{CH}_2\text{F}$	-108.12	-107.57	-108.25	-107.76	-108.44	-108.76	-108.48	-107.16	-108.83	-108.15	0.42
$\text{CH}_2\text{F}_2 + \text{CH}_3\text{CH}_2\text{CH}_3 = \text{CH}_3\text{F} + \text{CH}_3\text{CH}_2\text{CH}_2\text{F}$	-107.80	-107.41	-107.84	-107.75	-108.42	-108.58	-108.32	-107.08	-108.70	-107.99	0.43
$\text{CH}_2\text{F}_2 + \text{CH}_3\text{CH}_2\text{CH}_3 = \text{CH}_3\text{F} + \text{CH}_3\text{CHFCH}_3$	-107.78	-107.16	-107.81	-107.69	-108.22	-108.51	-108.38	-107.13	-109.31	-107.99	0.48
$\text{CH}_2\text{F}_2 + \text{CH}_3\text{CH}_2\text{CH}_3 = \text{CH}_3\text{CH}_2\text{CH}_2\text{F} + \text{CH}_3\text{CH}_2\text{F}$	-108.29	-107.18	-107.94	-107.40	-108.74	-108.93	-108.57	-106.34	-108.77	-108.02	0.67
$\text{CH}_2\text{F}_2 + \text{CH}_3\text{CH}_2\text{CH}_2\text{CH}_3 = \text{CH}_3\text{CH}_2\text{CH}_2\text{F} + \text{CH}_3\text{CH}_2\text{CH}_2\text{F}$	-108.07	-107.20	-108.00	-107.19	-108.79	-108.83		-106.20	-108.74	-107.88	0.72
$\text{CH}_2\text{F}_2 + \text{CH}_3\text{CH}_2\text{CH}_2\text{CH}_3 = \text{CH}_3\text{CH}_2\text{CH}_2\text{F} + \text{CH}_3\text{CHFCH}_3$	-108.05	-106.94	-107.97	-107.03	-108.59	-108.77		-106.26	-109.35	-107.87	0.76
Average^d	-108.00	-107.29	-107.97	-107.50	-108.48	-108.70	-108.38	-106.73	-108.79	-108.07^f	
STD^e	0.14	0.21	0.12	0.30	0.22	0.13	0.15	0.46	0.56		0.52 ^g

^a Heat of formation of target molecule, unit in kcal mol⁻¹. ^b Average of heat of formation of target molecule for each work reaction over seven calculation methods(CBS-QB3, M06, M06-2X, ω B97X, G4, CBS-APNO,W1U). ^c Standard deviation of heat of formation of target molecule for each work reaction under seven calculation levels(CBS-QB3, M06, M06-2X, ω B97X, G4, CBS-APNO,W1U). ^d Average of heat of formation of target molecule of all set of work reactions under one calculation level. ^e Standard deviation of heat of formation of target molecule of all set of work reactions under one calculation level. ^f Heat of formation of target molecule calculated from the set of work reactions and seven selected calculation levels (CBS-QB3, M06, M06-2X, ω B97X, G4, CBS-APNO,W1U). ^g Standard deviation of target molecule calculated from all set of work reaction over the seven selected calculation levels(CBS-QB3, M06, M06-2X, ω B97X, G4, CBS-APNO,W1U).

Table E.7 Isodesmic reactions, heat of formations, and deviations for 1,1-difluoroethane

Isodesmic reactions	$\Delta H_{f,298}^a$									Average ^b	STD ^c
	CBS-QB3	M06	M06-2X	ω B97X	G4	CBS-APNO	W1U	B3LYP	G4(MP2)-6X		
$\text{CH}_3\text{CHF}_2 + \text{CH}_4 = \text{CH}_3\text{F} + \text{CH}_3\text{CH}_2\text{F}$	-120.86	-120.67	-120.95	-120.53	-120.87	-121.28	-120.76	-119.47	-119.75	-120.57	0.24
$\text{CH}_3\text{CHF}_2 + \text{CH}_4 = \text{CH}_2\text{F}_2 + \text{CH}_3\text{CH}_3$	-120.71	-121.08	-120.67	-120.74	-120.39	-120.49	-120.26	-120.28	-118.89	-120.39	0.27
$\text{CH}_3\text{CHF}_2 + \text{CH}_3\text{CH}_3 = \text{CH}_3\text{CHFCH}_3$	-120.59	-120.87	-121.11	-120.87	-120.82	-120.71	-120.85	-120.42	-120.71	-120.82	0.19
$\text{CH}_3\text{CHF}_2 + \text{CH}_3\text{CH}_3 = \text{CH}_3\text{F} + \text{CH}_3\text{CH}_2\text{CH}_2\text{F}$	-120.58	-120.62	-121.08	-120.71	-120.62	-121.33	-120.91	-120.48	-121.33	-120.83	0.23
$\text{CH}_3\text{CHF}_2 + \text{CH}_3\text{CH}_2\text{CH}_3 = \text{CH}_3\text{CHFCH}_3$	-121.08	-120.65	-121.20	-120.52	-121.14	-120.78	-121.10	-119.69	-120.78	-120.85	0.34
$\text{CH}_3\text{CHF}_2 + \text{CH}_3\text{CH}_2\text{CH}_3 = \text{CH}_3\text{CH}_2\text{F} + \text{CH}_3\text{CH}_2\text{F}$	-120.77	-120.49	-120.80	-120.51	-121.11	-120.65	-120.95	-119.60	-120.65	-120.69	0.31
$\text{CH}_3\text{CHF}_2 + \text{CH}_3\text{CH}_2\text{CH}_3 = \text{CH}_3\text{CH}_2\text{CH}_2\text{F}$	-120.75	-120.24	-120.77	-120.35	-120.91	-121.26	-121.01	-119.66	-121.26	-120.69	0.36
$\text{CH}_3\text{CHF}_2 + \text{CH}_3\text{CH}_2\text{CH}_3 = \text{CH}_3\text{CHFCH}_3$	-120.54	-120.50	-120.86	-120.30	-121.16	-120.62		-119.47	-120.62	-120.59	0.38
$\text{CH}_3\text{CHF}_2 + \text{CH}_3\text{CH}_2\text{CH}_2\text{CH}_3 = \text{CH}_3\text{CH}_2\text{CH}_2\text{CH}_2\text{F}$	-120.51	-120.00	-120.80	-119.98	-120.76	-121.85		-119.58	-121.85	-120.58	0.46
$\text{CH}_3\text{CHF}_2 + \text{CH}_3\text{CH}_2\text{CH}_2\text{CH}_3 = \text{CH}_3\text{CHFCH}_3$	-120.87	-121.30	-120.88	-120.97	-120.58	-120.08	-120.61	-120.86	-120.08	-120.76	0.25
Average^d	-120.73	-120.64	-120.91	-120.55	-120.84	-120.59	-120.81	-119.95	-120.59	-120.87^f	
STD^e	0.12	0.36	0.15	0.27	0.23	0.29	0.25	0.53	0.90		0.30 ^g

^a Heat of formation of target molecule, unit in kcal mol⁻¹. ^b Average of heat of formation of target molecule for each work reaction over seven calculation methods(CBS-QB3, M06, M06-2X, ω B97X, G4, CBS-APNO,W1U). ^c Standard deviation of heat of formation of target molecule for each work reaction under seven calculation levels(CBS-QB3, M06, M06-2X, ω B97X, G4, CBS-APNO,W1U). ^d Average of heat of formation of target molecule of all set of work reactions under one calculation level. ^e Standard deviation of heat of formation of target molecule of all set of work reactions under one calculation level. ^f Heat of formation of target molecule calculated from the set of work reactions and seven selected calculation levels (CBS-QB3, M06, M06-2X, ω B97X, G4, CBS-APNO,W1U). ^g Standard deviation of target molecule calculated from all set of work reaction over the seven selected calculation levels(CBS-QB3, M06, M06-2X, ω B97X, G4, CBS-APNO,W1U).

Table E.8 Isodesmic reactions, heat of formations, and deviations for 1,1-difluoropropane

Isodesmic reactions	$\Delta H_{f,298}^a$									Average ^b	STD ^c
	CBS-QB3	M06	M06-2X	ω B97X	G4	CBS-APNO	W1U	B3LYP	G4(MP2)-6X		
$\text{CH}_3\text{CH}_2\text{CHF}_2 + \text{CH}_4 = \text{CH}_3\text{F} + \text{CH}_3\text{CH}_2\text{CH}_2\text{F}$	-125.52	-125.50	-125.63	-125.21	-126.57	-125.94		-124.13	-124.52	-125.38	0.48
$\text{CH}_3\text{CH}_2\text{CHF}_2 + \text{CH}_4 = \text{CH}_3\text{F} + \text{CH}_3\text{CHFCH}_3$	-125.50	-125.25	-125.60	-125.05	-126.37	-125.87		-124.19	-125.13	-125.37	0.47
$\text{CH}_3\text{CH}_2\text{CHF}_2 + \text{CH}_4 = \text{CH}_3\text{CH}_2\text{F} + \text{CH}_3\text{CH}_2\text{F}$	-126.01	-125.27	-125.73	-124.86	-126.89	-126.29		-123.40	-124.59	-125.38	0.73
$\text{CH}_3\text{CH}_2\text{CHF}_2 + \text{CH}_4 = \text{CH}_2\text{F}_2 + \text{CH}_3\text{CH}_2\text{CH}_3$	-125.69	-126.06	-125.76	-125.43	-126.12	-125.33		-125.03	-123.79	-125.40	0.32
$\text{CH}_3\text{CH}_2\text{CHF}_2 + \text{CH}_4 = \text{CH}_3\text{CHF}_2 + \text{CH}_3\text{CH}_3$	-125.60	-125.31	-125.20	-125.02	-126.44	-125.44		-124.39	-124.49	-125.23	0.50
$\text{CH}_3\text{CH}_2\text{CHF}_2 + \text{CH}_3\text{CH}_3 = \text{CH}_3\text{CH}_2\text{F} + \text{CH}_3\text{CH}_2\text{CH}_2\text{F}$	-125.74	-125.47	-125.88	-125.20	-126.84	-126.18		-124.35	-125.55	-125.65	0.58
$\text{CH}_3\text{CH}_2\text{CHF}_2 + \text{CH}_3\text{CH}_3 = \text{CH}_3\text{CH}_2\text{F} + \text{CH}_3\text{CHFCH}_3$	-125.72	-125.22	-125.85	-125.04	-126.64	-126.12		-124.41	-126.17	-125.65	0.59
$\text{CH}_3\text{CH}_2\text{CHF}_2 + \text{CH}_3\text{CH}_3 = \text{CH}_2\text{F}_2 + \text{CH}_3\text{CH}_2\text{CH}_2\text{CH}_3$	-125.64	-126.25	-125.85	-125.97	-126.03	-125.32		-126.12	-124.78	-125.74	0.32
$\text{CH}_3\text{CH}_2\text{CHF}_2 + \text{CH}_3\text{CH}_3 = \text{CH}_3\text{CHF}_2 + \text{CH}_3\text{CH}_2\text{CH}_3$	-125.65	-125.66	-125.77	-125.37	-126.41	-125.51		-125.43	-125.58	-125.67	0.36
$\text{CH}_3\text{CH}_2\text{CHF}_2 + \text{CH}_3\text{CH}_2\text{CH}_3 = \text{CH}_3\text{CH}_2\text{CH}_2\text{F} + \text{CH}_3\text{CH}_2\text{CH}_2\text{F}$	-125.42	-125.32	-125.47	-125.19	-126.82	-126.00		-124.27	-125.41	-125.49	0.61
$\text{CH}_3\text{CH}_2\text{CHF}_2 + \text{CH}_3\text{CH}_2\text{CH}_3 = \text{CH}_3\text{CHFCH}_3 + \text{CH}_3\text{CHFCH}_3$	-125.39	-124.82	-125.42	-124.87	-126.42	-125.87		-124.38	-126.65	-125.48	0.61
$\text{CH}_3\text{CH}_2\text{CHF}_2 + \text{CH}_3\text{CH}_2\text{CH}_3 = \text{CH}_3\text{CHF}_2 + \text{CH}_3\text{CH}_2\text{CH}_2\text{CH}_3$	-125.56	-125.49	-125.29	-125.56	-126.34	-125.43		-125.48	-125.48	-125.58	0.37
$\text{CH}_3\text{CH}_2\text{CHF}_2 + \text{CH}_3\text{CH}_2\text{CH}_3 = \text{CH}_3\text{CH}_2\text{CH}_2\text{CH}_3$	-125.76	-125.53	-125.41	-125.25	-126.63	-125.62		-124.97	-125.68	-125.61	0.49
Average^d	-125.63	-125.47	-125.60	-125.23	-126.50	-125.76		-124.66	-125.22	-125.82^f	
STD^e	0.13	0.36	0.19	0.33	0.23	0.29		0.77	0.82		0.47 ^g

^a Heat of formation of target molecule, unit in kcal mol⁻¹. ^b Average of heat of formation of target molecule for each work reaction over six calculation methods(CBS-QB3, M06, M06-2X, ωB97X, G4, CBS-APNO). ^c Standard deviation of heat of formation of target molecule for each work reaction under six calculation levels(CBS-QB3, M06, M06-2X, ωB97X, G4, CBS-APNO). ^d Average of heat of formation of target molecule of all set of work reactions under one calculation level. ^e Standard deviation of heat of formation of target molecule of all set of work reactions under one calculation level. ^f Heat of formation of target molecule calculated from the set of work reactions and six selected calculation levels (CBS-QB3, M06, M06-2X, ωB97X, G4, CBS-APNO). ^g Standard deviation of target molecule calculated from all set of work reaction over the six selected calculation levels(CBS-QB3, M06, M06-2X, ωB97X, G4, CBS-APNO).

Table E.9 Isodesmic reactions, heat of formations, and deviations for 2,2-difluoropropane

Isodesmic reactions	$\Delta H_{f,298}^a$						W1U	B3LYP	G4(MP2)-6X	Average ^b	STD ^c
	CBS-QB3	M06	M06-2X	ωB97X	G4	CBS-APNO					
CH ₃ CF ₂ CH ₃ + CH ₄ = CH ₃ F + CH ₃ CH ₂ CH ₂ F	-133.06	-133.54	-133.17	-132.76	-133.11	-133.36		-131.17	-130.56	-132.59	0.27
CH ₃ CF ₂ CH ₃ + CH ₄ = CH ₃ F + CH ₃ CHFCH ₃	-133.04	-133.29	-133.14	-132.60	-132.91	-133.29		-131.22	-131.18	-132.58	0.26
CH ₃ CF ₂ CH ₃ + CH ₄ = CH ₃ CH ₂ F + CH ₃ CH ₂ F	-133.55	-133.31	-133.26	-132.40	-133.43	-133.71		-130.43	-130.63	-132.59	0.46
CH ₃ CF ₂ CH ₃ + CH ₄ = CH ₂ F ₂ + CH ₃ CH ₂ CH ₃	-133.23	-134.10	-133.30	-132.98	-132.66	-132.75		-132.06	-129.83	-132.61	0.52
CH ₃ CF ₂ CH ₃ + CH ₄ = CH ₃ CHF ₂ + CH ₃ CH ₃	-133.14	-133.34	-132.74	-132.56	-132.97	-132.86		-131.42	-130.53	-132.45	0.28
CH ₃ CF ₂ CH ₃ + CH ₃ CH ₃ = CH ₃ CH ₂ F + CH ₃ CH ₂ CH ₂ F	-133.28	-133.51	-133.42	-132.75	-133.38	-133.60		-131.38	-131.59	-132.86	0.30
CH ₃ CF ₂ CH ₃ + CH ₃ CH ₃ = CH ₃ CH ₂ F + CH ₃ CHFCH ₃	-133.27	-133.26	-133.39	-132.59	-133.18	-133.54		-131.44	-132.21	-132.86	0.33
CH ₃ CF ₂ CH ₃ + CH ₃ CH ₃ = CH ₂ F ₂ + CH ₃ CH ₂ CH ₂ CH ₃	-133.19	-134.28	-133.39	-133.52	-132.56	-132.74		-131.15	-130.83	-132.96	0.62
CH ₃ CF ₂ CH ₃ + CH ₃ CH ₃ = CH ₃ CHF ₂ + CH ₃ CH ₂ CH ₃	-133.20	-133.70	-133.30	-132.92	-132.94	-132.94		-132.46	-131.63	-132.89	0.31
CH ₃ CF ₂ CH ₃ + CH ₃ CH ₂ CH ₃ = CH ₃ CH ₂ CH ₂ F + CH ₃ CH ₂ CH ₂ F	-132.97	-133.36	-133.01	-132.74	-133.35	-133.42		-131.30	-131.46	-132.70	0.28
CH ₃ CF ₂ CH ₃ + CH ₃ CH ₂ CH ₃ = CH ₃ CHFCH ₃ + CH ₃ CHFCH ₃	-132.93	-132.85	-132.95	-132.42	-132.95	-133.29		-131.41	-132.69	-132.69	0.28
CH ₃ CF ₂ CH ₃ + CH ₃ CH ₂ CH ₃ = CH ₃ CHF ₂ + CH ₃ CH ₂ CH ₂ CH ₃	-133.10	-133.53	-132.83	-133.11	-132.88	-132.85		-132.51	-131.52	-132.79	0.27
CH ₃ CF ₂ CH ₃ + CH ₃ OH = CH ₃ CHF ₂ + CH ₃ CH ₂ OH	-133.30	-133.57	-132.95	-132.80	-133.16	-133.04		-132.00	-131.72	-132.82	0.27
Average^d	-133.17	-133.51	-133.14	-132.78	-133.04	-133.18		-131.69	-131.26	-133.25 ^f	
STD^e	0.13	0.36	0.19	0.33	0.23	0.29		0.76	0.82		0.34 ^g

^a Heat of formation of target molecule, unit in kcal mol⁻¹. ^b Average of heat of formation of target molecule for each work reaction over six calculation methods(CBS-QB3, M06, M06-2X, ωB97X, G4, CBS-APNO). ^c Standard deviation of heat of formation of target molecule for each work reaction under six calculation levels(CBS-QB3, M06, M06-2X, ωB97X, G4, CBS-APNO). ^d Average of heat of formation of target molecule of all set of work reactions under one calculation level. ^e Standard deviation of heat of formation of target molecule of all set of work reactions under one calculation level. ^f Heat of formation of target molecule calculated from the set of work reactions and six selected calculation levels (CBS-QB3, M06, M06-2X, ωB97X, G4, CBS-APNO). ^g Standard deviation of target molecule calculated from all set of work reaction over the six selected calculation levels(CBS-QB3, M06, M06-2X, ωB97X, G4, CBS-APNO).

Table E.10 Isodesmic reactions, heat of formations, and deviations for trifluoromethane

Isodesmic reactions	$\Delta H_{f,298}^a$									Average ^b	STD ^c
	CBS-QB3	M06	M06-2X	ω B97X	G4	CBS-APNO	W1U	B3LYP	G4(MP2)-6X		
$\text{CHF}_3 + \text{CH}_4 = \text{CH}_3\text{F} + \text{CH}_2\text{F}_2$	-166.30	-166.41	-166.27	-165.81	-166.77	-167.42	-166.82	-164.17	-165.36	-166.15	0.51
$\text{CHF}_3 + \text{CH}_3\text{CH}_3 = \text{CH}_3\text{F} + \text{CH}_3\text{CHF}_2$	-166.27	-166.01	-166.28	-165.75	-167.06	-167.60	-167.24	-164.57	-167.15	-166.44	0.70
$\text{CHF}_3 + \text{CH}_3\text{CH}_2\text{CH}_3 = \text{CH}_3\text{CH}_2\text{F} + \text{CH}_2\text{F}_2$	-166.53	-166.39	-166.53	-165.79	-167.04	-167.66	-167.16	-164.39	-166.39	-166.43	0.61
$\text{CHF}_3 + \text{CH}_3\text{CH}_2\text{CH}_2\text{CH}_3 = \text{CH}_3\text{CH}_2\text{CH}_2\text{F} + \text{CH}_2\text{CHF}_2$	-166.13	-165.86	-166.02	-165.89	-166.16	-167.60	-167.60	-164.66	-167.08	-166.33	0.78
$\text{CHF}_3 + \text{CH}_3\text{CH}_2\text{CH}_2\text{CH}_2\text{CH}_3 = \text{CH}_3\text{CH}_2\text{CH}_2\text{CH}_2\text{F} + \text{CH}_2\text{CHF}_2$	-165.79	-165.04	-165.70	-165.55	-166.84	-167.39		-164.84	-168.25	-166.17	0.88
$\text{CHF}_3 + \text{CH}_3\text{CH}_2\text{CH}_2\text{CH}_2\text{CH}_2\text{CH}_3 = \text{CH}_3\text{CH}_2\text{CH}_2\text{CH}_2\text{CH}_2\text{F} + \text{CH}_2\text{CHF}_2$	-166.44	-165.63	-165.97	-165.38	-167.36	-167.77	-167.34	-163.76	-167.09	-166.30	0.94
$\text{CHF}_3 + \text{CH}_3\text{CH}_2\text{CH}_2\text{CH}_2\text{CH}_2\text{CH}_2\text{CH}_3 = \text{CH}_3\text{CH}_2\text{CH}_2\text{CH}_2\text{CH}_2\text{F} + \text{CH}_2\text{CHF}_2$	-166.21	-166.23	-166.12	-165.78	-167.02	-167.48	-167.01	-164.31	-166.26	-166.27	0.62
$\text{CHF}_3 + \text{CH}_3\text{CH}_2\text{CH}_2\text{CH}_2\text{CH}_2\text{CH}_2\text{CH}_2\text{CH}_3 = \text{CH}_3\text{CH}_2\text{CH}_2\text{CH}_2\text{CH}_2\text{CH}_2\text{F} + \text{CH}_2\text{CHF}_2$	-166.19	-165.98	-166.09	-165.62	-166.82	-167.42	-167.06	-164.36	-166.87	-166.27	0.65
$\text{CHF}_3 + \text{CH}_3\text{CH}_2\text{CH}_2\text{CH}_2\text{CH}_2\text{CH}_2\text{CH}_2\text{CH}_2\text{CH}_3 = \text{CH}_3\text{CH}_2\text{CH}_2\text{CH}_2\text{CH}_2\text{CH}_2\text{CH}_2\text{F} + \text{CH}_2\text{CHF}_2$	-166.39	-165.65	-166.18	-165.33	-166.53	-167.85		-163.78	-167.12	-166.10	0.88
$\text{CHF}_3 + \text{CH}_3\text{CH}_2\text{CH}_2\text{CH}_2\text{CH}_2\text{CH}_2\text{CH}_2\text{CH}_2\text{CH}_2\text{CH}_3 = \text{CH}_3\text{CH}_2\text{CH}_2\text{CH}_2\text{CH}_2\text{CH}_2\text{CH}_2\text{CH}_2\text{F} + \text{CH}_2\text{CHF}_2$	-166.06	-164.82	-165.86	-164.99	-167.20	-167.64		-163.96	-168.29	-166.10	1.14
$\text{CHF}_3 + \text{CH}_3\text{CH}_2\text{CH}_2\text{CH}_2\text{CH}_2\text{CH}_2\text{CH}_2\text{CH}_2\text{CH}_2\text{CH}_2\text{CH}_3 = \text{CH}_3\text{CH}_2\text{CH}_2\text{CH}_2\text{CH}_2\text{CH}_2\text{CH}_2\text{CH}_2\text{CH}_2\text{F} + \text{CH}_2\text{CHF}_2$	-166.22	-165.64	-166.03	-165.18	-167.40	-167.68		-163.62	-167.06	-166.10	0.99
$\text{CHF}_3 + \text{CH}_3\text{CH}_2\text{CH}_2\text{CH}_2\text{CH}_2\text{CH}_2\text{CH}_2\text{CH}_2\text{CH}_2\text{CH}_2\text{CH}_2\text{CH}_3 = \text{CH}_3\text{CH}_2\text{CH}_2\text{CH}_2\text{CH}_2\text{CH}_2\text{CH}_2\text{CH}_2\text{CH}_2\text{CH}_2\text{F} + \text{CH}_2\text{CHF}_2$	-166.20	-165.39	-166.00	-165.02	-167.20	-167.61		-163.67	-167.67	-166.10	1.01
$\text{CHF}_3 + \text{CH}_3\text{F} = \text{CH}_2\text{F}_2 + \text{CH}_2\text{F}_2$	-166.38	-166.79	-166.25	-166.00	-166.57	-166.87	-166.65	-165.20	-165.53	-166.25	0.31
$\text{CHF}_3 + \text{CH}_3\text{CH}_2\text{CH}_2\text{CH}_2\text{F} = \text{CH}_3\text{CHF}_2 + \text{CH}_2\text{CHF}_2$	-166.35	-165.82	-165.85	-165.55	-166.92	-167.11	-167.07	-164.83	-167.12	-166.29	0.66
Average^d	-166.25	-165.83	-166.08	-165.55	-166.92	-167.51	-167.11	-164.29	-166.95	-166.71^f	
STD^e	0.11	0.43	0.12	0.28	0.36	0.29	0.32	0.52	1.06		0.73 ^g

^a Heat of formation of target molecule, unit in kcal mol⁻¹. ^b Average of heat of formation of target molecule for each work reaction over seven calculation methods(CBS-QB3, M06, M06-2X, ω B97X, G4, CBS-APNO,W1U). ^c Standard deviation of heat of formation of target molecule for each work reaction under seven calculation levels(CBS-QB3, M06, M06-2X, ω B97X, G4, CBS-APNO,W1U). ^d Average of heat of formation of target molecule of all set of work reactions under one calculation level. ^e Standard deviation of heat of formation of target molecule of all set of work reactions under one calculation level. ^f Heat of formation of target molecule calculated from the set of work reactions and seven selected calculation levels (CBS-QB3, M06, M06-2X, ω B97X, G4, CBS-APNO,W1U). ^g Standard deviation of target molecule calculated from all set of work reaction over the seven selected calculation levels(CBS-QB3, M06, M06-2X, ω B97X, G4, CBS-APNO,W1U).

Table E.11 Isodesmic reactions, heat of formations, and deviations for 1,1,1-trifluoroethane

Isodesmic reactions	$\Delta H_{f,298}^a$									Average ^b	STD ^c
	CBS-QB3	M06	M06-2X	ω B97X	G4	CBS-APNO	W1U	B3LYP	G4(MP2)-6X		
$\text{CH}_3\text{CF}_3 + \text{CH}_4 = \text{CH}_2\text{F}_2 + \text{CH}_3\text{CH}_2\text{F}$	-180.50	-180.68	-180.41	-179.46	-180.45	-181.09	-180.20	-177.34	-177.89	-179.78	0.50
$\text{CH}_3\text{CF}_3 + \text{CH}_4 = \text{CH}_3\text{CHF}_2 + \text{CH}_3\text{F}$	-180.24	-180.31	-180.17	-179.42	-180.46	-181.03	-180.29	-177.52	-178.65	-179.79	0.48
$\text{CH}_3\text{CF}_3 + \text{CH}_4 = \text{CHF}_3 + \text{CH}_3\text{CH}_3$	-180.21	-180.53	-180.13	-179.91	-179.65	-179.67	-179.29	-179.19	-177.74	-179.59	0.42
$\text{CH}_3\text{CF}_3 + \text{CH}_3\text{CH}_3 = \text{CH}_2\text{F}_2 + \text{CH}_3\text{CH}_2\text{CH}_2\text{F}$	-180.23	-180.88	-180.57	-179.80	-180.40	-180.99	-180.29	-178.29	-178.85	-180.03	0.40
$\text{CH}_3\text{CF}_3 + \text{CH}_3\text{CH}_3 = \text{CH}_2\text{F}_2 + \text{CH}_3\text{CHFCH}_3$	-180.22	-180.63	-180.54	-179.64	-180.20	-180.92	-180.35	-178.35	-179.47	-180.03	0.40
$\text{CH}_3\text{CF}_3 + \text{CH}_3\text{CH}_3 = \text{CH}_3\text{CHF}_2 + \text{CH}_3\text{CH}_2\text{F}$	-180.47	-180.28	-180.42	-179.40	-180.73	-181.28	-180.62	-177.74	-179.68	-180.07	0.57
$\text{CH}_3\text{CF}_3 + \text{CH}_3\text{CH}_3 = \text{CHF}_3 + \text{CH}_3\text{CH}_2\text{CH}_3$	-180.27	-180.89	-180.69	-180.26	-179.62	-179.75	-179.52	-180.22	-178.84	-180.01	0.53
$\text{CH}_3\text{CF}_3 + \text{CH}_3\text{CH}_2\text{CH}_3 = \text{CH}_3\text{CH}_2\text{CHF}_2 + \text{CH}_3\text{CH}_2\text{CH}_2\text{F}$	-180.15	-180.12	-180.01	-179.39	-180.71	-181.10	-180.47	-177.65	-179.55	-179.91	0.55
$\text{CH}_3\text{CF}_3 + \text{CH}_3\text{CH}_2\text{CH}_3 = \text{CH}_3\text{CHF}_2 + \text{CH}_3\text{CHFCH}_3$	-180.13	-179.87	-179.98	-179.23	-180.51	-181.03	-180.53	-177.71	-180.16	-179.91	0.58
$\text{CH}_3\text{CF}_3 + \text{CH}_3\text{CH}_2\text{CH}_3 = \text{CH}_3\text{CF}_2\text{CH}_3 + \text{CH}_3\text{CH}_2\text{CH}_2\text{F}$	-180.32	-180.13	-180.16	-179.54	-179.83	-181.28		-177.82	-179.61	-179.84	0.59
$\text{CH}_3\text{CF}_3 + \text{CH}_3\text{CH}_2\text{CH}_2\text{CH}_3 = \text{CH}_3\text{CF}_2\text{CH}_3 + \text{CH}_3\text{CH}_2\text{F}$	-179.99	-179.30	-179.84	-179.21	-180.51	-181.07		-178.00	-180.78	-179.84	0.71
$\text{CH}_3\text{CF}_3 + \text{CH}_3\text{CH}_2\text{CH}_2\text{CH}_3 = \text{CHF}_3 + \text{CH}_3\text{CH}_2\text{CH}_2\text{CH}_3$	-180.17	-180.72	-180.22	-180.46	-179.55	-179.66		-180.28	-178.73	-179.97	0.45
$\text{CH}_3\text{CF}_3 + \text{CH}_3\text{CH}_2\text{CH}_2\text{CH}_3 = \text{CH}_3\text{CH}_2\text{CHF}_2 + \text{CH}_3\text{CH}_2\text{CH}_2\text{F}$	-180.10	-180.14	-180.23	-179.34	-179.88	-181.18		-177.68	-179.58	-179.77	0.60
$\text{CH}_3\text{CF}_3 + \text{CH}_3\text{CH}_2\text{CH}_2\text{CH}_3 = \text{CH}_3\text{CH}_2\text{CHF}_2 + \text{CH}_3\text{CHFCH}_3$	-180.08	-179.89	-180.20	-179.18	-179.68	-181.11		-177.74	-180.20	-179.76	0.64
$\text{CH}_3\text{CF}_3 + \text{CH}_3\text{CH}_2\text{CH}_2\text{CH}_3 = \text{CH}_3\text{CF}_2\text{CH}_3 + \text{CH}_3\text{CH}_2\text{CH}_2\text{F}$	-179.77	-179.31	-179.90	-179.00	-180.56	-180.97		-177.86	-180.75	-179.77	0.74
$\text{CH}_3\text{CF}_3 + \text{CH}_3\text{CH}_2\text{CH}_2\text{CH}_3 = \text{CH}_3\text{CF}_2\text{CH}_3 + \text{CH}_3\text{CHFCH}_3$	-179.75	-179.06	-179.87	-178.84	-180.36	-180.90		-177.92	-181.37	-179.76	0.77
$\text{CH}_3\text{CF}_3 + \text{CH}_3\text{CH}_2\text{F} = \text{CH}_3\text{CHF}_2 + \text{CH}_3\text{CHF}_2$	-180.06	-180.31	-179.90	-179.56	-180.28	-180.43	-180.20	-178.73	-179.58	-179.89	0.30
$\text{CH}_3\text{CF}_3 + \text{CH}_3\text{OH} = \text{CHF}_3 + \text{CH}_3\text{CH}_2\text{OH}$	-180.37	-180.76	-180.34	-180.14	-179.84	-179.85	-179.64	-179.77	-178.93	-179.96	0.39
Average^d	-180.17	-180.21	-180.20	-179.54	-180.18	-180.74	-180.13	-178.32	-179.47	-180.51^f	
STD^e	0.14	0.49	0.23	0.45	0.38	0.53	0.35	1.01	1.06		0.51 ^g

^a Heat of formation of target molecule, unit in kcal mol⁻¹. ^b Average of heat of formation of target molecule for each work reaction over seven calculation methods(CBS-QB3, M06, M06-2X, ω B97X, G4, CBS-APNO,W1U). ^c Standard deviation of heat of formation of target molecule for each work reaction under seven calculation levels(CBS-QB3, M06, M06-2X, ω B97X, G4, CBS-APNO,W1U). ^d Average of heat of formation of target molecule of all set of work reactions under one calculation level. ^e Standard deviation of heat of formation of target molecule of all set of work reactions under one calculation level. ^f Heat of formation of target molecule calculated from the set of work reactions and seven selected calculation levels (CBS-QB3, M06, M06-2X, ω B97X, G4, CBS-APNO,W1U). ^g Standard deviation of target molecule calculated from all set of work reaction over the seven selected calculation levels(CBS-QB3, M06, M06-2X, ω B97X, G4, CBS-APNO,W1U).

Table E.12 Isodesmic reactions, heat of formations, and deviations for 1,1,1-trifluoropropane

Isodesmic reactions	$\Delta H_{f,298}^a$									Average ^b	STD ^c
	CBS-QB3	M06	M06-2X	ω B97X	G4	CBS-APNO	WI U	B3LYP	G4(MP2)-6X		
$\text{CH}_3\text{CH}_2\text{CF}_3 + \text{CH}_4 = \text{CH}_2\text{F}_2 + \text{CH}_3\text{CH}_2\text{CH}_2\text{F}$	-185.41	-185.67	-185.17	-184.21	-185.52	-185.87	-182.02	-182.81	-184.58	0.59	
$\text{CH}_3\text{CH}_2\text{CF}_3 + \text{CH}_4 = \text{CH}_2\text{F}_2 + \text{CH}_3\text{CHFCH}_3$	-185.39	-185.42	-185.14	-184.05	-185.32	-185.81	-182.07	-183.42	-184.58	0.60	
$\text{CH}_3\text{CH}_2\text{CF}_3 + \text{CH}_4 = \text{CH}_2\text{CHF}_2 + \text{CH}_3\text{CH}_2\text{F}$	-185.64	-185.07	-185.02	-183.81	-185.86	-186.16	-181.47	-183.64	-184.58	0.84	
$\text{CH}_3\text{CH}_2\text{CF}_3 + \text{CH}_4 = \text{CH}_3\text{CH}_2\text{CHF}_2 + \text{CH}_3\text{F}$	-185.33	-185.30	-185.07	-184.31	-184.66	-185.99	-182.37	-183.63	-184.58	0.58	
$\text{CH}_3\text{CH}_2\text{CF}_3 + \text{CH}_4 = \text{CH}_3\text{CF}_2\text{CH}_3 + \text{CH}_3\text{F}$	-184.99	-184.47	-184.75	-183.98	-185.34	-185.78	-182.55	-184.80	-184.58	0.64	
$\text{CH}_3\text{CH}_2\text{CF}_3 + \text{CH}_4 = \text{CHF}_3 + \text{CH}_3\text{CH}_2\text{CH}_3$	-185.44	-185.68	-185.29	-184.67	-184.74	-184.63	-183.95	-182.79	-184.65	0.45	
$\text{CH}_3\text{CH}_2\text{CF}_3 + \text{CH}_3\text{CH}_3 = \text{CH}_3\text{CHF}_2 + \text{CH}_3\text{CH}_2\text{CH}_2\text{F}$	-185.38	-185.27	-185.17	-184.15	-185.80	-186.06	-182.42	-184.60	-184.86	0.66	
$\text{CH}_3\text{CH}_2\text{CF}_3 + \text{CH}_3\text{CH}_3 = \text{CH}_3\text{CHF}_2 + \text{CH}_3\text{CHFCH}_3$	-185.36	-185.02	-185.15	-183.99	-185.60	-185.99	-182.48	-185.21	-184.85	0.68	
$\text{CH}_3\text{CH}_2\text{CF}_3 + \text{CH}_3\text{CH}_3 = \text{CH}_3\text{CH}_2\text{CHF}_2 + \text{CH}_3\text{CH}_2\text{F}$	-185.55	-185.27	-185.33	-184.30	-184.93	-186.23	-182.58	-184.66	-184.86	0.64	
$\text{CH}_3\text{CH}_2\text{CF}_3 + \text{CH}_3\text{CH}_3 = \text{CH}_3\text{CF}_2\text{CH}_3 + \text{CH}_3\text{CH}_2\text{F}$	-185.22	-184.45	-185.00	-183.96	-185.61	-186.03	-182.76	-185.83	-184.86	0.75	
$\text{CH}_3\text{CH}_2\text{CF}_3 + \text{CH}_3\text{CH}_3 = \text{CHF}_3 + \text{CH}_3\text{CH}_2\text{CH}_2\text{CH}_3$	-185.40	-185.86	-185.38	-185.21	-184.65	-184.62	-185.04	-183.78	-184.99	0.48	
$\text{CH}_3\text{CH}_2\text{CF}_3 + \text{CH}_3\text{CH}_3 = \text{CH}_3\text{CF}_3 + \text{CH}_3\text{CH}_2\text{CH}_3$	-185.10	-185.02	-185.03	-184.63	-184.97	-184.83	-184.64	-184.92	-184.89	0.17	
$\text{CH}_3\text{CH}_2\text{CF}_3 + \text{CH}_3\text{CH}_2\text{CH}_3 = \text{CH}_3\text{CH}_2\text{CHF}_2 + \text{CH}_3\text{CH}_2\text{CH}_2\text{F}$	-185.23	-185.12	-184.92	-184.29	-184.91	-186.05	-182.50	-184.53	-184.69	0.57	
$\text{CH}_3\text{CH}_2\text{CF}_3 + \text{CH}_3\text{CH}_2\text{CH}_3 = \text{CH}_3\text{CH}_2\text{CHF}_2 + \text{CH}_3\text{CHFCH}_3$	-185.22	-184.87	-184.89	-184.13	-184.71	-185.99	-182.56	-185.14	-184.69	0.62	
$\text{CH}_3\text{CH}_2\text{CF}_3 + \text{CH}_3\text{CH}_2\text{CH}_3 = \text{CH}_3\text{CF}_2\text{CH}_3 + \text{CH}_3\text{CH}_2\text{CH}_2\text{F}$	-184.90	-184.29	-184.59	-183.95	-185.58	-185.84	-182.68	-185.69	-184.69	0.74	
$\text{CH}_3\text{CH}_2\text{CF}_3 + \text{CH}_3\text{CH}_2\text{CH}_3 = \text{CH}_3\text{CF}_2\text{CH}_3 + \text{CH}_3\text{CHFCH}_3$	-184.88	-184.04	-184.56	-183.79	-185.38	-185.78	-182.74	-186.31	-184.69	0.77	
$\text{CH}_3\text{CH}_2\text{CF}_3 + \text{CH}_3\text{CH}_2\text{CH}_3 = \text{CH}_3\text{CF}_3 + \text{CH}_3\text{CH}_2\text{CH}_2\text{CH}_3$	-185.01	-184.85	-184.56	-184.82	-184.90	-184.75	-184.69	-184.82	-184.80	0.15	
$\text{CH}_3\text{CH}_2\text{CF}_3 + \text{CH}_3\text{F} = \text{CH}_3\text{CHF}_2 + \text{CH}_3\text{CHF}_2$	-185.46	-185.07	-184.75	-183.95	-185.67	-185.56	-182.68	-184.57	-184.71	0.65	
$\text{CH}_3\text{CH}_2\text{CF}_3 + \text{CH}_3\text{CH}_2\text{CH}_2\text{F} = \text{CH}_3\text{CH}_2\text{CHF}_2 + \text{CH}_3\text{CH}_2\text{CHF}_2$	-185.32	-185.31	-184.95	-184.61	-183.60	-185.56	-183.74	-184.62	-184.71	0.72	
$\text{CH}_3\text{CH}_2\text{CF}_3 + \text{CH}_3\text{CHFCH}_3 = \text{CH}_3\text{CH}_2\text{CHF}_2 + \text{CH}_3\text{CH}_2\text{CHF}_2$	-185.34	-185.56	-184.98	-184.77	-183.80	-185.63	-183.68	-184.01	-184.72	0.68	
$\text{CH}_3\text{CH}_2\text{CF}_3 + \text{CH}_3\text{CH}_2\text{CH}_2\text{F} = \text{CH}_3\text{CF}_2\text{CH}_3 + \text{CH}_3\text{CF}_2\text{CH}_3$	-184.66	-183.66	-184.30	-183.94	-184.95	-185.15	-184.10	-186.96	-184.71	0.58	
$\text{CH}_3\text{CH}_2\text{CF}_3 + \text{CH}_3\text{CHFCH}_3 = \text{CH}_3\text{CF}_2\text{CH}_3 + \text{CH}_3\text{CF}_2\text{CH}_3$	-184.68	-183.91	-184.3	-184.10	-185.15	-185.21	-184.05	-186.34	-184.72	0.54	
$\text{CH}_3\text{CH}_2\text{CF}_3 + \text{CH}_3\text{OH} = \text{CH}_3\text{CF}_3 + \text{CH}_3\text{CH}_2\text{OH}$	-185.21	-184.89	-184.68	-184.51	-185.19	-184.94	-184.18	-185.02	-184.83	0.28	
Average^d	-185.22	-184.96	-184.91	-184.27	-185.08	-185.59	-183.13	-184.70	-185.48^f		
STD^e	0.13	0.45	0.19	0.45	0.56	0.44	1.15	1.26		0.56^g	

^a Heat of formation of target molecule, unit in kcal mol⁻¹. ^b Average of heat of formation of target molecule for each work reaction over six calculation methods(CBS-QB3, M06, M06-2X, ω B97X, G4, CBS-APNO). ^c Standard deviation of heat of formation of target molecule for each work reaction under six calculation levels(CBS-QB3, M06, M06-2X, ω B97X, G4, CBS-APNO). ^d Average of heat of formation of target molecule of all set of work reactions under one calculation level. ^e Standard deviation of heat of formation of target molecule of all set of work reactions under one calculation level. ^f Heat of formation of target molecule calculated from the set of work reactions and six selected calculation levels (CBS-QB3, M06, M06-2X, ω B97X, G4, CBS-APNO). ^g Standard deviation of target molecule calculated from all set of work reaction over the six selected calculation levels(CBS-QB3, M06, M06-2X, ω B97X, G4, CBS-APNO).

Table E.13 Isodesmic reactions, heat of formations, and deviations for tetrafluoromethane

Isodesmic reactions	$\Delta H_{f,298}^a$									Average ^b	STD ^c
	CBS-QB3	M06	M06-2X	ω B97X	G4	CBS-APNO	W1U	B3LYP	G4(MP2)-6X		
$CF_4 + CH_4 = CH_3F + CHF_3$	-222.50	-222.39	-222.35	-221.33	223.06	-223.85	-222.96	-219.22	-220.91	-222.06	0.78
$CF_4 + CH_4 = CH_2F_2 + CH_2F_2$	-222.64	-222.94	-222.36	-221.09	-223.39	-224.48	-223.37	-218.18	-219.20	-222.07	1.05
$CF_4 + CH_3CH_3 = CH_3F + CH_2CF_3$	-222.16	-221.73	-222.10	-221.30	-223.28	-224.05	-223.55	-219.90	-223.04	-222.35	1.03
$CF_4 + CH_3CH_3 = CH_2F_2 + CH_2CHF_2$	-222.61	-222.54	-222.36	-221.03	-223.67	-224.66	-223.79	-218.58	-221.99	-222.36	1.19
$CF_4 + CH_3CH_3 = CHF_3 + CH_2CH_2F$	-222.73	-222.36	-222.61	-221.32	-223.33	-224.09	-223.30	-219.43	-221.94	-222.35	0.88
$CF_4 + CH_3CH_2CH_3 = CH_3F + CH_2CH_2CF_3$	-221.79	-221.44	-221.79	-221.40	-223.05	-223.95		-220.00	-222.85	-222.03	1.03
$CF_4 + CH_3CH_2CH_3 = CH_2CH_2F + CH_2CF_3$	-222.33	-221.35	-221.79	-220.93	-223.58	-224.22	-223.65	-219.08	-222.98	-222.21	1.27
$CF_4 + CH_3CH_2CH_3 = CH_2CH_2CH_2F + CHF_3$	-222.41	-222.21	-222.20	-221.31	-223.30	-223.91	-223.15	-219.35	-221.81	-222.18	0.87
$CF_4 + CH_3CH_2CH_3 = CH_2CH_2CH_2F + CHF_3$	-222.39	-221.96	-222.17	-221.15	-223.10	-223.85	-223.20	-219.41	-222.42	-222.18	0.90
$CF_4 + CH_3CH_2CH_3 = CH_2CHFCH_3 + CHF_3$	-222.46	-222.39	-222.11	-221.17	-222.77	-224.66		-218.66	-221.92	-222.02	1.15
$CF_4 + CH_3CH_2CH_3 = CH_2F_2 + CH_2CH_2CHF_2$	-222.13	-221.56	-221.78	-220.83	-223.45	-224.45		-218.84	-223.09	-222.02	1.33
$CF_4 + CH_3CH_2CH_3 = CH_2F_2 + CH_2CF_2CH_3$	-222.52	-221.79	-221.81	-220.62	-223.98	-224.77	-223.98	-217.94	-222.69	-222.23	1.50
$CF_4 + CH_3CH_2CH_3 = CH_2CHF_2 + CH_2CHF_2$	-222.06	-221.23	-221.95	-220.84	-223.41	-224.20		-219.12	-222.89	-221.96	1.29
$CF_4 + CH_3CH_2CH_2CH_3 = CH_2CH_2F + CH_2CH_2CF_3$	-222.11	-221.36	-221.85	-220.73	-223.63	-224.12		-218.95	-222.95	-221.96	1.32
$CF_4 + CH_3CH_2CH_2CH_3 = CH_2CH_2CH_2F + CH_2CF_3$	-222.09	-221.11	-221.82	-220.56	-223.43	-224.06		-219.00	-223.56	-221.95	1.34
$CF_4 + CH_3CH_2CH_2CH_3 = CH_2CHFCH_3 + CH_2CF_3$	-222.47	-221.80	-222.02	-220.57	-223.15	-224.85		-217.97	-222.72	-221.94	1.44
$CF_4 + CH_3CH_2CH_2CH_3 = CH_2CHF_2 + CH_2CH_2CHF_2$	-222.47	-221.80	-222.02	-220.57	-223.15	-224.85		-217.97	-222.72	-221.94	1.44
$CF_4 + CH_3CH_2CH_2CH_3 = CH_2CHF_2 + CH_2CH_2CHF_2$	-222.14	-220.98	-221.70	-220.23	-223.83	-224.65		-218.15	-223.89	-221.94	1.69
$CF_4 + CH_3CH_2CH_2CH_3 = CH_2CHF_2 + CH_2CH_2CHF_2$	-222.58	-222.77	-222.33	-221.52	-222.85	-223.30	-222.79	-220.24	-221.08	-222.16	0.56
$CF_4 + CH_3F = CH_2F_2 + CHF_3$	-222.44	-222.22	-222.32	-221.77	-222.53	-222.67	-222.38	-221.28	-221.79	-222.16	0.29
$CF_4 + CH_2F_2 = CHF_3 + CHF_3$	-222.32	-222.39	-222.08	-221.48	-222.87	-223.24	-222.88	-220.43	-221.84	-222.17	0.59
$CF_4 + CH_3CH_2F = CH_2CHF_2 + CHF_3$	-222.01	-222.13	-221.82	-221.50	-222.81	-223.26	-223.04	-220.71	-222.18	-222.16	0.67
$CF_4 + CH_3CH_2F = CH_2F_2 + CH_2CF_3$	-221.96	-222.00	-221.92	-221.61	-222.60	-223.34		-220.89	-222.12	-222.06	0.63
$CF_4 + CH_3CH_2CH_2F = CH_2F_2 + CH_2CH_2CF_3$	-222.25	-221.53	-221.67	-221.10	-223.15	-223.55	-223.38	-220.16	-223.01	-222.20	0.99
$CF_4 + CH_3CH_2CH_2F = CH_2CHF_2 + CH_2CF_3$	-222.50	-222.40	-222.23	-221.63	-222.00	-223.42		-220.59	-221.90	-222.08	0.60
$CF_4 + CH_3CH_2CH_2F = CH_2CH_2CHF_2 + CHF_3$	-222.16	-221.57	-221.91	-221.29	-222.67	-223.21		-220.77	-223.07	-222.08	0.71
$CF_4 + CH_3CH_2CH_2F = CH_2CF_2CH_3 + CHF_3$	-221.98	-222.25	-221.95	-221.77	-222.80	-223.40		-220.83	-221.51	-222.06	0.62
$CF_4 + CH_2CHFCH_3 = CH_2F_2 + CH_2CH_2CF_3$	-222.26	-221.79	-221.70	-221.26	-223.35	-223.61	-223.32	-220.10	-222.40	-222.20	0.95
$CF_4 + CH_2CHFCH_3 = CH_2CHF_2 + CH_2CF_3$	-222.51	-222.56	-222.26	-221.79	-222.19	-223.48		-220.53	-221.29	-222.09	0.57
$CF_4 + CH_2CHFCH_3 = CH_2CH_2CHF_2 + CHF_3$	-222.18	-221.82	-221.94	-221.46	-222.87	-223.28		-220.72	-222.46	-222.09	0.69
$CF_4 + CH_2CHFCH_3 = CH_2CF_2CH_3 + CHF_3$											
Average ^d	-222.30	-221.95	-222.03	-221.19	-223.11	-223.88	-223.25	-219.62	-222.29	-223.15^f	
STD ^e	0.17	0.45	0.22	0.48	0.42	0.47	0.35	1.12	0.92		0.94 ^g

^a Heat of formation of target molecule, unit in kcal mol⁻¹. ^b Average of heat of formation of target molecule for each work reaction over seven calculation methods(CBS-QB3, M06, M06-2X, ω B97X, G4, CBS-APNO,W1U). ^c Standard deviation of heat of formation of target molecule for each work reaction under seven calculation levels(CBS-QB3, M06, M06-2X, ω B97X, G4, CBS-APNO,W1U). ^d Average of heat of formation of target molecule of all set of work reactions under one calculation level. ^e Standard deviation of heat of formation of target molecule of all set of work reactions under one calculation level. ^f Heat of formation of target molecule calculated from the set of work reactions and seven selected calculation levels (CBS-QB3, M06, M06-2X, ω B97X, G4, CBS-APNO,W1U). ^g Standard deviation of target molecule calculated from all set of work reaction over the seven selected calculation levels(CBS-QB3, M06, M06-2X, ω B97X, G4, CBS-APNO,W1U).

Table E.14 Isodesmic reactions, heat of formations, and deviations for t-butyl fluoride

Isodesmic reactions	$\Delta H_{f,298}^a$			Average ^b	STD ^c
	CBS-QB3	CBS-APNO	G4		
$(\text{CH}_3)_3\text{CF} + \text{CH}_3\text{CH}_2\text{CH}_3 = (\text{CH}_3)_3\text{CH} + \text{CH}_3\text{CHFCH}_3$	-85.81	-85.65	-85.65	-85.70	0.09
$(\text{CH}_3)_3\text{CF} + \text{CH}_3\text{CH}_2\text{CH}_2\text{CH}_3 = (\text{CH}_3)_3\text{CH} + \text{CH}_3\text{CHFCH}_2\text{CH}_3$	-85.73	-85.59	-85.67	-85.66	0.07
$(\text{CH}_3)_3\text{CF} + \text{CH}_3\text{CH}_2\text{CH}_2\text{CH}_3 = \text{CH}_3\text{CH}(\text{CH}_3)\text{CH}_2\text{CH}_3 + \text{CH}_3\text{CHFCH}_3$	-85.97	-85.72	-85.88	-85.86	0.13
$(\text{CH}_3)_3\text{CF} + \text{CH}_3\text{CH}_2\text{CH}_2\text{CH}_2\text{CH}_3 = \text{CH}_3\text{CH}(\text{CH}_3)\text{CH}_2\text{CH}_3 + \text{CH}_3\text{CHFCH}_2\text{CH}_3$	-85.80	-85.73	-85.80	-85.78	0.04
Average^d	-85.83	-85.67	-85.75	-85.75	
STD^e	0.10	0.11	0.07		0.11

^aHeat of formation of target molecule, unit in kcal mol⁻¹. ^bAverage of heat of formation of target molecule for each work reaction over three calculation methods(CBS-QB3, G4, CBS-APNO). ^cStandard deviation of heat of formation of target molecule for each work reaction under three calculation levels(CBS-QB3, G4, CBS-APNO). ^dAverage of heat of formation of target molecule of all set of work reactions under one calculation level. ^eStandard deviation of heat of formation of target molecule of all set of work reactions under one calculation level.

Table E.15 All the isodesmic reactions used for enthalpy of formation of methanol in this study

Isodesmic reactions	enthalpies of
$\text{CH}_3\text{OH} + \text{CH}_3\text{CH}_2\text{CH}_3 = \text{CH}_3\text{CH}_2\text{OH} + \text{CH}_3\text{CH}_3$	-48.08
$\text{CH}_3\text{OH} + \text{CH}_3(\text{CH}_2)_2\text{CH}_3 = \text{CH}_3\text{CH}_2\text{OH} + \text{CH}_3\text{CH}_2\text{CH}_3$	-48.15
$\text{CH}_3\text{OH} + \text{CH}_3(\text{CH}_2)_3\text{CH}_3 = \text{CH}_3\text{CH}_2\text{OH} + \text{CH}_3(\text{CH}_2)_2\text{CH}_3$	-47.91
$\text{CH}_3\text{OH} + \text{CH}_3\text{CH}_2\text{CH}_3 = \text{CH}_3\text{CH}_2\text{CH}_2\text{OH} + \text{CH}_4$	-48.43
$\text{CH}_3\text{OH} + \text{CH}_3(\text{CH}_2)_2\text{CH}_3 = \text{CH}_3\text{CH}_2\text{CH}_2\text{OH} + \text{CH}_3\text{CH}_3$	-48.03
$\text{CH}_3\text{OH} + \text{CH}_3(\text{CH}_2)_3\text{CH}_3 = \text{CH}_3\text{CH}_2\text{CH}_2\text{OH} + \text{CH}_3\text{CH}_2\text{CH}_3$	-47.85
$\text{CH}_3\text{OH} + \text{CH}_3\text{CH}_2\text{CH}_3 = \text{CH}_3\text{CH}(\text{OH})\text{CH}_3 + \text{CH}_4$	-48.62
$\text{CH}_3\text{OH} + \text{CH}_3(\text{CH}_2)_2\text{CH}_3 = \text{CH}_3\text{CH}(\text{OH})\text{CH}_3 + \text{CH}_3\text{CH}_3$	-48.22
$\text{CH}_3\text{OH} + \text{CH}_3(\text{CH}_2)_3\text{CH}_3 = \text{CH}_3\text{CH}(\text{OH})\text{CH}_3 + \text{CH}_3\text{CH}_2\text{CH}_3$	-48.05
Total average	-48.15^b

^a The average of enthalpy of formation obtained under B3LYP, CBS-QB3, CBS-APNO, M06, M06-2X, ω B97X, G4, and G4(MP2)-6X based on the same isodesmic reaction. ^b The total average of enthalpy of formation for methanol.

Table E.16 Work reactions used to determine the computational method uncertainty

Isodesmic reaction	ΔH_{rxn}^a	ΔH_{rxn}^b
$\text{CH}_3\text{CH}_2\text{F} + \text{CH}_4 = \text{CH}_3\text{F} + \text{CH}_3\text{CH}_3$	6.39	6.63
$\text{CH}_3\text{CH}_2\text{F} + \text{CH}_3\text{OH} = \text{CH}_3\text{F} + \text{CH}_3\text{CH}_2\text{OH}$	0.48	0.83
$\text{CH}_3\text{CH}_2\text{F} + \text{CH}_3\text{CH}_3 = \text{CH}_3\text{F} + \text{CH}_3\text{CH}_2\text{CH}_3$	3.62	3.89
$\text{CH}_3\text{CH}_2\text{F} + \text{CH}_3\text{F} = \text{CH}_2\text{F}_2 + \text{CH}_3\text{CH}_3$	-6.56	-6.14
$\text{CH}_3\text{CH}_2\text{F} + \text{CH}_2\text{F}_2 = \text{CHF}_3 + \text{CH}_3\text{CH}_3$	-12.40	-13.25
$\text{CH}_3\text{CH}_2\text{F} + \text{CHF}_3 = \text{CF}_4 + \text{CH}_3\text{CH}_3$	-12.29	-11.05
$\text{CH}_2\text{F}_2 + \text{CH}_4 = \text{CH}_3\text{F} + \text{CH}_3\text{F}$	12.95	12.77
$\text{CH}_2\text{F}_2 + \text{CH}_3\text{CH}_3 = \text{CH}_3\text{F} + \text{CH}_3\text{CH}_2\text{F}$	6.56	6.14
$\text{CHF}_3 + \text{CH}_3\text{CH}_3 = \text{CH}_3\text{CH}_2\text{F} + \text{CH}_2\text{F}_2$	12.40	13.25
$\text{CF}_4 + \text{CH}_4 = \text{CH}_2\text{F}_2 + \text{CH}_2\text{F}_2$	24.52	24.79
$\text{CF}_4 + \text{CH}_3\text{F} = \text{CHF}_3 + \text{CH}_2\text{F}_2$	5.73	4.91
$\text{CH}_3\text{CF}_3 + \text{CH}_4 = \text{CHF}_3 + \text{CH}_3\text{CH}_3$	12.70	11.55

^aTake the heat of formation of each species from Goos's table. ^bTake the heat of formation of each species from this study's suggestion. ^{a,b}Units in kcal mol⁻¹.

Table E.17 Calculated Enthalpies of Formation at 298 K of Three Species in Table A

Work Reaction	Calculation Methods	$\Delta_f H_{298}^\circ$
$y(\text{cco-cco}) + \text{CH}_3\text{CH}_3 = y(\text{cco}) + y(\text{cco})$	CBS-QB3	23.8
	CBS-APNO	23.4
	B3LYP/6-311+G(2d,d,p)	23.9
	B2PLYP/6-311+G(2d,d,p)	23.4
	M06/6-311+G(2d,d,p)	23.9
	M06-2X/6-311+G(2d,d,p)	26.0
	ω B97X/6-311+G(2d,d,p)	24.2
	ω B97XD/6-311+G(2d,d,p)	24.5
	Average	24.1
	Std	0.9
$y(\text{coo-oc}) + y(\text{cco}) = y(\text{coo}) + y(\text{cco-oc})$	CBS-QB3	-51.1
	CBS-APNO	-51.3
	B3LYP/6-311+G(2d,d,p)	-50.9
	M06/6-311+G(2d,d,p)	-51.4
	M06-2X/6-311+G(2d,d,p)	-51.4
	ω B97X/6-311+G(2d,d,p)	-51.9
	ω B97XD/6-311+G(2d,d,p)	-51.8
	Average	-51.4
	Std	0.4
	$y(\text{coo-oc}\bullet) + \text{CH}_3\text{OCH}_3 = y(\text{coo-oc}) + \text{CH}_3\text{OCH}_2\bullet$	CBS-QB3
CBS-APNO		-3.0
B3LYP/6-311+G(2d,d,p)		-2.9
M06/6-311+G(2d,d,p)		-3.3
M06-2X/6-311+G(2d,d,p)		-3.4
ω B97X/6-311+G(2d,d,p)		-2.4
ω B97XD/6-311+G(2d,d,p)		-2.3

	Average	-3.1
	Std	0.4
$y(\text{cjoo}) + y(\text{cco}) = y(\text{cjco}) + y(\text{coo})$	CBS-QB3	48.7
	CBS-APNO	48.3
	B3LYP/6-311+G(2d,d,p)	49.4
	M06/6-311+G(2d,d,p)	49.5
	M06-2X/6-311+G(2d,d,p)	49.7
	ω B97X/6-311+G(2d,d,p)	49.5
	ω B97XD/6-311+G(2d,d,p)	49.4
	Average	49.3
	Std	0.5

APPENDIX F

OPTIMIZED STRUCTURES OF STUDIED MOLECULES

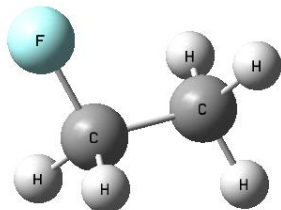


Figure F.1 Optimized geometry for CH₃CH₂F at B3LYP/6-31+G(d,p) level of theory. Chapter 2.

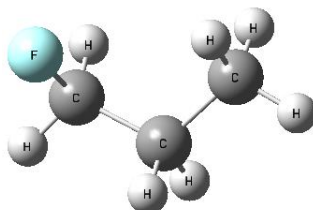


Figure F.2 Optimized geometry for CH₃CH₂CH₂F at B3LYP/6-31+G(d,p) level of theory. Chapter 2.

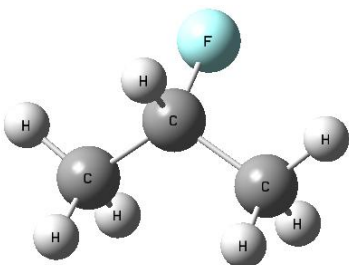


Figure F.3 Optimized geometry for CH₃CHFCH₃ at B3LYP/6-31+G(d,p) level of theory. Chapter 2.

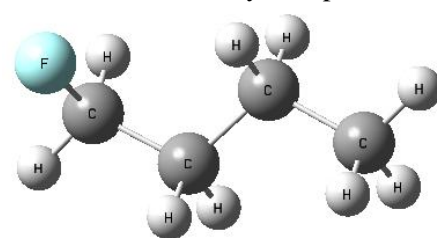


Figure F.4 Optimized geometry for CH₃CH₂CH₂CH₂F at B3LYP/6-31+G(d,p) level of theory.

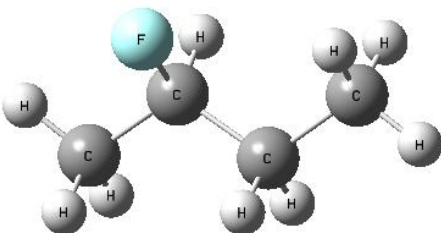


Figure F.5 Optimized geometry for CH₃CHFCH₂CH₃ at B3LYP/6-31+G(d,p) level of theory. Chapter 2.

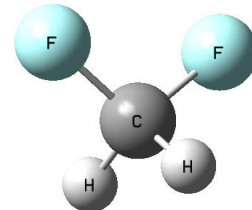


Figure F.6 Optimized geometry for CH₂F₂ at B3LYP/6-31+G(d,p) level of theory. Chapter 2.

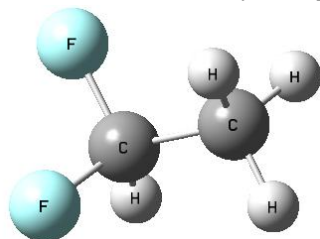


Figure F.7 Optimized geometry for CH₃CHF₂ at B3LYP/6-31+G(d,p) level of theory. Chapter 2.

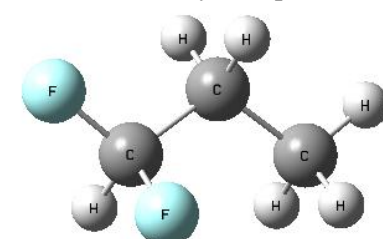


Figure F.8 Optimized geometry for CH₃CH₂CHF₂ at B3LYP/6-31+G(d,p) level of theory. Chapter 2.

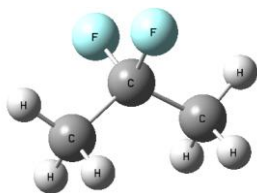


Figure F.9 Optimized geometry for $\text{CH}_3\text{CF}_2\text{CH}_3$ at B3LYP/6-31+G(d,p) level of theory. Chapter 2.

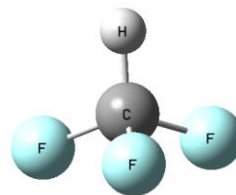


Figure F.10 Optimized geometry for CHF_3 at B3LYP/6-31+G(d,p) level of theory. Chapter 2.

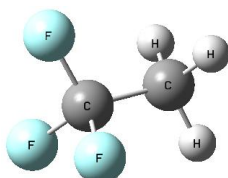


Figure F.11 Optimized geometry for CH_3CF_3 at B3LYP/6-31+G(d,p) level of theory. Chapter 2.

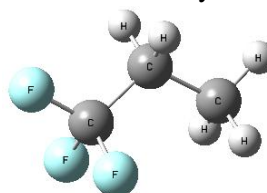


Figure F.12 Optimized geometry for $\text{CH}_3\text{CH}_2\text{CF}_3$ at B3LYP/6-31+G(d,p) level of theory. Chapter 2.

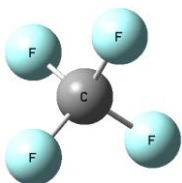


Figure F.13 Optimized geometry for CF_4 at B3LYP/6-31+G(d,p) level of theory. Chapter 2.



Figure F.14 Optimized geometry for $(\text{CH}_3)_3\text{CF}$ at B3LYP/6-31+G(d,p) level of theory. Chapter 2.

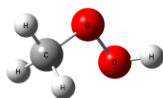


Figure F.15 Optimized geometry for CH_3OOH at B3LYP/6-31+G(d,p) level of theory. Chapter 3.

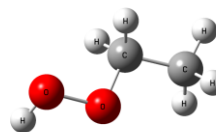


Figure F.16 Optimized geometry for $\text{CH}_3\text{CH}_2\text{OOH}$ at B3LYP/6-31+G(d,p) level of theory. Chapter 3.

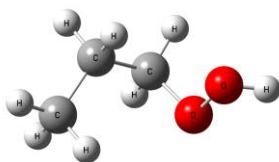


Figure F.17 Optimized geometry for $\text{CH}_3\text{CH}_2\text{CH}_2\text{OOH}$ at B3LYP/6-31+G(d,p) level of theory. Chapter 3.

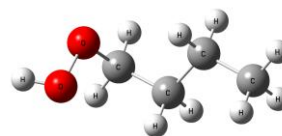


Figure F.18 Optimized geometry for $\text{CH}_3\text{CH}_2\text{CH}_2\text{CH}_2\text{OOH}$ at B3LYP/6-31+G(d,p) level of theory. Chapter 3.

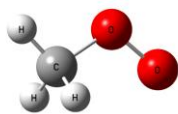


Figure F.19 Optimized geometry for CH_3OOj at B3LYP/6-31+G(d,p) level of theory. Chapter 3.

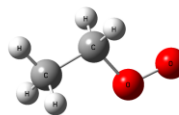


Figure F.20 Optimized geometry for $\text{CH}_3\text{CH}_2\text{OOj}$ at B3LYP/6-31+G(d,p) level of theory. Chapter 3.

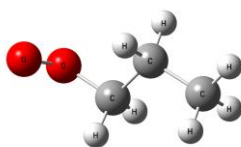


Figure F.21 Optimized geometry for $\text{CH}_3\text{CH}_2\text{CH}_2\text{OOj}$ at B3LYP/6-31+G(d,p) level of theory. Chapter 3.



Figure F.22 Optimized geometry for $\text{CH}_3\text{CH}_2\text{CH}_2\text{CH}_2\text{OOj}$ at B3LYP/6-31+G(d,p) level of theory.

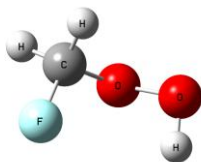


Figure F.23 Optimized geometry for CH_2FOOH at CBS-APNO level of theory. Chapter 4.

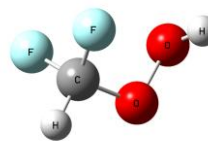


Figure F.24 Optimized geometry for CHF_2OOH at CBS-APNO level of theory. Chapter 4.

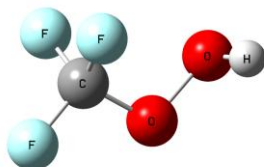


Figure F.25 Optimized geometry for CF_3OOH at CBS-APNO level of theory. Chapter 4.

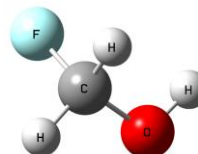


Figure F.26 Optimized geometry for CH_2FOH at CBS-APNO level of theory. Chapter 4.

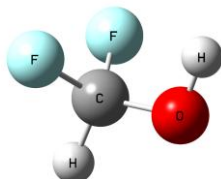


Figure F.27 Optimized geometry for CHF_2OH at CBS-APNO level of theory. Chapter 4.

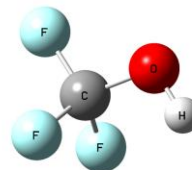


Figure F.28 Optimized geometry for CF_3OH at CBS-APNO level of theory. Chapter 4.

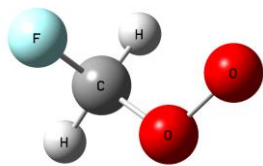


Figure F.29 Optimized geometry for CH_2FOOj at CBS-APNO level of theory. Chapter 4.

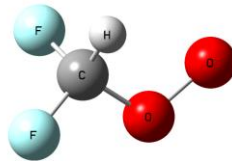


Figure F.30 Optimized geometry for CHF_2OOj at CBS-APNO level of theory. Chapter 4.

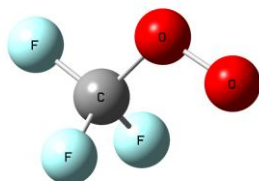


Figure F.31 Optimized geometry for CF_3OOj at CBS-APNO level of theory. Chapter 4.

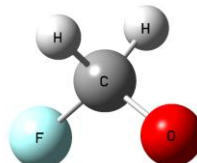


Figure F.32 Optimized geometry for CH_2FOj at CBS-APNO level of theory. Chapter 4.

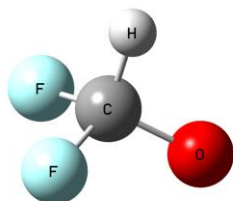


Figure F.33 Optimized geometry for CHF_2Oj at CBS-APNO level of theory. Chapter 4.

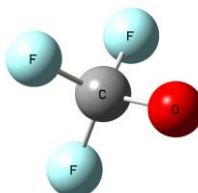


Figure F.34 Optimized geometry for CF_3Oj at CBS-APNO level of theory. Chapter 4.

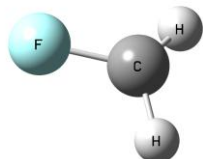


Figure F.35 Optimized geometry for CH_2Fj at CBS-APNO level of theory. Chapter 4.

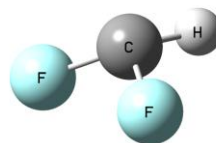


Figure F.36 Optimized geometry for CHF_2j at CBS-APNO level of theory. Chapter 4.

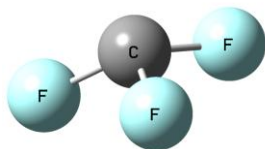


Figure F.37 Optimized geometry for CF_3 at CBS-APNO level of theory. Chapter 4.

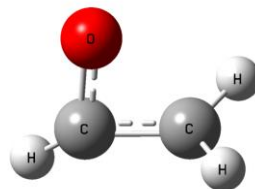


Figure F.38 Optimized geometry for TS1 at B3LYP/6-31+G(d,p) level of theory. Chapter 5.

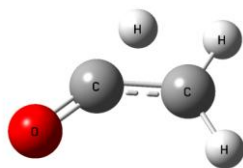


Figure F.39 Optimized geometry for TS2 at B3LYP/6-31+G(d,p) level of theory. Chapter 5.

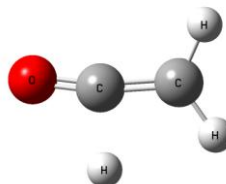


Figure F.40 Optimized geometry for TS3 at B3LYP/6-31+G(d,p) level of theory. Chapter 5.

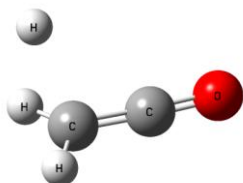


Figure F.41 Optimized geometry for TS4 at B3LYP/6-31+G(d,p) level of theory. Chapter 5.

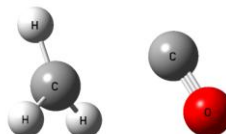


Figure F.42 Optimized geometry for TS52 at B3LYP/6-31+G(d,p) level of theory. Chapter 5.

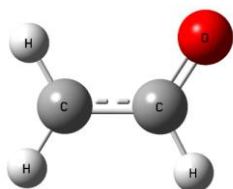


Figure F.43 Optimized geometry for cjcho at B3LYP/6-31+G(d,p) level of theory. Chapter 5.

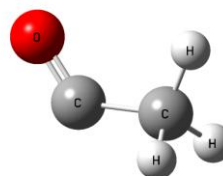


Figure F.44 Optimized geometry for ccj=o at B3LYP/6-31+G(d,p) level of theory. Chapter 5.

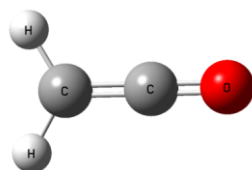


Figure F.45 Optimized geometry for c=c=O at B3LYP/6-31+G(d,p) level of theory. Chapter 5.

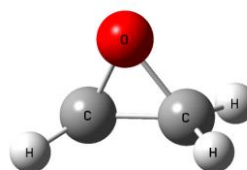


Figure F.46 Optimized geometry for y(cjco) at CBS-QB3 level of theory. Chapter 6.

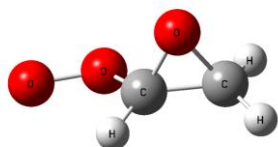


Figure F.47 Optimized geometry for y(cco)-qj at CBS-QB3 level of theory. Chapter 6.

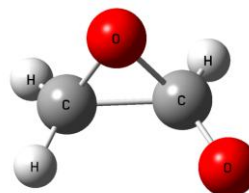


Figure F.48 Optimized geometry for y(cco)-oj at CBS-QB3 level of theory. Chapter 6.

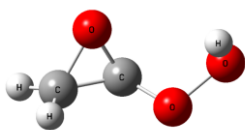


Figure F.49 Optimized geometry for y(ccjo)-q at CBS-QB3 level of theory. Chapter 6.

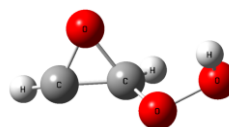


Figure F.50 Optimized geometry for y(cjco)-q at CBS-QB3 level of theory. Chapter 6.

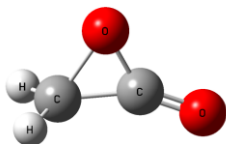


Figure F.51 Optimized geometry for y(cco)-do at CBS-QB3 level of theory. Chapter 6.

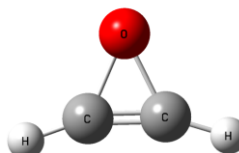


Figure F.52 Optimized geometry for y(cdco) at CBS-QB3 level of theory. Chapter 6.

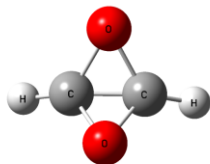


Figure F.53 Optimized geometry for yy(cco-cco) at CBS-QB3 level of theory. Chapter 6.

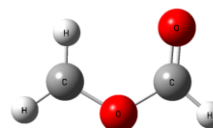


Figure F.54 Optimized geometry for cjocho at CBS-QB3 level of theory. Chapter 6.

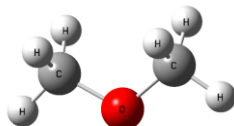


Figure F.55 Optimized geometry for CH₃OCH₃ at CBS-QB3 level of theory. Chapter 6.

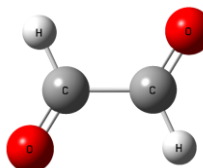


Figure F.56 Optimized geometry for cho-cho at CBS-QB3 level of theory. Chapter 6.

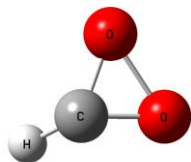


Figure F.57 Optimized geometry for y(cjoo) at CBS-QB3 level of theory. Chapter 6.

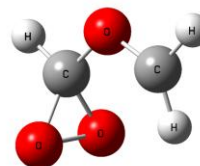


Figure F.58 Optimized geometry for y(coo)-ocj at CBS-QB3 level of theory. Chapter 6.

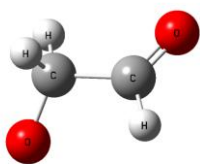


Figure F.59 Optimized geometry for ojc-cho at CBS-QB3 level of theory. Chapter 6.

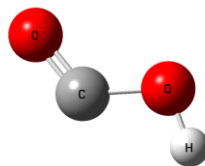


Figure F.60 Optimized geometry for cjdo-oh at CBS-QB3 level of theory. Chapter 6.

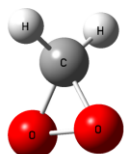


Figure F.61 Optimized geometry for y(coo) at CBS-QB3 level of theory. Chapter 6.

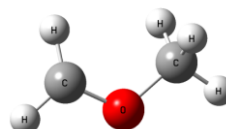


Figure F.62 Optimized geometry for cocj at CBS-QB3 level of theory. Chapter 6.

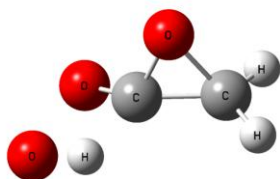


Figure F.63 Optimized geometry for TS1 at CBS-QB3 level of theory. Chapter 6.

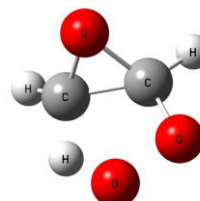


Figure F.64 Optimized geometry for TS2 at CBS-QB3 level of theory. Chapter 6.

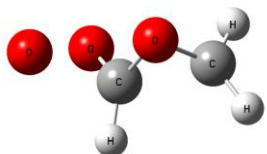


Figure F.65 Optimized geometry for TS3 at CBS-QB3 level of theory. Chapter 6.

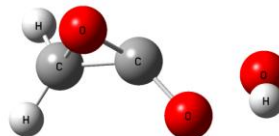


Figure F.66 Optimized geometry for TS4 at CBS-QB3 level of theory. Chapter 6.

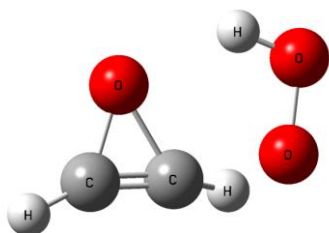


Figure HF.67 Optimized geometry for TS5 at CBS-QB3 level of theory. Chapter 6.

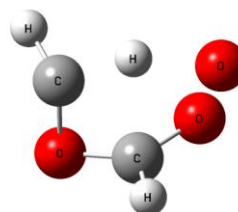


Figure F.68 Optimized geometry for TS6 at CBS-QB3 level of theory. Chapter 6.

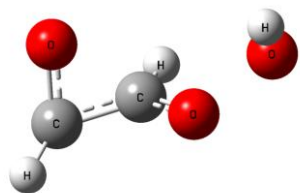


Figure F.69 Optimized geometry for TS7 at CBS-QB3 level of theory. Chapter 6.

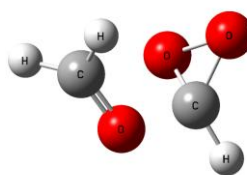


Figure F.70 Optimized geometry for TS8 at CBS-QB3 level of theory. Chapter 6.

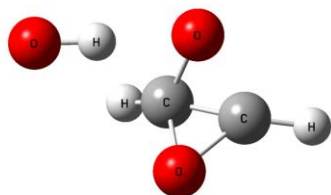


Figure F.71 Optimized geometry for TS9 at CBS-QB3 level of theory. Chapter 6.

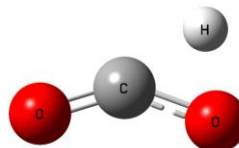


Figure F.72 Optimized geometry for TS10 at CBS-QB3 level of theory. Chapter 6.

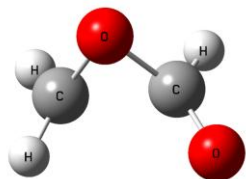


Figure F.73 Optimized geometry for TS11 at CBS-QB3 level of theory. Chapter 6.

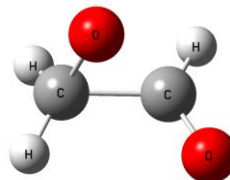


Figure F.74 Optimized geometry for TS12 at CBS-QB3 level of theory. Chapter 6.

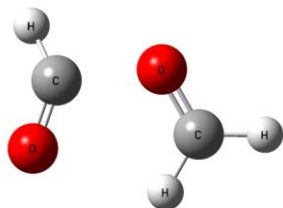


Figure F.75 Optimized geometry for TS13 at CBS-QB3 level of theory. Chapter 6.

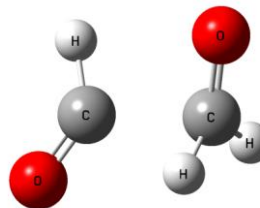


Figure F.76 Optimized geometry for TS14 at CBS-QB3 level of theory. Chapter 6.

APPENDIX G

POTENTIAL ENERGY PROFILES

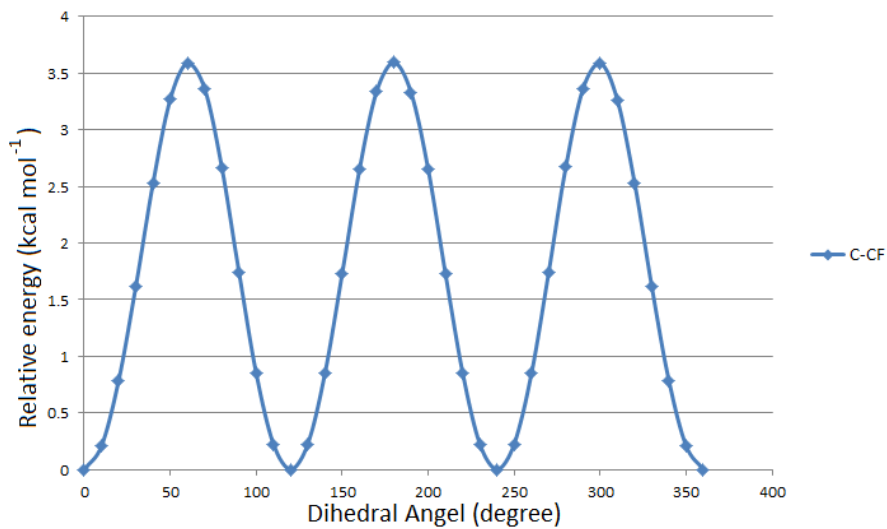


Figure G.1 Potential energy profile of C—C internal rotors for $\text{CH}_3\text{CH}_2\text{F}$ (dot points). The solid lines indicate Fourier series expansion.

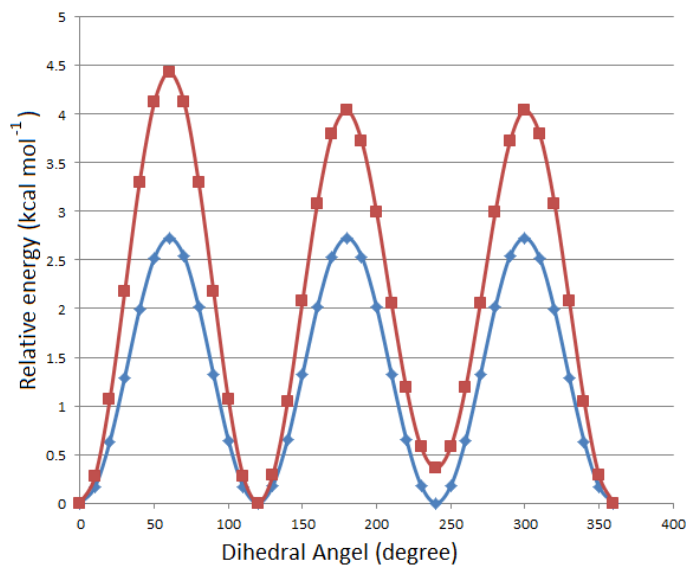


Figure G.2 Potential energy profile of C—C internal rotors for $\text{CH}_3\text{CH}_2\text{CH}_2\text{F}$ (dot points). The solid lines indicate Fourier series expansion.

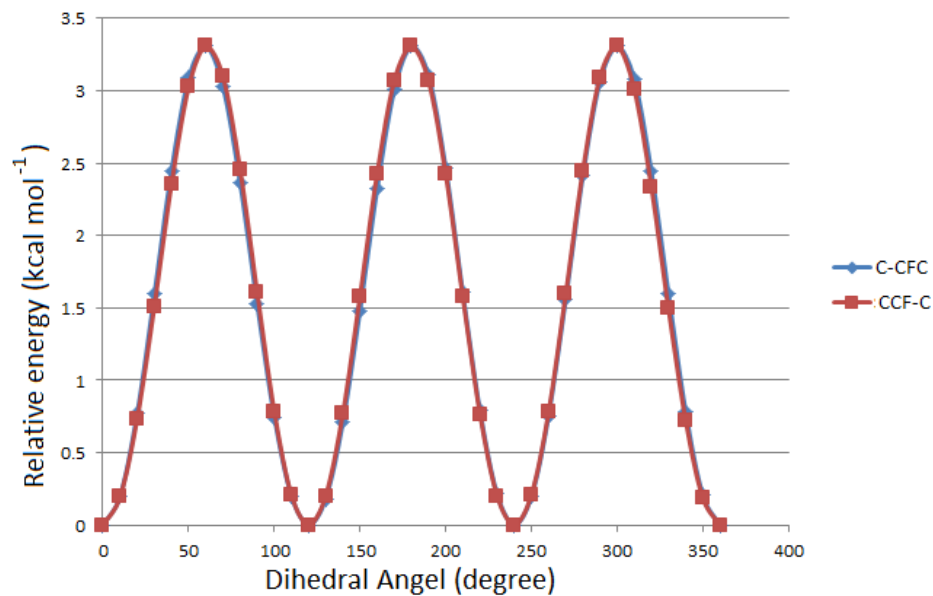


Figure G.3 Potential energy profile of C—C internal rotors for $\text{CH}_3\text{CHFCH}_3$ (dot points). The solid lines indicate Fourier series expansion.

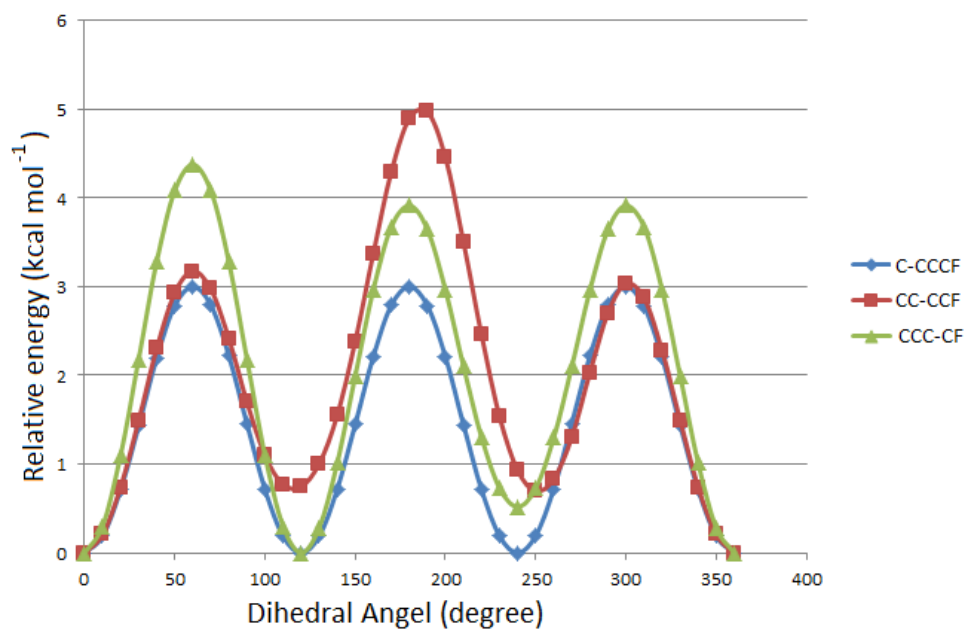


Figure G.4 Potential energy profile of C—C internal rotors for $\text{CH}_3\text{CH}_2\text{CH}_2\text{CH}_2\text{F}$ (dot points). The solid lines indicate Fourier series expansion.

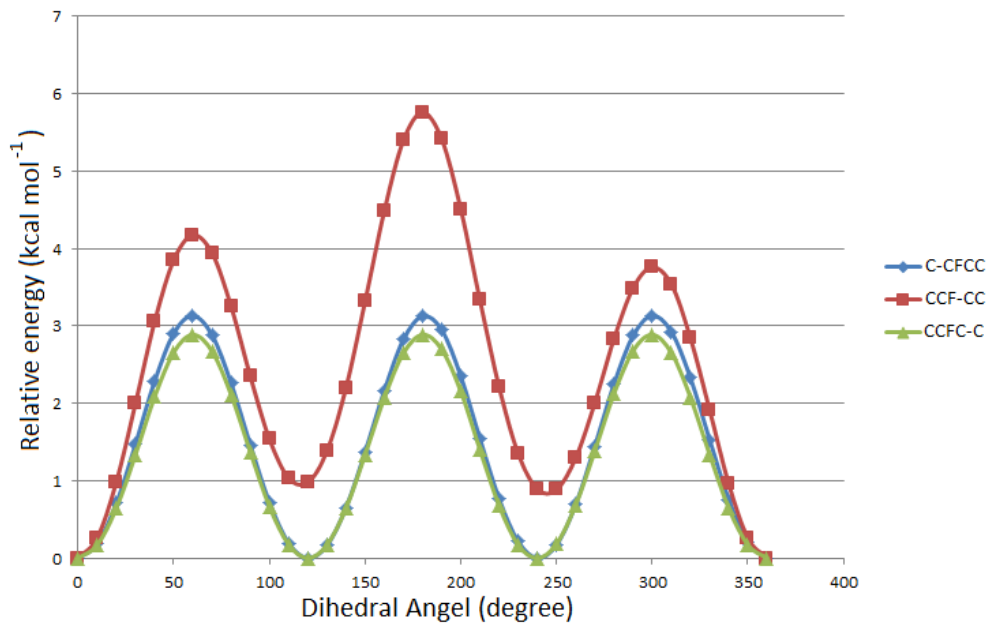


Figure G.5 Potential energy profile of C—C internal rotors for $\text{CH}_3\text{CHFCH}_2\text{CH}_3$ (dot points). The solid lines indicate Fourier series expansion.

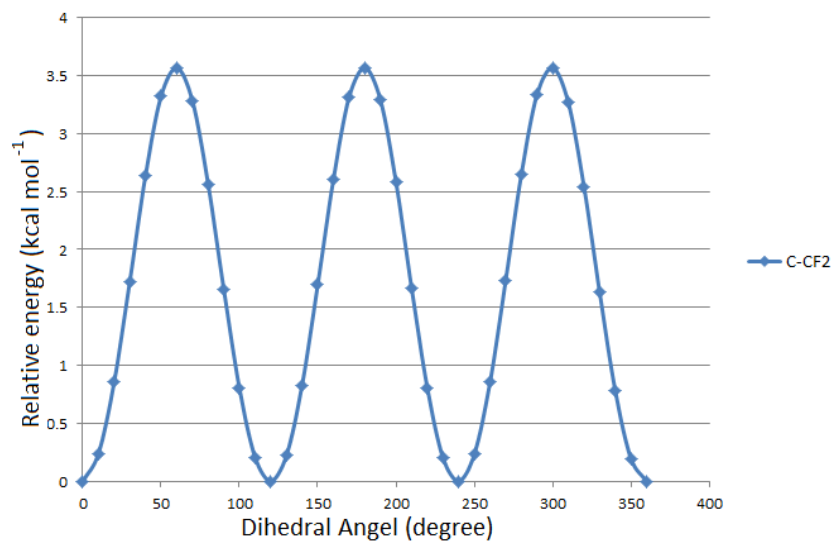


Figure G.6 Potential energy profile of C—C internal rotors for CH_3CHF_2 (dot points). The solid lines indicate Fourier series expansion.

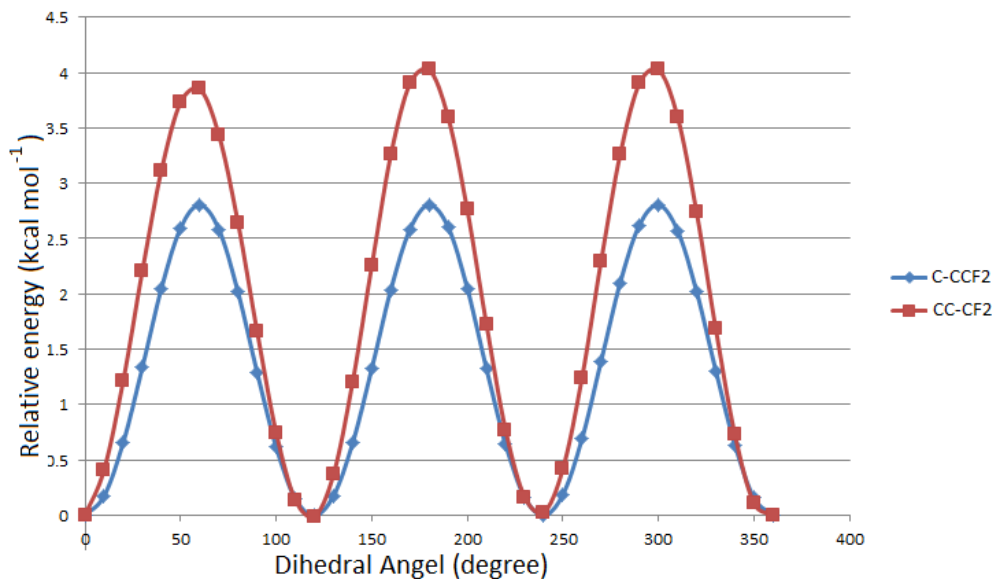


Figure G.7 Potential energy profile of C—C internal rotors for $\text{CH}_3\text{CH}_2\text{CHF}_2$ (dot points). The solid lines indicate Fourier series expansion.

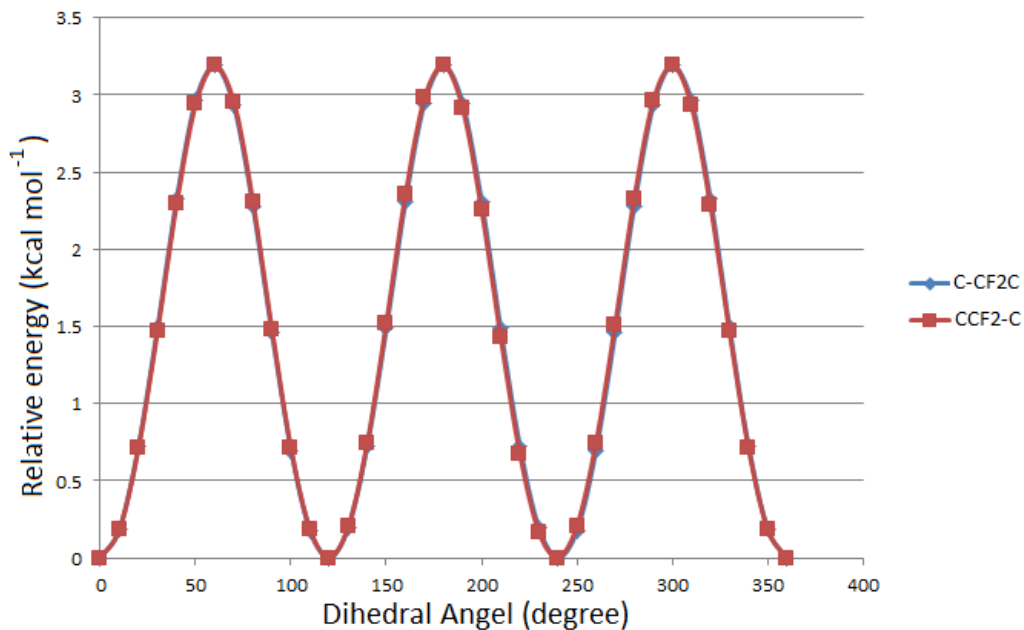


Figure G.8 Potential energy profile of C—C internal rotors for $\text{CH}_3\text{CF}_2\text{CH}_3$ (dot points). The solid lines indicate Fourier series expansion.

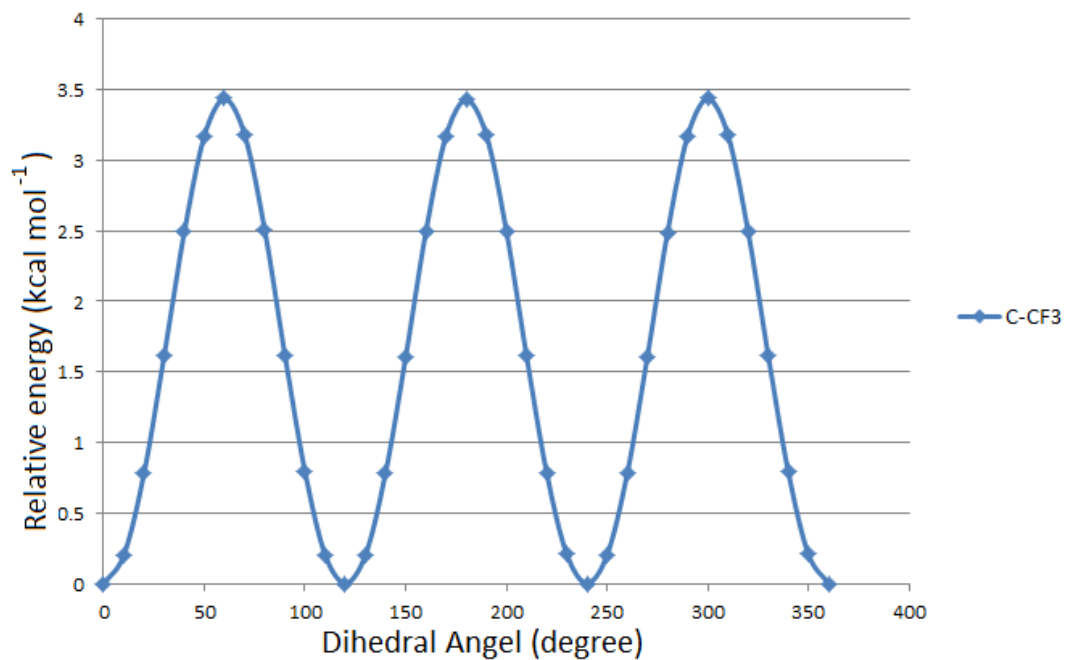


Figure G.9 Potential energy profile of C—C internal rotors for CH_3CF_3 (dot points). The solid lines indicate Fourier series expansion.

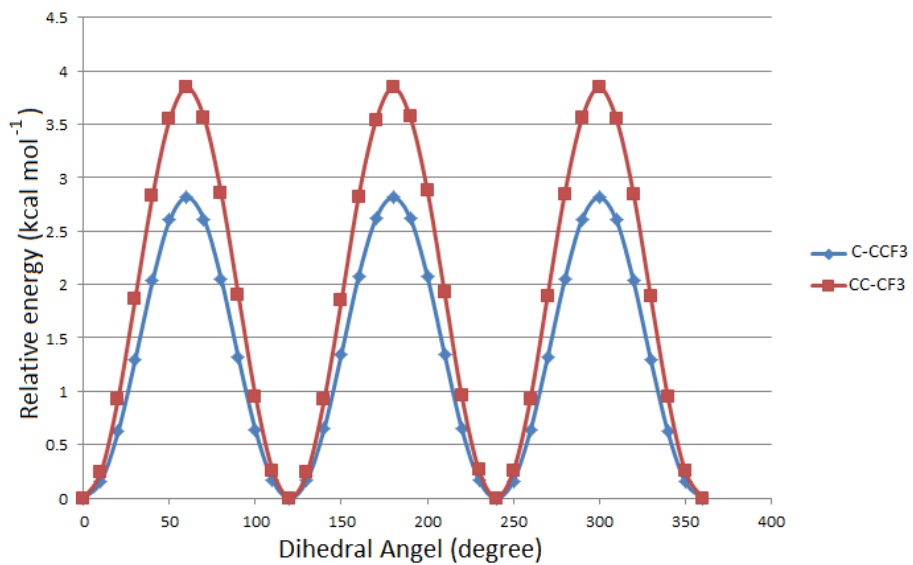


Figure G.10 Potential energy profile of C—C internal rotors for $\text{CH}_3\text{CH}_2\text{CF}_3$ (dot points). The solid lines indicate Fourier series expansion.

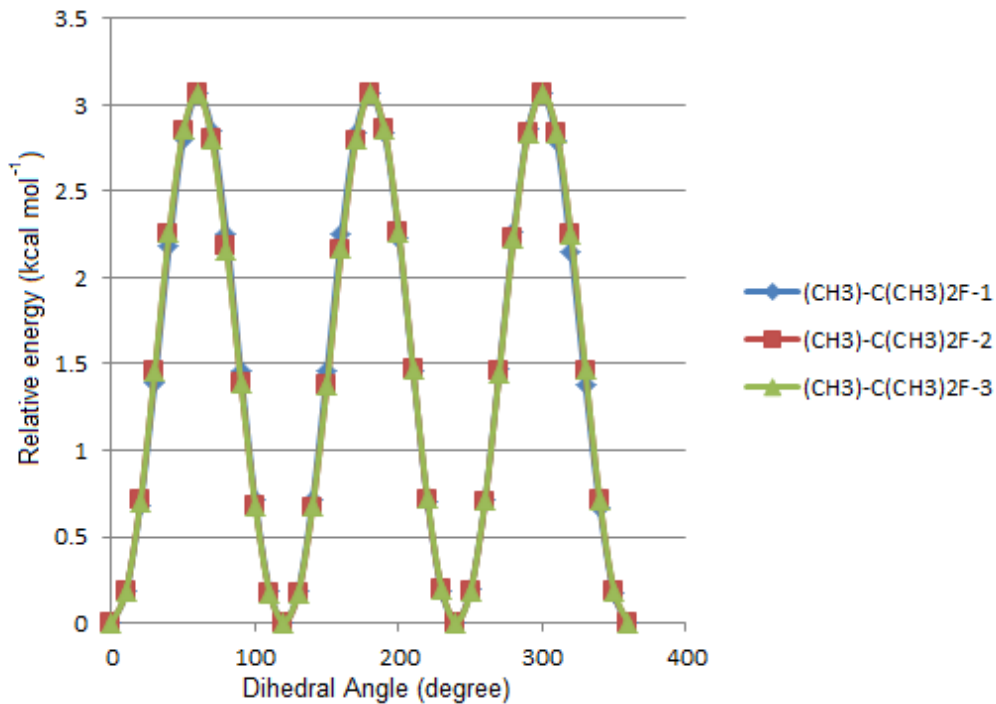


Figure G.11 Potential energy profile of C—C internal rotors for $(\text{CH}_3)_3\text{CF}$ (dot points). The solid lines indicate Fourier series expansion.

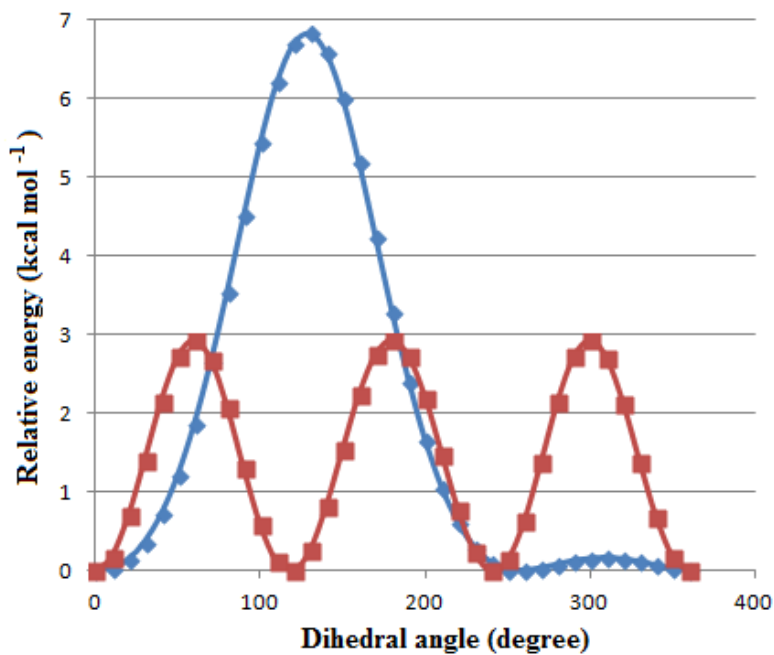


Figure G.12 Potential energy profile of CO-OH and C-OOH internal rotors for CH_3OOH (dot prints). The solid lines indicate Fourier series expansion.

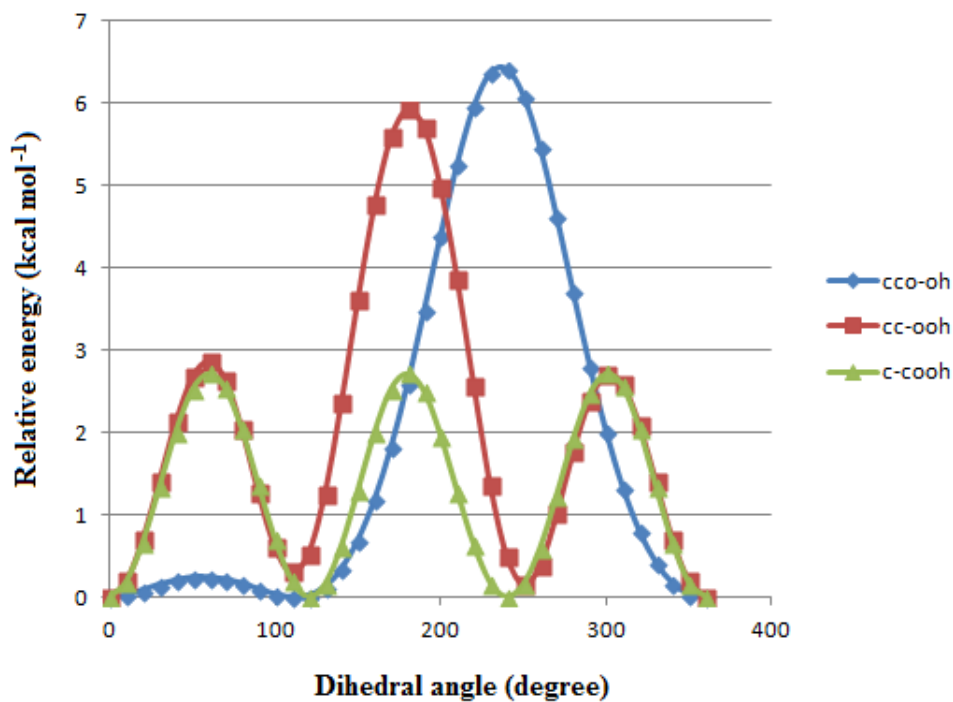


Figure G.13 Potential energy profile of CCO-OH, CC-OOH, and C-COOH internal rotors for $\text{CH}_3\text{CH}_2\text{OOH}$ (dot prints). The solid lines indicate Fourier series expansion.

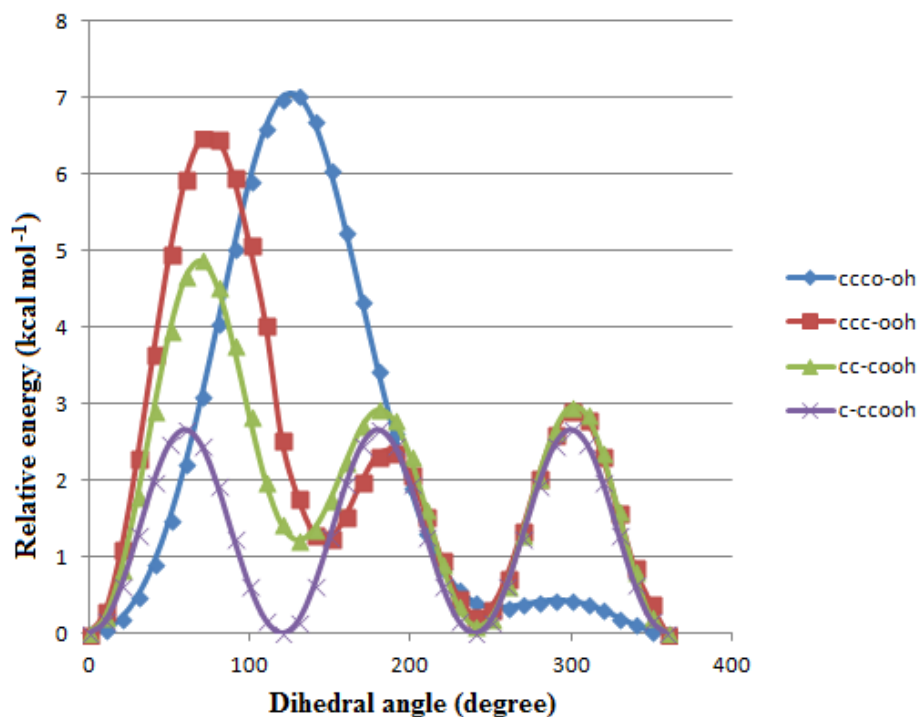


Figure G.14 Potential energy profile of CCCO-OH, CCC-OOH, CC-COOH and C-CCOOH internal rotors for $\text{CH}_3\text{CH}_2\text{CH}_2\text{OOH}$ (dot prints). The solid lines indicate Fourier series expansion.

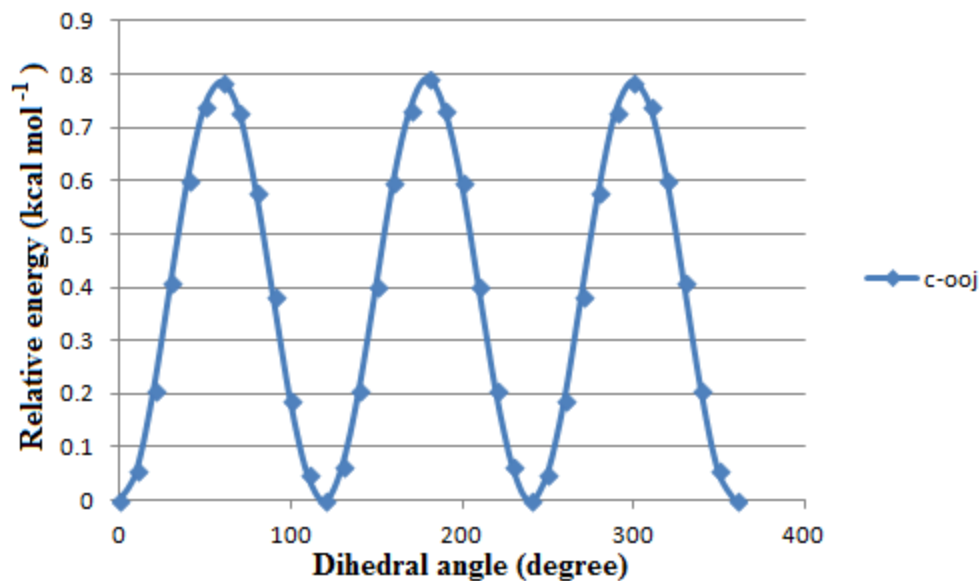


Figure G.15 Potential energy profile of C-OO internal rotors for CH₃OOj(dot prints). The solid lines indicate Fourier series expansion.

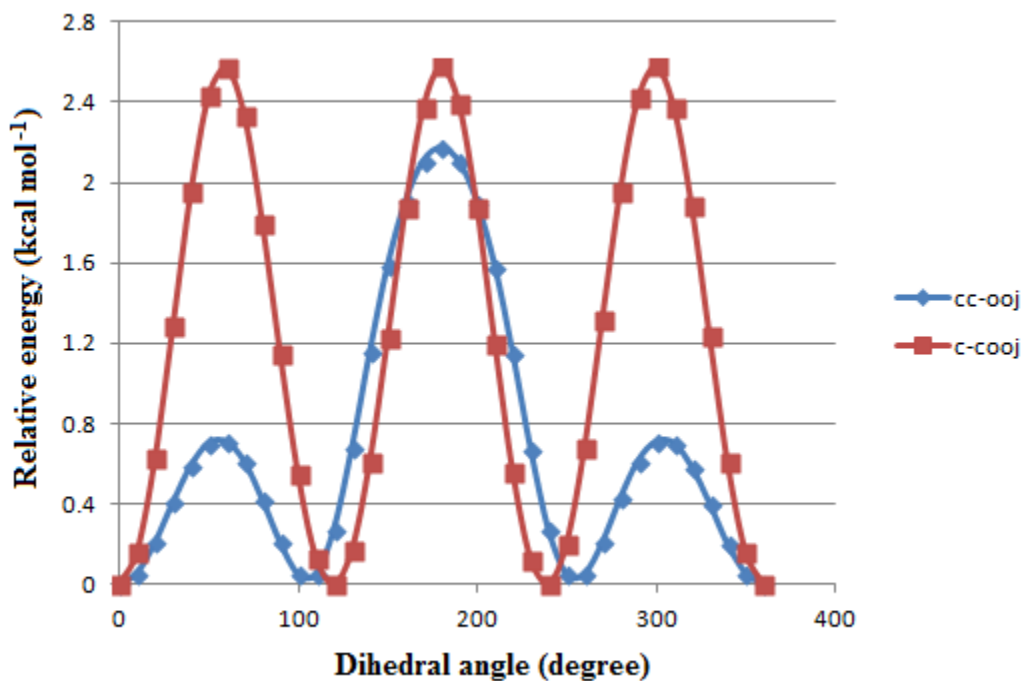


Figure G.16 Potential energy profile of CC-OOj and C-COOj internal rotors for CH₃CH₂OOj(dot prints). The solid lines indicate Fourier series expansion.

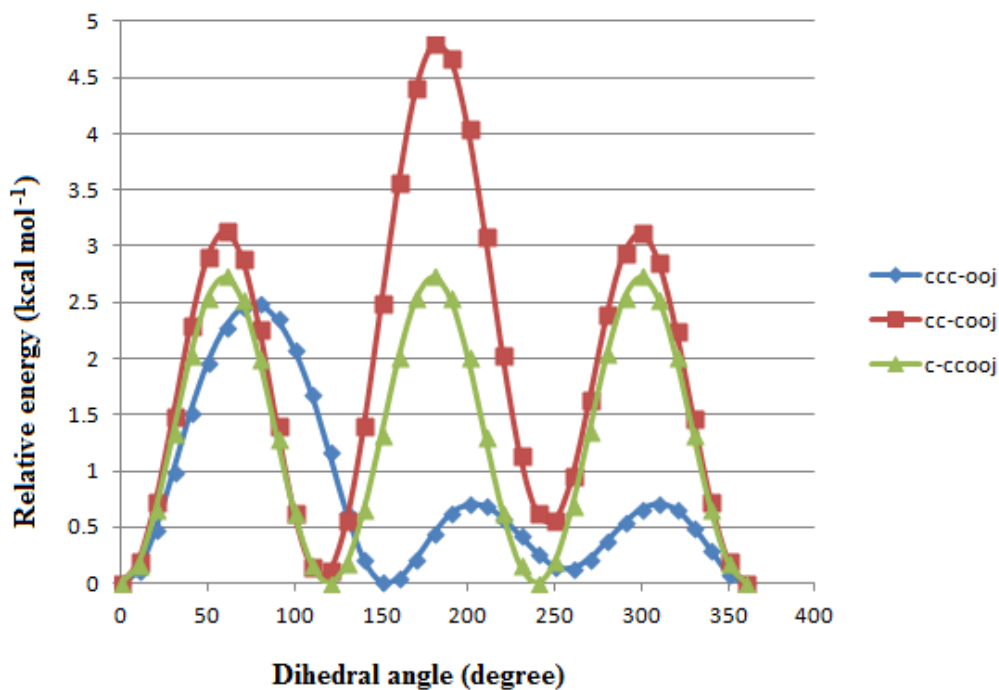


Figure G.17 Potential energy profile of CCC-OOj, CC-COOj, and C-CCOOj internal rotors for CH₃CH₂CH₂OOj(dot prints). The solid lines indicate Fourier series expansion.

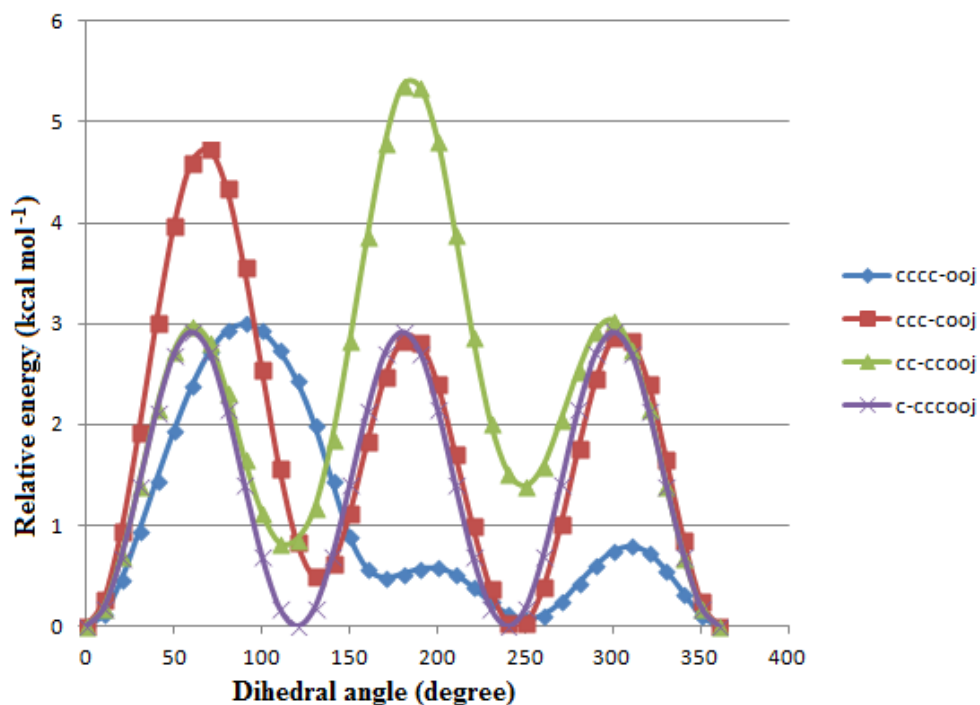


Figure G.18 Potential energy profile of CCCC-OOj, CCC-COOj, CC-CCOOj, and C-CCCCOOj internal rotors for CH₃CH₂CH₂CH₂OOj(dot prints). The solid lines indicate Fourier series expansion.

APPENDIX H
ORBITAL ANALYSIS

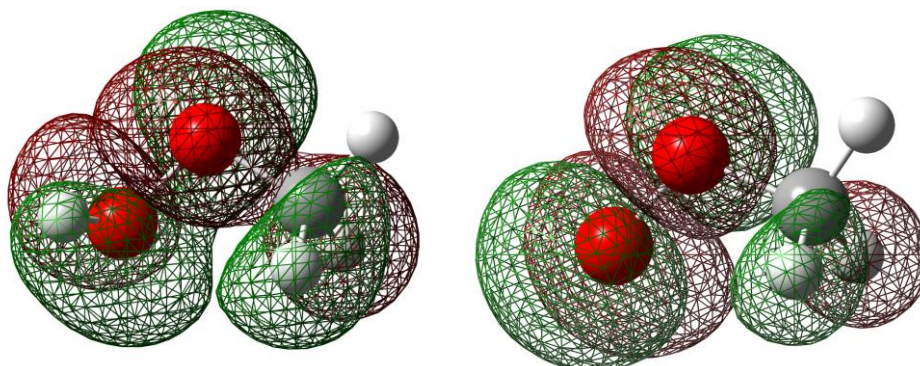


Figure H.1 HOMO analysis for CH_3OOH (left) and CH_3OOj (right).

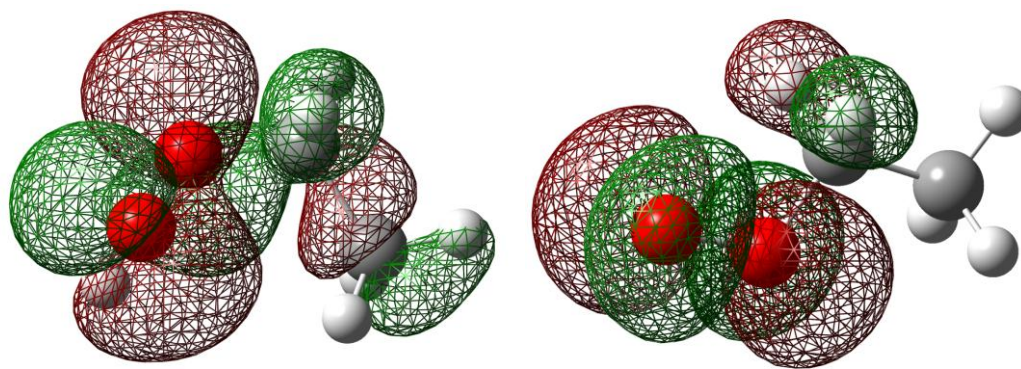


Figure H.2 HOMO analysis for $\text{CH}_3\text{CH}_2\text{OOH}$ (left) and $\text{CH}_3\text{CH}_2\text{OOj}$ (right).

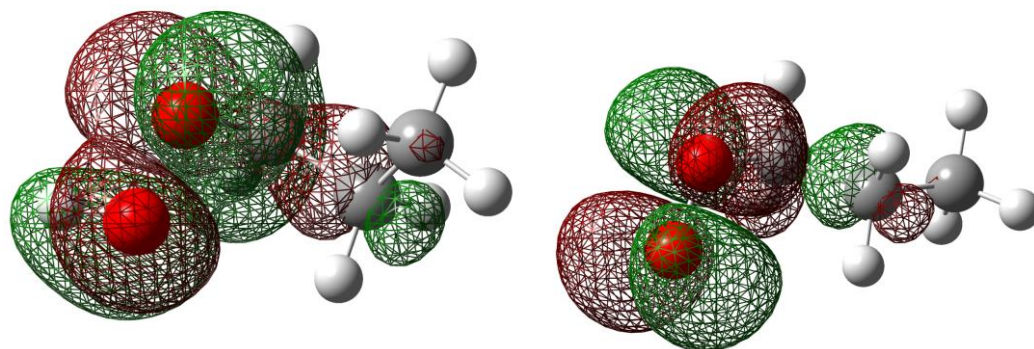


Figure H.3 HOMO analysis for $\text{CH}_3\text{CH}_2\text{CH}_2\text{OOH}$ (left) and $\text{CH}_3\text{CH}_2\text{CH}_2\text{OOj}$ (right).

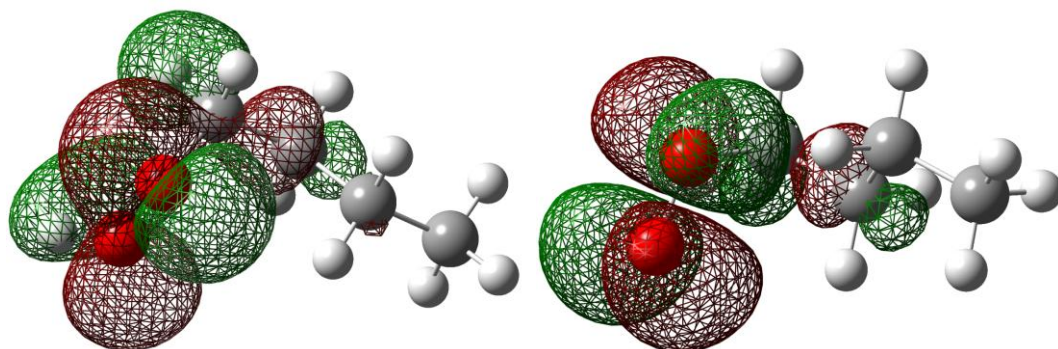


Figure H.4 HOMO analysis for $\text{CH}_3\text{CH}_2\text{CH}_2\text{CH}_2\text{OOH}$ (left) and $\text{CH}_3\text{CH}_2\text{CH}_2\text{CH}_2\text{OOj}$ (right).

REFERENCES

1. Wallington, T. J.; Schneider, W. F.; Worsnop, D. R.; Nielsen, O. J.; Sehested, J.; Debruyne, W. J.; Shorter, J. A., *Environ. Sci. Technol.* **1994**, *28*, 320A.
2. Berry, R. J.; Burgess, D. R. F.; Nyden, M. R.; Zachariah, M. R.; Melius, C. F.; Schwartz, M., *J. Phys. Chem.* **1996**, *100*, 7405.
3. Chen, Y.; Paddison, S. J.; Tschuikow-Roux, E., *J. Phys. Chem.* **1994**, *98*, 1100.
4. Haworth, N. L.; Smith, M. H.; Bacskay, G. B.; Mackie, J. C., *J. Phys. Chem. A* **2000**, *104*, 7600.
5. Nagy, B.; Csontos, B.; Csontos, J.; Szakács, P.; Kállay, M., *J. Phys. Chem. A* **2014**, *118*, 4824.
6. Yamada, T.; Bozzelli, J. W., *J. Phys. Chem. A* **1999**, *103*, 7373.
7. Yamada, T.; Bozzelli, J. W.; Berry, R. J., *J. Phys. Chem. A* **1999**, *103*, 5602.
8. Yamada, T.; Lay, T. H.; Bozzelli, J. W., *J. Phys. Chem. A* **1998**, *102*, 7286.
9. Zachariah, M. R.; Westmoreland, P. R.; Burgess, D. R.; Tsang, W.; Melius, C. F., *J. Phys. Chem.* **1996**, *100*, 8737.
10. Benson, S. W., *Thermochemical Kinetics*. 2nd ed.; New York, NY: Wiley-Interscience:1976.
11. Chase, M. W. J., *J. Phys. Chem. Ref. Data.* **1998**, *Monograph 9*, 1-1951.
12. Csontos, J.; Rolik, Z.; Das, S.; Kállay, M., *J. Phys. Chem. A* **2010**, *114*, 13093.
13. Goos, E.; Burcat, A.; Ruscic, B., Extended Third Millennium Ideal Gas and Condensed Phase Thermochemical Database for Combustion with Updates from Active Thermochemical Tables. March, 2014.
14. Kormos, B. L.; Liebman, J. F.; Cramer, C. J., *J. Phys. Org. Chem.* **2004**, *17*, 656.
15. Bartlett, R. J.; Purvis, G. D., *Int. J. Quantum Chem.* **1978**, *14*, 561.
16. Čížek, J.; Paldus, J., *Int. J. Quantum Chem.* **1971**, *5*, 359.
17. Paldus, J.; Čížek, J.; Shavitt, I., *Phys. Rev. A* **1972**, *5*, 50.

18. Pople, J. A.; Krishnan, R.; Schlegel, H. B.; Binkley, J. S., *Int. J. Quan. Chem.* **1978**, *14*, 545.
19. Halkier, A.; Helgaker, T.; Jørgensen, P.; Klopper, W.; Olsen, J., *Chem. Phys. Lett.* **1999**, *302*, 437.
20. Dunning, T. H., *J. Chem. Phys.* **1989**, *90*, 1007.
21. Kendall, R. A.; Dunning, T. H.; Harrison, R. J., *J. Chem. Phys.* **1992**, *96*, 6796.
22. Woon, D. E.; Dunning, T. H., *J. Chem. Phys.* **1993**, *98*, 1358.
23. Feller, D., *J. Chem. Phys.* **1992**, *96*, 6104.
24. Helgaker, T.; Klopper, W.; Koch, H.; Noga, J., *J. Chem. Phys.* **1997**, *106*, 9639.
25. Ruscic, B.; Pinzon, R. E.; Morton, M. L.; von Laszewski, G.; Bittner, S. J.; Nijssure, S. G.; Amin, K. A.; Minkoff, M.; Wagner, A. F., *J. Phys. Chem. A* **2004**, *108*, 9979.
26. Tajti, A.; Szalay, P. G.; Császár, A. G.; Kállay, M.; Gauss, J.; Valeev, E. F.; Flowers, B. A.; Vázquez, J.; Stanton, J. F., *J. Chem. Phys.* **2004**, *121*, 11599.
27. Bak, K. L.; Gauss, J.; Jørgensen, P.; Olsen, J.; Helgaker, T.; Stanton, J. F., *J. Chem. Phys.* **2001**, *114*, 6548.
28. Frisch, M. J.; Trucks, G. W.; Schlegel, H. B.; Scuseria, G. E.; Robb, M. A.; Cheeseman, J. R.; Scalmani, G.; Barone, V.; Mennucci, B.; Petersson, G. A.; Gaussian 09. Wallingford CT, 2009.
29. Bentz, J. L.; Olson, R. M.; Gordon, M. S.; Schmidt, M. W.; Kendall, R. A., *Comput. Phys. Commun.* **2007**, *176*, 589.
30. Olson, R. M.; Bentz, J. L.; Kendall, R. A.; Schmidt, M. W.; Gordon, M. S., *J. Chem. Theory Comput.* **2007**, *3*, 1312.
31. Piecuch, P.; Kucharski, S. A.; Kowalski, K.; Musiał, M., *Comput. Phys. Commun.* **2002**, *149*, 71.
32. Schmidt, M. W.; Baldrige, K. K.; Boatz, J. A.; Elbert, S. T.; Gordon, M. S.; Jensen, J. H.; Koseki, S.; Matsunaga, N.; Nguyen, K. A.; Su, S.; Windus, T. L.; Dupuis, M.; Montgomery, J. A., *J. Comput. Chem.* **1993**, *14*, 1347.
33. Becke, A. D., *J. Chem. Phys.* **1993**, *98*, 5648.
34. Lee, C.; Yang, W.; Parr, R. G., *Phys. Rev. B* **1988**, *3*, 785.

35. Montgomery, J. A.; Frisch, M. J.; Ochterski, J. W.; Petersson, G. A., *J. Chem. Phys.* **2000**, *112*, 6532.
36. Ochterski, J. W.; Petersson, G. A.; Montgomery, J. A., *J. Chem. Phys.* **1996**, *104*, 2598.
37. Zhao, Y.; Truhlar, D., *Theor. Chem. Acc.* **2008**, *120*, 215.
38. Chai, J.-D.; Head-Gordon, M., *J. Chem. Phys.* **2008**, *128*, 084106.
39. Barnes, E. C.; Petersson, G. A.; Montgomery, J. A.; Frisch, M. J.; Martin, J. M. L., *J. Chem. Theory Comput.* **2009**, *5*, 2687.
40. Martin, J. M. L.; de Oliveira, G., *J. Chem. Phys.* **1999**, *111*, 1843.
41. Curtiss, L. A.; Redfern, P. C.; Raghavachari, K., *J. Chem. Phys.* **2007**, *126*, 084108.
42. Chan, B.; Radom, L., *J. Chem. Theory Comput.* **2011**, *7*, 2852.
43. Hehre, W.; Radom, L.; Schleyer, P. R.; Pople, J. A., *Ab Initio Molecular Orbital Theory*. New York: NY, Wiley & Sons, 1986.
44. Pedley, J. B., *Thermochemical Data of Organic Compounds*. 2nd ed.; New York: NY, Chapman and Hall, 1986.
45. Burgess, D. R., "Thermochemical Data" in NIST Chemistry Webbook, NIST Standard Reference Database Number 69; Linstrom, P. J., Mallard, W. G., Eds., National Institute of Standards and Technology. Gaithersburg, MD.
46. Sheng, C. Ph.D. Dissertation. New Jersey Institute of Technology, 2002.
47. Lay, T. H.; Krasnoperov, L. N.; Venanzi, C. A.; Bozzelli, J. W.; Shokhirev, N. V., *J. Phys. Chem.* **1996**, *100*, 8240.
48. NIST Computational Chemistry Comparison and Benchmark Database, NIST Standard Reference Database Number 101, Release 16a; Johnson, R.D. III, Ed. NIST: Gaithersburg, MD, 2013.
49. Holmes, J. L.; Lossing, F. P., *J. Am. Chem. Soc.* **1982**, *104* (9), 2648.
50. Stull, D. R.; Westrum, E. F.; Sinke, G. C., *The Chemical Thermodynamics of Organic Compounds*. Florida: FL: Robert E. Krieger Publishing Company: Malabar, 1987.

51. M., F.; Kabo, G. J.; Marsh, K. N.; Roganov, G. N.; Wilhoit, R. C., *Thermodynamics of Organic Compounds in the Gas State*. Texas, TS: Texas A&M University System:College Station, 1994.
52. Williamson, A. D.; LeBreton, P. R.; Beauchamp, J. L., *J. Am. Chem. Soc.* **1976**, *98*, 2705.
53. Chen, S. S.; Rodgers, A. S.; Choo, J.; Wilhoit, R. C.; Zwolinski, B. J., *J. Phys. Chem. Ref. Data* **1975**, *4*, 441.
54. Berry, R. J.; Ehlers, C. J.; Burgess Jr, D. R.; Zachariah, M. R.; Nyden, M. R.; Schwartz, M., Halon thermochemistry: *THEOCHEM* **1998**, *422*, 89.
55. Luo, Y.-R.; Benson, S. W., *J. Phys. Chem. A* **1997**, *101*, 3042.
56. Bakowies, D., *J. Phys. Chem. A* **2009**, *113*, 11517.
57. Frenkel, M.; Kabo, G. J.; Marsh, K. N.; Roganov, G. N.; Wilhoit, R. C., *Thermodynamics of Organic Compounds in the Gas State*. Texas, TS: Texas A&M University System: Texas, 1994.
58. P., K. V., *Russ. Chem. Rev.* **1978**, *47*, 599.
59. Lord, A.; Goy, C. A.; Pritchard, H. O., *J. Phys. Chem.* **1967**, *71*, 2705.
60. Kolesov, V. P.; Papina, T. S., *Russ. Chem. Rev.* **1983**, *52*, 425.
61. Rodgers, A. S.; Chao, J.; Wilhoit, R. C.; Zwolinski, B. J., *J. Phys. Chem. Ref. Data* **1974**, *3*, 117.
62. Cohen, N., *J. Phys. Chem. Ref. Data* **1996**, *25*, 1411.
63. Li, S.; Sarathy, S. M.; Davidson, D. F.; Hanson, R. K.; Westbrook, C. K., *Combust. Flame* **2015**, *162*, 2296.
64. Nakamura, H.; Curran, H. J.; Polo Córdoba, A.; Pitz, W. J.; Dagaut, P.; Togbé, C.; Sarathy, S. M.; Mehl, M.; Agudelo, J. R.; Bustamante, F., *Combust. Flame* **2015**, *162*, 1395.
65. Z. Wang; L. Zhang; V.S.B. Shankar; K. Moshhammer; D.M.P.-Vaida; A. Lucassen; C. Hemken; D. Vuilleumier; N. Hansen; P. Dagaut; Sarathy, S. M., In *9th U.S. National Combustion Meeting*, Cincinnati, Ohio, 2015.
66. Crounse, J. D.; Knap, H. C.; Ørnsø, K. B.; Jørgensen, S.; Paulot, F.; Kjaergaard, H. G.; Wennberg, P. O., *J. Phys. Chem. A* **2012**, *116*, 5756-5762.

67. Di Tommaso, S.; Rotureau, P.; Crescenzi, O.; Adamo, C., *Phys. Chem. Chem. Phys.* **2011**, *13*, 14636.
68. Sharma, S.; Raman, S.; Green, W. H., *J. Phys. Chem. A* **2010**, *114*, 5689.
69. Zhu, L.; Bozzelli, J. W.; Kardos, L. M., *J. Phys. Chem. A* **2007**, *111*, 6361.
70. da Silva, G.; Bozzelli, J. W., *J. Phys. Chem. A* **2007**, *111*, 12026.
71. Van, M. A.; Ploemen, I. H. J., Improvements relating to alkylene oxide production. Google Patents: 2015.
72. Baker, G.; Littlefair, J. H.; Shaw, R.; Thynne, J. C. J., *J. Chem. Soc.* **1965**, 6970.
73. Rebbert, R. E.; Laidler, K. J., *J. Chem. Phys.* **1952**, *20*, 574.
74. Lay, T. H.; Bozzelli, J. W., *J. Phys. Chem. A* **1997**, *101*, 9505.
75. Stathis, E. C.; Egerton, A. C., *Trans.Fara. Soc.* **1940**, *35*, 606.
76. Egerton, A. C.; Emte, W.; Minkoff, G. J., *Discuss.Fara. Soc.* **1951**, *10*, 278.
77. Burke, S. M.; Simmie, J. M.; Curran, H. J., *J. Phys. Chem. Ref. Data* **2015**, *44*, 013101.
78. Chen, C.-J.; Bozzelli, J. W., *J. Phys. Chem. A* **2000**, *104*, 4997.
79. Sheng, C. Y.; Bozzelli, J. W.; Dean, A. M.; Chang, A. Y., *J. Phys. Chem. A* **2002**, *106*, 7276.
80. Sumathi, R.; Green, W. H., *J. Phys. Chem. A* **2002**, *106*, 7937.
81. Sebban, N.; Bozzelli, J. W.; Bockhorn, H., *J. Phys. Chem. A* **2004**, *108*, 8353-8366.
82. Janoschek, R.; Rossi, M. J., *Int. J. Chem. Kinet.* **2004**, *36*, 661.
83. Simmie, J. M.; Black, G.; Curran, H. J.; Hinde, J. P., *J. Phys. Chem. A* **2008**, *112*, 5010.
84. Goldsmith, C. F.; Magoon, G. R.; Green, W. H., *J. Phys. Chem. A* **2012**, *116*, 9033.
85. Khursan, S. L.; Martem'yanov, V. S., *Russ. J. Phys. Chem. (Engl. Transl.)* **1991**, *65*, 321.
86. Matthews, J.; Sinha, A.; Francisco, J. S., *J. Chem. Phys.* **2005**, *122*, 221101.

87. Blanksby, S. J.; Ramond, T. M.; Davico, G. E.; Nimlos, M. R.; Kato, S.; Bierbaum, V. M.; Lineberger, W. C.; Ellison, G. B.; Okumura, M., *J. Am. Chem. Soc.* **2001**, *123*, 9585.
88. Khachatryan, L. A.; Niazyan, O. M.; Mantashyan, A. A.; Vedeneev, V. I.; Teitel'boim, M. A., *Int. J. Chem. Kinet.* **1982**, *14*, 1231.
89. Knyazev, V. D.; Slagle, I. R., *J. Phys. Chem. A* **1998**, *102*, 1770.
90. Slagle, I. R.; Gutman, D., *J. Am. Chem. Soc.* **1985**, *107*, 5342.
91. Benson, S. W., *J. Am. Chem. Soc.* **1964**, *86*, 3922.
92. Nangia, P. S.; Benson, S. W., *J. Phys. Chem.* **1979**, *83*, 1138.
93. Chen, C.-J.; Bozzelli, J. W., *J. Phys. Chem. A* **1999**, *103*, 9731.
94. Bach, R. D.; Ayala, P. Y.; Schlegel, H. B., *J. Am. Chem. Soc.* **1996**, *118*, 12758.
95. Barker, J. R.; Benson, S. W.; Golden, D. M., *Int. J. Chem. Kinet.* **1977**, *9*, 31.
96. Blanksby, S. J.; Ellison, G. B., *Acc. Chem. Res.* **2003**, *36*, 255.
97. Kondo, O.; Benson, S. W., *J. Phys. Chem.* **1984**, *88*, 6675.
98. Jonsson, M., *J. Phys. Chem.* **1996**, *100*, 6814.
99. Fu, Y.; Liu, L.; Mou, Y.; Lin, B.-L.; Guo, Q.-X., *THEOCHEM* **2004**, *674*, 241-249.
100. Mitov, S.; Panchenko, A.; Roduner, E., *Chem. Phys. Lett.* **2005**, *402*, 485.
101. Wijaya, C. D.; Sumathi, R.; Green, W. H., *J. Phys. Chem. A* **2003**, *107*, 4908-4920.
102. Luo, Y.-R., *Handbook of Bond Dissociation Energies in Organic Compounds*. Florida, FL: CRC Press: Boca Raton, 2003.
103. Merle, J. K.; Hayes, C. J.; Zalyubovsky, S. J.; Glover, B. G.; Miller, T. A.; Hadad, C. M., *J. Phys. Chem. A* **2005**, *109*, 3637.
104. Schneider, W. F.; Wallington, T. J., *J. Phys. Chem.* **1993**, *97*, 12783.
105. Sawada, H., *Chem. Rev.* **1996**, *96*, 1779.
106. Hayman, G. D.; Derwent, R. G., *Environ. Sci. Technol.* **1997**, *31*, 327.
107. El-Taher, S., *J. Fluorine Chem.* **2006**, *127*, 54.

108. Reints, W.; Pratt, D. A.; Korth, H.-G.; Mulder, P., *J. Phys. Chem. A* **2000**, *104*, 10713.
109. Kosmas, A. M.; Mpellos, C.; Salta, Z.; Drougas, E., *Chem. Phys.* **2010**, *371*, 36.
110. Wang, H.; Castillo, Á.; Bozzelli, J. W., *J. Phys. Chem. A* **2015**, *119*, 8202.
111. Ruscic, B., *J. Phys. Chem. A* **2015**, *119*, 7810.
112. Batt, L.; Walsh, R., *Int. J. Chem. Kinet.* **1982**, *14*, 933.
113. Battin-Leclerc, F.; Rodriguez, A.; Husson, B.; Herbinet, O.; Glaude, P.-A.; Wang, Z.; Cheng, Z.; Qi, F., *J. Phys. Chem. A* **2014**, *118*, 673.
114. Dagaut, P.; Reuillon, M.; Cathonnet, M., *Combust. Flame* **1995**, *101*, 132-140.
115. Dagaut, P.; Reuillon, M.; Cathonnet, M.; Presvots, D., *Chromatographia* **40**, 147.
116. Yahyaoui, M.; Djebaïli-Chaumeix, N.; Dagaut, P.; Paillard, C. E.; Gail, S., *Combust. Flame* **2006**, *147*, 67.
117. Baldwin, R. R.; Pickering, I. A.; Walker, R. W., *J. Chem.Soc., Fara. Trans. I: Phys.Chem. in Condensed Phases* **1980**, *76*, 2374.
118. Zádor, J.; Taatjes, C. A.; Fernandes, R. X., *Progr. Energy Combust. Sci.* **2011**, *37*, 371.
119. Sun, H.; Bozzelli, J. W., *J. Phys. Chem. A* **2004**, *108*, 1694.
120. Bugler, J.; Somers, K. P.; Silke, E. J.; Curran, H. J., *J. Phys. Chem. A* **2015**, *119*, 7510.
121. Auzmendi-Murua, I.; Bozzelli, J. W., *J. Phys. Chem. A* **2014**, *118*, 3147.
122. Auzmendi-Murua, I.; Charaya, S.; Bozzelli, J. W., *J. Phys. Chem. A* **2013**, *117*, 378.
123. Joshi, A.; You, X.; Barckholtz, T. A.; Wang, H., *J. Phys. Chem. A* **2005**, *109*, 8016.
124. Grimme, S., *J. Chem. Phys.* **2006**, *124*, 034108.
125. Chai, J.-D.; Head-Gordon, M., *Phys. Chem. Chem. Phys.* **2008**, *10*, 6615.
126. Curtiss, L. A.; Raghavachari, K.; Redfern, P. C.; Rassolov, V.; Pople, J. A., *J. Chem. Phys.* **1998**, *109*, 7764.

127. Cizek, J., *Advances in Chemical Physics*. New York, NY: Weiley Interscience: **1969**.
128. Purvis, G. D.; Bartlett, R. J., *J. Chem. Phys.* **1982**, *76*, 1910.
129. Scuseria, G. E.; Janssen, C. L.; Schaefer, H. F., *J. Chem. Phys.* **1988**, *89*, 7382.
130. Scuseria, G. E.; Schaefer, H. F., *J. Chem. Phys.* **1989**, *90*, 3700.
131. Peterson, K. A., *J. Chem. Phys.* **2003**, *119*, 11099.
132. Peterson, K. A.; Puzzarini, C., *Theor. Chem. Acc.* **2005**, *114*, 283.
133. Kee, R. J.; Rupley, F. M.; Miller, J. A. *Chemkin-II: A Fortran chemical kinetics package for the analysis of gas-phase chemical kinetics*; **1989**.
134. Poling, B.; Prausnitz, J.; Connell, J. O., *The Properties of Gases and Liquids*. New York, NY: McGraw-Hill Education: **2000**.
135. Poling, B. E.; Prausnitz, J. P.; O'Connell, J. P., *The Properties of Gases and Liquids*. 5th ed.; New York, NY: McGraw-Hill Education, **2004**.
136. Zhu, L.; Bozzelli, J. W., *J. Phys. Chem. A* **2002**, *106*, 345.
137. Cox, J. D.; Wagman, D. D.; Medvedev, V. A., *CODATA Key Values for Thermodynamics*. New York, NY: Hemisphere Publishing, Corp., **1989**.
138. Asatryan, R.; Silva, G. d.; Bozzelli, J. W., *J. Phys. Chem. A* **2010**, *114*, 8302.
139. Lee, J.; Bozzelli, J. W., *J. Phys. Chem. A* **2003**, *107*, 3778.
140. Ruscic, B.; Boggs, J. E.; Burcat, A.; Császár, A. G.; Demaison, J.; Janoschek, R.; Martin, J. M. L.; Morton, M. L.; Rossi, M. J.; Stanton, J. F.; Szalay, P. G.; Westmoreland, P. R.; Zabel, F.; Bérces, T., *J. Phys. Chem. Ref. Data* **2005**, *34*, 573.
141. Bouchoux, G.; Chamot-Rooke, J.; Leblanc, D.; Mourgues, P.; Sablier, M., *ChemPhysChem* **2001**, *2*, 235.
142. Niiranen, J. T.; Gutman, D.; Krasnoperov, L. N., *J. Phys. Chem.* **1992**, *96*, 5881.
143. Tsang, W.; Martinho Simoes, J. A.; Greenberg, A.; Liebman, J. F., *Heats of Formation of Organic Free Radicals by Kinetic Methods in Energetics of Organic Free Radicals*. London: Blackie Academic and Professional, **1996**.

144. JANAF, *Thermochemical Tables; National Standard Reference Data Series.*; Washington DC, U.S. National Bureau of Standards: **1985**; Vol. 37.
145. Tabor, D. P.; Harding, M. E.; Ichino, T.; Stanton, J. F., *J. Phys. Chem. A* **2012**, *116*, 7668.
146. da Silva, G.; Bozzelli, J. W., *J. Phys. Chem. A* **2006**, *110*, 13058.
147. Baulch, D. L.; Bowman, C. T.; Cobos, C. J.; Cox, R. A.; Just, T.; Kerr, J. A.; Pilling, M. J.; Stocker, D.; Troe, J.; Tsang, W.; Walker, R. W.; Warnatz, J., *J. Phys. Chem. Ref. Data* **2005**, *34*, 757.
148. Frenklach, M.; Packard, A.; Djurisic, Z. M.; Golden, D. M.; Bowman, C. T.; Green, W. H.; McTae, G. J.; Allison, T. C.; Rosasco, G. J.; Pilling, M. J., *Process Informatics Model.* **2007**.
149. Baldwin, R. R.; Bennett, J. P.; Walker, R. W., *J. Chem. Soc., Fara. Trans. 1: Phys. Chem. in Condensed Phases* **1980**, *76*, 2396.
150. Baldwin, R. R.; Drewery, G. R.; Walker, R. W., *J. Chem. Soc., Fara. Trans. 1: Phys. Chem. in Condensed Phases* **1984**, *80*, 3195.
151. Baldwin, R. R.; Drewery, G. R.; Walker, R. W., *J. Chem. Soc., Fara. Trans. 2: Phys. Chem. in Condensed Phases* **1986**, *82*, 251.
152. Dagaut, P., *Phys. Chem. Chem. Phys.* **2002**, *4*, 2079.
153. Snitsiriwat, S.; Bozzelli, J. W., *J. Phys. Chem. A* **2014**, *118*, 4631.
154. Bauschlicher Jr, C. W., *Chem. Phys. Lett.* **1995**, *246*, 40.